The Role of Host Microenvironment in the Pathogenesis of Multiple Myeloma



Seint Thè Su Lwin

A thesis submitted in partial fulfilment for the requirement for the degree of

Doctor of Philosophy

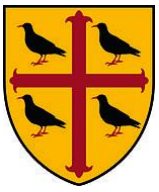

St. Edmund Hall
Nuffield Department of Surgical Sciences
University of Oxford
Michaelmas Term 2014

Statement of originality

All the work presented in this thesis is the result of my own research unless otherwise stated.

Dedication

To my beloved father, U Myint Lwin, who is the most fun, loving, best father that I could ever imagine, I really wish he could have known that I had an opportunity to study at Oxford. He would have been so proud of me. Of the many letters that he has written to me when I was studying in the US, one of the letters drew an analogy between studying and running a marathon, how they both need hard work and training for stamina. I understand his analogy better during my DPhil work. I am so lucky to have him as my father. I miss him dearly and great memories of him will forever stay in my heart.

I also would like to dedicate my thesis to my beloved mom Daw Hla Hla Win and, my sweet beloved baby brother Chan Myae Lwin, who love me unconditionally and support me with everything I need or want. My mom has always devoted her life for my brother and I, and still continues doing so even though we are both grown ups. My brother has been my best friend and my consultant in everything I do. Talking to him and hanging out with him always make me happy and calm. I love my family very much and words cannot express how happy and lucky I am to have my loving and devoted family.

Acknowledgements

Firstly, I would like to take this opportunity to show my deep appreciation to my supervisors Dr. Claire Edwards and Dr. James Edwards for their wonderful supervision, guidance, support, encouragement, giving me intellectual and personal freedom, and creating great opportunities throughout, before and beyond my DPhil work. Without Claire and James, I would have never dreamt of studying and working for a PhD, let alone being in Oxford. Their kind support and positive outlook in life during my time as a research assistant working for Claire at Vanderbilt University has made me believe that I could have what it takes to study for PhD. Whenever my experiments are not going well, somehow Claire and James have something positive to say to calm me down and made me believe that it really was not too bad after all. I feel very lucky to have met, worked for, and having Claire and James as my DPhil supervisors, and I could not have asked for anything better. I have learnt a lot from Claire and James both at personal and professional levels. I have thoroughly enjoyed everything that Oxford has to offer both academically and personally, as a University, college, or city itself.

Secondly, I am indebted to my best friend and lab sibling, Srinivasa Rao Rao. He has always been very kind, generous, supportive, and helpful. Rao has given me tireless help both professionally and personally. I am also grateful to Ann Snaith for bringing youthfulness and joy to the lab, and being such a fun and loving friend to hang out, and to travel. I also would like to thank Laurynas Pliuškys for helping me with initial set up writing my thesis and his fun and lovely friendship. I am very grateful to Dr. Philippa Hulley, Dr. Sarah Gooding, and Dr. Ed Hookway for giving me mock viva, which helped me tremendously. I also would like to thank Edwards lab members, Gloria, Siobhan, Sam, Jess, Emma and everyone in the lab for their friendship. Being with fun friends made everything easier. I am grateful to the members of Botnar Research Centre for any kind of help that they have given me.

Finally, I am indebted to Clarendon Fund at University of Oxford for supporting me throughout my DPhil work. Interactions with Clarendon members have been inspiring and priceless. I also appreciate the research-funding bodies that supported my DPhil work. I appreciate the members of my college, St Edmund Hall, for creating a nice and cosy environment, giving different sources of funding, and having formal dinners with one of the best and affordable food in Oxford. I am grateful to all my friends, teachers and family who has helped me, inspired me in any and many ways throughout my life. All in all, I had my best time here at Oxford, ever since I left home 15 years ago.

Contents

List of Figures ..... **x**

List of Tables ..... **xii**

Abbreviations ..... **xiv**

Chapter 1 : General Introduction **1**

1.1 Multiple myeloma 1

1.1.1 Incidence rate 1

1.1.2 Stages and symptoms of myeloma 4

1.2 Monoclonal Gammopathy of Undetermined Significance (MGUS) 6

1.3 Murine models of myeloma 7

1.4 Interactions between cells of the host microenvironment 11

1.4.1 The cells of the bone marrow microenvironment 12

1.4.2 Cross-talk between tumour cells and host microenvironment 19

1.4.3 Matrix metalloproteinases (MMPs) in matrix environment 20

1.4.4 Matrix Metalloproteinase 7 (MMP7) 22

1.4.5 TIMP1, an inhibitor of MMP7 26

1.4.6 Factors involved in enhanced osteoclastic bone resorption in myeloma 26

1.4.7 Inhibition of osteoblast formation in myeloma 30

1.5 Current Therapies 34

1.5.1 Proteasome inhibitors 35

1.5.2 Immunomodulators (IMiDs) 36

1.5.3 Bisphosphonates (BPs) 37

1.5.4 Denosumab 39

1.5.5 Autologous stem cell transplantation (ASCT) 39

1.5.6 Overview of the current National Institute for Health and Care Excellence (NICE) guidelines for management of myeloma 40

1.6 Association between myeloma and obesity 41

1.7 Obesity, MMPs, TIMPs and myeloma 42

1.8 The aim of the study 44

Chapter 2 : General Materials and Methods 46

2.1 Cell culture 46

2.1.1 Cell culture conditions 46

2.2 *In vivo* studies 47

2.3 Body composition analysis 48

2.4 Bone marrow isolation by centrifugation 48

2.5 Assessment of tumour burden by ELISA 49

2.6 Assessment of tumour burden by flow cytometry 51

2.7 Microcomputed tomography (MicroCT) analysis 51

2.8 Tissue processing and paraffin embedding for mouse hind legs and spleen 52

2.9 Tissue staining 53

2.9.1 Hematoxylin and eosin (H & E) staining 53

2.9.2 TRAP staining 53

2.9.3 Immunohistochemistry 54

2.9.4 TUNEL staining 55

2.10 Enzyme-linked Immunosorbent Assay (ELISA) 56

2.11 RNA isolation and quantitation 56

2.12 cDNA synthesis 57

2.12.1 Removal of genomic DNA from RNA preparations (DNase treatment) 57

2.12.2 iScript cDNA Synthesis 58

2.13 Polymerase Chain Reaction (PCR) 58

2.14 Quantitative Real Time Polymerase Chain Reaction (Real-time PCR) 58

2.15 Cell viability assay (MTS) 59

2.16 Protein extraction 61

2.16.1 Procedure for lysis of cells cultured in suspension or murine bone marrow cells 61

2.16.2 Procedure for lysis of monolayer-cultured adherent cells 61

2.17 Quantitation of protein concentration 62

2.18 Western blotting 62

2.19 Statistical analysis 64

2.20 List of antibodies 65

Chapter 3 : The role of host-derived MMP7 in myeloma development *in vivo* 66

3.1 66

3.1 Introduction.....66

3.1.1 MMP7 and osteolytic bone disease 66

3.1.2 Substrates of MMP7 67

3.1.3 Aim 70

3.2 Materials and Methods.....71

3.2.1 Overexpression of MMP7 by transduction.....71

3.2.2 *In vivo* studies 71

3.2.3 Viability assay.....72

3.2.4 Silver staining 73

3.2.5 Co-culture experiments.....73

3.2.6 Human patient samples.....74

3.2.7 ELISAs.....74

3.2.8 Western blotting.....74

3.2.9 Real-time PCR 75

3.2.10 Gelatin and casein zymography.....76

3.2.11 MMP7 activity assay 77

3.3 Results.....78

3.3.1 Tumour burden is increased in myeloma-bearing MMP7$^{-/-}$ mice..78

3.3.2 Increased osteolytic bone disease in myeloma-bearing MMP7$^{-/-}$ mice.....79

3.3.3 Patients with myeloma have a decrease in circulating MMP7 activity with no change in concentration 80

3.3.4 The endogenous MMP inhibitor TIMP-1 is increased in patients with myeloma and myeloma-bearing mice.....83

3.3.5 Exogenous MMP7 decreases myeloma cell viability *in vitro* 84

3.3.6 Tumour-derived MMP7 has no effect on myeloma tumour burden *in vivo*.....87

3.3.7 MMP7 cleaves OPN *in vitro*.....88

3.3.8 Effect of full length and MMP7-cleaved OPN on 5TGM1-GFP myeloma cells *in vitro*.....89

.....90

3.3.9 Expression of full length, cleaved, and total OPN in serum of myeloma patients 90

3.3.10 Role of cleaved OPN in murine myeloma progression *in vivo* 92

3.3.11 MMP-7 cleaves galectin-3 and the effect of galectin-3 to promote myeloma cell proliferation is decreased in the presence of MMP7 *in vitro* 93

3.3.12 Full length galectin-3 is increased in myeloma-bearing MMP7$^{-/-}$ mice 96

3.3.13 Ratio of full:cleaved galectin-3 is increased in patients with myeloma 99

..... 101

3.3.14 Positive correlation between serum MMP7 activity and cleaved:full galectin-3 in patients with myeloma 102

3.4 Discussion 103

Chapter 4 : The role of obesity in myeloma development *in vivo* 108

4.1 Introduction 108

4.1.1 Aim 109

4.2 Materials and methods 110

4.2.1 Animal studies 110

4.2.2 Measurement of adipocyte number in murine bone marrow tissue 111

4.2.3 ELISAs 112

4.2.4 Western blotting 112

4.3 Results 113

4.3.1 Increased bone marrow adiposity, body weight, and total fat with decreased trabecular bone volume in myeloma-permissive C57BL/KaLwRij mice 113

4.3.2 Diet-induced obesity increases myeloma tumour burden and the associated bone disease in non-permissive C57BL/6 mice *in vivo* 115

..... 116

4.3.3 Removal of high fat diet decreases myeloma tumour burden in C57BL/6 mice 117

4.3.4 Effect of high fat diet in myeloma permissive KaLwRij mice 118

4.3.5 The effect of diet-induced obesity on serum IGF-1, IL-6, DKK1, and adiponectin levels in myeloma development 119

4.4 Discussion 121

Chapter 5 : Pharmacological targeting of adipogenic factor (PPARγ) to alter the myeloma microenvironment 126

5.1 Introduction 126

5.1.1 PPARγ, a master regulator of adipogenesis 126

5.1.2 PPARγ ligands 127

5.1.3 AMPK signalling 128

5.1.4 Aim 129

5.2 Materials and Methods 130

5.2.1 *In vivo* studies 130

5.2.2 PPARγ activity assay 131

5.2.3 Treatment of myeloma cells *in vitro* 131

5.2.4 Dual-coloured fluorescence assay with co-culture experiments 132

5.2.5 Real-time PCR 132

5.2.6 Western blotting 132

5.3 Results 134

5.3.1 The PPARγ ligand, BADGE, significantly decreased tumour burden in a murine myeloma model 134

5.3.2 BADGE increased bone marrow adipocytes and the mRNA expression of adipocyte markers in myeloma-bearing mice *in vivo* 136

5.3.3 Direct anti-tumour effects of BADGE on myeloma cells *in vitro* 139

5.3.4 Effect of BADGE on the AMPK signalling pathway 142

5.3.5 The direct anti-tumour effect of BADGE on myeloma cells *in vitro* is independent of SIRT1 145

5.3.6 Effect of BADGE on NFκB p65 expression *in vitro* 146

5.3.7 Effect of BADGE on the expression of osteolineage markers 147

5.4 Discussion 150

Chapter 6 : Conclusion and Significance 155

Appendix I : Primer sequences 162

Appendix II 164

A-II.1 Publication 164

A-II.2 Manuscript in preparation 164
A-II.3 Abstract presented 164
Appendix III : Awards 165
References 166

List of Figures

Figure 1.1. Average number of new cases per year and age-specific incidence rates per 100,000 population, UK, 2009-2011 (Cancer research UK, 2014). 1

Figure 1.2. Schematic diagram of B cell development. 3

Figure 1.3. Radiographs showing osteolytic lesions and pathological fractures in myeloma patients. 6

Figure 1.4. Development of myeloma in the bone marrow of RAG2$^{-/-}$ and KaLwRij mice. 10

Figure 1.5. Schematic of osteoclastogenesis. 14

Figure 1.6. Schematic of osteoblast differentiation. 16

Figure 1.7. Schematic of MMP structure 22

Figure 1.8. Structure of MMP7 23

Figure 1.9. Vicious cycle in myeloma bone disease. 27

Figure 1.10. 5TGM1 myeloma in KaLwRij mice. 44

Figure 1.11. Overall aims of the study. 45

Figure 2.1. Flushing of bone marrow by centrifugation 49

Figure 3.1. Experimental design for *in vivo* studies investigating the role of MMP7 in myeloma development. 72

Figure 3.2. MMP7-/-mice inoculated with 5TGM1-GFP myeloma (MM) cells resulted in a significant increase in the rate of tumour growth. 79

Figure 3.3. Myeloma-bearing (MM) MMP7$^{-/-}$ mice have a significant increase in osteolytic bone disease. 80

Figure 3.4. MMP7 activity is decreased in the serum of patients with multiple myeloma. 82

Figure 3.5. The endogenous MMP inhibitor TIMP1 is increased in patients with myeloma and myeloma-bearing mice. 84

Figure 3.6. Exogenous MMP7 inhibits the growth of myeloma cells. 86

Figure 3.7. Effect of tumour-derived MMP7 *in vivo*. 88

Figure 3.8. Cleavage of OPN by MMP7. 89

Figure 3.9. Effect of full length and MMP7-cleaved OPN on myeloma cell viability *in vitro*. 90

Figure 3.10. OPN protein expression in serum of control and myeloma (MM) patients. 91

Figure 3.11. OPN Expression in RAG2$^{-/-}$ WT and RAG2$^{-/-}$ MMP7$^{-/-}$ mice. 93

Figure 3.12. Effect of galectin-3 to promote myeloma cell growth is decreased in the presence of MMP7. 95

Figure 3.13. Increased full length galectin-3 protein expression in serum of myeloma bearing mice. 98

Figure 3.14. The ratio of cleaved:full-length galectin-3 is decreased in patients with myeloma. 101

Figure 3.15. Correlation between serum MMP7 activity and cleaved:full-lenth galectin-3 in patients with myeloma. 102

Figure 3.16. Schematic of potential mechanism for protective effect of host-derived MMP7 in myeloma pathogenesis. 107

Figure 4.1. Overall hypothesis. 109

Figure 4.2. Schematic experimental design for diet-induced obesity. 111

Figure 4.3. Phenotype comparison between non-tumour bearing myeloma non-permissive C57BL/6 and permissive KaLwRij mice. 114

Figure 4.4. A high fat diet increases tumour burden in non-permissive C57Bl6 mice. 116

Figure 4.5. Removal of a high fat diet decreases tumour burden in C57Bl6 mice. 118

Figure 4.6. A high fat diet in myeloma-permissive KaLwRij mice does not further promote myeloma development. 119

Figure 4.7. Serum concentrations of IGF-1, IL-6, DKK1, and adiponectin in myeloma-inoculated C57Bl6 mice on high fat diet. 120

Figure 5.1. Experimental design for *in vivo* studies investigating the role of BADGE in myeloma development. 130

Figure 5.2. PPARγ ligand, BADGE, significantly decreased tumour burden in a murine myeloma model of C57BL/KaLwRij mice inoculated with 5TGM1-GFP myeloma cells. 135

Figure 5.3. Increased number of adipocytes and mRNA expression of adipocyte markers in the bone marrow of myeloma-bearing mice treated with BADGE. 138

Figure 5.4. Direct anti-tumour effect of BADGE on myeloma cells. 141

Figure 5.5. BADGE induced activation of AMPK, SIRT1, increased mRNA expression of autophagy marker Atg3 and decreased VEGFα. 144

Figure 5.6. Inhibition of SIRT1 activity does not prevent the anti-tumour effect of BADGE. 146

Figure 5.7. BADGE treatment has no effect on NFκB p65 protein expression *in vitro*. 147

Figure 5.8. BADGE selectively increases *mRNA* expression of osteolineage markers. 149

Figure 6.1. Role of MMP7, obese microenvironment, and BADGE in myeloma development. 161

List of Tables

Table 1.1 Substrates of MMP7 24
Table 2.1 List of cell lines 46
Table 2.2 List of primary antibodies 65
Table 2.3 List of secondary antibodies 65
Table 3.1 List of primary antibodies for western blotting 75
Table 4.1: Experimental design of treatments 111

The Role of Host Microenvironment in the Pathogenesis of Multiple Myeloma

Seint Thè Su Lwin

St Edmund Hall

A thesis submitted for the degree of Doctor of Philosophy

Michaelmas Term 2014

Abstract

Interactions between myeloma cells and cells of the bone marrow microenvironment promote tumour growth, survival and osteolytic bone disease. A greater understanding of the contributions of the host microenvironment to myeloma pathogenesis will ultimately identify new therapeutic approaches. An association between obesity and myeloma, or monoclonal gammopathy of undetermined significance (MGUS) has been shown previously. Matrix metalloproteinases (MMPs) are key regulators of tumour: host interactions due to their ability to alter the activity of multiple substrates. MMP7 has been implicated in breast and prostate cancer-mediated osteolysis. Interestingly, changes in serum MMP7 levels are found to correlate with changes in obesity, suggesting possible cross-talk between these mechanisms.

The overall aim of my thesis was to investigate the role of MMP7 and/or adiposity in the development of myeloma and the associated bone disease. To achieve this, 3 distinct but related approaches were taken. The role of host-derived MMP7 in myeloma pathogenesis *in vivo* was determined using genetically modified mice deficient in MMP7. The role of adiposity in myeloma was investigated *in vivo* by firstly studying the effect of diet-induced obesity on myeloma development, and secondly by using a pharmacological approach to alter bone marrow adiposity.

In vivo, *in vitro*, and patient data suggest that MMP7 activity plays a protective role in myeloma pathogenesis and that host-derived MMP7 inhibits MM growth *in vivo*, in part via processing of galectin-3. *In vivo* studies demonstrated that diet-induced obesity created a permissive environment for the development of a myeloma-like disorder in otherwise non-permissive C57BL/6 mice, associated with increase tumour burden, decrease bone and increase IGF-1. Although targeting the host microenvironment by treatment with bisphenol A diglycidyl ether (BADGE) did not decrease adipocyte number as anticipated, a significant decrease in tumour burden and bone disease was observed. Direct anti-myeloma effects of BADGE *in vitro* were associated with an increase in phospho-AMPK and SIRT1 protein expression, via a SIRT1 independent mechanism.

Taken together, my studies have identified a direct anti-myeloma effect of BADGE and new mechanisms by which the host microenvironment contributes to myeloma growth, through changes in obesity or MMP7.

Abbreviations

ALP	alkaline phosphatase
AML	acute myeloid leukaemia
AMPK	AMP-activated protein kinase
ASCT	Autologous stem cell transplantation
BADGE	bisphenol A diglycidyl ether
BLI	bioluminescent imaging
BSA	bovine serum albumin
BM	bone marrow
BMI	body mass index
BMP	bone morphogenetic protein
BMSCs	bone marrow stromal cells
BSP	bone sialoprotein
BV/TV	bone volume/tissue volume
CAFs	carcinoma associated fibroblasts
cDNA	complementary DNA
CO_2	carbon dioxide
CRD	carbohydrate-recognition domain
CEBPα	CCAAT/enhancer-binding protein alpha
CFU-GM	colony-forming unit granulocyte/macrophage
DMEM	Dulbecco's Modified Eagle's medium
DAB	3’-3’-diaminobenzidine
DMSO	dimethyl sulphoxide
DNA	deoxyribonucleic acid
DPX	distyrene-plasticzer-xylene
DKK1	dickkopf-related protein1, Wnt-signalling antagonist

ECM	extracellular matrix
EDTA	ethylenediaminetetraacetic acid
ELISA	enzyme-linked immunosorbent assay
ER	estrogen receptor
FACS	fluorescence activated cell sorting
Fas-L	Fas-ligand
FBS	fetal bovine serum
GAPDH	glyceraldehyde-3-phosphate dehydrogenase
GFP	green fluorescence protein
H & E	haematoxylin and eoisin
H_20	water
H_20_2	hydrogen peroxide
HMW	high molecular weight
HRP	horseradish-peroxidase
HRpQCT	high-resolution peripheral quantitative computed tomography
hrs	hours
IGF-1	insulin-like growth factor-1
IgG	immunoglobulin G
IHC	immunohistochemistry
IP	intra-peritoneal
KO	knockout
M	molar
mg	milligram
M-CSF	macrophage-colony stimulating factor
MGUS	monoclonal gammopathy of undetermined significance
MIP-1α	macrophage inflammatory protein-1α
ml	millilitre

mm	millimetre
mM	millimolar
MM	multiple myeloma
MMPs	matrix metalloproteinases
MMP-7	matrix metalloproteinase-7
MMP-8	matrix metalloproteinase-8
MMP-9	matrix metalloproteinase-9
MRI	magnetic resonance imaging
mRNA	messenger RNA
ng	nanogram
nM	nanomolar
NFκB	nuclear factor kappa-light-chain-enhancer of activated B cells
NIK	NFκB-inducing kinase
OCN	osteocalcin
Obs	osteoblasts
OD	optical density
OPG	osteoprotegerin
PARP	poly (ADP-ribose) polymerase
PBS	phosphate buffered saline
PCR	polymerase chain reaction
PE	phycoerythrin
pg	picogram
PPARγ	peroxisome-proliferator activated receptor γ
RAG-2	recombinase-activating gene-2
RANKL	receptor activator of NFκB ligand
RNA	ribonucleic acid
RPMI 1640	Roswell Park Memorial Institute 1640

RT	room temperature
RT-PCR	reverse transcriptase-PCR
SDS	sodium dodecyl sulphate
SIRT1	Sirtuin 1
Spec	spectrophotometer
SCC	squamous cell carcinoma
SDF-1α	Stromal derived factor-1 α
TBS	tris-buffered saline
TE	tris-EDTA buffer
TNF-α	tumour necrosis factor-α
TNFR	TNF receptor
TRAP	tartrate-resistant acid phosphatase
UK	United Kingdom
UPR	unfolded protein response
USA	United States of America
µg	microgram
µl	microlitre
µm	micrometre
µM	micromolar
vBMD	volumetric bone mineral density
NT	Non-tumour
MM	multiple myeloma
VEGFα	vascular endothelial growth factor-α
WB	western blot
Wnt	Wingless-type

Chapter 1 : General Introduction

1.1 Multiple myeloma

1.1.1 Incidence rate

Multiple myeloma (MM) is a fatal haematological malignancy with a median survival of only four years. According to Cancer Research UK, myeloma is the 17th most common cancer in the UK (2010), with an annual incidence rate of 8 new cases/100,000 males and 7 new cases/100,000 females. The occurrence of myeloma correlates positively with age, with a high incidence above 50 years old, reaching peak rates (per 100,000) at over 85 years old (Figure 1.1).

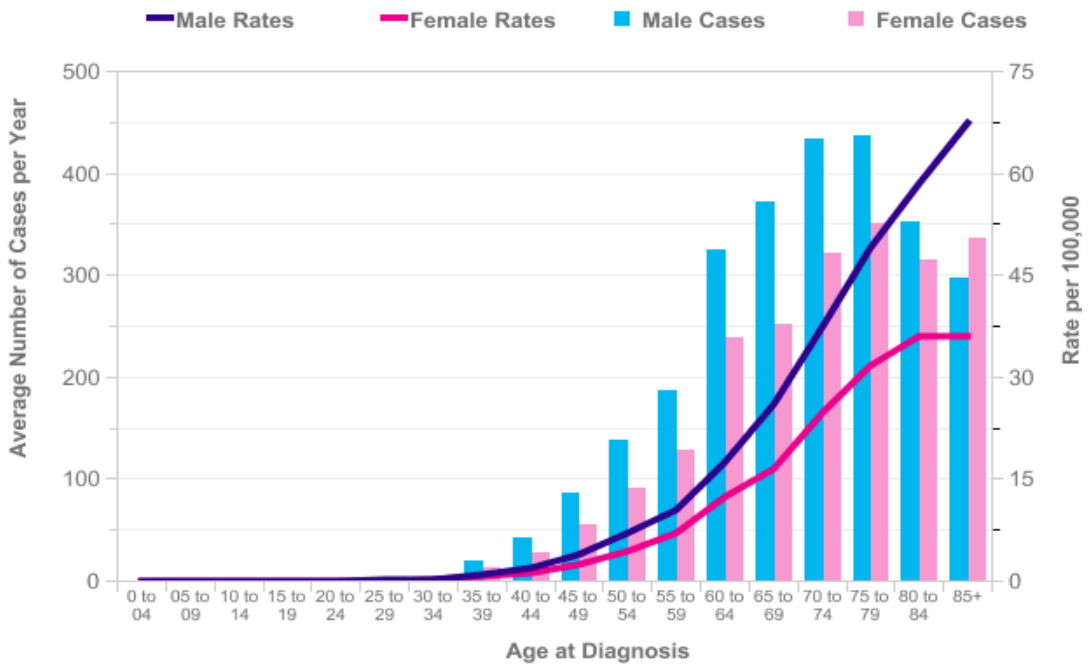

Figure 1.1. Average number of new cases per year and age-specific incidence rates per 100,000 population, UK, 2009-2011 (Cancer research UK, 2014).

Ethnicity appears to be important in myeloma development, as age-standardised average incidence rates are 6.3/100,000 for white males, 5/100,000 for Asian males, and 14.5/100,000 for black males, which is significantly higher. A similar trend was observed for females, with incidence rates of 3.9 to 4.2 for white females and 2.3 to 4.4 for asian females per 100,000, and significantly higher rates ranging from 6.6 to 11.5 per 100,000 for black females (Cancer research UK, 2014).

Myeloma is characterized as a clonal expansion of greater than 10% plasma cells in the bone marrow. Plasma cells are mature B cells that produce specific antibodies to fight against antigens under normal conditions. Development of plasma cells initiates in the bone marrow in the following order; haematopoietic stem cells, pro-B cell, pre-B cell, immature naive B cell, plasmablast, which then differentiate into plasma cells or memory B cells. B cell activation occurs when exposed to antigens, which induce their enlargement and proliferation, the process known as blasting to develop into a plasmablast. Plasmablasts secrete measurable amount of antibodies while proliferating, they then fully develop into antibody producing non-proliferated plasma cells (Figure 1.2) (Oracki et al., 2010). Therefore, clonotypic B cells are stem-cell like precursors for myeloma cells and perform as antigen presenting cells and develop into memory B cell upon activation by antigen (Szczepek et al., 1997). However, in a diseased condition such as myeloma, over production of malignant plasma cells in the bone marrow leads to insufficient production of other haematopoietic cells and abnormal antibody production. This results in anaemia and fatigue, and patients with myeloma are prone to infections as a result of failure to protect against pathogens by dysfunctional monoclonal antibodies produced by malignant plasma cells. A characterization study from myeloma patients has shown the presence of CD19-CD34+ as a potential marker of myeloma precursor cells (Conway et al., 2009).

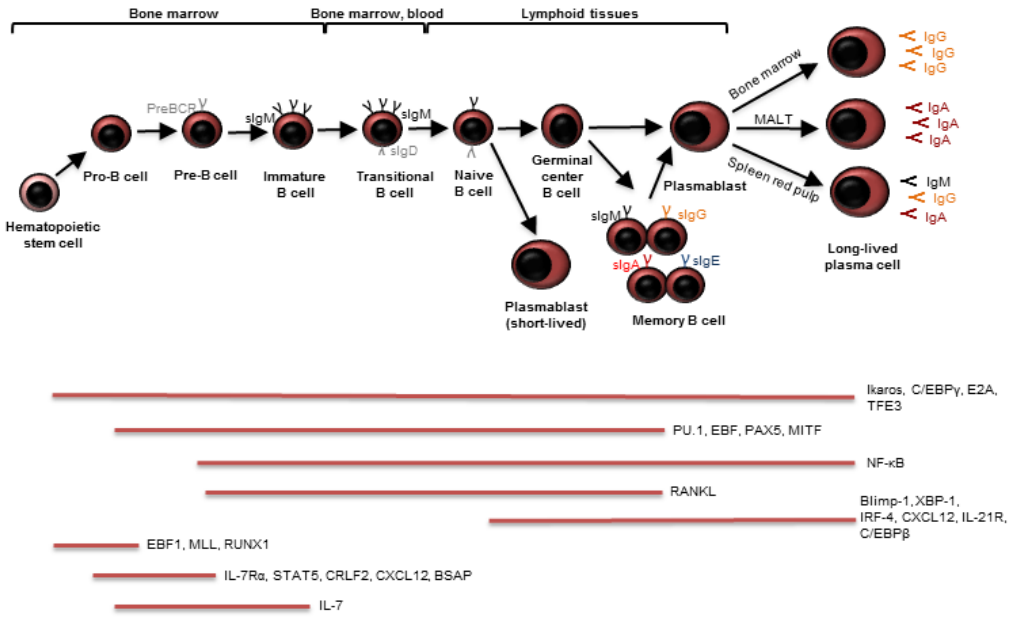

Figure 1.2. Schematic diagram of B cell development. B cells develop from hematopoietic stem cell in the bone marrow, leaves bone marrow as immature B cell, and mature in lymphoid tissues. The red lines below the diagram indicates some of the markers involved in B cell differentiation. Abbreviations: BCR (B cell receptor), sIg (soluble immunoglobulins), MALT (mucosal-associated lymphoid tissues), Ikaros (zinc finger transcription factor), C/EBP γ (CCAAT/enhancer binding protein γ), E2A (immunoglobulin enhancer binding factors E12/E47), TFE3 (transcription factor E3), PU.1 (transcriptor factor that binds to PU box), EBF (early B cell factor), PAX5 (Paired box 5), MITF (microphthalmia-associated transcription factor), NF-κB (nuclear factor kappa-light-chain-enhancer of activated B cells), RANKL (receptor activator of nuclear factor kappa-B ligand), Blimp-1 (B lymphocyte-induced maturation protein-1), XBP-1 (X-box binding protein 1), IRF-4 (Interferon regulatory factor 4), CXCL12, C-X-C motif chemokine 12, IL-21R (interleukin-21 receptor), C/EBPβ (CCAAT/enhancer binding protein β), MLL (Myeloid/lymphoid or Mixed lineage leukemia), RUNX1 (Runt-related transcription factor 1), IL-7 (interleukin 7), IL-7Rα (interleukin 7 receptor α), STAT5 (signal transducer and activator of transcription 5), CRLF2 (Cytokine receptor-like factor 2), BSAP (B-cell lineage specific activator protein (Glimcher and Singh, 1999;Tangye, 2011;Juárez-Velázquez et al., 2013;Manilay and Zouali, 2014).

Myeloma cells secrete high levels of monoclonal paraproteins into the blood stream, which are later excreted through the kidney, and contribute to the renal failure commonly seen in patients with myeloma. Myeloma bone disease is associated with an increase in osteoclastic bone resorption and a decrease in osteoblastic bone formation, thereby increasing overall bone loss (Edwards, Zhuang and Mundy, 2008). Patients

with myeloma suffer from osteolytic bone disease due to the uncoupling of the normal bone remodelling process. Overall bone loss leads to hypercalcaemia, pathological fractures, and bone pain. Despite new advances in drug development for the treatment of myeloma and the associated bone destruction, this disease remains fatal. My research is focused on investigating new mechanisms and factors involved in the progression of multiple myeloma and its destructive bone disease.

1.1.2 Stages and symptoms of myeloma

Staging of myeloma is important for assessing suitable and appropriate treatment options and prediction of patients' survival. The widely used Durie-Salmon staging system is based on the amount of abnormal monoclonal proteins in the serum or urine, blood calcium levels, bone disease, and blood haemoglobin (Fechtner et al., 2010). Durie-Salmon plus staging system was also introduced to incorporate new imaging techniques such as whole body magnetic resonance imaging (MRI) and whole body computerised tomography (CT) (Durie, 2006). Alternatively, the international staging system can be used, which is based on serum β-2 microglobulin and serum albumin levels (Hari et al., 2009). Generally, stages of myeloma can be divided into the precursor condition monoclonal gammopathy of undetermined significance (MGUS), smouldering myeloma and symptomatic myeloma. MGUS is characterised by having less than 30g/L of the serum monoclonal proteins, also known as M proteins, less than 10% clonal plasma cells in the bone marrow, and without organ or tissue damage related to myeloma (Leung et al., 2012). Patients with smouldering myeloma have more than 30g/L of the serum monoclonal proteins, and/or greater than 10% clonal plasma cells in the bone marrow by biopsy, and without organ or tissue damage related to myeloma. Symptomatic myeloma can be characterised by having greater than 30g/L of the monoclonal proteins in the serum or urine, and/or greater than 10% of the clonal

plasma cells in the bone marrow by biopsy or quantifiable amount of clonal plasma cells in other tissues by biopsy, and evidence of hypercalcemia, renal or kidney damage, anaemia, and osteolytic lesions (Graham-Rowe, 2011).

Myeloma patients may present with multiple osteolytic lesions, spinal cord compressions, and pathological fractures (Figure 1.3). Once the malignant plasma cells start growing in the bone marrow, they interact with different types of cells including osteoblasts, osteoclasts, and stromal cells, which are usurped to promote tumour cell expansion and myeloma associated bone disease (Mundy, 1998). Understanding the molecular mechanism of how myeloma cells interact with these cells within the host bone marrow microenvironment will help to identify a potential therapeutic target against myeloma.

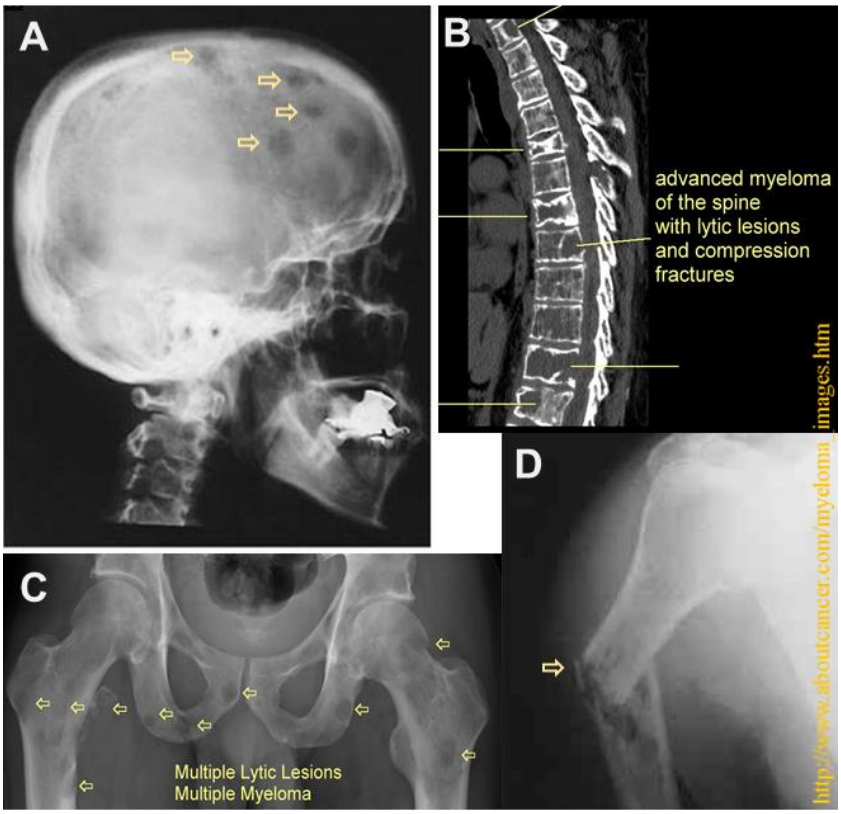

Figure 1.3. Radiographs showing osteolytic lesions and pathological fractures in myeloma patients. (A) Osteolytic lesions in skull, (B) spinal cord compression and fractures associated with myeloma pathogenesis (C) osteolytic lesions in pelvis and femurs, and (D) pathological fracture in the right humerus of a myeloma patient. Source: http://www.aboutcancer.com/myeloma_images.htm

1.2 Monoclonal Gammopathy of Undetermined Significance (MGUS)

Myeloma is known to develop from the benign precursor condition MGUS. MGUS is monoclonal protein without evidence of myeloma or macroglobulinemia (Kyle et al., 1972;Kyle, 1978). MGUS is known to affect 3% of people over the age of 50 and patients with MGUS have a 1% risk of developing myeloma yearly (Palladino, Bruno and Boccadoro, 2014). Like myeloma, MGUS affects African/black individuals twice as much as white population, whereas Asians are less affected by MGUS (Bianchi et al., 2010).

There are 3 established risk factors to assess the progression of MGUS to myeloma; quantifying the presence of non-IgG type M protein, the concentration of monoclonal protein, and the free light chain ratio (Bianchi et al., 2010). Once diagnosed, MGUS patients are advised to have yearly check-ups to monitor blood count, creatinine, calcium, and serum paraprotein level to detect symptoms of myeloma if it were to develop (Palladino, Bruno and Boccadoro, 2014). However, there is no evidence to suggest that early detection of MGUS and intervention prior to myeloma progression could improve prognosis or prolong survival. Bianchi et al. suggest individualized follow-up of patients with MGUS according to the level of risk for progression (Bianchi et al., 2010). The factors involved in the progression of MGUS to myeloma remain to be characterised. Hence, it is important to identify the differences in molecular or biological markers between MGUS that progress to myeloma, and MGUS that do not.

The Edwards lab has identified a decrease serum level of adiponectin in the MGUS patients who progress to myeloma as compared to the age, sex, BMI-matched MGUS patients who do not progress to myeloma (Fowler et al., 2011). A study conducted by Alvin et al. has shown that MGUS patients have increased serum level of DKK1 and MIP-1α, and a significantly decreased overall and trabecular volumetric bone mineral density (vBMD) as compared with the controls, measured by high-resolution peripheral quantitative computed tomography (HRpQCT) (Ng et al., 2011). Elevated serum DKK1 and MIP-1α levels are also known to be associated with myeloma bone disease.

1.3 Murine models of myeloma

Preclinical studies using murine models of myeloma play a crucial role in understanding the mechanisms involved in the progression of myeloma and ultimately finding potential therapeutic targets. Radl et al. identified that 0.5% of ageing

C57BL6/KaLwRij mice spontaneously develop myeloma, which recapitulates many features of human myeloma including the associated bone disease. Myeloma and associated osteolytic lesions can be induced in synergistic young C57BL6/KaLwRij mice by inoculation of freshly isolated bone marrow cells from older mice with myeloma, also known as the 5T Radl model or 5TMM murine model of myeloma bone disease (Radl et al., 1979). However, a limitation to this method is that the number of myeloma cells in the bone marrow may vary between animals.

From the 5T Radl murine myeloma model, a series of myeloma cell lines were established from different original donors, such as 5T2, 5T33, and 5TGM1. Inoculation of these cell lines into synergistic C57BL6/KaLwRij mice resulted in myeloma growth within the bone marrow, increased myeloma specific serum paraprotein, and osteolytic bone disease (Radl et al., 1988;Manning et al., 1992;Garrett et al., 1997). There is no known evidence in the literature indicating that C57BL6/KaLwRij mice or the 5T Radl model have any immune deficiencies.

Interestingly, 5TGM1 myeloma cells will only grow when inoculated intravenously into immune competent well-characterised 5T Radl murine model or C57BL6/KaLwRij mice, but not in closely related C57BL/6 mice. One of the limitations of the 5T Radl myeloma model is that it cannot be crossed with genetically modified murine models which makes it impossible to manipulate at a molecular level to understand the specific mechanisms involved in myeloma. Intriguingly, a recent study has shown that C57BL6/KaLwRij mice have a deficient mRNA and protein expression of the *Samsn1* gene (Noll et al., 2014).

The Edwards lab has previously shown that recombinase-activating gene-2 (RAG-2) immunodeficient mice on a C57BL/6 background are permissive for 5T myeloma

growth (Fowler et al., 2009). B and T lymphocytes recognise antigens through variable domains of immunoglobulin or T cell receptor respectively. During the early stages of B and T lymphocyte differentiation, those variable domains are constructed together from germline variable (V), diversity (D), and joining (J) gene segments by a V(D)J recombination process. RAG-2 is critical for V(D)J recombination, and RAG-2 defieient mice are unable to initiate V(D)J rearrangement and lack mature B and T cells (Shinkai et al., 1992). RAG-2 knockout mice create a myeloma permissive environment, as the inoculation of GFP tagged 5TGM1 myeloma cells resulted in the same features of myeloma seen in the well-established 5T Radl model (Figure 1.4). The RAG-2 model can be crossed with genetically modified mice to allow for the manipulation of the host microenvironment at a molecular level. Tumour burden in this model was assessed by measuring the serum concentration of myeloma paraprotein IgG2bκ using ELISA, and by quantitating the percentage of GFP positive myeloma cells in the bone marrow using flow cytometry analysis. Myeloma bone disease was measured by μCT analysis and histology.

In the present study, C57BL/6, C57BL6/KaLwRij, and RAG-$2^{-/-}$ mice were used. Also, RAG-$2^{-/-}$ mice were crossed with MMP$7^{-/-}$ mice to generate RAG-$2^{-/-}$;MMP$7^{-/-}$ (MMP$7^{-/-}$) or RAG-$2^{-/-}$;MMP$7^{+/+}$ (WT) mice to manipulate the host microenvironment at a molecular level.

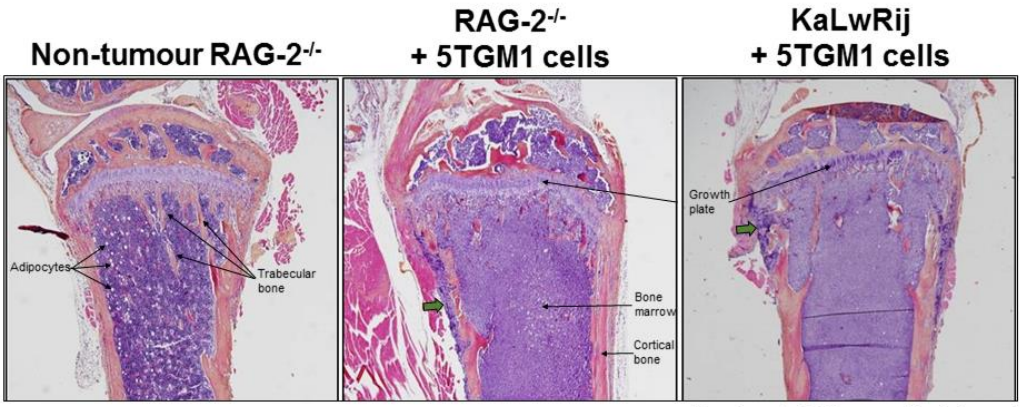

Figure 1.4. Development of myeloma in the bone marrow of RAG2$^{-/-}$ and KaLwRij mice. Hematoxylin and eosin staining showing the comparison of bone marrow sections in non-tumour RAG2-/-, myeloma-bearing RAG2-/- and KaLwRij mice. Similar pathology of myeloma cell growth within the bone marrow cavity, and osteolytic lesions through the cortical bone (green arrows) was observed in myeloma-bearing RAG2-/- mice and the well-established 5T Radl KaLwRij murine model of myeloma.

Alternatively, myeloma development can be induced in mice with genetically determined severe combined immunodeficiency (SCID) (also known as SCID-hu/rab model), which are deficient in both B and T cells. Hence, primary human myeloma cells colonizing either fetal human or rabbit bone are implanted subcutaneously into SCID mice (Yaccoby, Barlogie and Epstein, 1998). These immune-compromised mice are useful tools to accept foreign human myeloma cells, but would not be useful in revealing components of the normal host microenvironment, which may support the initial pathogenesis of the disease.

Similarly, Fryer et al. have shown that the acute myeloid leukaemia model NOD/SCIDγcnull mice develops myeloma that mimicked the clinical features of human myeloma when inoculated intra-tibially with luciferase tagged U266 human myeloma cells or primary human plasma cells (Fryer et al., 2013). In this model, myeloma development was assessed weekly by bioluminescent imaging (BLI), measurement of paraprotein levels by ELISA, magnetic resonance imaging (MRI), and histology at end

point. In this study, myeloma development began between 5 and 7 weeks after inoculation and the mice were reported to be paraplegic between week 8 and 9 after inoculation with myeloma cells. The IP injection of these NOD/SCIDγcnull mice with currently used anti-myeloma therapies such as bortezomib and an aminopeptidase inhibitor, tosedostat, resulted in the decrease in myeloma tumour burden.

Carrasco et al. have explored the genetics of myeloma pathogenesis by using a transgenic mouse model named Eμ-XBP-1s. XBP-1 is a transcription factor involved in the differentiation of plasma cells. Inactive unspliced XBP-1 can be modified into active spliced XBP-1 (XBP-1s) by removal of a 26-nucleotide intron by activated inositol-requiring enzyme 1 α (IRE1α) endoribonuclease (Yoshida et al., 2001). A XBP-1 spliced isoform is responsible for the unfolded protein or endoplasmic reticulum stress response. Overexpression of spliced XBP-1 is one of the features seen in human myeloma patients. These researchers reported that Eμ-XBP-1s transgenic mice has an MGUS phenotype and some of these ageing mice developed myeloma with similar features to the human disease, such as elevated serum paraprotein and osteolytic lesions (Carrasco et al., 2007).

1.4 Interactions between cells of the host microenvironment

The "seed and soil theory" of Dr. Stephen Paget from 1889 first described the mutual relationship between breast cancer cells (the seeds) and the host microenvironment (the soil) for further promotion of cancer growth. Attachment of myeloma cells in the stroma of the host microenvironment can activate different biological pathways involved in promoting cancer cell growth, adhesion, migration, invasion, blood vessel growth, and the breakdown of bone (Hughes, 2011). Unfortunately, bone is a favourable site for tumour growth and survival.

1.4.1 The cells of the bone marrow microenvironment

Osteoclasts

Osteoclasts are highly motile, large multinucleated bone resorbing cells, which can contain up to 10 to 20 nuclei per cell (Galson and Roodman, 2011). Osteoclasts are derived from myeloid progenitors committed to the monocyte/macrophage lineage and form by fusion of mononuclear precursors (Galson and Roodman, 2011). Osteoclasts play a major role in the bone remodelling process. The resorptive function of osteoclasts is responsible for the removal of old or abnormal bone that becomes weakened by age or mechanical stress.

Osteoclasts express H^+ and Cl^- ions to acidify the sealed resorption lacunae and dissolve inorganic bone components, but also to activate proteases such as cathepsin K (CatK) and matrix metalloproteinase 9 (MMP9) to degrade organic bone matrix. Decreased CatK enzymatic activity in patients with pycnodysostosis results in defective bone remodelling, poor bone structure and hypomineralization. CatK deficient mice have mild osteopetrosis with a high osteoclast number, but impaired osteoclast function (Kiviranta et al., 2005;Pennypacker et al., 2009). MMP9 expressed by osteoclasts plays a major role in the induction of osteoclast migration and angiogenesis (Cackowski et al., 2010). MMP9 deficient mice showed a delay in endochondral ossification, vessel invasion, and healing of long bone fractures (Vu et al., 1998). Tartrate-resistant acid phosphatase (TRAP) is used to identify osteoclasts. TRAP appears early during osteoclast differentiation, just prior to fusion of mononuclear precursors into mutinucleated cells, and continues to increase as the osteoclast matures.

Osteoclast differentiation begins from haematopoietic stem cells which commit to progenitor precursors known as colony-forming unit granulocyte/macrophage

population (CFU-GM) (Figure 1.5). Macrophage-colony stimulating factor (M-CSF), encoded by *Csf1* gene, induces differentiation of macrophages and mutation of the *Csf1* gene leads to a severe osteopetrosis in murine models, indicating the important role of M-CSF in osteoclastogenesis (Galson and Roodman, 2011). M-CSF directs CFU-GM cells toward the formation of mononuclear precursor cells through the binding of the M-CSF receptor, c-fms, which upregulates the expression of receptor activator of NFκB (RANK)(Crockett et al., 2011).

RANK ligand (RANKL) is expressed by cells of the bone microenvironment including osteoblasts and fibroblasts. The binding of RANKL to the receptor RANK on osteoclast precursor cells leads to the formation of osteoclasts from myeloid progenitors and bone resorption in mature osteoclasts. OPG is a soluble decoy receptor that binds to RANKL and blocks the interaction between RANKL and RANK, thereby inhibiting osteoclastic bone resorption. OPG is secreted by osteoblasts and bone marrow stromal cells. The loss of RANK or RANKL leads to high bone mass and mice deficient in OPG have a severe low bone mass phenotype (Mizuno et al., 1998;Li et al., 2000). The crucial role of the RANK/RANKL/OPG system, TNF and TNF receptor superfamily members, in osteoclast formation and activity has been well documented (Anderson et al., 1997;Lacey et al., 1998).

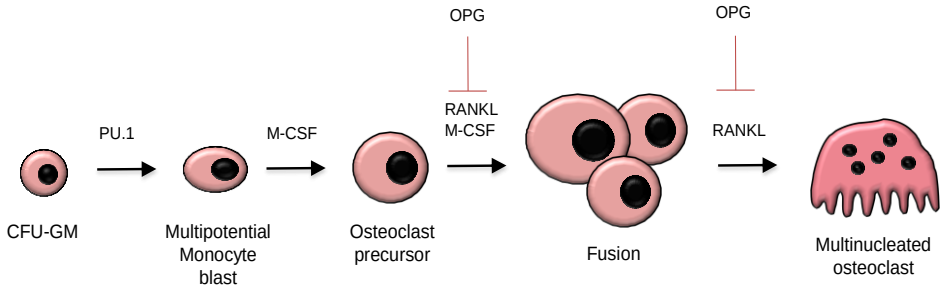

Figure 1.5. Schematic of osteoclastogenesis. Differentiation of osteoclast from CFU-GM to multinucleated osteoclast with key markers involved in osteoclastogeneisis**.**

Osteoblasts

Osteoblasts are single nucleated bone-forming cells that lay down organic matrix during skeletal development and after unwanted bone is resorbed by osteoclasts. They are descended from mesenchymal precursor cells which can also be stimulated to form a number of other cells including myocytes, adipocytes and chondrocytes (Figure 1.6) (Ducy, Schinke and Karsenty, 2000). Bone formation involves multiple steps including osteoblast differentiation and proliferation, matrix deposition, matrix maturation, and mineralization. Runx2 is a master regulator of osteoblast differentiation, and can further regulate the expression of osteoblastogenic markers; alkaline phosphatase (ALP), type I collagen (Col1), bone sialoprotein (BSP), osteopontin (OPN), and osteocalcin (OCN). ALP is considered an early marker and OCN a late marker of osteoblast differentiation (Krause et al., 2009).

Runx2 regulates the transition of mesechymal cells to osteoprogenitors, and governs the functions of bone forming cells by maintaining the mature osteoblast phenotype (Martin, Sims and Quinn, 2011). Mice deficient in Runx2 die at birth due to a complete failure to form osteoblasts and consequently, impaired skeletal mineralization

(Karsenty, 2001). ALP is found within the mineralized matrix and ALP knock out mice have impaired mineralization (Anderson et al., 2004). ALP hydrolyzes inhibitors of mineral deposition such as pyrophosphates and increases local phosphate concentration. Type I collagen (ColI) is the building block of the bone matrix fiber network and it binds and accomodates other proteins that nucleate hydroxyapatite deposition. Mutations in *ColI* may lead to osteogenesis imperfecta (Boskey and Robey, 2013). The expression of BSP is upregulated during mineralization in culture and BSP knock out mice have impaired osteoblast and osteoclast function, suggesting that it may also regulate bone remodelling (Wade-Gueye et al., 2010;Gordon et al., 2007). Both BSP and OPN help anchor osteoclasts to bone, and support cell attachment. In addition, OPN binds to cells and collagen, regulates cell proliferation, and osteoblastic maturation (Boskey and Robey, 2013). Serum OCN could be used as a marker of bone turn over in metabolic diseases (Pagani, Francucci and Moro, 2005). OCN knock out mice have increased bone mineral density (BMD) as compared to wild type mice (Ducy et al., 1996).

Furthermore, the Wingless-type (Wnt) signalling pathway is known to regulate bone formation and mutations that inactivate the Wnt co-receptor LDL receptor-related protein-5 (LRP5) resulted in osteoporosis, suggesting that LRP5 mediated Wnt signalling is important in proper bone growth and establishment of peak bone mass (Gong et al., 2001). On the other hand, mutations of 'gain of function' in LRP5 resulted in a syndrome of hereditary high bone density (Boyden et al., 2002).

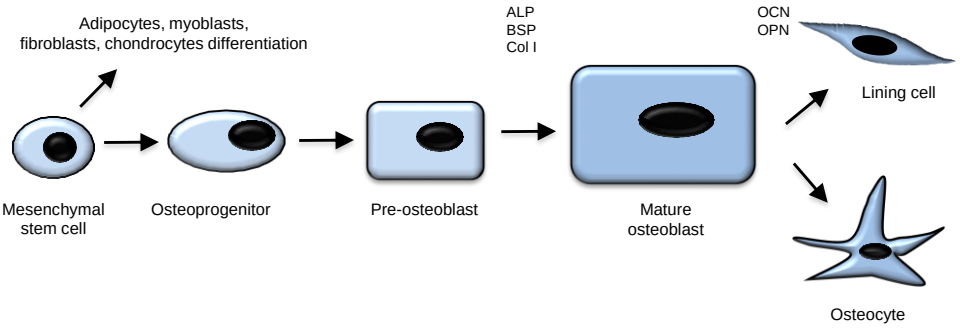

Figure 1.6. Schematic of osteoblast differentiation. Osteoblast lineage from mesenchymal stem cell to mature osteoblast and osteocyte with key markers involved in osteoblastogeneisis.

Adipocytes

Bone marrow adipocytes are fat cells that take up abundant space in the bone marrow and their function includes lipid metabolism, energy storage, and support (Gimble et al., 1996a). Adipocytes derive from the same precursor mesenchymal cells as osteoblasts, myocytes, and chondrocytes. Increased bone marrow adipogenesis on ageing is related to reduction in bone mass and osteoblastogenesis (Meunier et al., 1971). Bone marrow fat and bone mineral density are inversely related, where increasing marrow adipocytes leads to decreasing bone mineral density. As a result, an increase in bone marrow adiposity is also associated with age-related osteoporosis (Nuttall and Gimble, 2004). Adiponectin is an adipokine produced by adipocytes and was shown to increase proliferation of hematopoietic stem cells (DiMascio et al., 2007).

Adipogenesis is regulated by transcription factors peroxisome proliferator-activated receptors (PPAR) α, δ, and γ, CAAT/enhancer binding proteins (C/EBP) α, β, and δ (Gimble et al., 1996b). The ligands of PPARγ and PPARδ such as thiazolidinediones, commonly used as anti-diabetic drugs, have been shown to increase insulin sensitivity,

increase adiposity, reduce bone mass, and increase fracture risk (Habib et al., 2010). Furthermore, pharmacological doses of fibroblast growth factor 21 (FGF21) was shown to suppport the differentiation of adipocytes instead of osteoblasts, thereby, reducing overall bone mass in mice (Wei et al., 2012).

Interestingly, an increase in bone marrow adiposity was observed after the loss of bone mineral density, followed by calorie restriction (Devlin et al., 2010). This was probably due to decreased concentrations of leptin, estrogen, and insulin-like growth factor-1 (IGF-1), and FGF21, followed by calorie restriction. Furthermore, a recent study has shown that calorie restriction induced an increase in adiponectin secretion by bone marrow adipose tissue, and mice with impaired bone marrow adipose tissue expansion resulted in decreased adiponectin level and altered the skeletal muscle adaptation to calorie restriction, suggesting bone marrow adipose tissue as an endocrine organ. (Cawthorn et al., 2014).

Bone marrow stromal cells

Bone marrow stromal cells (BMSCs) can be precursors of various cell types and can be differentiated into bone cells, adipocytes, myoblasts, and neural cells (Prockop, 1997;Sanchez-Ramos et al., 2000). Interactions between BMSCs and cancer cells have been shown to promote the growth of various cancers including myeloma (Saad et al., 2000;Scott et al., 2001;Fowler et al., 2012). Upon adhesion of cancer cells to BMSCs, there is an up-regulation of multiple growth factors and cell cycle regulating proteins including IL-6, VEGF, IGF-1, and RANKL (Mancino et al., 2001;Manier et al., 2012).

RANKL, M-CSF, IL-11, and VEGF, IL-6 are osteoclast-activating factors produced by BMSCs (Silbermann and Roodman, 2013). These factors not only increase osteoclastogenesis, but also are growth factors for tumourigenesis. BMSCs also produce DKK1, an osteoblast inhibiting factor. The Edwards lab has shown that co-inoculation

of BMSCs from myeloma-permissive mice and myeloma cells created a permissive myeloma environment in otherwise non-permissive mice (Fowler et al., 2012). Similarly, subcutaneous injection of the mixture of carcinoma associated fibroblasts (CAFs) derived from bone marrow mesenchymal precursor cells, and breast cancer cells increased metastasis to lung and mammary gland (Karnoub et al., 2007). Furthermore, glucose-regualted protein 78 (GRP78), an endoplasmic recticulum chaperone, secreted by colon cancer cell lines induced differentiation of human and murine BMSCs to CAFs (Li, Peng and Li, 2013). These studies highlight the mutual relationship between cancer cells and BMSCs.

Osteocytes

Osteocytes are the most abundant of all bone cells (90-95%) in the adult skeleton, compared to approximately 4-6% osteoblasts and 1-2% osteoclasts (Bonewald, 2013). They connect to each other and cells on the bone surface through dendritic processes that disperse towards the bone surface, bone marrow, and blood supply. Osteocytes take part in sending signals of bone formation or resorption in response to mechanical strain (Bonewald, 2013). Osteocyte-like cell line MLO-Y4 regulates bone remodelling by induction of osteoclast formation and osteoblast differentiation (Heino, Hentunen and Kalervo Vnnen, 2002). Osteocytes may regulate bone-remodelling process through their own apoptosis as a result of microdamage. The damaged osteocytes are thereby cleaned up by osteoclasts (Verborgt et al., 2002). Disease conditions that lead to skeletal fragility such as osteoporosis and osteoarthritis are associated with the death of osteocytes (Weinstein, Nicholas and Manolagas, 2000). Skeletal fragility is induced by the inability to sense and/or repair the microdamage. Estrogen deficiency could induce osteocyte apoptosis, whereas exercise could preserve the viability of osteocyte and bone strength following ovariectomy (Fonseca et al., 2011). Blocking sclerostin, a selective

marker of osteocytes, by neutralising antibody was shown to increase or maintain the bone mass (Paszty, Turner and Robinson, 2010). Sclerostin inhibits the Wnt-signalling pathway, an important mediator of bone remodelling (Li et al., 2005). Mechanical loading was shown to have bone anabolic effects and oscillatory fluid flow decreased mRNA and protein expression of sclerostin in mature osteoblasts (Papanicolaou et al., 2009). Furthermore, an increase in sclerostin expression was observed following mechanical unloading and inhibition of sclerostin by neutralsing antibody decreased skeletal deterioration caused by the reduction of mechanical loading (Spatz et al., 2013).

1.4.2 Cross-talk between tumour cells and host microenvironment

To fully elucidate the role of the host microenvironment in myeloma development, a better understanding of the interaction between myeloma cells and the surrounding bone marrow stromal cells, osteoclasts, osteoblasts and other cell types is required. Interestingly, myeloma cells are often located in close proximity to sites of active bone resorption (Mundy et al., 1974). As described previously, myeloma cells secrete osteoclastogenic factors, which in turn gives rise to the production of pro-myeloma growth factors within the microenvironment. This reciprocal relationship between myeloma cells and osteoclasts contributes to an increase in the secretion of pro-angiogenic factors and vascular tubule formation (Tanaka et al., 2007). An increase in angiogenesis and tumour growth factors is a common feature of cancer progression and metastasis.

Co-culture or direct contact of myeloma cells and bone marrow stromal cells (BMSCs) increase myeloma cell proliferation, migration, and survival via the NFκB pathway (Michigami et al., 2000). In addition, this interaction up-regulated known

osteoclastogenic factors interleukin-6 (IL-6) and RANKL, and decreased osteoprotegerin (OPG) secretion by BMSCs, thereby disrupting balance of the system, resulting in overall bone loss (Shipman and Croucher, 2003;Giuliani et al., 2001). Abe et al. found that inhibition of cellular contact between myeloma cells and osteoclasts hindered myeloma growth and survival induced by osteoclast activation, which highlights the crucial role of direct contact between myeloma cells and osteoclasts (Abe et al., 2004).

Increased osteoclastic activity was mediated via the interaction between alpha4-beta1 integrin and vascular cell adhesion molecule 1 (VCAM-1), and treatment with a monoclonal antibody to alpha4 integrin inhibited myeloma development and the associated osteolysis in the 5TGM1 murine model of myeloma (Michigami et al., 2000;Mori et al., 2004). The study conducted by Fowler et al has shown that co-inoculation of myeloma cells with BMSCs isolated from myeloma permissive C57BL6/KaLwRij mice, resulted in the development of myeloma and osteolytic bone disease in otherwise non-permissive C57BL/6 mice (Fowler et al., 2012). The same study has shown that inoculation of those BMSCs from myeloma-permissive mice with high expression of DKK1, an inhibitor Wnt signalling pathway, resulted in suppression of osteoblasts in non-permissive mice. DKK1 level is known to be elevated in patients with myeloma and MGUS (Corre et al., 2007;Ng et al., 2011). This study further confirms the critical role of BMSCs in myeloma and the associated bone destruction.

1.4.3 Matrix metalloproteinases (MMPs) in matrix environment

Matrix metalloproteinases are enzymes that can degrade the extracellular matrix. MMPs are zinc-dependent endopeptidases, which exist as a latent or inactive zymogen form, and can be activated by various mechanisms. The MMP pro-enzymes include an amino-

terminal pro-domain about 80 amino acids long, a zinc-and calcium binding catalytic domain of about 170 amino acids, and a linker peptide or hinge region and a hemopexin-like carboxy-terminal domain of 200 amino acids (Figure 1.7) (Nagase et al, 2006). MMP7 (Figure 1.8), MMP26 and MMP23 do not have the linker peptide and hemopexin domain. MMPs can be divided into collagenases (MMP 1, 8, and 13), gelatinases (MMP 2 and 9), stromelysins (MMP 3, 10, and 11), matrilysins (MMP 7 and 26), enamelysin (MMP 20), metalloelastase (MMP 12), membrane-type MMPs (MMP 14, 15, 16, 17, 24, and 25), and other MMPs (MMP 19, 21, 23A, 23B, 27, and 28) (Nagase, Visse and Murphy, 2006).

The functions of MMPs go beyond their proteolytic activity. MMP12 deficient mice display an ineffective anti-bacterial effect in murine macrophages, and the adhesion of MMP12 to the bacterial cell wall disrupts the cell membrane, which leads to bacterial death (Houghton et al., 2009). Interestingly, Gonzalo et al. showed the important role of MT1-MMP (MMP14) in osteoclast formation via macrophage fusion, both *in vitro* and *in vivo*, through Rac1 signalling independent of its catalytic activity. Rac1 is a small GTPase that regulates cell motility (Gonzalo et al., 2010). These studies expand our knowledge of MMPs outside their ability for proteolytic cleavage.

MMPs can activate one another, for example MMP14 can activate MMP2 and MMP13 (Nagase et al., 2006). Active MMPs can cleave multiple substrates and alter their activities in various physiological processes. MMPs have been shown to regulate the tumour microenvironment and the progression of various cancers, including prostate, breast, and liver cancer (Lynch et al., 2005;Takafuji et al., 2007;Thiolloy et al., 2009). The function of MMPs is dependent on the balance between the protein expression/activity and the availability of endogenous MMP inhibitors, where tissue inhibitors of matrix metalloproteinases (TIMPs) negatively regulate the function of

MMPs (Bramhall et al., 1997). TIMPs have an N-terminal and C-terminal domains with 184-194 amino acids in length and are divided into TIMP 1, 2, 3, and 4. TIMPs inhibit activity of MMPs by blocking the active site (Nagase et al., 2006).

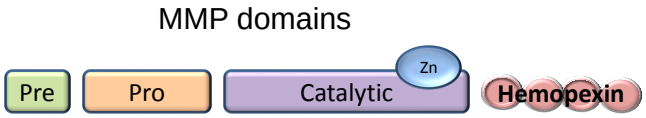

Figure 1.7. Schematic of MMP structure

1.4.4 Matrix Metalloproteinase 7 (MMP7)

My studies focused on the role of MMP7, also known as matrilysin, in the progression of myeloma and the associated bone destruction. MMP7 is produced by epithelial cells osteoclasts, macrophages and stromal cells of the bone marrow microenvironment, and plays a role in a number of biological processes including tissue remodelling and wound healing (Lynch et al., 2005;Nagase, Visse and Murphy, 2006). Biological effects caused by the cleavage of its substrates by MMP7 are summarised in Table 1.1 (Nagase et al., 2006).

More importantly, MMP7 also plays a role in tumour-induced bone disease, and is involved in prostate and breast cancer-induced osteolysis. Interestingly, both osteolytic and osteoblastic metastases are notable forms of bone metastatsis in prostate and breast cancer, whereas myeloma is exclusively associated with osteolytic bone destruction (Yin, Pollock and Kelly, 2005). MMP7 knockout mice have decreased osteolytic bone disease in the presence of prostate cancer cells, possibly mediated by the processing of

soluble RANKL, and suggesting that MMP7 may promote tumour induced bone disease (Lynch et al., 2005). Also, MMP7 deficient mice have reduced osteolytic lesions and increased trabecular bone volume compared to WT control, following intra-tibial inoculation with breast cancer cells (Thiolloy et al., 2009). Based on these studies, we hypothesized that MMP7 may play a role in the development and progression of myeloma and the associated bone disease.

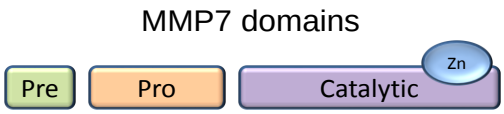

Figure 1.8. Structure of MMP7

Table 1.1 Substrates of MMP7

Substrates	Function
E-cadherin	Epithelial repair, wound healing, cell-cell adhesion, signal transduction, invasion promoter, increased circulating soluble E-cadherin in myeloma patients (Syrigos et al., 2004;Fingleton et al., 2010;Armstrong et al., 2011).
β4 Integrin (CD104)	Hemidesmosome formation, cell adhesion and survival (Von Bredow et al., 1997;Dowling, Yu and Fuchs, 1996).
Tumour necrosis factor-α (TNFα)	Increases cell death by apoptosis, the hearts of MMP7-/- mice have decreased TNFα release after ischemia, TNF receptor-1 (TNFR1) tends to be more pro-apoptotic than TNF receptor-2 (TNFR2) (Gearing et al., 1994;Kast, 2005;Reil et al., 2007).
FasL	Cell apoptosis, MMP7-/- mice have a reduction in the apoptotic index in the involuting prostate compared with WT (Crawford et al., 2002;Powell et al., 1999).
Epidermal Growth Factor (EGF)	Stimulates cell growth, proliferation, and differentiation by binding to its receptor EGFR. EGFR inhibition blocks MM cell growth factor activity of HB-EGF (Rude Voldborg et al., 1997;Mahtouk et al., 2004).
Fibronectin (FN)	Influences cell adhesion, growth, migration, differentiation, attachment, wound healing, embryonic development, signal transduction, reduced level in myeloma patients with high-level plasmacytosis, and high plasma FN in myeloma patients (Clark et al., 1985;Paizi et al., 1991;Habeck, 2000;Kraft et al., 2001).
Receptor Activator of Nuclear κB Ligand (RANKL)	Mediates osteoclast activation, highly expressed in MM patients (Sezer et al., 2002;Boyle, Simonet and Lacey, 2003;Sezer et al., 2003;Lynch et al., 2005).
Osteopontin (OPN)	Wound healing, inflammation, cell adhesion and migratory stimulus *in vitro* through cell surface integrins, secreted high levels in numerous cancers (Agnihotri et al., 2001;Caers et al., 2006;Robbiani et al., 2007).
N-cadherin	Mediates the interaction of myeloma cells with the bone marrow microenvironment, in particular the osteoblasts. Cell adhesion, cell motility, metastasis, neurite outgrowth, embryonic development, early heart development and other morphogenetic processes (Williams et al., 2010;Groen et al., 2011;Jones et al., 2002;Derycke and Bracke, 2004).
Collagen Type 4	Plays a role in glomerular development and function, found in basement membranes and basal lamina structures and functions as filtration system (Harvey et al., 1998;Kraft et al., 2001).
Laminin-1	Epithelial development, morphogenesis, acts as attachment protein, cell survival *in vitro*, overexpression increases tumour growth, induce migration of myeloma cells (Faisal Khan et al., 2002;Vande Broek et al., 2001).
Elastin	Provides elasticity and resilience to many vertebrate tissues and organs, deficiency causes acquired cutis laxa (Abramson et al., 1995;Filippov et al., 2003;Morava et al., 2009).
Versican	Cell adhesion, migration, and proliferation. Expressed in various tumours. Often considered an anti-adhesive molecule, because of its large structure, it could hinder integrin interaction with cells (Yamagata and Kimata, 1994;Halpert et al., 1996;Ricciardelli et al., 2009).
Tenascin	ECM glycoproteins, abundant in the ECM of developing vertebrate embryos, reappear around healing wounds and in the stroma of some tumours (Oyama et al., 1991;Saarialho-Kere et al., 1999).
Plasminogen	MMP7 hydrolysis to generate angiostatin which is one of the most potent inhibitors of angiogenesis (Patterson and Sang, 1997;Rajkumar et al., 2000).

Substrates	**Function**
Fibrinogen	The plasma protein that serves as the precursor for the fibrin network formed during the clotting of blood (Bini et al., 1999;Ariëns, 2013).
Collagen Type 18	Component of the basement membrane of blood vessels and epithelial cells in various organs of the body, important role in retinal structure and in neural tube closure (Sertié et al., 2000;Lin et al., 2001).
Carboxylated Transferrin	Frequently used to measure enzyme activities (Yu et al., 2012).
Cryptdins/defensins	Plays important role in intestinal mucosal defense by regulating the activity of defensins (Wilson et al., 1999;Droin et al., 2009).
Tissue Factor Pathway Inhibitor-1	Effect coagulation mediated by tissue factor (Belaaouaj et al., 2000).
MMP-1	Important in rheumatoid and osteo-arthritis. Expression can be induced by myeloma cells (Abramson et al., 1995;Barillé et al., 1997;Nagase, Visse and Murphy, 2006).
MMP-2	Role in normal tissue remodelling events such as embryonic development, angiogenesis, ovulation, mammary gland involution and wound healing. MMP2 is also involved in osteoblastic bone formation and/or inhibits osteoclastic bone resorption. Activation of MMP2 favors the spread of myeloma (Barillé et al., 1999;Thiolloy et al., 2012).
MMP-8	Human myeloma cells express it and probably plays a role in proliferation and invasion (Balbín et al., 1998;Van Valckenborgh et al., 2004).
MMP-9	Promote myeloma, $MMP9^{-/-}$ mice have reduced myeloma tumour burden (Von Bredow et al., 1998;Fowler et al., 2009).
ADAM28	Plays a role in the adhesive and proteolytic events that occur during lymphocyte emigration or function in ectodomain shedding of lymphocyte surface target proteins, such as FASL and CD40L. Sperm maturation. Activate IGFBP3, overexpressed in non small cell lung carcinoma and breast carcinoma. Enhancing bioavailability of insulin growth factor-1 released from the complex insulin-like growth factor binding protein-3/insulin growth factor-1 (Mochizuki et al., 2004;Ohtsuka et al., 2006).
Insulin-like growth factor-binding protein 1 (IGFBP1)	Binding of this protein prolongs the half-life of the IGFs and alters their interaction with cell surface receptors (Nakamura et al., 2005).
Insulin-like growth factor-binding protein 2 (IGFBP2)	Inhibit the mitogenic action of IGF-I on osteoblasts (Nakamura et al., 2005;Govoni, 2012).
Insulin-like growth factor-binding protein 3 (IGFBP3)	Enhance osteoblast proliferation in response to IGF-I (Nakamura et al., 2005;Govoni, 2012).
Insulin-like growth factor-binding protein 4 (IGFBP4)	Expressed by human MM cell ARH-77, inhibit the mitogenic action of IGF-I on osteoblasts, indirectly decrease bone formation (Feliers, Woodruff and Abboud, 1999;Nakamura et al., 2005;Govoni, 2012).
Insulin-like growth factor-binding protein 5 (IGFBP5)	Enhance osteoblast proliferation in response to IGF-I, decreased level in aging with bone loss (Nakamura et al., 2005;Govoni, 2012).
Insulin-like growth factor-binding protein 6 (IGFBP6)	Expressed by human MM cell ARH-77 (less than IGFBP4), may inhibit the mitogenic effect of IGF-II on osteoblasts (Nakamura et al., 2005;Yan et al., 2001).
Heprin Binding Epidermal Growth Factor (HB-EGF)	Promotes cellular proliferation, overexpressed in myeloma cell lines (Yu et al., 2002;Yue et al., 2002).
Syndecan-1	HB-EGF coreceptor, plasma cell differentiation, marker of myeloma cells (Aref, Goda and El-Sherbiny, 2003;Chen et al., 2009).
Decorin	Binds TGF-β, releases TGF-β upon MMP7 cleavage (Imai et al., 1997).
Galectin-3	Expressed by myeloma cells, inhibition increased myeloma cell apoptosis, and increased serum levels observed in patients with various cancers (Iurisci et al., 2000;Streetly et al., 2010;Puthenedam et al., 2011;Mirandola et al., 2011).

1.4.5 TIMP1, an inhibitor of MMP7

As described previously, tissue inhibitor of matrix metalloproteinases (TIMPs) regulate the functions of MMPs. TIMP1 has been shown to be an inhibitor of MMP7 and importantly, high serum levels of TIMP1 are positively correlated with advanced stages of myeloma and poor prognosis in patients with myeloma (Watelet et al., 2004;Terpos et al., 2010). Furthermore, TIMP1 is shown to decrease apoptosis induced by serum starvation in mouse bone marrow stromal cells (BMSCs) by decreasing caspase-3 activation (Guo et al., 2006). Treatment with physiological concentrations of TIMP1 directly increased the bone resorptive activity of mature osteoclasts isolated from rabbit (Sobue et al., 2001).

1.4.6 Factors involved in enhanced osteoclastic bone resorption in myeloma

Myeloma bone disease is associated with uncoupled bone remodelling with an increase in bone resorption and a decrease in bone formation, which results in the overall bone loss in patients with myeloma (Figure 1.9). Increased osteoclastic bone resorption is partly due to changes in RANKL, OPG, macrophage inflammatory protein-1α (MIP-1α), IL-6 and tumour necrosis factor (TNF) (Edwards, Zhuang and Mundy, 2008).

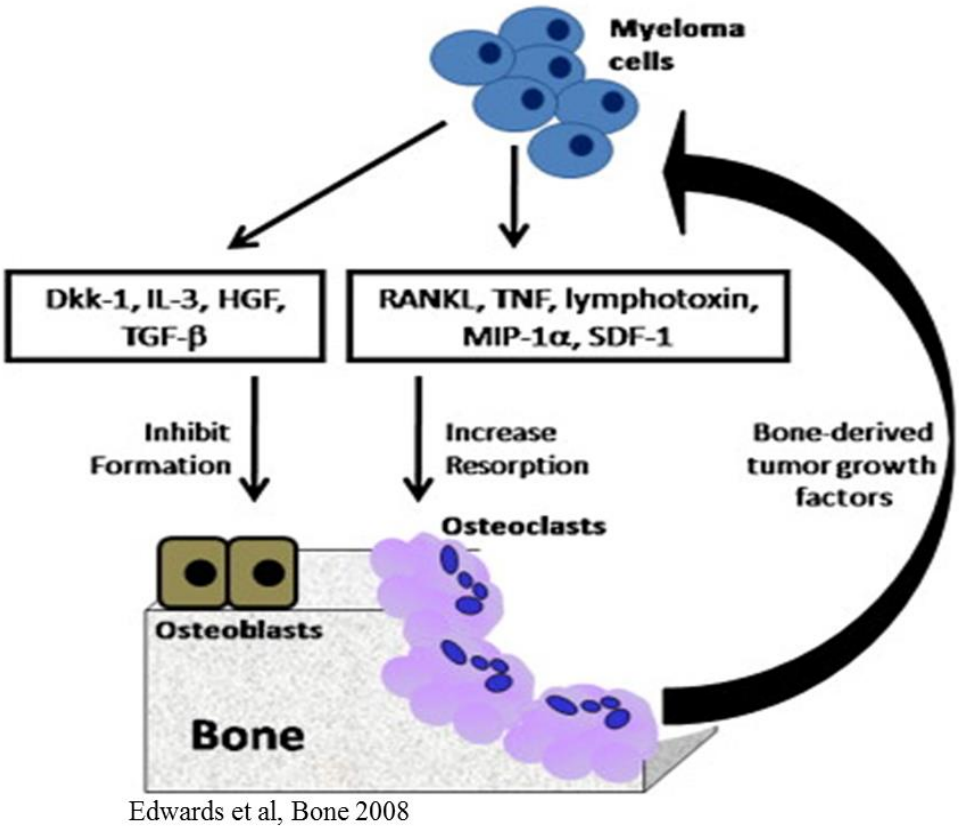

Figure 1.9. Vicious cycle in myeloma bone disease. Osteolytic bone disease developed by myeloma is associated with an increase in osteoclastic bone resorption and a reduction in osteoblastic bone formation. Factors secreted by myeloma cells promote increased osteoclast number and activation which in turn secrete bone-derived tumour growth factors that further enhance myeloma growth.

The RANK/RANKL/OPG system

As previously described, regulation of the RANK/RANKL/OPG system is crucial in osteoclastogenesis. The ratio of RANKL to OPG was shown to be increased in the serum of myeloma patients, which correlates with the overall bone loss associated with those suffering with myeloma (Terpos et al., 2003;Goranova-Marinova et al., 2007;Hofbauer and Schoppet, 2004). *In vitro* and *in vivo* studies have shown that the imbalance of the RANKL:OPG ratio in myeloma can be rescued by OPG protein, a decoy receptor to RANKL, to decrease osteolytic bone lesions (Giuliani et al.,

2001;Croucher et al., 2001;Vanderkerken et al., 2003) and highlight the importance of the RANK/RANKL/OPG system in myeloma.

Macrophage inflammatory protein-1 α (MIP-1α)

MIP-1α is a cytokine that can induce osteoclast differentiation from osteoclast progenitors and is also expressed by myeloma cells (Lentzsch, 2010). Myeloma patients have increased levels of MIP-1α in serum and bone marrow plasma, and a neutralising antibody to MIP-1α decreased osteoclast activity in myeloma patients (Choi et al., 2000). *In vivo* studies have shown that inhibiting the osteoclastogenic activity of MIP-1α by using an anti-sense construct or a neutralising antibody decreased the development of myeloma bone disease in SCID and 5TGM1 murine model of myeloma respectively (Oyajobi et al., 2003;Choi et al., 2001). Interestingly, injection of MIP-1α over calvariae in RANK deficient mice did not have MIP-1α mediated osteoclastogenic effect, suggesting that MIP-1α may be partially acting through RANKL to regulate osteoclastogenic activity (Oyajobi et al., 2003). MIP-1α also increases adhesion of myeloma cells to BMSCs through interactions between CCR1 on osteoclasts and CCR5 on myeloma cells, and promotes myeloma growth and the associated bone destruction (Oba et al., 2005).

Vascular endothelial growth factor (VEGF)

VEGF plays a critical role in angiogenesis, promoting the growth of various solid tumours. VEGF is secreted by myeloma cells and it has been reported that myeloma patients have an increase in the microvessel density in the bone marrow, which has a positive correlation with disease progression and poor prognosis (Vacca et al., 1994). It has been well-established that the addition of M-CSF and RANKL to cultures of monocytes and macrophages can induce osteoclast differentiation *in vitro*. Niida et al

demonstrated that VEGF could be used instead of M-CSF in the induction of osteoclast differentiation (Niida et al., 1999). Futhermore, Tanaka et al reported that inhibition of angiogenesis and bone resorption enhanced by co-culture of myeloma cells and osteoclasts could be achieved by the blockage of both VEGF and osteopontin (Tanaka et al., 2007). These data suggests that osteoclastic bone resorption in myeloma may be partly mediated by VEGF.

Stromal derived factor-1α (SDF1α)

Stromal derived factor-1 alpha (SDF1; CXCL12) is a CXC chemokine (a member of the chemokine subfamily), expressed by bone marrow stromal cells and endothelial cells. SDF-1α binds to its receptor CXCR4, and is thought to be involved in the migration and homing of myeloma cells (Alsayed et al., 2007). Hematopoeitic stem cells and lymphocytes, malignant cells and osteoclast precursors express CXCR4 (Juarez and Bendall, 2004;Yu et al., 2003;Smith et al., 2004). It has been shown that SDF-1α increases osteoclast motility and bone resorbing activity and a CXCR-4 specific inhibitor can decrease the osteoclast activation stimulated by myeloma cells (Zannettino et al., 2005). A combination of these data suggests the importance of SDF-1α in myeloma pathogenesis and the associated bone disease.

Interleukin-6 (IL-6)

IL-6 is a known myeloma growth factor and is produced by BMSCs, osteoblasts and myeloma cells. IL-6 can act through a membrane bound receptor complex of 130-kDa glycoprotein (gp130) to stimulate osteoclast formation, where combined treatment of IL-6 and its soluble receptor sIL-6R induced osteoclast formation, whereas separate treatment of each did not have an effect (Tamura et al., 1993) The interaction between myeloma cells and BMSCs promotes myeloma growth and induces the secretion of IL-

6 from BMSCs. The increase in IL-6 production triggers myeloma cells to increase the secretion of VEGF, a known proangiogenic factor, which in turns further promotes myeloma growth (Manier et al., 2012)**.**

Insulin growth factor-1 (IGF-1)

Myeloma cell proliferation is associated with the increased production of IGF-1 by BMSCs and osteoblasts in the bone marrow microenvironment (Manier et al., 2012). Myeloma patients expressing IGF-1 receptor (IGF-1R) on myeloma cells have a poorer prognosis than patients negative for IGF-1R due to the activation of IGF-1 signalling through IGF-1 binding to IGF-1R (Sprynski et al., 2009). IGF-1 is also produced by liver upon activation of growth hormone and its receptor. There is a positive correlation between IGF-1 levels and cancer risk and increased levels of IGF-1 are observed in obesity (Cohen et al. 2012). A calorie restricted diet decreased IGF-1 levels in murine models, suggesting that decreasing IGF-1 levels pharmacologically or by calorie restriction could be beneficial against cancer risk (Hursting et al., 2003).

1.4.7 Inhibition of osteoblast formation in myeloma

One of the major problems in myeloma bone disease is the imbalance of osteoclastic bone resorption and osteoblastic bone formation, thus uncoupling the normal bone remodelling process. An ideal therapy would not only have anti-tumour effects but also target the bone destruction induced by myeloma whilst simultaneously stimulating new bone formation.

Wingless-type (Wnt) signalling pathway

As previously described, the canonical Wnt signalling pathway plays a major role in the regulation of bone formation, and non-canonical Wnt signalling is also involved in the

differentiation of osteoblasts from mesenchymal stem cells by inhibiting adipocyte differentiation (Takada et al., 2007). An increase in bone mass *in vivo* was achieved by increasing Wnt signalling through inhibition of glycogen synthase kinase-3β (GSK-3β) (Clément-Lacroix et al., 2005). GSK-3β, a serine-threonine kinase, is involved in cell proliferation and is expressed by human myeloma cell lines and primary plasma cells isolated from myeloma patients. Knockdown of GSK-3β decreased human myeloma cell viability (Piazza et al., 2010). Furthermore, our group has previously identified that activation of the Wnt signalling pathway by lithium chloride (LiCl) treatment in the C57BL6/KaLwRij murine myeloma model decreased tumour burden and increased bone mineral density and trabecular bone volume by inhibiting GSK-3β (Edwards et al., 2008).

Inhibitors of Wnt signalling pathway

Molecules that inhibit Wnt signalling include Dickkopfs-1 (DKK-1) and the secreted frizzled-related proteins-2 (sFRP-2), both of which play a role in bone formation and myeloma pathogenesis. They are the major soluble Wnt inhibitors, produced in murine osteoblasts, that block early osteoblastogenesis and induce immature cell death (Galli et al., 2006;Niida et al., 2004;Li et al., 2006). DKK-1 is also expressed by BMSCs and myeloma cells, in addition to osteoblasts, and it mediates osteoblastic dysfunction in myeloma bone disease and DKK-1 levels in bone marrow plasma or peripheral blood in patients with myeloma were elevated as compared with healthy controls or MGUS patients (Tian et al., 2003). DKK-1 overexpression is associated with severe osteopenia and its deficiency resulted in increased bone mass in murine models (Li et al., 2006;Morvan et al., 2006). Moreover, myeloma development is mediated through the interaction between myeloma cells and local bone marrow microenvironment, and this

interaction has been shown to up-regulate DKK1 expression by osteoblasts (Oyajobi et al., 2004).

Another antagonist of Wnt signalling pathway, sFRP-2 is expressed by human myeloma cells. Myeloma cells from patients with advanced osteolytice bone disease also express sFRP-2, suggesting the possibility that sFRP-2 may play a role in myeloma bone disease. Treatment with conditioned media from sFRP-2 expressing RPMI8226 and U266 human myeloma cells decreased osteoblast mineralization and alkaline phosphatase activity *in vitro*. Moreover, exogenous sFRP-2 also decreased osteoblast differentiation (Oshima et al., 2005).

In addition to DKK-1 and sFRP-2, the product of *SOST* gene sclerostin was shown to be an antagonist of Wnt signalling pathway. It is mainly expressed by osteocytes, and recent studies have shown the expression of sclerostin in human myeloma cell lines and bone marrow plasma cells from myeloma patients with bone disease, with increased *SOST* expression in patients with higher skeletal problems (Colucci et al., 2011;Habibi et al., 2013). A decrease in osteoblast differentiation was observed when BMSCs were co-cultured with human myeloma cell lines when compared with BMSCs alone. However, inhibition of sclerostin by blocking antibody had rescued effects on osteoblast differentiation in the same co-culture system (Colucci et al., 2011). These studies suggest a potential role for sclerosotin in myeloma associated osteolytic bone disease.

Transforming growth factor- β (TGF-β)

TGF-β is a bone matrix protein and a multifunctional growth factor that is secreted during osteoclastic bone resorption and inhibits osteoblast differentiation (Edwards, Zhuang and Mundy, 2008). A pharmacological approach of blocking TGF-β by using a

neutralising antibody, 1D11, increased bone mineral density and bone volume (Edwards et al., 2010). *In vitro* studies have shown that osteoblast differentiation from BMSCs and MC3T3-E1 preosteoblast cells was suppressed by TGF-β, whereas inhibitors of TGF-β were able to restore osteoblast differentiation that was initially suppressed by conditioned media from myeloma cells and bone marrow plasma from patients with myeloma (Takeuchi et al., 2010). These data suggest the potential for targeting TGF-β as a treatment of myeloma bone disease.

Activin A

Activin A, a member of the TGF-β superfamily, is produced by BMSCs and an increased level of activin was observed in the bone marrow plasma of myeloma patients with osteolysis (Vallet et al., 2010). Targeting activin A by a soluble decoy receptor type IIA fusion protein stimulated bone formation and inhibit myeloma-induced bone loss in 5T2 myeloma-bearing mice and xenograft model SCID/hu mice, suggesting an important role of activin A in myeloma bone disease (Chantry et al., 2010;Vallet et al., 2010).

Runt-related transcription factor 2 (Runx2)

Runx2 is a transcription factor that regulates bone formation and differentiation of osteoblasts from precursor mesenchymal stem cells. Myeloma patients with osteolytic lesions are presented with reduction in Runx2 positive stromal and osteoblastic cells, as compared to myeloma patients without osteolysis. The same study has shown that soluble factors secreted by myeloma cells have the ability to suppress Runx2 activity upon cell to cell contact between myeloma cells and osteoprogenitors cells (Giuliani et al., 2005). The expression of a bone matrix protein osteopontin was shown to be dependent upon active Runx2 protein expression in human myeloma cells, which in

turn increased angiogenesis in the bone marrow of myeloma patients (Colla et al., 2005).

Interleukin-3 (IL-3)

Studies have reported IL-3 as a potential inhibitor of osteoblasts in myeloma bone disease (Ehrlich et al., 2005). Patients with myeloma have elevated levels of IL-3 in the bone marrow plasma, as compared with healthy patients or MGUS patients (Lee et al., 2004). Moreover, bone marrow plasma from patients with myeloma with elevated levels of IL-3 decreased osteoblast differentiation, whereas this inhibitory effect was reversed when treated with a neutralising antibody to IL-3 (Ehrlich et al., 2005). The same study has shown that IL-3 has no significant effect on Runx2 expression and activity in both murine and human bone marrow cells.

Hepatocyte growth factor (HFG)

Myeloma cells produced HGF, and myeloma patients have elevated levels of serum HGF (Seidel et al., 1998). Furthermore, serum levels of HGF have been shown to be negatively correlated with bone specific alkaline phosphatase and survival in patients with myeloma (Andersen et al., 2005;Standal et al., 2007). Additionally, HGF also inhibited osteoblastogenesis induced by bone morphogenic protein, and transcription factors involved in bone formation Runx2 and Osterix (Standal et al., 2007).

1.5 Current Therapies

Despite current therapies, myeloma remains fatal and incurable. Current therapeutic strategies include proteasome inhibitors, immune modulators, autologous stem cell transplantation, monoclonal antibodies, bisphosphonates, radiation therapy, surgery, kyphoplasty and vertebroplasty. Over the years, these treatment options have improved

survival of patients substantially (Engelhardt et al., 2014). In order to defeat this devastating disease, an ideal therapy would not only target tumour cells directly, but also inhibit or disrupt the congenial tumour growth factors contributed by the host microenvironment.

1.5.1 Proteasome inhibitors

Proteasome inhibitors are widely used as an anti-myeloma therapy. Proteasomes mainly degrade or process unwanted, damaged or improperly folded proteins by breaking down the peptide bonds of those proteins. Proteasome inhibitors disrupt unfolded protein response (UPR), a pathway that regulates proper folding of the protein, and immunoglobulin (IgG) secretion in myeloma cells (Lee et al., 2003;Ling et al., 2012). Proteasome inhibition prevents the normal elimination of misfolded proteins, resulting in an accumulation of these unwanted proteins, ultimately leading to cell death (Edwards and Mundy, 2010). Therefore, proteasome inhibitors are widely used as novel anti-cancer agents.

It has been shown that myeloma patients have increased levels of proteasomal activity, which may indicate that proteasome inhibitors would prove effective as a novel tool to prevent myeloma development (Jakob et al., 2007). Our group has previously shown that 5TGM1 myeloma cells showed an increase in proteasome activity, after inoculation *in vivo* using a succinyl luminogenic proteasome substrate (Suc-LLVY-aminoluciferin) assay, compared to the original 5TGM1 cells prior to inoculation (Edwards et al., 2009). The same study demonstrated that proteasome inhibition by Bortezomib has stronger anti-myeloma effect, when myeloma cells were located within the bone marrow as compared to tumour at an extra-osseous site/subcutaneous plasmacytoma, suggesting an enhanced anti-myeloma effect of proteasome inhibition from within the

host bone marrow microenvironment.

Furthermore, administration of Bortezomib alone or in combination with chemotherapeutic agents and/or dexamethasone was shown to be an effective treatment at the early stage or after relapse in patients with myeloma (Yang et al., 2003;Jagannath et al., 2005). Bortezomib is also used as part of an induction and maintenance therapy before and after autologous stem cell transplant in patients with myeloma (Engelhardt et al., 2014). However, peripheral neuropathy affects 50% of the myeloma patients treated with Bortezomib (Sonneveld et al., 2012).

In addition to anti-myeloma effects of proteasome inhibitors, they are also shown to promote increase in bone volume and bone formation rate *in vivo* and inhibition of bone morphogenetic protein 2 (BMP2) abrogated bone formation effect of proteasome inhibitors. The same study has shown that proteasome inhibition increased osteoblastogenesis by increasing BMP2 expression *in vitro*, suggesting that proteasome inhibition regulates bone formation through BMP2 (Garrett et al., 2003). Moreover, an increase in bone formation following Bortezomib treatment in myeloma patients was associated with a significant increase in bone formation marker alkaline phosphatase, suggesting a dual benefit of proteasome inhibitors as anti-myeloma and osteoblast activation agent in the treatment of myeloma (Zangari et al., 2005).

1.5.2 Immunomodulators (IMiDs)

IMiDs such as thalidomide can be used for the treatment of patients who are not eligible for transplant and as maintenance therapy, following conventional therapy and autologous stem cell transplant, for progression free and to improve overall survival of myeloma patients (Engelhardt et al., 2014). Pomalidomide and lenalidomide, derivatives of thalidomide were shown to be effective treatment against myeloma

(Dimopoulos et al., 2007). Both pomalidomide and lenalidomide were shown to downregulate PU.1, a transcription factor critical for inhibition of osteoclast development (Breitkreutz et al., 2008). Mice deficient in PU.1 have been shown to develop osteopetrosis due to inhibition of osteoclast activity (Tondravi et al., 1997). Thalidomide, or non-steriodal anti-inflammatory drugs (NSAIDs) were shown to be potent inhibitors of osteoclastic activity, thereby decreasing osteolysis in myeloma.

Osteoclast formation and activity were inhibited by an NSAIDs SDX-308, through downregulation of NFκB activity and decreased myeloma cell growth in a human primary bone marrow culture (Feng et al., 2007). These data suggests that SDX-308 not only decreases osteoclast formation, but also has a direct anti-myeloma effect. However, as with many other drugs, NSAIDs also have side effects such as nausea, vomiting, gastric ulceration, bleeding and diarrhea (Lentzsch 2010). Peripheral neuropathy is a side effect in 50% of the patients treated with thalidomide (Sonneveld et al., 2012). Moreover, treatment with IMiDs does not have an effect on bone formation, assessed by measuring bone alkaline phosphatase and osteocalcin level (Terpos et al., 2005).

1.5.3 Bisphosphonates (BPs)

Unfortunately, myeloma patients who respond well to anti-myeloma therapies may still present with associated skeletal problems such as bone pain, hypercalcemia, and fractures (Belch et al., 1991;Kyle et al., 1975). Bisphosphonates are potent inhibitors of osteoclastic activity and shown to reduce bone pain, inhibit bone loss, and represent an effective treatment for inhibiting the myeloma associated bone disease (Berenson et al., 1996). BPs can be categorized into nitrogen containing (eg. Pamidronate and Zoledronate), and non-nitrogen containing BPs (eg. Clodronate) (Berenson, 2010).

In vitro studies have shown that the concentration and time dependent direct anti-tumour effect of Pamidronate (PAM) and a more potent bisphosphonate, Zoledronate (ZOL), in human myeloma cell lines and primary myeloma cells from patients (Aparicio et al., 1998). Intravenous administration of PAM and ZOL are shown to be effective in reducing skeletal-related diseases in patients with myeloma (Berenson et al., 1998;Rosen et al., 2003). Increase in overall survival was observed in myeloma patients treated with ZOL or oral administration of clodronate (CLO) treatment, independent of skeletal related disease, suggesting the anti-myeloma effect of bisphosphonates (Morgan et al., 2010). Following the BPs treatment, myeloma patients were monitored for the effectiveness of the treatment using bone resorption markers, N-terminal cross-linking telopeptide of type I collagen (NTX) and C-terminal cross-linking telopeptide of type I collagen generated by MMPs (ICTP). A significant decrease in the levels of NTX and ICTP were observed in myeloma patients with osteolysis, following the treatment of CLO, PAM, and ZOL (Withold et al., 1998;Terpos et al., 2000;Coleman et al., 2005;Terpos et al., 2001;Elomaa et al., 1996;Berenson et al., 2001).

Similar to IMiDs treatment, despite the advantage of inhibiting bone resorption in myeloma, bisphosphonates lack the ability to increase bone formation in myeloma. Therefore, combination therapy with bone anabolic agents will be beneficial for treatment of myeloma bone disease (Berenson 2010). Furthermore, some patients with myeloma develop osteonecrosis of the jaw or renal toxicity as side effects of bisphosphonate treatment (Kyle et al., 2007).

1.5.4 Denosumab

The human monoclonal antibody specific to RANKL, denosumab, has been shown to be effective in decreasing the bone resorptive markers in patients with breast cancer with bone metastasis and myeloma with bone lesions (Body et al., 2006). Denosumab is administered to patients subcutaneously and it appeared to be more effective than BPs by maintaining the inhibition of bone resorptive markers. Another advantage of denosumab over BPs is that the side effects from the treatment include limited toxicity, including asthenia and peripheral edema (Body et al., 2003). A randomized trial that involved less than 200 myeloma patients, comparing the effectiveness of denosumab versus zoledronic acid, has shown a poorer survival in myeloma patients treated with denosumab, suggesting a larger trial to draw more assessable conclusion (Henry et al., 2011). Hence, the use of denosumab in myeloma is currently being assessed in a larger trial with more than 200 myeloma patients. Taken together, although denosumab is approved for use as a therapy for prostate and breast cancer associated bone disease, current available data from clinical trials still do not support its use against myeloma bone disease (Engelhardt et al., 2014).

1.5.5 Autologous stem cell transplantation (ASCT)

ASCT is considered a standard frontline treatment for younger and fit patients with myeloma. High dose of chemotherapy agents is given to patients as induction regimens prior to ASCT with the goal of decreasing myeloma tumour burden, improving symptoms, and allowing successful stem cell collection. The aim of the combination of ASCT and novel agents is for better quality of the response, progression free survival, and overall survival (Moreau and Minvielle, 2013). Proteasome inhibitors, alkylating agents, corticosteroids, and IMiDs are classes of drugs used as induction regimens, and

induction therapy includes 2 or 3 those drugs (Kumar et al., 2012). Examples of these classes of drugs are bortezomib (V), cyclophosphamide (C), dexamethasome (D), and lenalidomide (R). In current clinical practice, preferred regimens contain VDR or VCD (Kumar et al., 2012). The three drug induction regimens give better response, however increased toxicity was observed with more than three drugs.

Overall survival of the patients appeared to be no different when having ASCT early or at the time of relapse, however, early transplantation seemed to give better outcome (Fermand et al., 2005). The limitation of stem cell transplant therapy is that it is not suitable for older patients above the age of 65 (Dolgin, 2011).

1.5.6 Overview of the current National Institute for Health and Care Excellence (NICE) guidelines for management of myeloma

Bortezomib with dexamethasone or together with dexamethasone and thalidomide is approved for adult myeloma patients as a treatment prior to high dose chemotherapy and autologous stem cell transplantation (NICE, 2014). Thalidomide is approved as a first line of treatment to myeloma patients who are not suitable for high dose drug treatment together with a stem cell treatment. Thalidomide is also approved as first treatments when combined with an alkylating agent such as melphalan and corticosteroids such as prednisolone. The same NICE guidline suggests that Bortezomib can be given to patients who cannot tolerate the side effects of thalidomide as first treatments (NICE, 2011). Lenalidomide in combination with dexamethasone is approved for patients who had at least two other treatments (NICE, 2009). Monotherapy using Bortezomib is recommended for patients who relapsed after having one treatment, who had bone marrow transplant, or who had no more than four cycles of treatment (unless the patient did not respond well to Bortezomib) (NICE, 2007).

1.6 Association between myeloma and obesity

Obesity is characterised as a nutritional disorder with an excess of adipose tissue and there is a convincing association between obesity and cancer incidence, including colon, breast, endometrial, kidney, esophageal, liver, pancreatic cancer and myeloma (Wolin, Carson and Colditz, 2010). Men with 5 kg/m^2 increase in BMI were shown to be associated with high risk of colon, renal, thyroid, and oesophageal adenocarcinoma, whereas women with the same increase in BMI were associated with strong risk for gallbladder, endometrial, renal and oesophageal adenocarcinoma (Renehan et al., 2008). The association between obesity and cancer risk appeared to be similar in different demographic studies with the exception of higher incidence of various cancers in African American population as compared to Hispanics. Higher incidence of premenopausal and postmenopausal breast cancer was associated with increased BMI in Asia-Pacific population. It has been reported that patients obese at diagnosis have a poorer prognosis, higher mortality rate, and increased risk of metastasis in breast cancer as compared to patients with normal weight (Reeves et al., 2014).

Obesity or increased BMI has been reported to increase the risk of haematological malignancies such as leukemia, lymphoma, and myeloma (Lichtman, 2010). A high BMI is significantly associated with the increased relative risk of mortality from myeloma, within a BMI range of 29.9 to 39.9 kg/m^2 (De Pergola and Silvestris, 2013). Studies have shown that a mean weight loss of 14-27% 15 years after bariatric surgery (in the Swedish patient population) or weight loss after gastric bypass surgery (in U.S. patients population) has decreased the risk from cancer death as compared to BMI-matched controls.

Overweight or obese cancer survivors are encouraged to maintain healthy normal weight or modest weight loss of 5-10% body weight to decrease the risk of cardiovascular disease and diabetes and to decrease the level of cancer growth factors or inflammatory cytokines (Reeves et al., 2014). An increase in physical activity is proven to promote a better quality of life in cancer survivors (Wolin, Carson and Colditz, 2010). Pendyala et al. reported that biopsies from 10 obese premenopausal women with diet-induced weight loss showed the decrease level of inflammatory and cancer related cytokines such as TNF-α, IL-1β, IL-8, and NFκB (Pendyala et al., 2011).

On the other hand, it has been shown that obese patients with metastatic castration-recurrent prostate cancer are more protected against overall mortality compared to patients with normal BMI, possibly due to the fact that obese patients might be protected from cachexia (Halabi et al., 2007). A better understanding of the mechanism responsible for the association between cancer and obesity is essential to identify potential therapeutic targets. Also, various molecular mechanisms appear to play differential roles within different cancer contexts. For instance, estrogen signalling appears to be responsible for obesity induced breast and endometrial cancer, whereas insulin signalling accounts for colon and prostate cancer incidences associated with weight gain (Wolin, Carson and Colditz, 2010).

1.7 Obesity, MMPs, TIMPs and myeloma

The constitution and distribution of the matrix components in the extracellular matrix (ECM) were reformed during adipocyte differentiation, suggesting the importance of ECM organization in differentiation and maintenance of adipocytes (Kubo et al., 2000). MMPs and their regulators TIMPs play a crucial role in concomitant extracellular protein degradation (Lilla, Stickens and Werb, 2002). Expression profiles of mRNA for

MMP-2, MMP-3, MMP-7, MMP-12, MMP-14, MMP-19 and their inhibitors TIMP-1 and TIMP-3 were studied by Chavey et al in epididymal fat pads of the murine models of obesity, leptin protein deficient ob/ob mice and leptin receptor activity deficient db/db mice. Interestingly, a decrease in MMP7 mRNA expression and an increase in its inhibitor TIMP-1 mRNA level was observed in obese tissue as compared with the lean tissue (Chavey et al., 2003). This study highlights the importance of the balance between MMPs and their inhibitors in obesity-induced fat mass development. I have previously mentioned the association between obesity and increased risk of myeloma. In addition, reduced MMP7 levels were observed in obese individuals and normal levels of MMP7 can be restored by weight reduction after bariatric surgery.

Mice deficient in MMP3, MMP11 or MMP19 have increased adiposity during diet-induced obesity, suggesting that these MMPs, in addition to MMP7, may act as negative regulators of diet-induce obesity (Lijnen et al., 2002;Pendás et al., 2004;Maquoi et al., 2003). *In vitro* studies have shown that the murine bone marrow adipocytic cell line 14F1.1 increased 5T33 myeloma cell proliferation and migration, and decreased myeloma cell apoptosis in a co-culture system (Caers et al., 2007). Moreover, the inhibitor of MMP7, TIMP1, was shown to be upregulated in myeloma and obesity (Chavey et al., 2003;Kralisch et al., 2007;Guedez and Stetler-Stevenson, 2010).

Taken together, these studies led us to investigate whether there is a role for MMP7 and/or obesity on myeloma development.

1.8 The aim of the study

The overall goal of my thesis is to identify novel ways in which the host microenvironment contributes to the pathogenesis of multiple myeloma. The role of osteoblasts and osteoclasts have been well studied, however the causative role of other cell types and factors within the bone marrow microenvironment are poorly understood. We have extensive experience with the 5T Radl model of multiple myeloma, which is a well-characterized murine model that mimics many features of the human myeloma disease, including elevated levels of the myeloma specific paraprotein (IgG2bκ), cortical lesions and generalized bone destruction. Importantly, 5TGM1 myeloma cells will only grow when inoculated intravenously into immune competent C57BL/KaLwRij mice, and not in the closely related C57BL/6 mice (Figure 1.10). This model has proven to be particularly useful to begin to elucidate the contribution of the host microenvironment to myeloma pathogenesis *in vivo*. The Edwards Lab has recently described the importance of host-derived adiponectin, Dkk1 and MMP-9 in myeloma pathogenesis *in vivo* (Fowler et al., 2009;Fowler et al., 2011;Fowler et al., 2012).

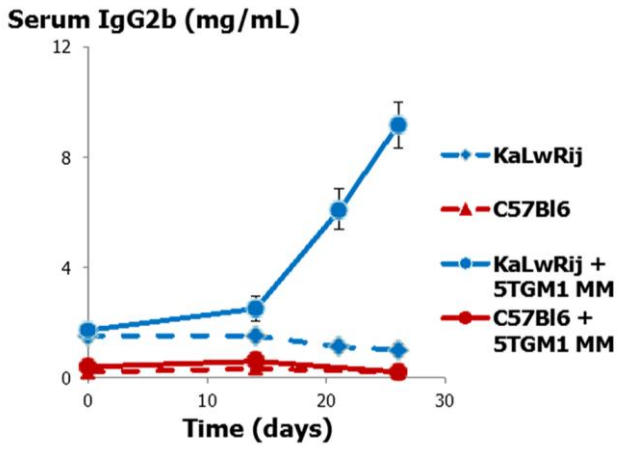

Figure 1.10. 5TGM1 myeloma in KaLwRij mice. Age- and sex-matched C57BL/6 and KaLwRij mice were inoculated with 5TGM1 myeloma cells. Tumour burden was quantitated by myeloma specific paraprotein IgG2bk ELISA (Fowler et al. 2011).

Adiponectin is negatively correlated with obesity, and there is increasing evidence to support an association between obesity and myeloma, or MGUS (Landgren et al., 2010). MMPs are also emerging as important regulators of cancer-induced bone disease, with strong evidence for the role of MMP-7 in prostate cancer and breast cancer-induced osteolysis (Lynch et al., 2005;Thiolloy et al., 2009). Intriguingly, serum MMP-7 levels are altered by changes in obesity, suggesting potential cross-talk between these mechanisms (Ress et al., 2010).

Based on these studies, the overall aim of my thesis was to determine whether MMP-7 or adiposity promote the development of myeloma and the associated bone disease *in vivo*. I have taken three complementary, yet distinct, approaches to address this (Figure 1.11). The role of host-derived MMP7 in myeloma pathogenesis *in vivo* was determined using genetically modified mice deficient in MMP7. The role of adiposity in myeloma was investigated *in vivo* by firstly studying the effect of diet-induced obesity on myeloma development, and secondly by using a pharmacological approach to alter bone marrow adiposity.

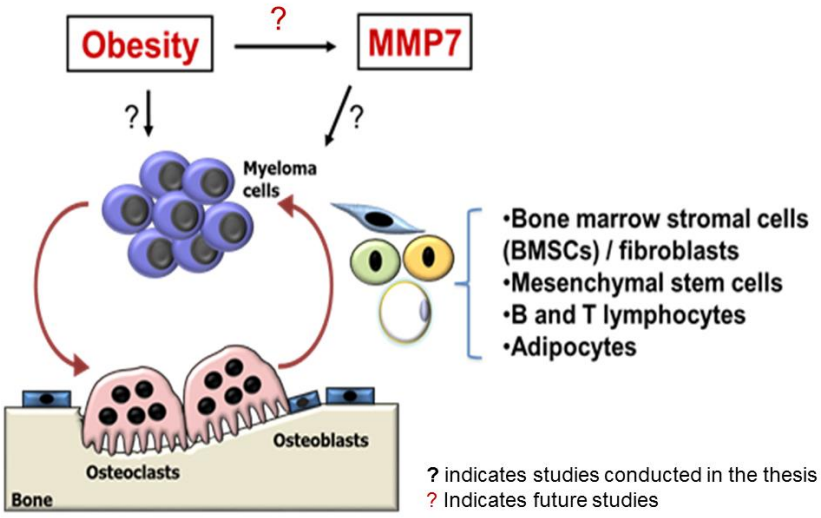

Figure 1.11. Overall aims of the study. Investigating the role of obesity and MMP7 in myeloma host microenvironment.

Chapter 2 : General Materials and Methods

Materials and techniques used in my overall research work are outlined in this chapter with techniques specific to each experimental chapter expanded in the respective chapters.

2.1 Cell culture

Table 2.1 List of cell lines

Cell Line	Species Origin	Type
5TGM1-GFP	Mouse	Immortalized myeloma cell line
RPMI 8226-eGFP	Human	Immortalized myeloma cell line
ST2	Mouse	Immortalized BMSCs
14M1	Mouse	Immortalized BMSCs from KaLwRij mice
2T3	Mouse	Immortalized pre-osteoblast cell line
HS5-mCherry	Human	Immortalized BMSCs

Abbreviations - BMSCs; bone marrow stromal cells

2.1.1 Cell culture conditions

Suspension cell lines, 5TGM1-GFP and RPMI 8226 myeloma cell lines utilized in my work were cultured in Roswell Park Memorial Institute medium (RPMI 1640) media supplemented with 10% fetal bovine serum (Biosera), 1% L-glutamine, 1% sodium pyruvate, 1% non-essential amino acid, and 1% penicillin/streptomycin (Sigma-Aldrich). The adherent cell lines, ST2 murine bone marrow stromal cells (BMSCs), 2T3 murine osteoblasts, and HS5 human BMSCs were cultured with Dulbecco's Modified Eagle's medium (DMEM) supplemented with 10% fetal bovine serum (Biosera), 1% L-glutamine, and 1% penicillin/streptomycin (Sigma-Aldrich). Media containing all components listed above were referred to in the text as complete media. All cell lines

were maintained at 37°C in 5% CO_2 atmosphere. All frozen cell lines were stored in 10% DMSO (Sigma) in FBS in liquid nitrogen.

Suspension cell lines were split at approximately 1:5 dilution and replaced with fresh RPMI 1640 complete media twice a week. When adherent cell lines were confluent, 1 x PBS (Sigma-Aldrich) was added to the flask to wash and aspirated, then cells were incubated with 0.25% trypsin in 1 mM EDTA (Sigma-Aldrich) at 37°C for 2-5 minutes to detach the cells, followed by the addition of fresh media containing FBS to neutralize the trypsin. Cell suspensions were split at 1:7 dilution and replaced with the fresh media. All tissue culture flasks and plates were obtained from Corning Inc.

2.2 *In vivo* studies

Studies were performed using 6- to 10-week-old female C57BL/6, C57BL/KaLwRijHsd male and female mice (Harlan Netherlands, Horst, The Netherlands), RAG-$2^{-/-}$ and RAG-$2^{-/-}$/MMP-$7^{-/-}$mice (provided by Dr. Conor C. Lynch, Vanderbilt University).

Myeloma development was induced by the intravenous inoculation of $5x10^5$ 5TGM1-GFP tagged myeloma (MM) cells in 100µL of phosphate buffered saline (PBS). The mice developed features of myeloma approximately 4 weeks after the inoculation. Tumour burden was analysed by quantifying the myeloma specific IgG paraprotein in the serum and GFP positive cells in the bone marrow and spleen. Bone disease was assessed by microcomputed tomography (microCT) and histology.

All *in vivo* experiments, except for the studies in section 3.3.6 were conducted at Vanderbilt University and analysed at University of Oxford. All *in vivo* experiments (both at Vanderbilt University and University of Oxford) were performed and analysed

by Seint Lwin. Studies were approved by the Institution of Animal Care and Use Committee at Vanderbilt University and conducted in accordance with the National Institute of Health (NIH) Guide for the Care and Use of Laboratory Animals (National Research Council. Guide for the Care and Use of Laboratory Animals 1985; Washington, DC National Academy Press pp. 86–23 NIH publication no.). *In vivo* experiments with MMP7-overexpressing 5TGM1-GFP myeloma cells were conducted and analysed at the University of Oxford and experiments were carried out by the approval of ethics committees at University of Oxford and by the United Kingdom Home Office.

2.3 Body composition analysis

Body composition analysis was measured weekly by using the LF50 minispec body composition analyser (BRUKER). This device measured overall percentage of fat, lean tissue/muscle and free fluid in live mice using a Time Domain Nuclear Magnetic Resonance (TD-NMR) method. After 6 hours of fasting before the measurement, each experimental mouse was placed in the restrainer. The restrainer was then placed in the minispec body composition analyser, for approximately 90 seconds for each mouse.

2.4 Bone marrow isolation by centrifugation

At the end-point of *in vivo* studies, mice were sacrificed and hind legs from experimental mice were harvested and the muscle stripped off. One end of both tibia and femur were cut off to allow for the bone marrow cells to go through the bone, followed by placing them in 0.5 mL eppendorf tubes with holes at the bottom of the tubes. Eppendorf tubes with bones were then placed in the 1.5mL eppendorf tubes with 500 µL of PBS in each tube. Bone marrow was isolated by centrifuging mouse tibia and

femur at full speed for 2 minutes (Figure 2.1). Bone marrow lysates were then washed with PBS and red blood cells were lysed for 5 minutes on ice, using lysis buffer consisting of 155mM NH_4Cl, 0.1M KCO_3, and 0.5M Na_2EDTA. Cells were then washed with PBS, and fixed with 4% formalin for further analysis or proceed with appropriate method as required.

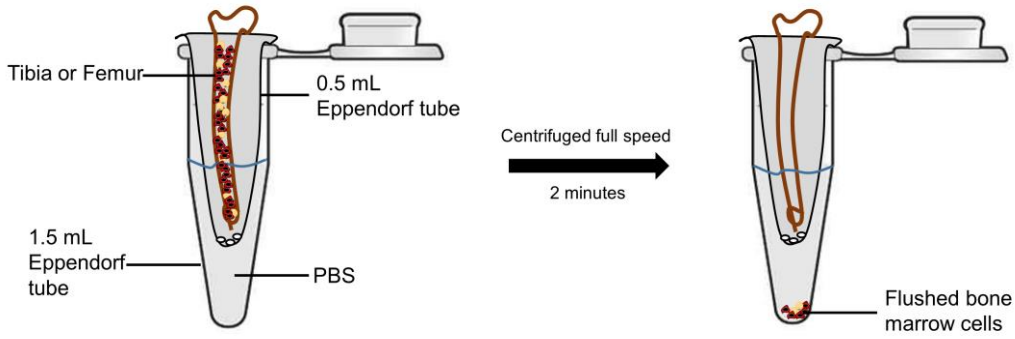

Figure 2.1. Flushing of bone marrow by centrifugation

2.5 Assessment of tumour burden by ELISA

An ELISA was used to determine the concentration of antigen or the soluble protein of interest in serum or cell culture supernatant. This method involved the formation of antigen-antibody complexs, which was quantified and visualised by the emission of a detection chromogen. Firstly, the capture antibody was coated to a 96-well plate, before adding the control or experimental sample to the wells. The antigen in the sample was bound to the capture antibody forming an antigen-antibody complex. Unbound or non-specific proteins were washed away with PBS and addition of the conjugated secondary antibody allowed for the visualisation of the complex followed by the addition of a chromogenic reagent such as H_2O_2-tetramethylbenzidine solution. The colour

developed was proportional to the amount of antigen bound or protein of interest in the sample and was quantitated by using a colorimetric plate reader.

Blood was taken weekly from mice used in the *in vivo* studies to obtain serum. Blood was clotted in BD microtainer serum separator tubes (BD Biosciences) and centrifuged at 4000 rcf for 5 minutes at 4°C and serum was collected and stored at -80°C. Using the concept described above, tumour burden was assessed by enzyme linked immunosorbent assay (ELISA) analysis of the myeloma specific immunoglobulin IgG2bκ in the serum, as developed previously (Dallas et al., 1999). A high binding ELISA plate (Costa) was coated overnight at 4°C with 2µg/mL of IgG2bκ capture antibody (Research Diagnostics, Fitzgerald Industries). The capture antibody was aspirated and washed 3 times in PBS/0.05% tween 20 before blocking in PBS/3% BSA for 3h at room temperature. An 8-point standard curve of 500, 100, 20, 4, 0.8, 0.16, 0.032, 0 ng/ml was generated from recombinant mouse IgG2bκ serially diluted in 1:5 in PBS/0.3% BSA. Serum was diluted 1:20,000 for baseline, week 2, week 3 and endpoint. The blocking solution was aspirated and the plate washed 2 times with PBS/0.05% tween 20. Standards and diluted test samples were transferred to the plate at 100µl per well and incubated at 37°C for 1h. Peroxidase-conjugated rat anti-mouse IgG detection antibody (provided by Dr. Oyajobi, University of Texas, San Antonio) was diluted 1:5000 in PBS/0.3% BSA at 30 minutes to 1h before use. Standards and test samples were aspirated and washed 6 times with PBS/0.05% tween 20 at the end of incubation time. Diluted detection antibody of 100 µl was added to each well of the plate and incubated at 37°C for 1h. The detection antibody was aspirated and washed 6 times with PBS/0.05% tween 20. The substrate reagent used for detection was O-phenylene-diamine with 0.05% H_2O_2 (Sigma-Aldrich) in H_2O. Upon colour

development (~15min), ELISA plates were read at 450nm OD using a SPECTRA max 384 plus plate reader (Molecular devices).

2.6 Assessment of tumour burden by flow cytometry

Bone marrow was flushed from the tibia and femur of each myeloma-bearing mouse as described in section 2.4. Cells from the spleen of the myeloma-bearing mice were obtained by homogenization in PBS. Cell suspensions from both bone marrow and spleen were filtered through a 70 μm filter (Thermo Scientific) followed by analysis for GFP fluorescence by 5TGM1 myeloma cells using a 3 laser BD LSRFortessa (BD Biosciences).

2.7 Microcomputed tomography (MicroCT) analysis

Hind legs from *in vivo* studies were fixed in 10% neutral buffered formalin (Thermo Scientific) and scanned at an isotropic voxel size of 12μm using a microCT40 (SCANCO Medical, Bassersdorf, Switzerland). MicroCT analysis of the proximal tibia was used to measure cortical bone lesions and the ratio of bone volume to total tissue volume (% BV/TV) within the cortical bone. For analysis of cortical bone lesions, cross-sectional images of the entire metaphysis including the cortices and extending 0.25 mm from the growth plate were exported in tiff format then imported into AMIRA 3-D graphics software (Mercury Computer Systems, Chelmsford, MA). AMIRA software generated a 3-D reconstruction of the metaphyses using a consistent threshold. The number of osteolytic lesions that completely penetrate the cortical bone seen in the virtual reconstruction were counted. To measure overall bone volume and structural characteristics of the trabecular, contours were drawn within the cortices of the

proximal tibia using the microCT40. The analysis provided % BV/TV within the drawn contours in the cortical bone.

2.8 Tissue processing and paraffin embedding for mouse hind legs and spleen

Hind legs and spleens harvested from the mice were fixed in 10% neutral buffered formalin (Thermo Scientific) for a minimum period of 48 hrs. Fixed bones were then scanned by microCT analysis to determine the trabecular bone volume and to quantitate osteolytic lesions, following the removal of muscle attached to hind legs. Bones were then placed in histological cassettes and were decalcified in 10% EDTA in distilled water (pH 7.2) for 2 weeks. Decalcification involved a chelation process where calcium ions in the mineralized matrix were dissociated and bound by EDTA, which gently removed calcium ions and preserved tissue proteins. Upon successful decalcification, bones were processed in the tissue processor (Leica) through a dehydration procedure in graded ethanol for 2 changes of 1 hour each in 70% and 95% ethanol, 3 changes of 1 hour each in 100% ethanol and xylene, and 2 changes of 1 hour each in paraffin wax at 60°C.

The tissues were then taken out of the second change of paraffin wax, and immersed in a small amount of hot 60°C paraffin wax with labelled cassettes and cooled on a cold plate (Leica), which resulted in a block of tissue embedded in wax.

2.9 Tissue staining

2.9.1 Hematoxylin and eosin (H & E) staining

Paraffin embedded bones and spleens were sectioned at 5µm thickness and stained with hematoxylin and eosin. Tissue sections were dewaxed in clearene for 2 x 5 minues (Leica Microsystems) and rehydrated through graded ethanol for 2 minutes each in 2 x 100%, 2 x 95%, 1 x 70% ethanol, 1 x distilled water. The slides were then immersed in working Harris Hematoxylin solution (Thermo Scientific) for 1 minute. Slides were thoroughly rinsed in tap water and the nuclear stain was enhanced by dipping the sections in 5% ammonium water for 10 seconds (Thermo Scientific). Tissue sections were then counterstain with eosin working solution with 2% orange G (Sigma-Aldrich) for 2 minutes. Finally, sections were rinsed through graded ethanol, 2 changes of clearene, and coverslipped using DPX mountant (Sigma-Aldrich).

2.9.2 TRAP staining

Tissue sections were dewaxed in clearene, rehydrated through graded ethanol, and distilled water as mentioned above. The slides were then incubated in a tartrate/napthol AS-BI phosphate substrate solution pH 5 (Sigma-Aldrich) at 42°C for 30 minutes. Immediately after the incubation period, slides were transferred directly to a pararosaniline/nitrite colour reaction solution (Sigma-Aldrich) for 10 minutes at room temperature. Slides were thoroughly rinsed in distilled water and counterstained with Harris Hematoxylin solution for 1 minute (Thermo Scientific), rinsed through graded ethanol, 2 changes of clearene, and coverslipped using DPX mountant (Thermo Scientific).

2.9.3 Immunohistochemistry

Paraffin embedded tissue sections (bones and spleens) of 5µm thickness were dewaxed, rehydrated, and rinsed in distilled water (as described in section 2.9.1), rinsed in Tris buffered saline (TBS; 10mM Tris at pH 7.4, 150mM NaCl) with Tween-20 (0.05%) (TBST), and rinsed again in 1xTBS. The slides were then immersed in 100% methanol for 2 minutes at room temperature.

Endogenous peroxidases in the tissue were quenched using 2% H_2O_2 solution in methanol for 30 minutes at room temperature, followed by incubating in methanol for 2 minutes. The sections were then washed in TBS twice.

An antigen retrieval method was necessary for formalin fixed paraffin sections, as methylene based cross-linking occurs as a result of fixation, where an alteration of the tertiary protein structure can mask antigenic sites. To unmask or reveal the antigenic sites, tissue sections were immersed in a plastic jar containing 250ml of 10mM citrate buffer at pH 6 (2.94g sodium citrate or citric acid in 1L distilled water) (Sigma-Aldrich) and heated at full power in the microwave for 2 minutes. This heating process was monitored to avoid boiling, as this causes the bones to peel from the slide. Tissue sections were then cooled and washed in TBS several times.

Tissue sections were blocked using blocking solution (1% bovine serum albumin (BSA) and 5% serum of the species in which the secondary antibody was raised), for 1 hour at room temperature. The slides were then incubated in primary antibodies (optimised concentration diluted in blocking solution) overnight at 4°C in a humidified tray. Slides were then washed extensively in TBST prior to the addition of a species-specific biotinylated secondary antibody diluted in TBS for 1 hour at room temperature. Slides

were washed in TBS, followed by incubation with avidin-peroxidase complex using Vectastain kit (Vector laboratories) for 45 minutes at room temperature.

Following washing in TBS, the antigen-antibody-polymer complex was visualised by 5-15 minutes incubation with 3'-3'-diaminobenzidine (DAB) solution (Vector Laboratories). The slides were then thoroughly washed in running tap water and immersed in distilled water. The sections were then counterstained with Harris hematoxylin (Thermo Scientific) for 30 seconds, rinsed in running tap water and the slides placed in distilled water. The slides were then rinsed through graded ethanol, 2 changes of clearene, and coverslipped using DPX mountant (Thermo Scientific).

2.9.4 TUNEL staining

Quantification of apoptosis in bone marrow was performed using *In Situ* Cell Death Detection Kit, AP (Roche). Tibia and spleen tissue sections from myeloma-bearing mice were de-waxed and rehydrated according to standard protocol in 2.9.1. After dipping the slides in distilled water, the slides were placed in a plastic jar containing 250ml 0.1M citrate buffer, pH 6 (Sigma-Aldrich) for antigen retrieval treatment. Slides were then microwaved at full power for 2 minutes and monitored not to let it boil to prevent the bones from peeling off the slides. The slides were cooled rapidly by immediately adding distilled water. After washes with PBS, sections were blocked for 30 min at room temperature in Tris-HCL, 0.1M pH 7.5 solution containing 3% BSA and 20% FBS.

The manufacture's protocol was followed accordingly. TUNEL reaction mixture (enzyme and label solution) was prepared immediately before use and kept on ice until use and sections were incubated in mixture for 1h at 37°C in a humidified chamber in

the dark. Slides were washed with PBS following incubation and then incubated with converter-AP for 30 minutes at 37ºC. After washing the sections with PBS, the substrate solution, dissolved one Fast Red tablet (Sigma-Aldrich) in 2mL of 0.1M Tris-HCl, pH 8.2, was applied for 10 minutes at room temperature in the dark and the slides were rinsed in PBS. The sections were then counterstained with Harris hematoxylin (Thermo Scientific) for 10 seconds, rinsed in running tap water and the slides placed in distilled water. The slides were mounted with fluoshield aqueous mountant (Dako). Microscopic images for 4x4 fields of view were taken at 40x magnification from below the growth plate towards the distal tibia. Number of cells positive for apoptotic or proliferating myeloma cells in those fields of view were quantified using ImageJ analysis software.

2.10 Enzyme-linked Immunosorbent Assay (ELISA)

Using the concept described in section 2.5, commercially available ELISA kits were used and followed according to the manufacturer's instruction. Specific ELISA kits used for experiments such as MMP7, TIMP-1, osteopontin, DKK-1, IL-6, and IGF-1, were noted in relevant chapters.

2.11 RNA isolation and quantitation

RNeasy midi kit (Qiagen) was used to extract total RNA from cultured cells or murine bone marrow. Cells were lysed by adding 350µl or 600µl (for $< 5 \times 10^6$ or $> 5 \times 10^6$ respectively) of buffer RLT with 1% v/v β-Mercaptoethanol (Sigma) and pipetting vigorously for suspension cells and by using the cell scrapers for adherent cells, after washing with 1 x PBS. The cell lysate was transferred to the QIAshredder columns (Qiagen) and centrifuged at 18400 rcf for 2 minutes to homogenize. The flow through

was mixed with 1:1 volume 70% ethanol. The mixture was transferred to the RNeasy spin column in a 2ml collection tube and centrifuged at 9400 rcf for 15 secs. The flow through was discarded and 700 µl of Buffer RW1 was added and centrifuged as mentioned above. The flow through was discarded and 500 µl of Buffer RPE was added to the column and centrifuged as above. This was repeated as above and centrifuged at 9400 rcf for 2 minutes. The flow through was discarded and the column was transferred to a new collection tube and centrifuged at full speed for 1 minute to remove the excess remaining ethanol. The dry column was placed in a 1.5 ml RNase free eppendorf tube and 30 µl of RNase free water was added to the column and centrifuged at 9400 rcf for 1 minute to elute the RNA. The concentrations of RNA samples were assessed using Nano drop ND-1000 spectrophotometer (Labtech Inc). An RNA sample volume of 2µl was loaded on the calibrated Nano drop and 260/280 ratio and concentration in ng/mL was recorded.

2.12 cDNA synthesis

The volume containing 1µg of RNA was treated with DNase I (Fermentas Life Sciences) for removal of excess genomic DNA. RNA samples were then reverse transcribed using the iScript cDNA synthesis kit (Bio-Rad).

2.12.1 Removal of genomic DNA from RNA preparations (DNase treatment)

The volume containing 1 µg of RNA, 1µL of 10X reaction buffer with $MgCl_2$, 1µL of RNase-free DNase I, and DEPC-treated water to make up the 10µL reaction were added to an RNase-free tube and incubated at 37°C for 30 minutes, followed by the addition of 1 µL of 50 mM EDTA and incubated at 65°C for 10 minutes.

2.12.2 iScript cDNA Synthesis

The prepared DNase treated RNA was mixed with 4µL of 5x iScript reaction mix and nuclease-free water to make up 20µL reaction for each sample, and incubated at 25ºC for 5 minutes, at 42ºC 30 minutes, at 85ºC for 5 minutes, and then held at 4ºC before use or storage at -20ºC for further analysis.

2.13 Polymerase Chain Reaction (PCR)

To determine the expression of mRNA of interest, PCR analysis was performed using platinum PCR supermix (Invitrogen) along with the thermal cycler (Life Technologies). The cDNA synthesized from reverse transcription RNA, was amplified using specific primers to gene of interest by PCR analysis. Primer sequences and PCR reaction protocol used are described in each relevant Chapter.

After amplification of the specific gene of interest, the PCR product was visualised on an agarose gel (Sigma) along with a 100 base pair DNA ladder (Fermentas). Agarose gel was made with 1xTE (Sigma) buffer and the percentage of the gel used depended on the size of the amplicon of interest, ranging from 1-3 % agarose, with high percentage agarose used for smaller PCR products and a low percentage agarose used for larger amplicons. Expression analysis was achieved by comparing the band intensity normalised to a control gene product such as GAPDH.

2.14 Quantitative Real Time Polymerase Chain Reaction (Real-time PCR)

Real-time PCR was used to achieve relative quantitation of the mRNA expression of the gene of interest. Fast SYBR green master mix with DNA binding fluorochrome

(Life Technologies), 0.4 nM of specific forward and reverse primers for gene of interest, and the volume containing 0.2 µg cDNA were mixed and the real-time PCR reaction was run using the Viia7 real time PCR system (Life Technologies) to determine the relative gene expression. The fluorochrome in the reaction mix was excited by the laser light and emissions recorded every second. A relative value of the gene expression was obtained as the fluorochrome signal was produced proportional to the amplification of the PCR product. Untreated control sample from each experiment or known sample that expressed a gene of interest were used as standards. The volume containing 0.4 µg cDNA was used as the highest concentration of 1, and serially diluted 1:2 to generate a 6-point standard curve of 1, 0.5, 0.25, 0.125, 0.0625, 0.0313, and 0, and a relative expression quantity was calculated based on the standard curve generated. The relative data obtained was then normalised to the relative expression of endogenous control *GAPDH*. Specificity of PCR amplification and absence of primer dimers were ensured using melt-curve analysis. Primers were ordered from Eurofins and primer sequences are described in Appendix I.

2.15 Cell viability assay (MTS)

Suspension cell lines such as 5TGM1-GFP murine myeloma cells or RPM1 8226 human myeloma cells were plated at $5x10^5$ cells/ml and treated with appropriate compound of interest for the length of times indicated. Adherent cell lines such as ST2 murine bone marrow stromal cells (BMSCs), 2T3 murine osteoblasts, or HS5 human BMSCs were plated at 5×10^4 cells/ml and treated with appropriate compound of interest for different time points. Cells were treated in either complete medium or serum free condition, according to the experimental requirements. At the end of experimental

time points, cell viability *in vitro* was measured using a colorimetric CellTiter 96® AQueous Non-Radioactive Cell Proliferation Assay (Promega).

This assay used the novel tetrazolium compound (3-(4,5-dimethylthiazol-2-yl)-5-(3-carboxymethoxyphenyl)-2-(4-sulfophenyl)-2H-tetrazolium, inner salt; MTS) and the electron coupling reagent, phenazine methosulfate (PMS). MTS was chemically reduced by cells into formazan, which was soluble in tissue culture medium. The measurement of the absorbance of the formazan was carried out using 96 well microplates at 492nm without additional processing. The conversion of MTS into aqueous, soluble formazan was accomplished by dehydrogenase enzymes found in metabolically active cells. The quantity of formazan product as measured by the amount of 490nm absorbance was directly proportional to the number of living cells in culture.

Since the production of formazan was proportional to the number of living cells, the intensity of the produced colour was a good indication of the viability of the cells. MTS solutions were prepared according to the manufacturer's instructions as follows. Stock PMS (Sigma) was dissolved in PBS at a concentration of 0.92mg/ml (0.92mg/ml PMS in PBS was also included with the CellTiter 96® AQueous Assay System from Promega). The solutions were then stored in light-protected tubes at -20°C. MTS and PMS detection reagents were mixed, using a ratio of 20:1 (MTS:PMS), immediately prior to addition to the cell culture at a ratio of 1:5 (detection reagents:cell culture medium), and incubated for 3 h before the 492nm absorbance reading using SPECTRA max 384 plus plate reader (Molecular devices).

2.16 Protein extraction

Protein extraction from treated or untreated suspension cells, adherent cells, and bone marrow lysates from murine models was performed using RIPA buffer (Thermo Scientific), protease inhibitors (Roche), and phosphatase inhibitors (Sigma-Aldrich). Protease (50x) and phosphatase inhibitors (100x) were added to RIPA buffer immediately before use to a final concentration of 1x and protein extraction procedures for suspension and adherent cells were followed as described below.

2.16.1 Procedure for lysis of cells cultured in suspension or murine bone marrow cells

The suspension cells were pelleted by centrifugation at 2500g for 5 minutes. For protein extraction from murine bone marrow cells, bone marrow was first flushed by centrifuging mouse tibia and femur as described in section 2.4. The supernatant was discarded and cells were washed twice in cold PBS, followed by centrifugation at 2500g for 5 minutes. RIPA Buffer was added to the cell pellet, 300 µL of RIPA buffer was used for 40mg (approximately 5×10^6 cells) of wet cell pellet. The mixture was pipetted up and down to suspend the pellet. To increase yields, the pellet was sonicated for 30 seconds. The mixture was then gently shaken for 15 minutes on ice, followed by centrifugation at 14,000g for 15 minutes to pellet the cell debris. Supernatant was transferred to a new tube for further analysis.

2.16.2 Procedure for lysis of monolayer-cultured adherent cells

Cultured medium from adherent cells was carefully removed (decanted) and cells were then washed twice with cold PBS. Cold RIPA Buffer was added to the cells, 300 µL of buffer was used per $75cm^2$ flask with approximately 5×10^6 cells. The lysate was

gathered to one side using a cell scraper, the lysate was collected and transferred to a microcentrifuge tube. Samples were then centrifuged at ~14,000 rcf for 15 minutes to pellet the cell debris. To increase yields, cell pellet was sonicated for 30 seconds and supernatant was transferred to a new tube for further analysis.

2.17 Quantitation of protein concentration

The total concentration of the protein was determined by using the total protein assay (Micro BCA Reagent, Pierce). Firstly, a 9 point standard curve, 2000, 1500, 1000, 750, 500, 250, 125, 25, 0 µg/ml, was prepared by diluting 2mg/ml bovine serum albumin (BSA) (Pierce). Sample protein lysates were diluted 1:10 in RIPA buffer and samples were added to the clear 96-well plate in duplicate. Working substrate solution was prepared by making 50:1 ratio for substrate A:B solution as per manufacturer's instruction. 200µl/well of working substrate solution was added to the standards and sample wells, and mixed by gentle tapping of the plate, and incubated in the 37°C incubator for 30 minutes. At the end of the incubation time, the plate was read at 562nm using an SPECTRA max 384 plus plate reader (Molecular devices). The total protein concentration was calculated from the standard curve generated by the standards.

2.18 Western blotting

Western blot analysis was performed to measure the protein expression of interest in cell lines, serum of murine models and human patients, and murine bone marrow lysates. Total protein BCA assay was performed as mentioned in the previous section, to ensure equal loading 20µg of total protein of each experimental sample was used. To each 20µg experimental protein sample, 4x NuPAGE LDS sample buffer (1/4 of total volume) and 10x NuPAGE sample reducing agent (1/10 of total volume) (Life

Technologies) were added and protein samples were denatured in dry heat block for 5 minutes.

The gel tank was prepared using Tris-HCl 4-20% gradient pre-cast gels (Bio-rad) and filled with 1x tris glycine SDS running buffer (100mL of 10x tris glycine SDS running buffer + 900mL of distilled water, Bio-Rad). The calculated volume for 20µg protein was loaded in each well of the gel, along with a protein standard ladder, Precision Plus Protein Kaleidoscope (Bio-rad). The gel was run at 170 volts for 30-45 minutes until the dye front reached the bottom of the gel.

The PVDF membrane (Millipore) was activated in 100% methanol (Thermo Scientific) for 1 minute. The activated membrane and filter papers were soaked in 1x transfer buffer (100mL of 10x tris glycine transfer buffer + 200mL methanol+700mL of distilled water, Bio-Rad). The gel was removed from the gel tank and trimmed to remove the loading gel and excess areas. A Trans-Blot Turbo transfer system (Bio-Rad) was used to transfer the protein from the gel to the PVDF membrane, A sandwich was placed in the Trans-Blot in the following order; a piece of filter paper, membrane, gel, and second piece of filter paper. The appropriate program/time for transfer was selected according to the molecular weight of the protein of interest, ranging from 3-30 minutes for low-high molecular weight proteins. Once the transfer process was completed, the membrane was removed, rinsed briefly in methanol and allowed to air dry.

The membrane was placed in the blocking buffer with 5% bovine serum albumin (BSA, Sigma-Aldrich) in tris buffered saline (TBS, Sigma-Aldrich) with 0.1% tween 20 (Sigma-Aldrich) to block the non-specific binding to the membrane, and incubated for 1h at room temperature while shaking gently on a plate shaker. At the end of the blocking period, the membrane was incubated in the primary antibody in the blocking

buffer overnight at 4°C. The following day, the membrane was washed 3 x 10 minutes in TBS with 0.1% tween 20 (TBST), before incubating with secondary antibody diluted in 5% milk in TBST for 1h at room temperature. The membrane was washed 3 x 10 minutes with TBST.

While the membrane was being washed, luminescent reagent (ECL plus, Amersham Life Sciences) was prepared as 40:1 ratio of reagent A:B. the membrane was then incubated in luminescent mixture for 5 minutes at room temperature, before transferring to cling film and taped smoothly to a film developing cassette. Photographic film (FUJI) was exposed to the membrane in the dark room from seconds to minutes based on the signal strength of the protein expression of interest. The film was then developed using a Curix 60 processor (AGFA).

To strip and re-probe with a different antibody of interest, the membrane was incubated in restore plus western blot stripping buffer (Thermo Scientific) for 20 minutes at room temperature. The membrane was then washed with TBST for 6 x 5 minutes. Then the membrane was ready to repeat the entire process of blocking, incubating with a different primary antibody as described above. Protein expression of interest was quantitated by densitometry, using ImageJ analysis.

2.19 Statistical analysis

Statistical significance was determined using a student T test or one-way anova and Tukey-Kramer posthoc test or multiple comparisons were used for analysis of multiple groups in both *in vivo* and *in vitro* studies. *In vivo* experiments were repeated twice and *in vitro* studies were repeated at least 3 times and considered significant given $p<0.05$. Data were represented as mean ± SE unless otherwise stated.

2.20 List of antibodies

All antibodies used were listed in the tables below, except for the primary antibodies used in Chapter 3 listed separately under section 3.2.7, Table 3.1.

Table 2.2 List of primary antibodies

Antibody (Name)	Host	Reactivity	Type	Source	Application
Phospho-histone H3	Rabbit	H, M	polyclonal	Millipore (06-570)	IHC 1:1000
IgG2b (heavy chain)	Rat	M	monoclonal	Fitzgerald (10R-I118A)	ELISA 1:500
Adiponectin	Rabbit	M	polyclonal	Abcam (ab3455)	WB 1:1000
Cleaved-caspase 3	Rabbit	H, M	polyclonal	Cell signalling (9664)	WB 1:1000
Cleaved-PARP	Rabbit	H, M	polyclonal	Cell signalling (9544S)	WB 1:1000
p53	Rabbit	M	polyclonal	Cell signalling (2524)	WB 1:1000
Phospho-AMPK	Rabbit	H, M	polyclonal	Cell signalling (2537S)	WB 1:1000
AMPK	Rabbit	H, M	polyclonal	Cell signalling (2532S)	WB 1:1000
SIRT1	Rabbit	H, M	polyclonal	Millipore (07-131)	WB 1:1000
NFκB p65	Rabbit	H, M	polyclonal	Abcam (ab16502)	WB 1:1000
β-actin	Mouse	H, M	monoclonal	Sigma aldrich (A53160)	WB 1:20,000

Abbreviations - H; human, M; mouse

IHC; immunohistochemistry, ELISA; enzyme linked immunosorbent assay, WB; western blot

Table 2.3 List of secondary antibodies

Antigen (Name)	Host	Source	Application
Anti-Mouse immunoglobulins/peroxidase	Rat	Dr. Oyajobi, University of Texas, San Antonio	ELISA 1:5000
Biotinylated Anti-Rabbit IgG	Goat	Vector Labs (BA-1000)	IHC 1:1000
Anti-Goat immunoglobulins/HRP	Rabbit	Dako (P0160)	WB 1:2000
Anti-Mouse immunoglobulins/HRP	Rabbit	Cell signalling (7076S)	WB 1:5000
Anti-Rabbit immunoglobulins/HRP	Horse	Cell signalling (7074S)	WB 1:5000

Abbreviations - HRP; horseradish peroxidase

IHC; immunohistochemistry, WB; western blot, ELISA; enzyme linked immunosorbent assay

Chapter 3 : The role of host-derived MMP7 in myeloma development *in vivo*

3.1 Introduction

3.1.1 MMP7 and osteolytic bone disease

Despite new advances in therapeutic drug development for myeloma and the associated bone destruction, this disease remains fatal. There is increasing evidence demonstrating the important role of the host bone marrow microenvironment in the myeloma pathogenesis. Once the malignant plasma cells start growing in the bone marrow, they interact with different types of cells including osteoblasts, osteoclasts, and stromal cells. Understanding the molecular mechanism of how myeloma cells interact with these cells within the host bone marrow microenvironment will help identify potential therapeutic targets against myeloma.

MMPs have been shown to regulate the tumour microenvironment and to be involved in the progression of various cancers, including prostate, breast, and liver cancer (Lynch et al., 2005;Takafuji et al., 2007;Thiolloy et al., 2009). The functions of MMPs depend on the balance between the MMPs and their inhibitors. Tissue inhibitors of matrix metalloproteinases (TIMPs) are known to negatively regulate the function of MMPs (Bramhall et al., 1997). In myeloma, we have previously shown that MMP9$^{-/-}$ decreased myeloma growth and the osteolytic bone disease as compared to wild type mice *in vivo*, suggesting that host-derived MMP9 promotes myeloma pathogenesis (Fowler et al., 2009).

MMP7 has been shown to be involved in prostate and breast cancer-induced osteolysis. $MMP7^{-/-}$ mice have been shown to have decreased osteolytic bone disease in the presence of prostate cancer cells via processing of soluble RANKL, suggesting that MMP7 may promote tumour induced bone disease (Lynch et al., 2005). Also, it has been shown that MMP7 deficient mice have a reduction in osteolytic lesions and an increase in trabecular bone volume when breast cancer cells are inoculated intra-tibially, compared to WT control (Thiolloy et al., 2009). In addition, reduced MMP7 levels and increased levels of its inhibitor, TIMP1, has been shown to be involved in obesity where a normal level of MMP7 can be restored by weight reduction (Ress et al., 2010;Meissburger et al., 2011). Based on these studies, we hypothesized that MMP7 may play a role in the development and progression of myeloma and the associated bone disease. Fowler et al. has demonstrated that $RAG2^{-/-}$ mice are permissive to myeloma growth, similar to the well-established 5T Radl murine model of myeloma which develops features that mimics human myeloma pathogenesis and the associated bone disease (Fowler et al., 2009). To investigate this, $RAG2^{-/-}$; $MMP7^{-/-}$ mice were used to look into the murine myeloma model that can be manipulated at the molecular level.

3.1.2 Substrates of MMP7

It has been reported that MMP7 can cleave multiple substrates (Section 1.4.4). In the present study, two known substrates of MMP7, osteopontin and galectin-3 were investigated to determine whether these substrates play a role in myeloma pathogenesis in relation to MMP7.

Osteopontin

Osteopontin (OPN) is produced by tumour cells, osteoblasts and stromal cells of the bone environment. OPN is known to be cleaved by MMP3, MMP7, MMP9, and thrombin (Agnihotri et al., 2001;Takafuji et al., 2007;Hasegawa et al., 2011). OPN is a matrix component shown to be associated with myeloma and bone remodelling, which makes it a good candidate to investigate in my study (Alford and Hankenson, 2006). In addition, OPN has been shown to act as a chemo-attractant for myeloma cell migration (Caers et al., 2006).

Importantly, OPN is known to be associated with myeloma both in mouse models and in patients, where elevated OPN levels correlate with disease severity (Robbiani et al., 2007;Caers et al., 2006). Takafuji et al. demonstrated that a 5kDa OPN fragment cleaved by MMP9 has a crucial role for tumour cell invasion in hepatocellular carcinoma (Takafuji et al., 2007). OPN cleaved by caspase 8 has been shown to mediate hypoxia induced HeLa cell death through p53 and a caspase cleavage-resistant OPN mutant suppressed hypoxia induced cell death (Kim et al., 2009). These data suggest that cleavage and alterations in functional OPN levels may play a different role from a full length un-cleaved OPN.

A positive correlation between OPN and MMP9 was observed in patients with prostate cancer. Plasma levels of OPN and MMP9 were significantly increased with prostate cancer progression and prostatectomy (Castellano et al., 2008). Overexpression of OPN was observed in 4T1 bone metastatic murine breast cancer cells as compared to the non-metastatic 4T07 cell line from the same parental population (Mi et al., 2004). Interestingly, thrombin-cleaved carboxy-terminal OPN peptide was shown to bind with

a metastatic marker cyclophilin to CD147 (a cell surface glycoprotein and extracellular MMP inducer), which in turn promoted migration and invasion (Mi et al., 2007).

Galectin-3

Using a candidate list of substrates of MMP7, galectin-3 was identified. Galectin-3 is cleaved by MMP7 and inhibition of galectin-3 induces myeloma cell death both *in vitro* and *in vivo*, which makes it a good candidate for this study (Puthenedam et al., 2011;Streetly et al., 2010;Mirandola et al., 2011). Furthermore, galectin-3 is expressed by myeloma cells, and an increase in serum concentrations of galectin-3 was observed in patients with various cancers, although serum levels of galectin-3 have not been investigated in myeloma (Iurisci et al., 2000). A galectin-3 antagonist GCS-100 was shown to induce human and primary myeloma cell death through activation of caspase-8 and -9, and down regulation of activated NFκB/AKT pathways (Streetly et al., 2010). Additionally, intravenous treatment of galectin-3C (N-terminally truncated dominant negative inhibitor of galectin-3) was shown to enhance the anti-myeloma effect of bortezomib in a model where U266 human myeloma cells were subcutaneously injected into NOD/SCID mice (Mirandola et al., 2011).

Galectin-3 is a part of the protein family that contain β-galactoside-binding lectins. Its structure is composed of 3 distinct domains including; the carboxy-terminal domain with carbohydrate-recognition domain (CRD), the amino-terminal N domain, and R domain with repeating Pro-Gly-Tyr rich motifs (Herrmann et al., 1993). The CRD domain of galectin-3 appears to play a major role in cell-cell adhesion and metastasis. Adhesion of cancer cells to endothelial cells and adhesion between cancer cells are critical steps in various cancer intravascular metastases. Zou et al has reported that blocking the galectin-3 CRD domain with galectin-3 specific synthetic peptides

inhibited the cell adhesion of the human breast cancer cell line MDA-MB-435 to HBME-1 endothelial cells, and the aggregation of those breast cancer cells (Zou et al., 2005).

Galectin-3 has been shown to be involved in the metastasis of various cancers and Simone et al reported that galectin-3 coats the breast cancer cell membrane by CRD and that membrane coating galectin-3 has an enhanced metastatic phenotype as compared to the free circulating galectin-3 (Simone et al., 2014).

Galectin-3 is also cleaved by MMP2 and MMP9 at the Ala62-Tyr63 site, and the cleavage product of 22kDa fragment with intact CRD increased the binding affinity to the glycoconjugates by changing the CRD domain. This change leads to an alteration of biological function of galectin-3 (Ochieng et al., 1998). This study suggests that full-length 30kDa galectin-3 protein may have different biological impact from the cleaved galectin-3 fragments.

3.1.3 Aim

The aim of this study was to determine the effect of host-derived MMP7 in myeloma pathogenesis and to determine the effect of cleavage of MMP7 susbtrates osteopontin or galectin-3 in disease development.

To achieve these aims, myeloma development in MMP7 deficient mice was studied. *In vitro* studies were conducted to determine the effect of MMP7, OPN and galectin-3 in myeloma cells and osteoblasts. Serum levels of MMP7, OPN and galectin-3 in myeloma patients were analysed to correlate with *in vivo* and *in vitro* studies.

3.2 Materials and Methods

3.2.1 Overexpression of MMP7 by transduction

5TGM1 murine myeloma cells were transduced with 10^5 IFU/ml of lentiviral particles made from pLenti-suCMV(mMMP7)-Rsv(Puro)MMP7 and empty vector control lentivector (Amsbio). MMP7 overexpressed and empty vector (EV) transduced 5TGM1 myeloma cell lines were cultured in suspension with RPMI 1640 media supplemented with 10% fetal bovine serum (Biosera), 1% L-glutamine, 1% sodium pyruvate, 1% non-essential amino acid, and 1% penicillin/streptomycin and 5µg/ml puromycin (Sigma-Aldrich) at 37°C in 5% CO_2. Previous work in the Edwards lab has shown that 5µg/mL of puromycin was sufficient to kill 5TGM1 myeloma cells. After transduction, MMP7 expression was confirmed by real-time PCR analysis.

3.2.2 *In vivo* studies

To determine the effect of host-derived MMP7 on myeloma (MM) development *in vivo*, 5TGM1-GFP myeloma cell growth in $MMP7^{-/-}$ mice on a $RAG2^{-/-}$ background was assessed. In this study, $RAG2^{-/-}$;$MMP7^{-/-}$ ($MMP7^{-/-}$) or $RAG2^{-/-}$;$MMP7^{+/+}$ (WT) littermate mice were intravenously inoculated with $5x10^5$ 5TGM1-GFP murine myeloma cells or PBS control (WT, n=7; $MMP7^{+/+}$, n=4; WT MM, n=8; $MMP7^{+/+}$ MM, n=5) (Figure 3.1A).

To determine the effect of tumour-derived MMP7, KaLwRij mice were intravenously inoculated with 5 x 10^5 MMP7-overexpressing or empty vector 5TGM1-GFP myeloma cells, generated as described in section 3.2.1. Myeloma tumour burden and the associated bone disease was assessed by ELISA, number of GFP positive cells in the bone marrow and spleen, microCT and histological analysis (Chapter 2 and Figure

3.1B). All the mice used in these studies were age, sex, weight matched and studies were approved by the ethics committee of the Vanderbilt University, University of Oxford and the United Kingdom Home Office.

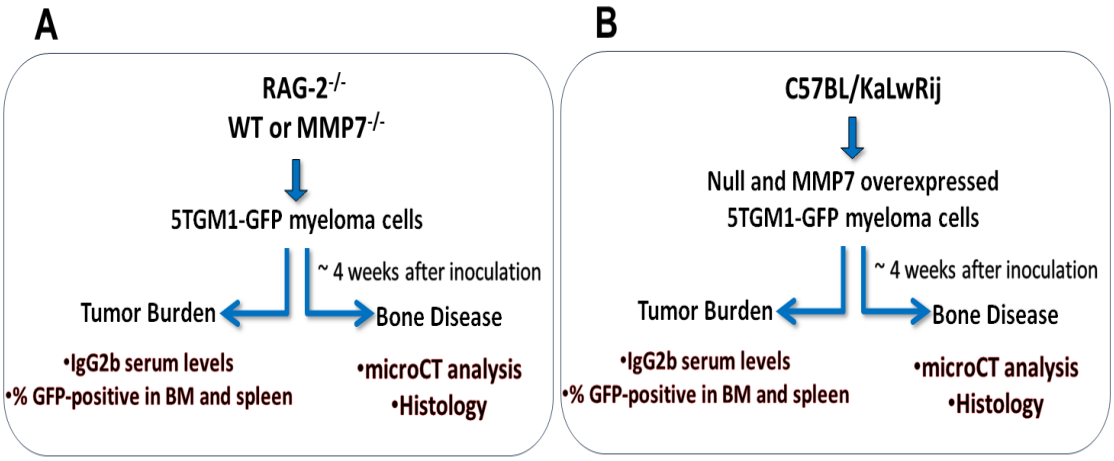

Figure 3.1. Experimental design for *in vivo* studies investigating the role of MMP7 in myeloma development.

3.2.3 Viability assay

5TGM1-GFP murine or RPMI 8226 human myeloma cells were plated at $5x10^5$ cells/mL in 96-well plate and treated with 0-50 ng/mL recombinant human active MMP7 (Millipore) for 48h, or with 0-20 µg/mL recombinant mouse OPN (R and D Systems) for 48h, or with 5µg/mL recombinant mouse OPN and 100ng/mL active MMP7 (pre-incubated at 37°C for 20 minutes to allow for the cleavage of OPN by MMP7) for 24 and 48h, or with 0-3 µg/mL recombinant mouse galectin-3 (R and D Systems) for 48h, or with 5µg/mL recombinant mouse galectin-3 and 200 ng/mL active MMP7 (pre-incubated at 37°C for 20 h to allow for the cleavage of galectin-3 by MMP7) for 24 and 48h. All cell lines were treated in serum free media. At the end of

each time point, viability was measured using a colorimetric CellTiter 96® AQueous Non-Radioactive Cell Proliferation Assay (Promega) as described in section 2.15.

3.2.4 Silver staining

Full-length and MMP7-cleaved galectin-3 fragments were visualized by silver staining of proteins in polyacrylamide gel, using high sensitivity silver ammonia staining with formaldehyde fixation protocol developed by Chevallet et al. (Chevallet, Luche and Rabilloud, 2006). The gel was placed in water following electrophoresis, and was rinsed for 5–10 minutes. It was then submerged in 20% ethanol containing 10% (v/v) formalin for 1 hour, followed by rinsing 2×15 min in water. The gel was sensitized overnight in 0.05% naphtalene disulfonate, followed by rinsing 6×20 minutes in water and impregnating for 30–60 minutes in silver-ammonia solution. The gel was rinsed 3×5 minutes in water and image was developed for 5–10 minutes in acidic developer (350 μ M citric acid containing 1 ml formalin per litre). The most intense bands or spots appeared within 1–2 minutes. Development was stopped in EA stop solution, 0.5% (v/v) ethanolamine and 2% (v/v) acetic acid, and left in it for 30–60 minutes. Finally, the gel was rinsed with several changes of water prior to scanning on the Epson transparency scanner.

3.2.5 Co-culture experiments

2T3 osteoblasts were plated at $5x10^4$ cells/ml in black 96-well plates with the volume of 100µl/well. Once 2T3 cells adhered after 6 h, the volume of 100µl/well at $1x10^5$ cells/ml of 5TGM1-GFP myeloma cells were added directly on top of the 2T3 cells to set up a direct co-culture *in vitro* system. The cells were treated with 2µg/mL of anti-galectin-3 neutralising antibody or isotype control (Novus Biologicals) in serum free

conditions for 72h and the number of 5TGM1-GFP myeloma cells were measured by GFP fluorescence reading using FLUOstar OPTIMA (BMG) (Ramasamy et al., 2012).

3.2.6 Human patient samples

Serum samples from myeloma patients, patients with MGUS, and the age, sex, and body mass index (BMI) -matched controls were obtained from Matthew T. Drake, M.D., Ph.D., Mayo Clinic, Rochester, MN, USA. Studies were conducted with approval from the Institutional Review Board and Biospecimen Protocol Review Group of the Mayo Clinic.

3.2.7 ELISAs

Serum concentrations of myeloma paraprotein IgG2bκ in myeloma-bearing and non-tumour (NT) mice were measured as described in section 2.5. Serum concentrations of human and murine MMP7, TIMP1, OPN were measured according to the manufacturers' instructions using commercially available ELISA kits (R and D Systems).

3.2.8 Western blotting

Recombinant OPN or galectin-3 were incubated with MMP7 at 37ºC for 20 minutes or 20h respectively prior to gel electrophoresis. The expressions of full length and cleaved OPN and galectin-3 were determined in serum of myeloma patients, or serum and bone marrow of myeloma-bearing mice. 20 µg of protein from bone marrow lysates or 1 µL of both human and murine serum samples diluted in PBS were loaded to each lane of the gel. Samples were then separated by 4-20% precast SDS-PAGE gels (Bio-Rad), transferred to PVDF membranes, blocked in TBS plus 5% BSA and 0.1% TWEEN-20 for 1 hr, and incubated with primary antibody of interest (Table 3.1) at 4ºC overnight.

Antigen-antibody complexes were detected using secondary antibodies conjugated to HRP, anti-rabbit (1:5000 dilution, Cell signalling), anti-goat antibody (1:2000 dilution, Dako), anti-mouse antibody (1:5000 dilution, Cell signalling), and visualized by enhanced chemiluminescence plus reagent (GE Healthcare). Densitometry was performed using ImageJ software.

Table 3.1 List of primary antibodies for western blotting

Antigen (Name)	Epitope	Host	Reactivity	Type	Source	Dilution
OPN*		Rb	H	polyclonal	Rockland (100-401-4040)	1:1000
OPN#		G	M	polyclonal	R and D systems (AF-808)	1:1000
Galectin-3#	C-terminus	Rb	H, M, R	polyclonal	Abcam (ab53082)	1:1000
Galectin-3*	C-terminus	Rb	H	polyclonal	Abcam (ab31707)	1:700
Galectin-3*	N-terminus	Rb	H, M, P	polyclonal	LSBio (LS-B4682)	1:1000
Galectin-3#	N-terminus	M	H, M	monoclonal	Novus Biologicals (NBP1-42384)	1:500

H = human, M = mouse, R = rat, P = pig, Rb = rabbit, G = goat
* used for human, # used for mouse samples

3.2.9 Real-time PCR

RNA from cell lines and bone marrow lysates was isolated using the RNeasy kit (Qiagen). The cDNA was generated using iScript cDNA synthesis kit (Bio-Rad). Mouse MMP7 and galectin-3 were detected using Fast SYBR green Gene Expression assay primer sets (Life Technologies). Relative gene expression of MMP7 and galectin-3 was normalized to the Fast SYBR Green Gene Expression assay for human/mouse GAPDH (Life Technologies). All primers were purchased from Eurofins and primer sequences are described in Appendix I.

3.2.10 Gelatin and casein zymography

The activity of MMP9 and MMP2, or MMP7 in serum samples from patients were quantitated using gelatin or casein zymography respectively as described in Galewska et al. (Galewska et al., 2010).

To investigate the activity of MMP9 and MMP2, 1 µL of serum sample from patients with myeloma and controls were diluted in 9 µL of PBS, and 2.5 µL of 4x loading buffer (Life Technologies) added to each sample, mixed well, and loaded into 10% precast gelatin zymogram gels (1% geletin) from Life Technologies and electrophoresed in western blot running buffer (TGS) at 125V for 90 minutes.

To determine MMP7 activity, 3 µL of serum sample from patients with myeloma and controls were diluted in 7 µL of PBS, and added 2.5 µL of 4x loading buffer (Life Technologies) to each sample, mixed well, and loaded into 4-16% precast zymogram blue casein gels (Life Technologies) and electrophoresed in western blot running buffer (TGS) at 125V for 120 minutes.

After electrophoresis, the gels were washed in 2.5% (v/v) Triton-X 100 in milliQ water for 30 minutes at room temperature to extract SDS from the gel. After washing, the gels were transferred to the developing buffer (0.05M Tris HCl pH 7.4, 0.2M NaCl, 0.005M $CaCl_2$, 0.02% NaN_3 sodium azide, 1% Triton X-100) and incubated at 37ºC overnight for gelatin zymography or 72h for casein zymography. The gels were then stained by coomassie blue staining and destain with 1% acetic acid, 50% methanol in water. Clear white protease bands should appear on the blue gel at 92kDa for MMP9, 72kDa for MMP2, or at approximately 100kDa for pro-MMP7 and at 75kDa for active MMP7 activity. The gels were then scanned using a transparency scanner and quantitated by densitometry using ImageJ software.

3.2.11 MMP7 activity assay

MMP7 activity in serum of myeloma patients and controls were measured according to the manufacturers' instructions using a substrate based proprietary MMP7 activity assay kit in development (QuickZyme).

This assay in development was aimed to measure MMP7 activity in various biological samples such as serum, plasma, urine, and conditioned culture media. It used a modified pro-enzyme as a substrate in a 96-well plate format. Each well of the 96-well plate was coated with anti-MMP7 capture antibody for 2 hours at 37° C, followed by the addition of diluted (1:15) serum samples to the wells and incubated overnight at 4° C. The wells were washed with wash buffer provided in the kit. Detection reagent containing detection enzyme and chromogenic substrate was added to each well. Active MMP7 in the serum samples was able to release colour from a chromogenic peptide substrate. Colorometric absorbance was read at 405nm using SPECTRA max 384 plus plate reader (Molecular devices).

3.3 Results

3.3.1 Tumour burden is increased in myeloma-bearing MMP7$^{-/-}$ mice

To determine the role of host-derived MMP7 in the development of multiple myeloma, MMP7$^{-/-}$ or littermate WT mice were inoculated with 5TGM1-GFP myeloma cells and tumour burden was analysed by quantifying the myeloma specific IgG paraprotein and GFP positive cells. A significant increase in tumour burden in myeloma-bearing MMP7$^{-/-}$ mice was observed by an increase in IgG2bκ levels and GFP-positive myeloma cells in the bone marrow and spleen, as compared to myeloma-bearing WT mice (Figure 3.2A and B). Further analysis showed that proliferation of myeloma cells within the MMP7$^{-/-}$ environment was greater than that in WT animals by phospho-histone H3 staining (Figure 3.2C). A significant decrease in myeloma cell apoptosis was observed in myeloma-bearing MMP7$^{-/-}$ mice by TUNEL staining (Figure 3.2D). The group size of animals used in each experiment was partially dependent on the number of animals available from breeding provided by the collaborators.

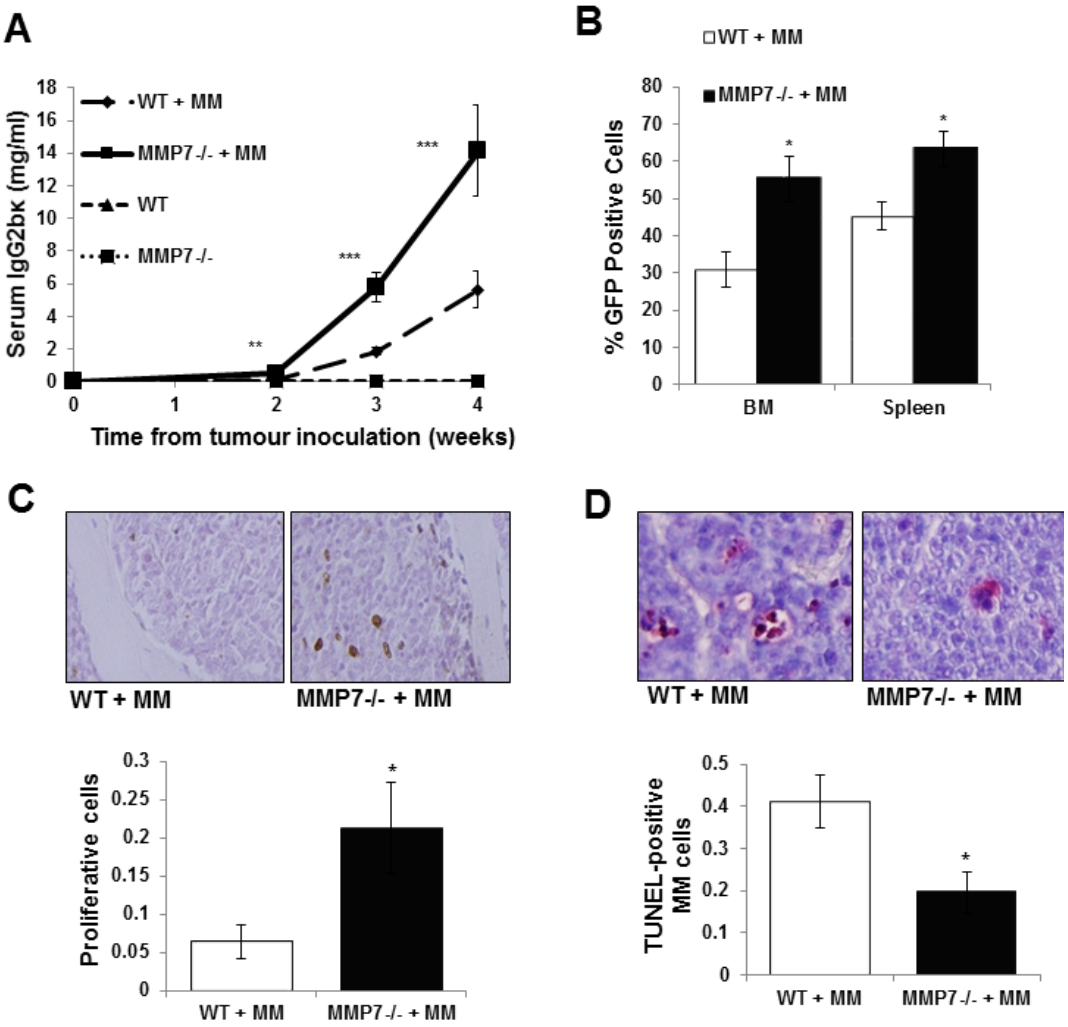

Figure 3.2. MMP7-/-mice inoculated with 5TGM1-GFP myeloma (MM) cells resulted in a significant increase in the rate of tumour growth. Tumour burden measured by (A) serum IgG2bκ concentrations, (B) % of GFP-positive myeloma cells in the bone marrow and spleen, by FACS analysis, (C) myeloma cell proliferation in the bone marrow, quantitated by phosphor-histone H3 IHC staining, (D) myeloma cell apoptosis, quantitated by TUNEL staining. Data represent as mean ± SEM. *p<0.05, **p<0.01, ***p<0.001 as compared to WT. (WT, n=7; KO, n=4; WT MM, n=8; KO MM, n=5), group size dependent on number of animals available from breeding by the collaborators.

3.3.2 Increased osteolytic bone disease in myeloma-bearing MMP7$^{-/-}$ mice

MicroCT analysis demonstrated a significant decrease in trabecular bone volume and an increase in osteolytic lesions in myeloma-bearing MMP7$^{-/-}$mice as compared with myeloma-bearing WT mice (Figure 3.3A and B). Combined data of tumour burden and the associated bone disease suggests that host MMP7 plays a protective role in

myeloma. Interestingly, this study has shown the opposite result from the contributory role of MMP7 in prostate and breast cancer (Lynch et al., 2005;Thiolloy et al., 2009). However, at this stage, the mechanism through which MMP7 may be protective against myeloma is unclear.

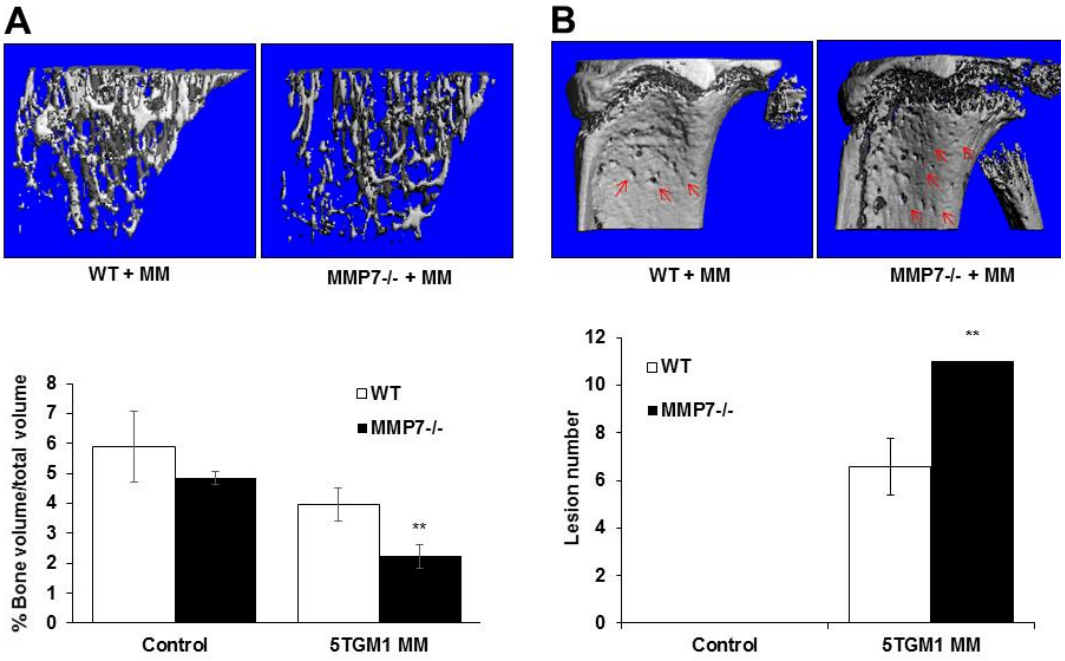

Figure 3.3. Myeloma-bearing (MM) MMP7$^{-/-}$ mice have a significant increase in osteolytic bone disease. (A) Trabecular bone volume was decreased, and (B) osteolytic lesions were increased in myeloma bearing MMP7$^{-/-}$ mice, as compared to myeloma bearing WT mice quantitated by microCT analysis. Data represent as mean ± SEM. **p<0.01 as compared to WT. (WT, n=7; KO, n=4; WT MM, n=8; KO MM, n=5)

3.3.3 Patients with myeloma have a decrease in circulating MMP7 activity with no change in concentration

To determine the clinical relevance of my *in vivo* data, the activity of MMP7 in the serum of myeloma patients was measured by casein zymography and confirmed by substrate based MMP7 activity assay. Galewska et al. has reported that using casein zymography, high molecular weight complexes of MMP7 were detected above 54kDa, which was observed in serum samples in this study (Galewska et al., 2010). Using

zymography and a substrate based assay, a significant decrease in MMP7 activity was observed in serum of myeloma patients as compared to the matched controls (Figure 3.4A and B) with no difference in the concentration of MMP7 as measured by ELISA (Figure 3.4C).

There was a negative correlation between the level of MMP7 activity (densitometry quantitation from casein zymography) and serum monoclonal protein level in the serum of myeloma patients (Figure 3.4D). The Edwards lab has previously shown that in contrast to MMP7, host-derived MMP9 promotes myeloma (Fowler et al., 2009). As a control for MMP7 activity, gelatin zymography was carried out to measure MMP9 and MMP2 activity in serum of myeloma patients and controls. No significant difference was found in MMP9 and MMP2 activity (Figure 3.4E). Myeloma is preceded with a non-malignant condition known as monoclonal gammopathy of undetermined significance (MGUS). In contrast to patients with myeloma, no significant difference in MMP7 activity was found in the serum of MGUS patients with progression and no progression to myeloma, as measured by casein zymography (Figure 3.4F). Tumour-bearing mice also have decreased MMP7 activity measured by substrate based MMP7 activity assay as compared to non-tumour mice (Figure 3.4G).

Taken together, these data suggests a specific reduction in MMP7 activity is associated with myeloma.

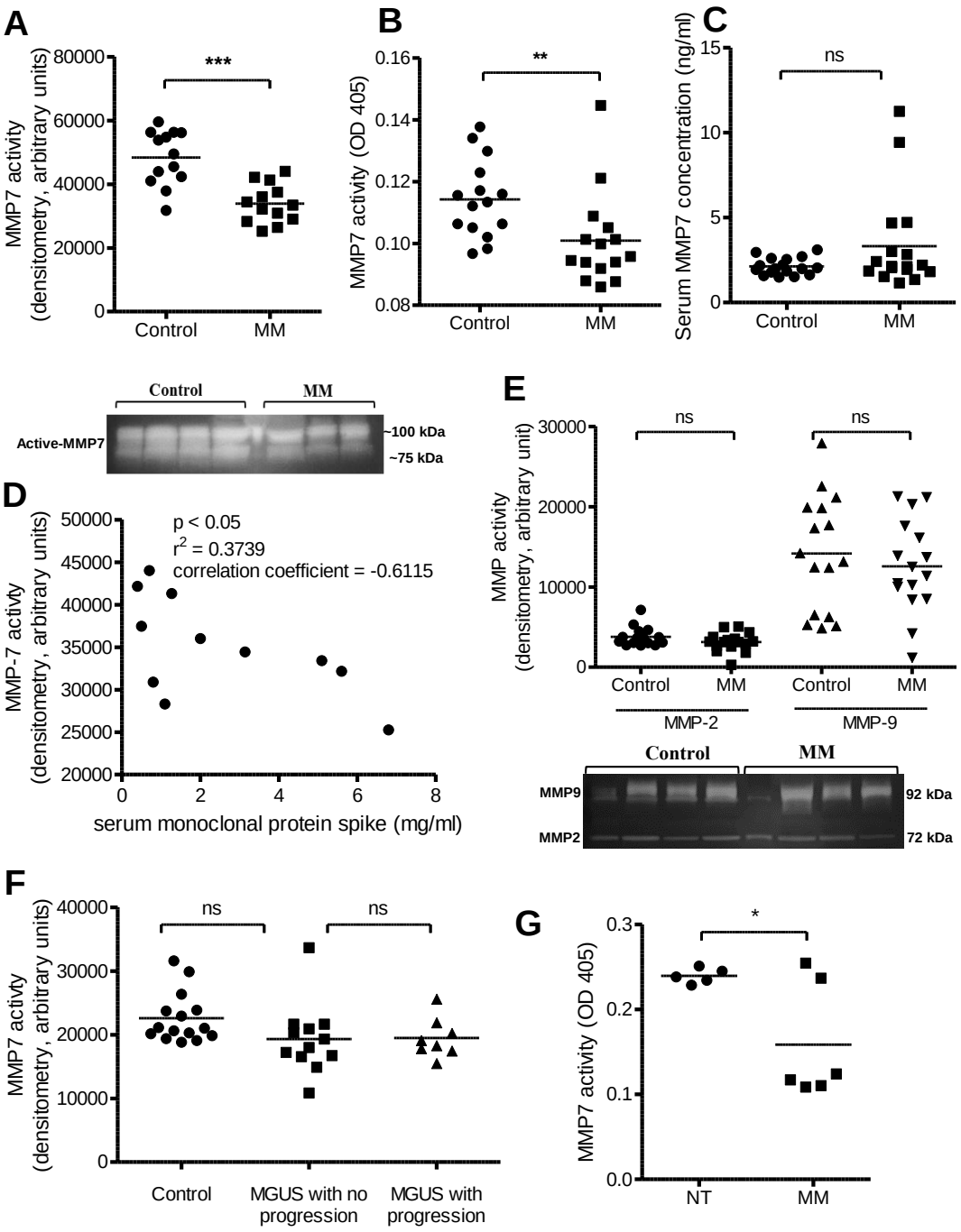

Figure 3.4. MMP7 activity is decreased in the serum of patients with multiple myeloma. Analysis of MMP7 activity in serum of control and myeloma patients (A) using casein zymography, quantitation by densitometry (B) using MMP7 activity assay (C) MMP7 expression in serum of control and myeloma patients, measured by ELISA (D) MMP7 activity relative to serum monoclonal protein expression in patients with multiple myeloma (E) Analysis of MMP9 and MMP2 activity in serum of control and myeloma patients, using gelatin zymography, quantitation by densitometry (control, n=16; MM, n=16) (F) Casein zymography analysis of MMP7 activity in serum of MGUS patients and matched controls, quantitation by densitometry (control; n=20, MGUS with no progression; n=12; MGUS with progression; n=8). (G) MMP7 activity in serum of control and myeloma bearing mice, using MMP7 activity assay (NT, n=5; MM, n=6). Gels images are representative images of the replicates. Data represent as mean ± SEM. *p<0.05, **p<0.01, ***p<0.001.

3.3.4 The endogenous MMP inhibitor TIMP-1 is increased in patients with myeloma and myeloma-bearing mice

Since my data suggest that MMP7 activity is decreased in myeloma, I have begun to investigate regulators of MMP7 in myeloma progression. TIMP1 is known to be a negative regulator of MMP7, MMP1, MMP3, and MMP9 (Bramhall et al., 1997).

PCR analysis for the expression of the inhibitor of MMP7, TIMP1, showed that 5TGM1-GFP myeloma cells express TIMP1 along with the osteoblast 2T3 cell line and normal mouse bone marrow stromal ST2 cell line while the mouse bone marrow stromal 14M1 cell line derived from myeloma permissive KaLwRij mice, do not express TIMP1 (Figure 3.5A). A significant increase in the level of TIMP1 expression was observed in serum of myeloma bearing KaLwRij and RAG2$^{-/-}$ mice as compared to non-tumour controls (Figure 3.5B). A significant increase in the level of TIMP1 expression was observed in the serum of myeloma patients, compared to controls (Figure 3.5C). These data indicate that a decrease in MMP7 activity in the serum of myeloma patients and myeloma-bearing mice is paralleled by an increase in the endogenous MMP inhibitor, TIMP1. However, the mechanism by which host-derived MMP7 protects against myeloma remains unknown.

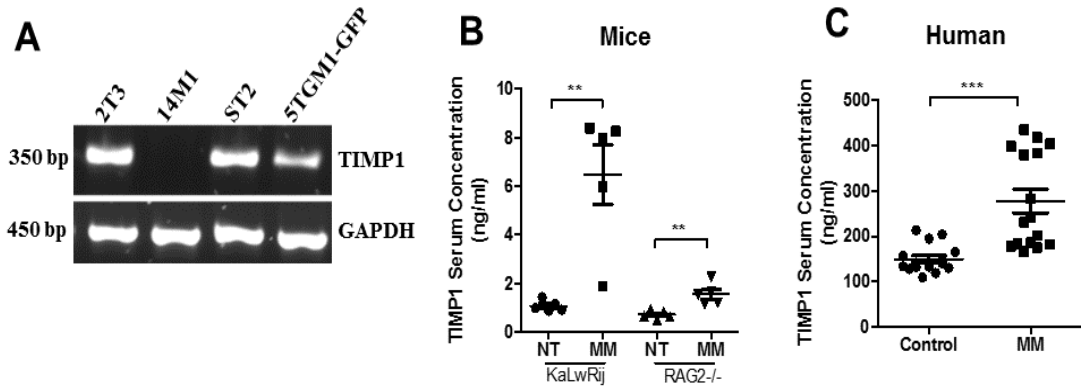

Figure 3.5. The endogenous MMP inhibitor TIMP1 is increased in patients with myeloma and myeloma-bearing mice. (A) TIMP1 expression is detected in 5TGM1 myeloma cells. (B) An increase in the serum concentration of TIMP1 in myeloma bearing KaLwRij and RAG2$^{-/-}$ mice (NT, n=5; MM, n=5 for each strain of mice) and (C) patients with multiple myeloma was detected by ELISA (control; n=16, MM; n=16). Data are mean ± SEM. **p<0.01, ***p<0.001.

3.3.5 Exogenous MMP7 decreases myeloma cell viability *in vitro*

My studies suggest that a loss of host-derived MMP7 promotes myeloma *in vivo*. To investigate whether tumour-derived MMP7 may also contribute to myeloma pathogenesis in the current study, MMP7 RNA expression was measured in 5TGM1-GFP myeloma cells by RT-PCR analysis. My data demonstrates that in contrast to osteoclasts, 5TGM1-GFP cells have very low expression of MMP7, suggesting that the effect of MMP7 in our murine model is most likely via host-derived and not tumour derived MMP7 (Figure 3.6A).

In contrast to human myeloma cells shown to express MMP7, 5TGM1-GFP murine myeloma cells used in the *in vivo* experiments have very low expression of MMP7 (Barillé et al., 1999). Hence, the direct effect of recombinant MMP7 *in vitro* was investigated in these murine myeloma cells. Treatment of 5TGM1 murine and RPMI 8226 human myeloma cells with recombinant MMP7 for 24 and 48h decreased their viability (Figure 3.6B).

To investigate the effect of tumour-derived and exogenous MMP7, 5TGM1 myeloma cells and 2T3 osteoblasts were transduced with empty vector (EV) control or MMP7 overexpression lentiviral particles and pooled stable cell lines were established. The expression of MMP7 after transduction was confirmed by real time PCR (Figure 3.6C). There was no significant decrease in the viability of control or MMP7 overexpressed 5TGM1 myeloma cells, measured by MTS assay (Figure 3.6D).

To determine the effect of exogenous MMP7 on myeloma cell viability, 5TGM1-GFP myeloma cells were co-cultured with empty vector control 2T3 osteoblasts or MMP7 overexpressing 2T3 osteoblasts. There was a significant increase in myeloma cell viability when co-cultured with control 2T3 osteoblasts, whereas this effect was abrogated when MMP7 was overexpressed in 2T3 osteoblasts, suggesting an anti-myeloma effect of exogenous MMP7 *in vitro* (Figure 3.6E).

However, MMP7 protein expression or activity was not determined in MMP7 overexpressing 5TGM1 myeloma cells and 2T3 osteoblasts. Therefore, it was difficult to draw a conclusion of whether anti-myeloma effect of exogenous MMP7 was dependent upon MMP7 actvity or expression remained unclear. Further studies are necessary to measure MMP7 protein expression or activity in MMP7 overexpressing 5TGM1 myeloma cell line and 2T3 osteoblast cells. Another limitation of this experiment was that generation of stable MMP7 overexpressing cell lines might have selected for non-functional variants with possible advantage to proliferation. Using inducible system in the presence of an inducer that allows for gene expression of interest might have an advantage over generating stable cell lines to produce the required gene expressing cell line without the transgene expression.

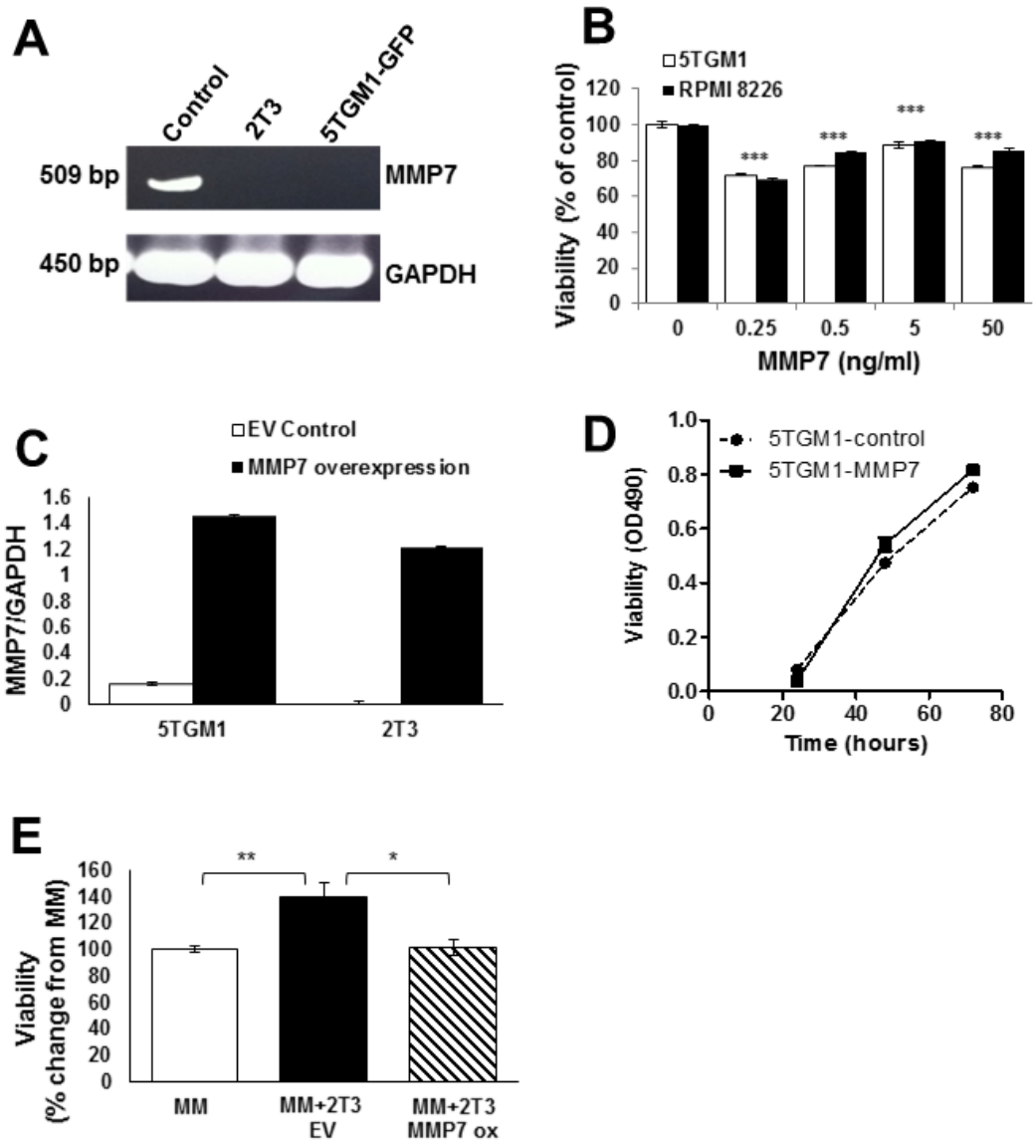

Figure 3.6. Exogenous MMP7 inhibits the growth of myeloma cells. (A) RT-PCR analysis of MMP7 expression in osteoclast cells as positive control, 2T3 osteoblast cells, and 5TGM1-GFP myeloma cells, (B) Effect of recombinant MMP7 treatment on 5TGM1-GFP murine and RPMI 8226 human MM cell viability, measured by MTS assay at 48h *in vitro* (C) qRT-PCR analysis of MMP7 expression in empty vector (EV) control and MMP7 overexpressing 5TGM1 myeloma cells and 2T3 osteoblasts. (D) Viability of EV control and MMP7 overexpressing 5TGM1 myeloma cells, measured by MTS analysis. (E) Viability of 5TGM1 myeloma cells (MM) when co-cultured with EV and MMP7 overexpressing (ox) 2T3 osteoblasts, measured by GFP fluorescence. Data are mean ± SEM. *p<0.05 and **p<0.01. ***p<0.001, as compared to control.

3.3.6 Tumour-derived MMP7 has no effect on myeloma tumour burden *in vivo*

To determine the effect of tumour-derived MMP7 *in vivo*, MMP7 overexpressing 5TGM1-GFP myeloma cells were inoculated into the KaLwRij murine myeloma model. There was no significant difference in myeloma development in the bone marrow or spleen or paraprotein, measured by the amount of myeloma specific serum paraprotein IgG2bk and the percentage of GFP positive cells in the bone marrow and spleen by flow cytometry respectively in mice inoculated with MMP7 over-expressed 5TGM1 myeloma cells as compared to controls (Figure 3.7A and B). This may be due to TIMP1 produced by myeloma cells inhibiting the MMP7 activity *in vivo* and abolishing the protective effect of MMP7. Alternatively, MMP7 expressed by the host stroma could be at a maximal saturated amount that additional MMP7 expression by the tumour cells did not have enhanced anti-tumour effect *in vivo*. It was also possible that MMP7 overexpressing 5TGM1 myeloma cells may not have a functional MMP7 protein expression or activity.

These data may further enhance the importance of host derived MMP7 rather than the tumour derived MMP7 in myeloma progression. However, the low tumour burden could likely be due to prolonged culture of cells, and renders it difficult to definitely draw conclusions from this study. Future studies will determine MMP7 activity in MMP7 overexpressing 5TGM1 myeloma cells. If there is an increase in MMP7 activity in those cells, inoculating them into MMP7 deficient mice will determine the effect of tumour derived MMP7 activity in myeloma pathogenesis *in vivo.*

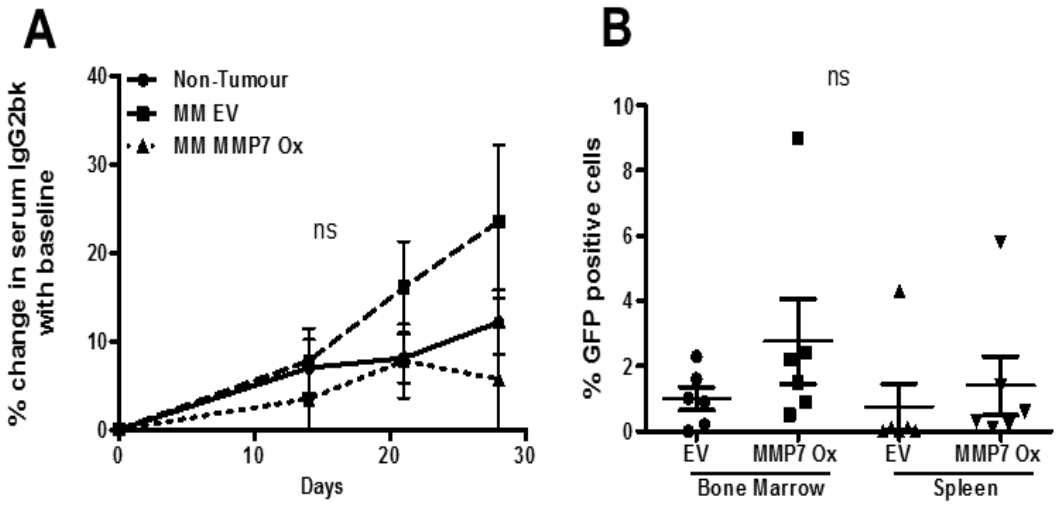

Figure 3.7. Effect of tumour-derived MMP7 *in vivo*. (A) tumour burden measured by myeloma specific serum IgG2bκ paraprotein (B) tumour burden measured by the percentage of GFP positive myeloma cells in the bone marrow (BM) and spleen in KaLwRij mice inoculated with empty vector (EV) and MMP7-overexpressed 5TGM1-GFP MM cells (Non-tumour, n=5; MM EV, n=6, MM MMP7 ox, n=6). Data are mean ± SEM, ns = no significant difference as compared to control or non-tumour mice.

3.3.7 MMP7 cleaves OPN *in vitro*

As the current study demonstrates that host-derived MMP7 plays a protective role in myeloma development, I hypothesized that the ability of MMP7 to cleave specific substrates may explain the mechanism through which MMP7 is protective against myeloma. My initial studies focused on OPN, and whether full-length and MMP7-cleaved OPN fragments play distinct roles in myeloma pathogenesis *in vitro*.

Since MMP7 had only been reported to cleave human OPN (Agnihotri et al., 2001), I confirmed that MMP7 can cleave murine OPN into distinct fragments, using recombinant protein incubated with increasing concentrations of MMP7 (Figure 3.8). Recombinant murine OPN was cleaved by MMP7 at 37˚C for 20 min, and western

blotting analysis was conducted to determine whether mouse OPN antibodies can detect the specific MMP7-cleaved OPN fragments.

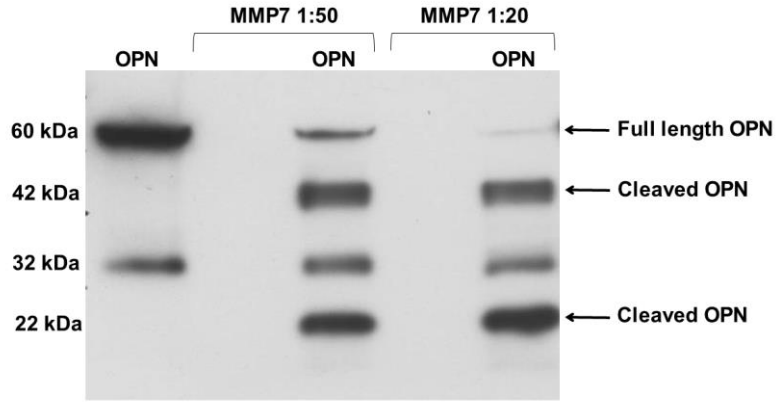

Figure 3.8. Cleavage of OPN by MMP7. Active MMP7 can cleave murine OPN into distinct fragments, using recombinant protein incubated with increasing concentrations of MMP7, measured by OPN western blot analysis.

3.3.8 Effect of full length and MMP7-cleaved OPN on 5TGM1-GFP myeloma cells *in vitro*

In order to determine the effects of full-length and MMP7 cleaved OPN on myeloma *in vitro*, recombinant murine OPN and MMP7 were pre-incubated for 20 minutes at 37˚C to allow for the cleavage of OPN by MMP7 before being added to the cells. 5TGM1-GFP myeloma cells were treated with recombinant murine full length and MMP7-cleaved OPN and their effects on myeloma cell viability determined. Full length OPN stimulated myeloma cell viability at 24h (Figure 3.9A). In separate experiments, the same increase in myeloma cell viability was observed by the addition of full length OPN at 24 and 48h, with no difference in the presence of MMP7 when compared with full length OPN alone (Figure 3.9B and C). This suggests that full length and MMP7 cleaved forms of OPN do not have different effects in myeloma cell viability *in vitro.*

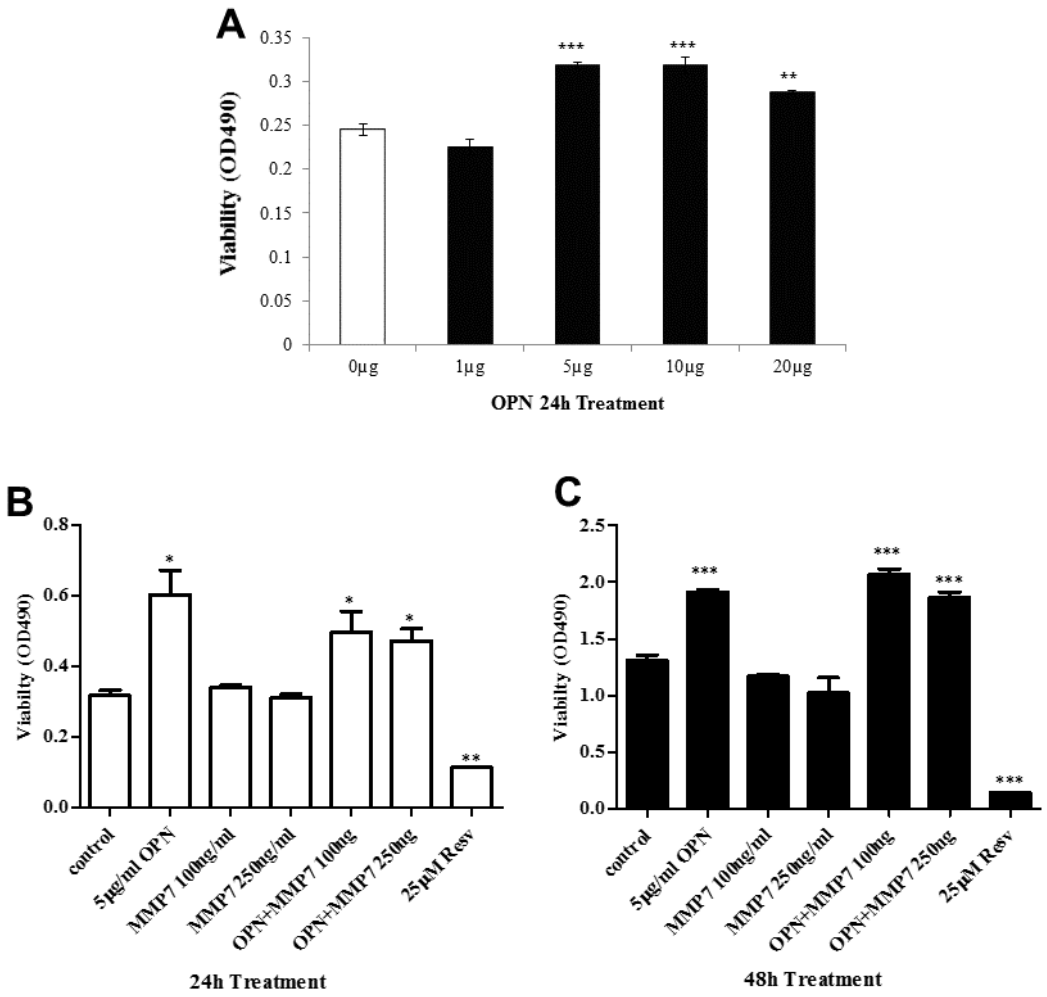

Figure 3.9. Effect of full length and MMP7-cleaved OPN on myeloma cell viability *in vitro.* (A) Murine recombinant OPN promoted 5TGM1-GFP myeloma cell viability dose dependently (B) Effect of full length and MMP7-cleaved OPN on 5TGM1-GFP myeloma cell viability. Resveratrol was used as a positive control for decreased cell viability, (B) 24h (C) 48h.*p<0.05, **p<0.01, ***p<0.001 as compared with control.

3.3.9 Expression of full length, cleaved, and total OPN in serum of myeloma patients

To begin to correlate MMP7 activity with OPN expression, the protein expression levels of full length and cleaved OPN was measured in serum of myeloma patients by western blot analysis and total OPN by ELISA. Quantitation by densitometry of the western blotting analysis showed that serum of myeloma patients has a significant

increase in full length OPN as compared to controls (Figure 3.10A, B and C). This suggests that the balance of full length and cleaved OPN may be important in myeloma pathogenesis. No significant difference was found in total OPN levels as measured by ELISA, in the serum of myeloma patients and controls (Figure 3.10D).

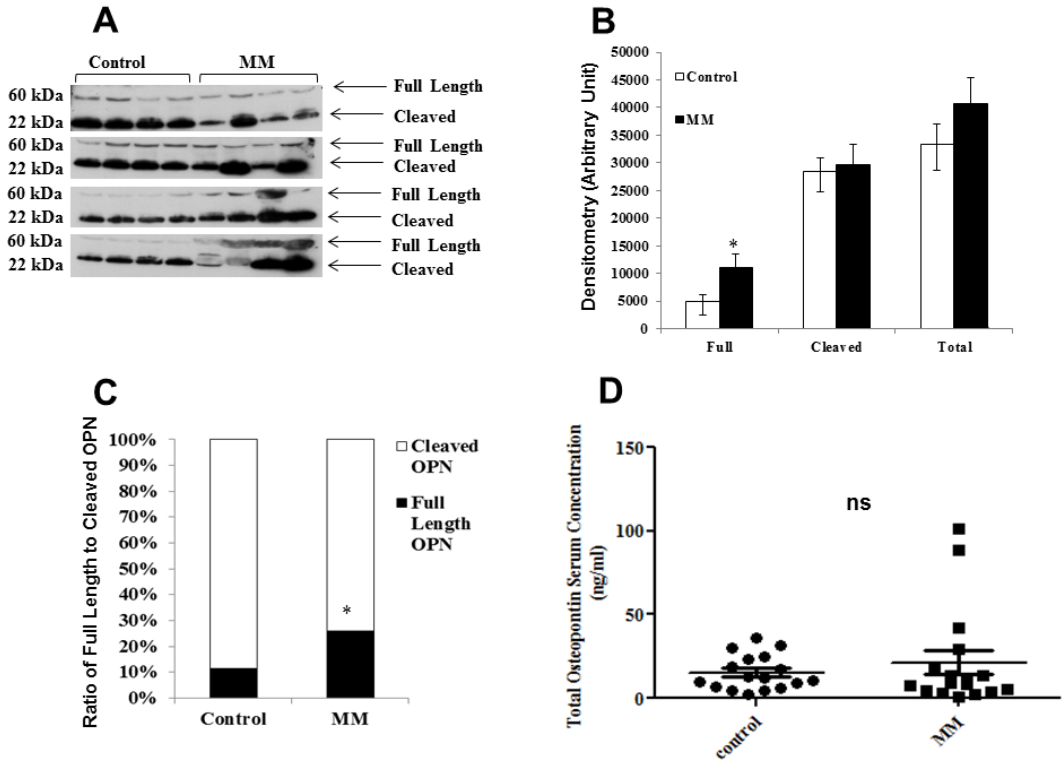

Figure 3.10. OPN protein expression in serum of control and myeloma (MM) patients. Full length and cleaved OPN protein expression in serum of control and myeloma patients (A) Western blot analysis, (B) Quantitation by densitometry, (C) The ratio of full length to cleaved OPN in myeloma patients' serum as compared to control, (D) Total OPN levels, measured by ELISA, myeloma patients (n=16) or matched controls (n=16). *$p<0.05$, ns = no significant difference as compared to control. Data are expressed as mean ± SEM.

3.3.10 Role of cleaved OPN in murine myeloma progression *in vivo*

A significant increase in total OPN levels in serum from MMP7$^{-/-}$ mice was identified, as compared to WT controls (Figure 3.11A). However, it is important to determine the expression of cleaved OPN, since MMP7-cleaved OPN may play a role in myeloma.

To determine the expression of full length and cleaved OPN fragments *in vivo*, western blot analysis was carried out using serum from WT and MMP7$^{-/-}$mice. Surprisingly, myeloma bearing WT and MMP7$^{-/-}$ mice have a significant increase in cleaved OPN expression, with no difference in expression between WT and MMP7$^{-/-}$ (Figure 3.11B). This cleaved OPN fragment is the same size as the MMP7-cleaved fragment at 25kDa that was detected by western blotting using recombinant OPN and MMP7 (Figure 3.8). Since serum concentration may not accurately reflect the local microenvironment, western blot analysis was carried out using the bone marrow lysates from WT and MMP7$^{-/-}$ mice. Different anti-OPN antibodies were used for mouse and human samples. No difference in OPN protein expression was observed between WT and MMP7$^{-/-}$ mice (Figure 3.11C). This cleaved OPN fragment is approximately 32kDa as seen with recombinant OPN and MMP7 (Figure 3.8). Therefore, although significant differences in OPN are seen in myeloma patients, the results in the murine system suggest that OPN cleavage does not explain the protective effects of MMP7.

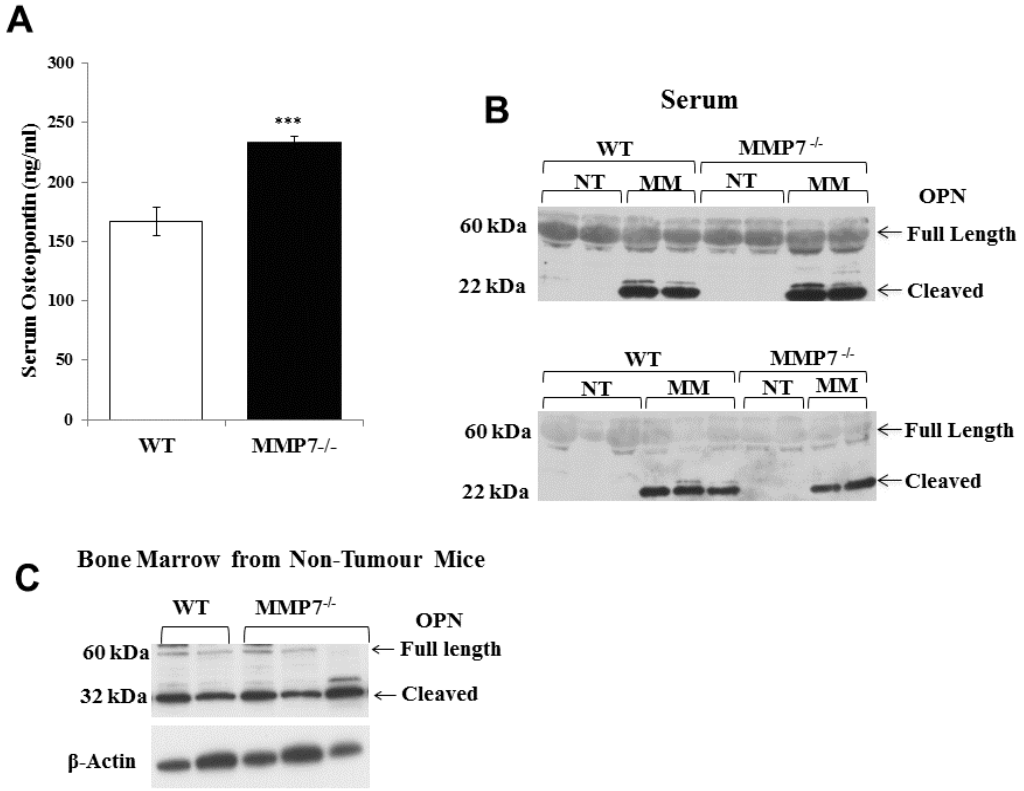

Figure 3.11. OPN Expression in RAG2$^{-/-}$ WT and RAG2$^{-/-}$ MMP7$^{-/-}$ mice. (A) Increased serum OPN levels in MMP7$^{-/-}$ mice compared to WT controls measured by ELISA. (B) Western blot analysis of full length and cleaved OPN protein expression in serum (C) in bone marrow of WT controls and MMP7$^{-/-}$ mice. Data are mean ± SEM. ***p<0.001.

3.3.11 MMP-7 cleaves galectin-3 and the effect of galectin-3 to promote myeloma cell proliferation is decreased in the presence of MMP7 *in vitro*

Using the candidate list of substrates of MMP7, galectin-3 has been shown to be cleaved by MMP7 and inhibiting galectin-3 has anti-myeloma effects *in vitro* (Puthenedam et al., 2011;Streetly et al., 2010;Mirandola et al., 2011). Firstly, I investigated whether galectin-3 was expressed by the 5TGM1 myeloma cells, ST2 BMSCs, bone marrow isolated from KaLwRij mice, and 2T3 osteoblasts. Except for 5TGM1 myeloma cells, all the above cells expressed galectin-3, measured by qRT-PCR analysis (Figure 3.12A).

Previous studies have shown that human recombinant galectin-3 is cleaved by MMP7 (Puthenedam et al., 2011). I determined whether murine recombinant galectin-3 is also cleaved into distinct fragments by MMP7. After 20h incubation of galectin-3 and increasing concentrations of MMP7 at 37ºC, silver staining of the gel demonstrated the cleavage of murine recombinant galectin-3 by MMP7 (Figure 3.12B).

I investigated the effect of galectin-3 in 5TGM1-GFP murine myeloma cell proliferation. Recombinant full-length murine galectin-3 significantly increased myeloma cell viability at 48h in a dose dependent manner (Figure 3.12C).

As 2T3 osteoblast cells express galectin-3 and 5TGM1-GFP myeloma cells do not, myeloma cells were cultured in the presence and absence of 2T3 osteoblasts and treated with a neutralizing antibody to galectin-3 to determine the role of host-derived galectin-3 in myeloma cell proliferation. A significant decrease in myeloma cell number was observed when blocking the galectin-3 expressed by 2T3 osteoblasts with the neutralising antibody to galectin-3 (Figure 3.12D). The number of myeloma cells was measured by GFP fluorescence.

To determine the effect of MMP7-cleaved galectin-3 in myeloma cell viability, 5TGM1 myeloma cells were treated with MMP7-cleaved galectin-3 (1µg/mL of recombinant murine galectin-3 incubated with 200ng/mL active MMP7 for 20h at 37ºC to allow for the cleavage of galectin-3) for 24 and 48h. The significant increase in myeloma cell viability by full-length galectin-3 was abrogated by the presence of MMP7 suggesting an anti-myeloma effect of exogenous MMP7 *in vitro* (Figure 3.12E). These results demonstrate that whereas full-length galectin-3 promotes myeloma cell growth, this is decreased by MMP7.

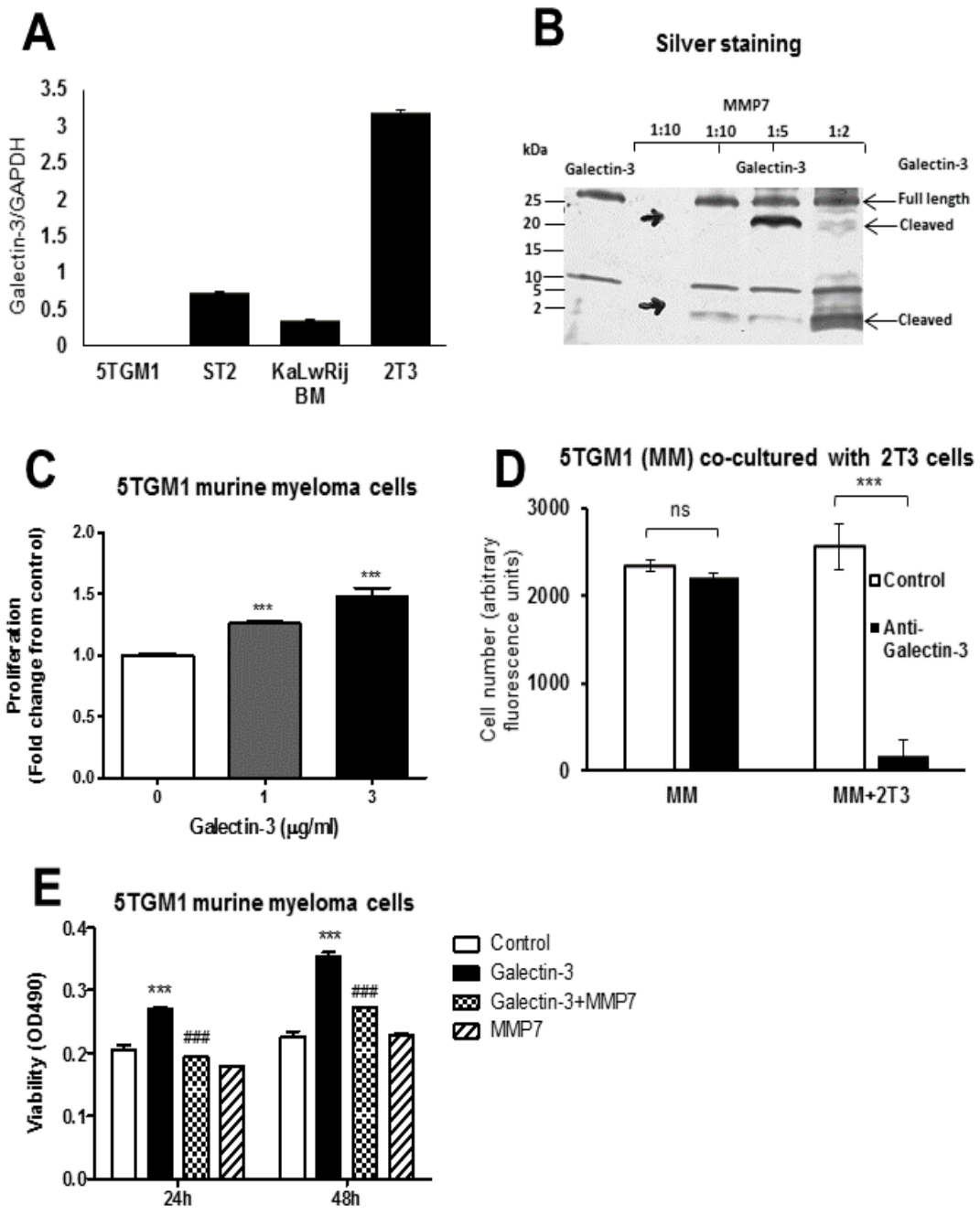

Figure 3.12. Effect of galectin-3 to promote myeloma cell growth is decreased in the presence of MMP7. (A) Galectin-3 is expressed by bone marrow cells (ST2 murine cell line and bone marrow isolated from myeloma-permissive KaLwRij mice) and 2T3 osteoblasts. (B) MMP7 can cleave murine galectin-3 into distinct fragments, using recombinant protein incubated with increasing concentrations of MMP7, detected by silver staining. (C) Full length galectin-3 promotes myeloma cells proliferation dose dependently *in vitro* 48h, ***p<0.001 as compared with control. (D) Myeloma cells were cultured in the presence and absence of 2T3 osteoblasts and treated with a neutralizing antibody to galectin-3 or isotype control. Myeloma cell number was determined measuring GFP fluorescence. (E) Myeloma cells were treated with galectin-3 in the presence and absence of MMP-7. Viability was determined using a MTS assay. Data represent as mean ± SEM. ***p<0.001 as compared to control, ### p<0.001 as compared to galectin-3.

3.3.12 Full length galectin-3 is increased in myeloma-bearing MMP7$^{-/-}$ mice

Western blot analysis using an antibody against C-terminal galectin-3 (reactive to both mouse and human) has shown that increasing concentration of MMP7 increased the expression of cleaved galectin-3 with no apparent change in full-length galectin-3, when recombinant murine galectin-3 was incubated with active MMP7 for 20h. However, only very weak detection of cleaved galectin-3 protein expression was observed between 10 and 15kDa, which was a different molecular weight to that detected by silver staining at approximately 2 and 20kDa in figure 3.12B (Figure 3.13A). C-terminal anti-galectin-3 antibody used for these murine samples recognises 161-200 amino acid residues of galectin-3. These data suggest that C-terminal galectin-3 antibody may not be best suited for detection of cleaved form in murine samples as the epitope only detects a small fragment between 161-200 amino acids.

A decrease in the expression of N-terminus full-length galectin-3 with increasing concentration of active MMP7 was observed (Figure 3.13B). To determine the circulating full-length galectin-3 expression *in vivo*, western blot analysis was carried out using serum of non-tumour and myeloma-bearing WT and MMP7$^{-/-}$ mice. Different C-terminal and N-terminal anti-galectin-3 antibodies were used for mouse and human samples. N-terminal anti-galectin-3 antibody used for murine samples recognises an epitope within the first 45 amino acids. A significant increase in full-length galectin-3 was observed in the serum of myeloma-bearing mice as compared to the serum of non-tumour mice (Figure 3.13C). Most importantly, serum of myeloma bearing MMP7$^{-/-}$ mice have a significant increase in full length N-terminus galectin-3 expression as compared to myeloma bearing WT mice with no difference in C-terminus galectin-3 expression (Figure 3.13D and E). These data indicates that loss of host derived MMP7 promotes myeloma development *in vivo* thereby increasing the circulating full length

galectin-3 at N-terminal end. Interestingly, MMP7 appeared to cleave galectin-3 at the N-terminal by mass spectrometry analysis of MMP7 cleaved galectin-3 fragments (data not shown). However, more studies are needed to determine whether MMP7 is cleaving at N-terminal end of murine galectin-3.

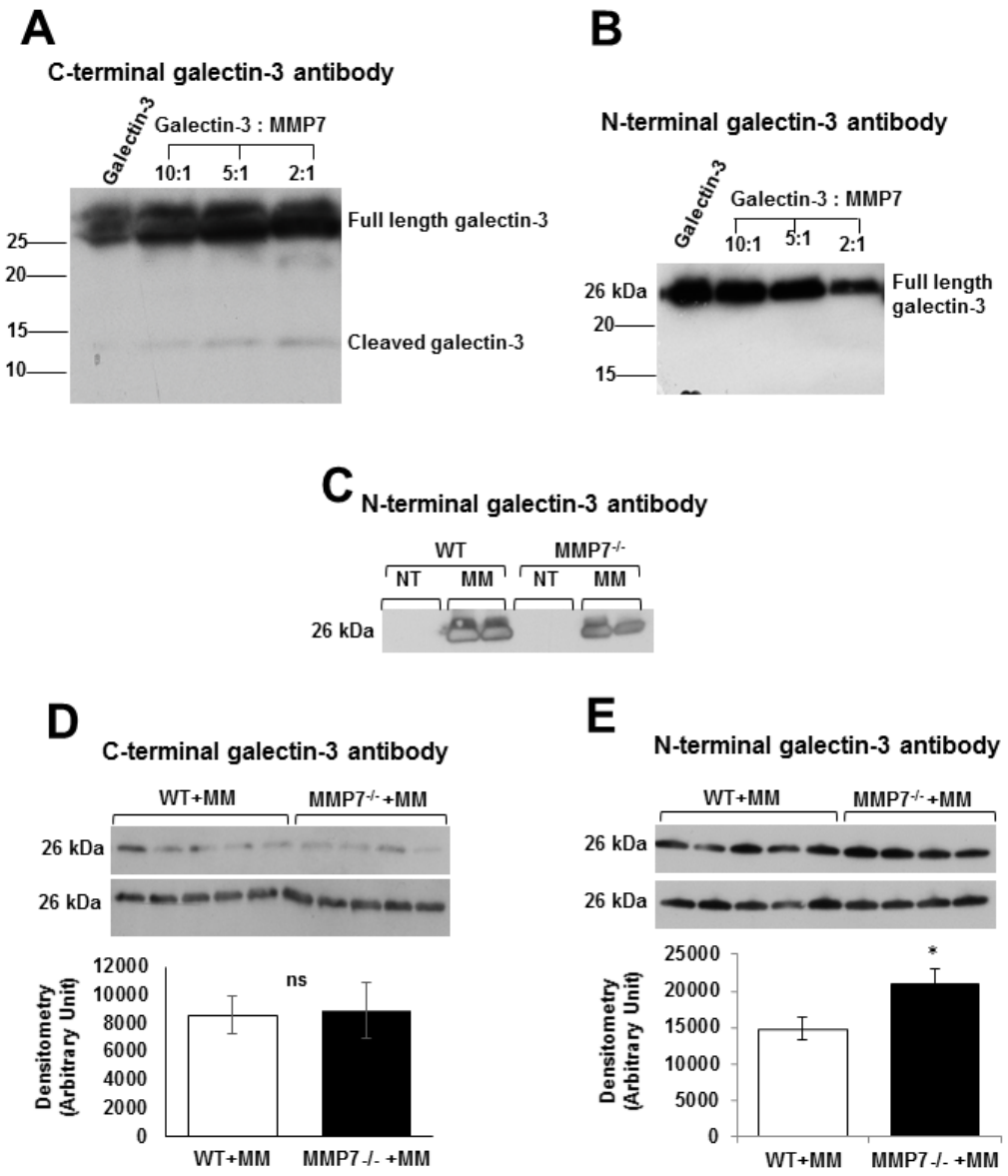

Figure 3.13. Increased full length galectin-3 protein expression in serum of myeloma bearing mice. Figure A and B at the top panel showed C- and N-terminal galectin-3 protein expression in murine recombinant proteins and Figure C, D and E at the bottom panel showed C- and N-terminal galectin-3 protein expression in murine serum. Western blot analysis of recombinant full length galectin-3, ~26kDa, and MMP7-cleaved galectin-3 with increasing concentrations of MMP7 detected by antibody against (A) C-terminal galectin-3, (B) N-terminal galectin-3; Western blot analysis of full length galectin-3 in serum of (C) non-tumour and myeloma bearing WT and MMP7$^{-/-}$ mice using N-terminal galectin-3 antibody, (D) WT and MMP7$^{-/-}$ myeloma bearing mice using C-terminal galectin-3 antibody, (E) WT and MMP7$^{-/-}$ myeloma bearing mice using N-terminal galectin-3 antibody, quantitation by densitometry. (WT NT, n=4; MMP7$^{-/-}$ NT, n=4; WT MM, n=10; MMP7$^{-/-}$ MM, n=8). Data represent as mean ± SEM. *$p<0.05$.

3.3.13 Ratio of full:cleaved galectin-3 is increased in patients with myeloma

The cleavage of recombinant human galectin-3 by active MMP7 was also confirmed by western blot analysis. C-terminal anti-galectin-3 antibody used for human recombinant and serum samples recognises an epitope within 200 amino acid residues to C-terminus of human galectin-3. A decrease in full length and an increase in cleaved C-terminal galectin-3 fragments were observed with increasing concentration of MMP7 (using C-terminus galectin-3 antibody specific to human), when recombinant human galectin-3 was incubated with active MMP7 for 20h, suggesting that there were multiple cleavage sites by MMP7 (Figure 3.14A). A decrease in the expression of full length N-terminal galectin-3 with increasing concentration of active MMP7 was observed (Figure 3.14B). N-terminal anti-galectin-3 antibody used for human samples recognises 38-87 amino acids of galectin-3 (reactive to both mouse and human), different epitope recognised by N-terminal anti-galectin-3 antibody used for murine samples, which was an epitope within the first 45 amino acids.

To determine the clinical relevance of galectin-3 in myeloma pathogenesis, the ratio of full length and cleaved galectin-3 protein expression in the serum of myeloma patients and matched controls was measured by western blotting analysis. Different C-terminal and N-terminal anti-galectin-3 antibodies were used for mouse and human samples. Quantitation by densitometry showed that there was no significant difference in N-terminal galectin-3 expression (Figure 3.14D). This result was different from increased full-length N-terminus galectin-3 expression observed in serum of myeloma bearing $MMP7^{-/-}$ mice as compared to myeloma bearing WT mice (Figure 3.13E). This difference may be due to the different epitopes recognised by different antibodies described above.

Interestingly, serum of myeloma patients has a significant increase in full:cleaved C-terminal galectin-3 and a significant decrease in C-terminal cleaved:full galectin-3 as compared to controls (Figure 3.14C). This may suggest that the balance of full length and cleaved galectin-3 may be important in myeloma pathogenesis. Furthermore, this supports my *in vivo* and *in vitro* data, confirming that full-length galectin-3 promotes myeloma pathogenesis and cleaved galectin-3 may protect against it.

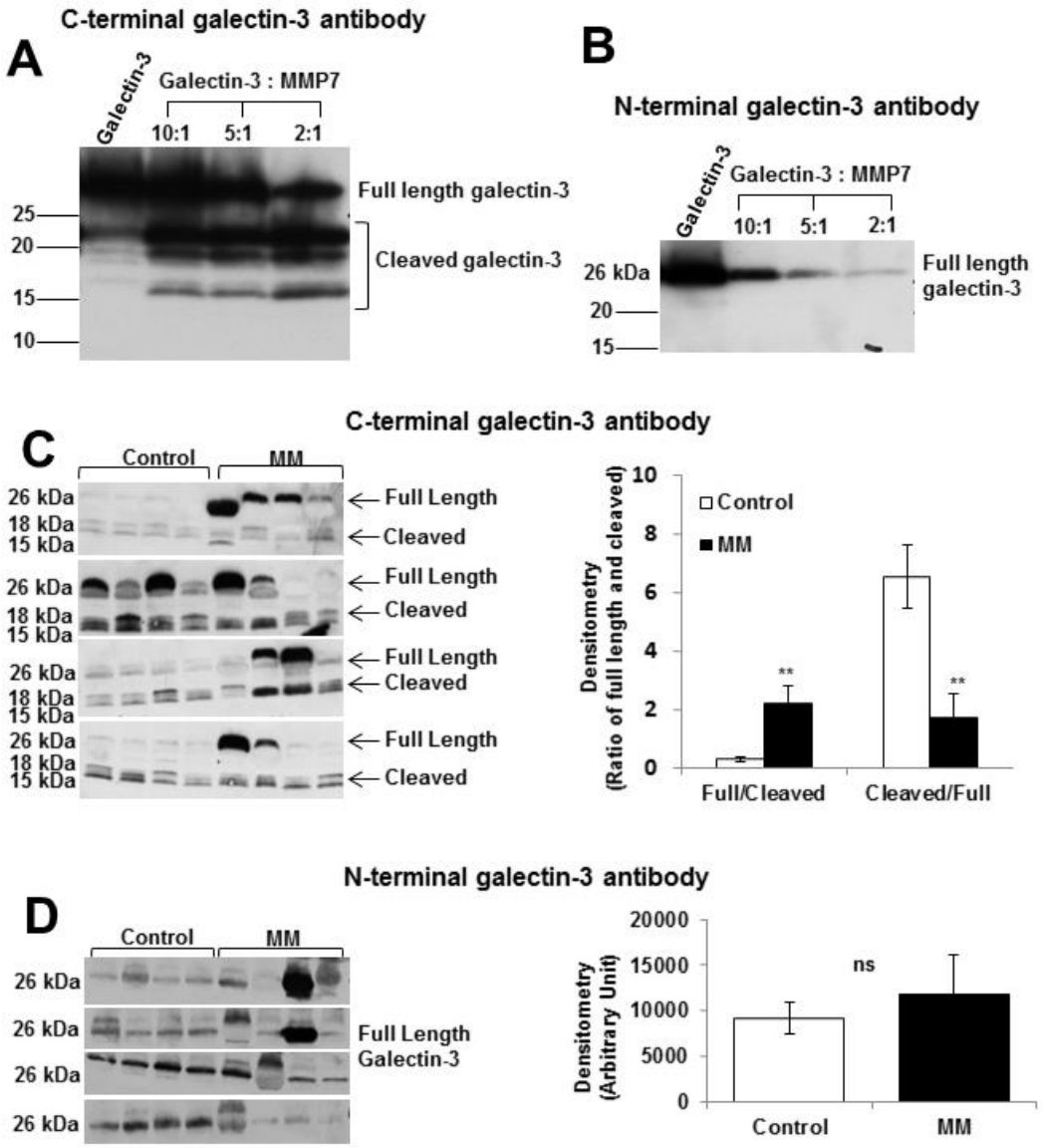

Figure 3.14. The ratio of cleaved:full-length galectin-3 is decreased in patients with myeloma. Figure A and B at the top panel showed C- and N-terminal galectin-3 protein expression in human recombinant proteins and Figure C and D at the bottom showed C- and N-terminal galectin-3 protein expression in serum of myeloma patients and matching controls. Western blot analysis of recombinant full length and MMP7-cleaved galectin-3 with increasing concentrations of MMP7 detected by antibody against (A) C-terminal galectin-3, (B) N-terminal galectin-3; Western blot analysis of in serum of control and myeloma patients (C) full length and cleaved galectin-3 using C-terminal galectin-3 antibody, quantitation by densitometry, the ratio of full length to cleaved galectin-3 and cleaved to full length galectin-3 in myeloma patients' serum as compared to control, (D) full length galectin-3 using N-terminal galectin-3 antibody, quantitation by densitometry. (control, n=16; MM, n=16). Data represent as mean ± SEM. **p<0.01, ns = no significant difference as compared with control.

3.3.14 Positive correlation between serum MMP7 activity and cleaved:full galectin-3 in patients with myeloma

To determine whether there is a correlation between MMP7 activity and the ratio of cleaved:full-length galectin-3, the serum MMP7 activity (determined by densitomentry quantitation of casein zymography) was plotted against cleaved: full-length galectin-3 expression from western blot analysis, quantitated by densitometry. A positive correlation between MMP7 activity and the ratio of cleaved:full-length galectin-3 was observed (Figure 3.15).

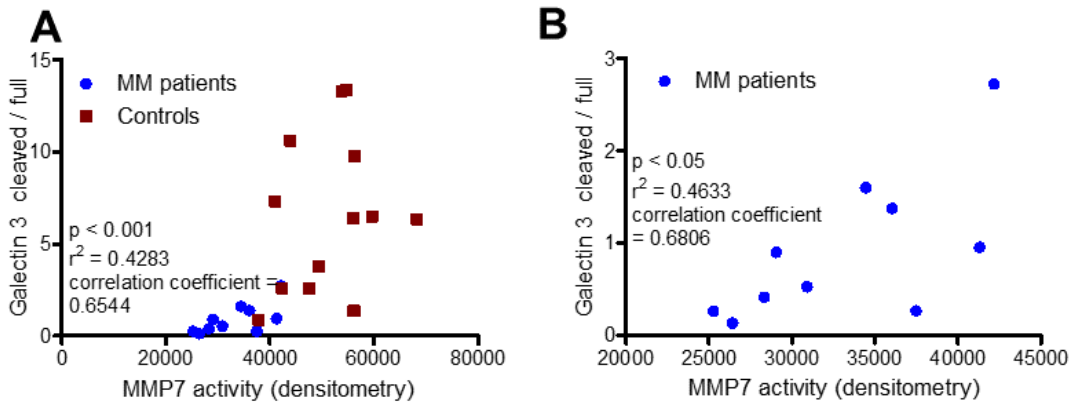

Figure 3.15. Correlation between serum MMP7 activity and cleaved:full-lenth galectin-3 in patients with myeloma. (A) A positive correlation between serum MMP7 activity and cleaved:full galectin-3 was detected in both patients with multiple myeloma and healthy controls. (B) Expansion of the same correlation in serum of myeloma patients (MM) only.

3.4 Discussion

This study demonstrates that host-derived MMP7 plays a protective role in myeloma pathogenesis, as MMP7 deficient mice have an increase in myeloma tumour burden and the associated bone disease. Interestingly, this protective effect is contrary to its contributory role in prostate and breast cancer (Lynch et al., 2005;Thiolloy et al., 2009). Barille et al. showed that MMP7 was expressed by human myeloma cell lines and primary myeloma cells isolated from bone marrow aspirates of myeloma patients, however, MMP7 activity was not investigated directly in those cells. Co-culture of myeloma cells with bone marrow stromal cells (BMSCs) induced the activation of MMP2 expressed by BMSCs, and using a MMP inhibitor 1-10 phenanthroline prevented the activation of MMP2, suggesting that a MMP produced by myeloma cells is responsible for the activation of MMP2 (Barillé et al., 1999). However, the limitation of this study was that 1-10 phenanthroline is not a specific inhibitor for MMP7, as it inhibits zinc MMPs, which makes it difficult to conclude that it was MMP7 that activate MMP2. Furthermore, the role of MMP2 in myeloma pathogenesis is not well studied and whether activation of MMP2 has a negative or positive effect on myeloma development remains to be seen.

While many MMPs play a role in promoting tumour invasion, other MMPs play a protective role. MMP8 has been shown to have a protective role in oral cancer and lymph node metastasis (Decock et al., 2008;Korpi et al., 2008). On the other hand, loss of host-derived MMP9 resulted in a decrease in myeloma tumour burden *in vivo* (Fowler et al., 2009). This study is the first to show a protective role of MMP7 in cancer progression. A decrease in MMP7 activity was observed in serum of both myeloma

patients and mice as compared to serum of control patients and non-tumour mice, which further strengthens the notion of a protective role for MMP7 in myeloma pathogenesis.

My studies reveal that myeloma is associated with an increase in TIMP1, an inhibitor of MMP7, which may have suppressed MMP7 activity both in patients and in a murine model. The 5TGM1-GFP myeloma cells in this study express TIMP1, therefore, the greater the increase in tumour burden, the more TIMP1 is being produced by these myeloma cells, thereby decreasing overall MMP7 activity. This may explain the fact that MMP7-overexpressing 5TGM1-GFP myeloma cells have no effect on myeloma progression when inoculated intravenously *in vivo*, as compared to mice inoculated with empty vector 5TGM1-GFP myeloma cells. The potential protective effect of overexpression of MMP7 may be cancelled by the increased expression of its inhibitor, TIMP1. However, prolonged culture of the transduced cells could have affected the function of these cells *in vivo* and definitive conclusions could not be made based on these data.

To investigate further the mechanism underlying how MMP7 was protective against myeloma progression, I looked into the substrates of MMP7. One of the substrates, osteopontin (OPN), is a matrix component shown to be associated with myeloma and bone remodelling, which identified it as a good candidate to investigate in my study (Agnihotri et al., 2001).

OPN was expressed by 5TGM1-GFP myeloma cells while MMP7 was not. As myeloma cells proliferate, an increasing amount of full length OPN will be secreted from them, while exogenous MMP7 will be a limiting factor. This could explain an increase in myeloma cell proliferation with MMP7-cleaved OPN treatment at 48h while myeloma cell proliferation was blocked by MMP7-cleaved OPN at the 24h time point.

An increase in total OPN protein expression was identified in the serum of MMP7$^{-/-}$ mice and a significant increase in the ratio of full-length to cleaved OPN in serum of myeloma patients, as compared to control. Serum of myeloma bearing WT and MMP7$^{-/-}$ mice surprisingly have a significant increase in cleaved OPN with no difference in expression between WT and MMP7$^{-/-}$. This most likely reflects tumour cell expression of OPN. The lack of difference in cleaved substrate between WT and MMP7$^{-/-}$ may suggest that OPN is not responsible for the effect of MMP7 in myeloma.

Substrates of MMP7 other than OPN could play a role in the current *in vivo* system. Therefore, it was important to look into other substrates of MMP7 that may play a protective role in myeloma progression. A number of substrates were identified following an extensive literature review. One of the substrates that stood out was galectin-3, as inhibition of galectin-3 was shown to increase myeloma cell apoptosis (Mirandola et al., 2011).

An increased serum galectin-3 level was identified in myeloma-bearing MMP7$^{-/-}$mice as compared to WT. Clinical analysis demonstrated that serum of myeloma patients had a significant increase in the ratio of full-length:cleaved galectin-3 and a significant decrease in the ratio of cleaved:full-length galectin-3 as compared to control, suggesting that full-length and cleaved galectin-3 may be important and that cleaved galectin-3 may play a protective role in myeloma. In contrast, cleaved galectin-3 was associated with advanced prostate and breast cancer progression (Nangia-Makker et al., 2007;Wang et al., 2009). These studies further highlighted the differences between the effects of host-derived MMP7 or galectin-3 in myeloma progression versus prostate and breast cancer progression. Further studies looking into the cleaved galectin-3 expression using a customized antibody in the bone marrow of patients with myeloma and

myeloma-bearing MMP7 deficient mice will give better insight into the local effect of cleaved galectin-3.

In vitro studies demonstrated that full-length galectin-3 induced myeloma cell proliferation while co-cultured 5TGM1-GFP myeloma cells with MMP7-overexpressed-2T3 cells decreased myeloma cell proliferation as compared to co-cultures with 2T3 cells that do not express MMP7 *in vitro*. On the other hand, blocking the expression of galectin-3 using a neutralizing antibody in the same co-cultured system decreased myeloma cell proliferation. As empty vector and MMP7-overexpressed 2T3 cells express galectin-3, these co-culture results may suggest that full-length galectin-3 increased myeloma cell proliferation, however, this effect was lost when MMP7 was expressed by 2T3 cells when co-cultured with myeloma cells, which may indicate the protective effect of MMP7-cleaved galectin-3 in myeloma proliferation. Further studies are needed to further investigate the role of galectin-3 and MMP7 ratios in myeloma progression.

Overall, my studies suggest that host-derived MMP7 inhibits myeloma growth *in vivo*, at least in part by processing of galectin-3 (Figure 3.16). This protective effect of MMP7 is contrary to its role in promoting prostate and breast cancer progression and the associated bone disease. This major difference in function of MMP7 is an intriguing point of study, demonstrating that an inhibitor of MMP7 as a therapeutic approach for myeloma will not be beneficial. On the other hand, inhibiting MMP9 will be beneficial as it plays a contributory role in myeloma progression (Fowler et al., 2009). These studies demonstrate that MMPs can play differential roles in specific disease contexts and support the rationale for the design of selective MMP inhibitors for the treatment of myeloma bone disease. Further studies looking into other substrates of MMP7 using a

proteomic approach will dissect further the protective effect of MMP7 in myeloma pathogenesis.

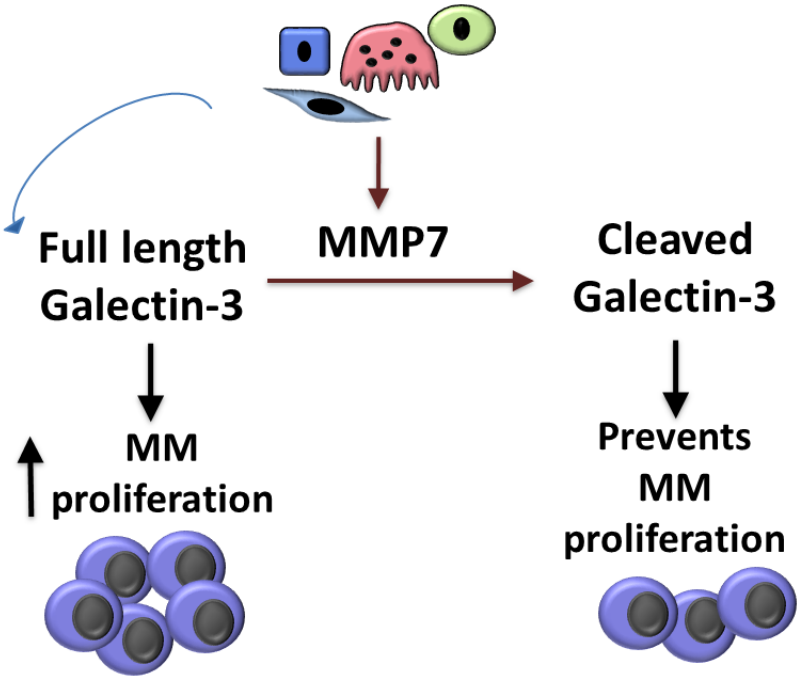

Figure 3.16. Schematic of potential mechanism for protective effect of host-derived MMP7 in myeloma pathogenesis.

Chapter 4 : The role of obesity in myeloma development *in vivo*

4.1 Introduction

Multiple myeloma is preceded by the non-malignant plasma cell disorder MGUS, characterized by an increase in monoclonal immunoglobulin secretion, less than 10% clonal plasma cells within the bone marrow in the absence of lytic bone lesions. The mechanisms underlying the pathogenesis of MGUS and progression to myeloma are complex with a major role attributed to the host microenvironment. The Edwards lab has previously demonstrated a role for host-derived adiponectin in the progression of MGUS to myeloma, and myeloma development (Fowler et al., 2011).

Adiponectin is an adipokine that is inversely linked to obesity, with increasing epidemiological evidence to support an association between obesity and MGUS or myeloma (Landgren et al., 2010;Hofmann et al., 2012;Wallin and Larsson, 2011). Therefore, it is possible that obesity plays an important role in the development of myeloma. To address this, I used the Radl 5T mouse model of myeloma which shares many of the clinical features seen in human myeloma and is widely used to study myeloma pathogenesis *in vivo* (Radl et al., 1988;Radl et al., 1979). In this model, myeloma is propagated by inoculation of 5T myeloma cells into the syngeneic C57BL/KaLwRij strain. However, myeloma does not develop when 5T cells are inoculated into closely related C57BL/6 strain mice, emphasizing the importance of the microenvironment in disease pathogenesis (Fowler et al., 2011).

4.1.1 Aim

The aim of this study was to investigate the role of adiposity, including diet-induced obesity on myeloma development in non-permissive C57BL/6 mice and the myeloma-permissive C57BL/KaLwRij murine model *in vivo*.

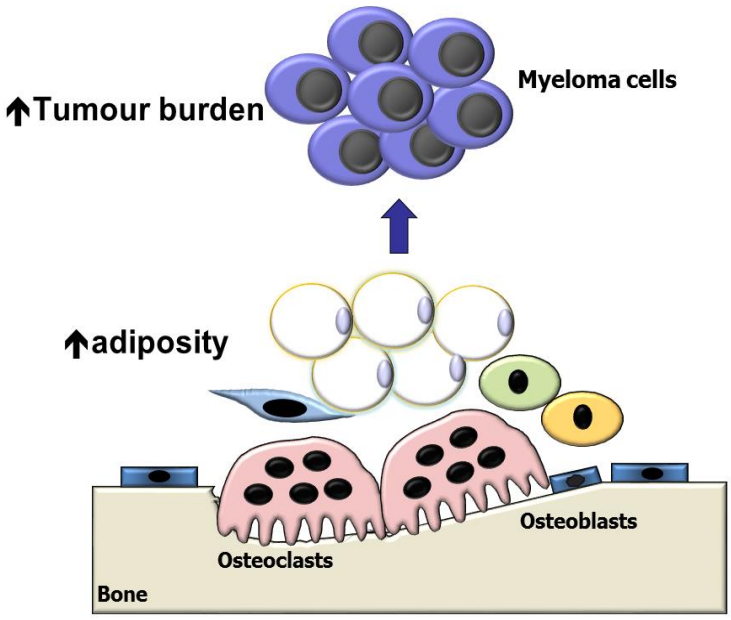

Figure 4.1. Overall hypothesis. Obesity and/or diet-induced obesity may promote myeloma development *in vivo*.

4.2 Materials and methods

4.2.1 Animal studies

In vivo studies were performed using 8- to 10-week old age- and sex-matched C57BL/6 (Harlan U.S., Indianapolis, Indiana) or C57BL/KaLwRij mice (Harlan Netherlands B.V.). Studies were approved by the Institution of Animal Care and Use Committee at Vanderbilt University and conducted in accordance with the National Institute of Health (NIH) Guide for the Care and Use of Laboratory Animals. Mice were fed either control 10% or 42% fat diet (Harlan-Teklad, TD.88137) for 5 weeks prior to tumour cell inoculation. High fat diet (HFD) was either maintained throughout the experiment up to 9 weeks or withdrawn upon detection of an increase in IgG2bκ indicating increased tumour burden (Table 1). Myeloma was propagated by the intravenous inoculation of 5 x 10^5 5TGM1-GFP myeloma cells in 100μL of PBS (Figure 4.2). Tumour burden was determined by serum IgG2bκ ELISA and flow cytometry, and trabecular bone volume assessed by microcomputed tomography as described previously in Chapter 2. To compare the phenotype of the non-permissive C57BL/6 mice and permissive C57BL/KaLwRij mice, body composition analysis was carried out using the minispec body composition analyser (LF50, BRUKER).

Table 4.1: Experimental design of treatments

No	Diet	Group	N	Treatments
1	Control	NT	5	Basal diet (10% fat) - diet maintained thoughout the experiment
2	HFD	NT	5	High fat diet (42% fat) - diet maintained thoughout the experiment
3	Control	MM	12	Basal diet (10% fat) - diet maintained thoughout the experiment
4	HFD	MM	12	High fat diet (42% fat) - diet maintained thoughout the experiment
5	HFD removed	MM	12	High fat diet (42% fat) - HFD removed at IgG level spike at week 7

HFD = high fat diet

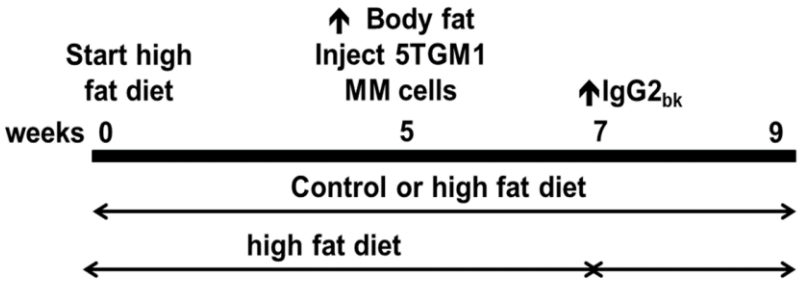

Figure 4.2. Schematic experimental design for diet-induced obesity.

4.2.2 Measurement of adipocyte number in murine bone marrow tissue

Bone marrow sections from both myeloma-permissive KaLwRij and non-permissive C57BL/6 mice were stained with hematoxylin and eosin (C57BL/6, n=5; KaLwRij, n=5). Microscopic images for 4x4 fields of view were taken at 40x magnification from below the growth plate towards the distal tibia. The number of adipocytes in those fields of view were quantified using the cell counter tool in ImageJ analysis software.

4.2.3 ELISAs

Serum concentrations of myeloma paraprotein IgG2bκ in myeloma-bearing and non-tumour (NT) mice on control and high fat diet were measured as described in section 2.5. Serum concentration of murine IGF-1 and DKK1 (R and D Systems), and IL-6 (eBioscience) were measured according to the manufacturers' instructions using commercially available ELISA kits.

4.2.4 Western blotting

To determine adiponectin expression in the serum of myeloma-inoculated C57BL/6 mice on control and high fat diet, 1 µL of serum from each mouse was mixed with PBS, loading buffer, and reducing buffer and loaded in each lane of the gel. Western blotting procedure was followed as described in section 2.18 using rabbit anti-adiponectin polyclonal antibody (Abcam) (Fowler et al., 2011).

4.3 Results

4.3.1 Increased bone marrow adiposity, body weight, and total fat with decreased trabecular bone volume in myeloma-permissive C57BL/KaLwRij mice

To determine the role of adiposity in myeloma development, I investigated whether myeloma-permissive C57BL/KaLwRij (KaLwRij) mice differ in their weight and fat distribution as compared to the non-permissive C57BL/6 mice. Bone marrow adiposity was compared, quantitated by ImageJ analysis on hematoxylin and eosin stained tibial sections and overall body weight and fat percentage, measured by body composition analysis using mini-spec body composition analyser, in age- and sex-matched myeloma-permissive KaLwRij and non-permissive C57BL/6 mice. Myeloma-permissive KaLwRij mice had a significant increase in the number of bone marrow adipocytes, total body weight and percentage fat mass as compared with non-permissive C57BL/6 mice (Figure 4.3A, B, and C). As myeloma is associated with osteolytic bone disease, the trabecular bone volume was also compared by microCT analysis. A significant decrease in the trabecular bone volume was observed in non-tumour myeloma-permissive KaLwRij compared to non-permissive C57BL/6 mice (Figure 4.3D).

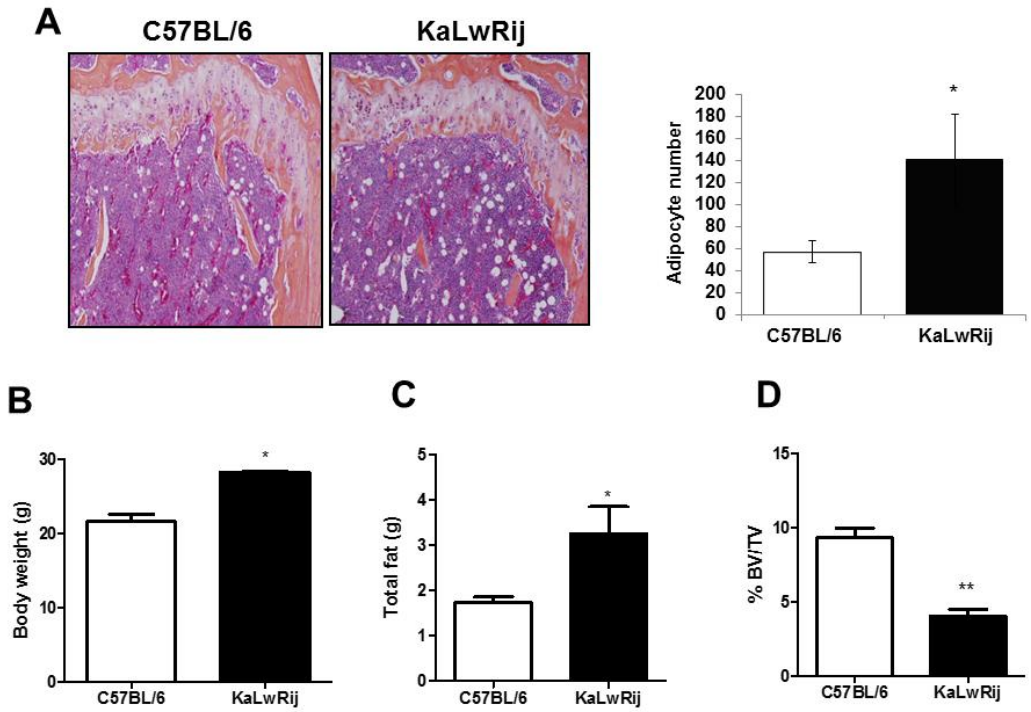

Figure 4.3. Phenotype comparison between non-tumour bearing myeloma non-permissive C57BL/6 and permissive KaLwRij mice. Histology, body composition, and microCT analysis revealed a significant increase in (A) bone marrow adiposity, analysed by hematoxylin and eosin staining and quantitated by ImageJ analysis, (B) body weight, (C) total body fat, (D) and decrease in trabecular bone volume in non-tumour bearing myeloma-permissive KaLwRij mice as compared to non-permissive C57BL/6 mice (C57BL/6, n=5; KaLwRij, n=5). *$p<0.05$, **$p<0.01$ as compared with C57BL/6 mice.

4.3.2 Diet-induced obesity increases myeloma tumour burden and the associated bone disease in non-permissive C57BL/6 mice *in vivo*

As myeloma-permissive KaLwRij mice have an increase in body fat and increased bone marrow adiposity (Figure 4.3), I investigated whether diet-induced obesity would enable myeloma development in the non-permissive C57BL/6 mice *in vivo*. C57BL/6 mice were placed on a high fat diet (42% fat) or control diet. A significant increase in body fat (measured by body composition analysis) (Figure 4.4A), and body weight (Figure 4.4B) was detected following 5 weeks of diet, at which point mice were inoculated with either 5TGM1 myeloma cells or vehicle control as described in Chapter 2 : Materials and Methods.

The diet was maintained for the duration of the experiment. C57BL/6 mice fed a high-fat diet prior to inoculation with 5TGM1 cells developed features of myeloma, including a significant increase in the serum concentration of myeloma-specific IgG2bκ paraprotein (Figure 4.4C) and accumulation of GFP-positive myeloma cells in the bone marrow and spleen (Figure 4.4D). Measurement of tibial trabecular bone volume by microCT analysis revealed a trend towards a reduction in trabecular bone volume in myeloma-bearing mice on a high-fat diet (Figure 4.4E). The combined assessment of tumour burden and bone loss revealed that 50% of mice on a high-fat diet exhibited both tumour growth within bone and bone loss, with a further 42% having detectable tumour, as compared to only 9% of mice on a control diet developing detectable tumour burden with no evidence of bone loss (Figure 4.4F).

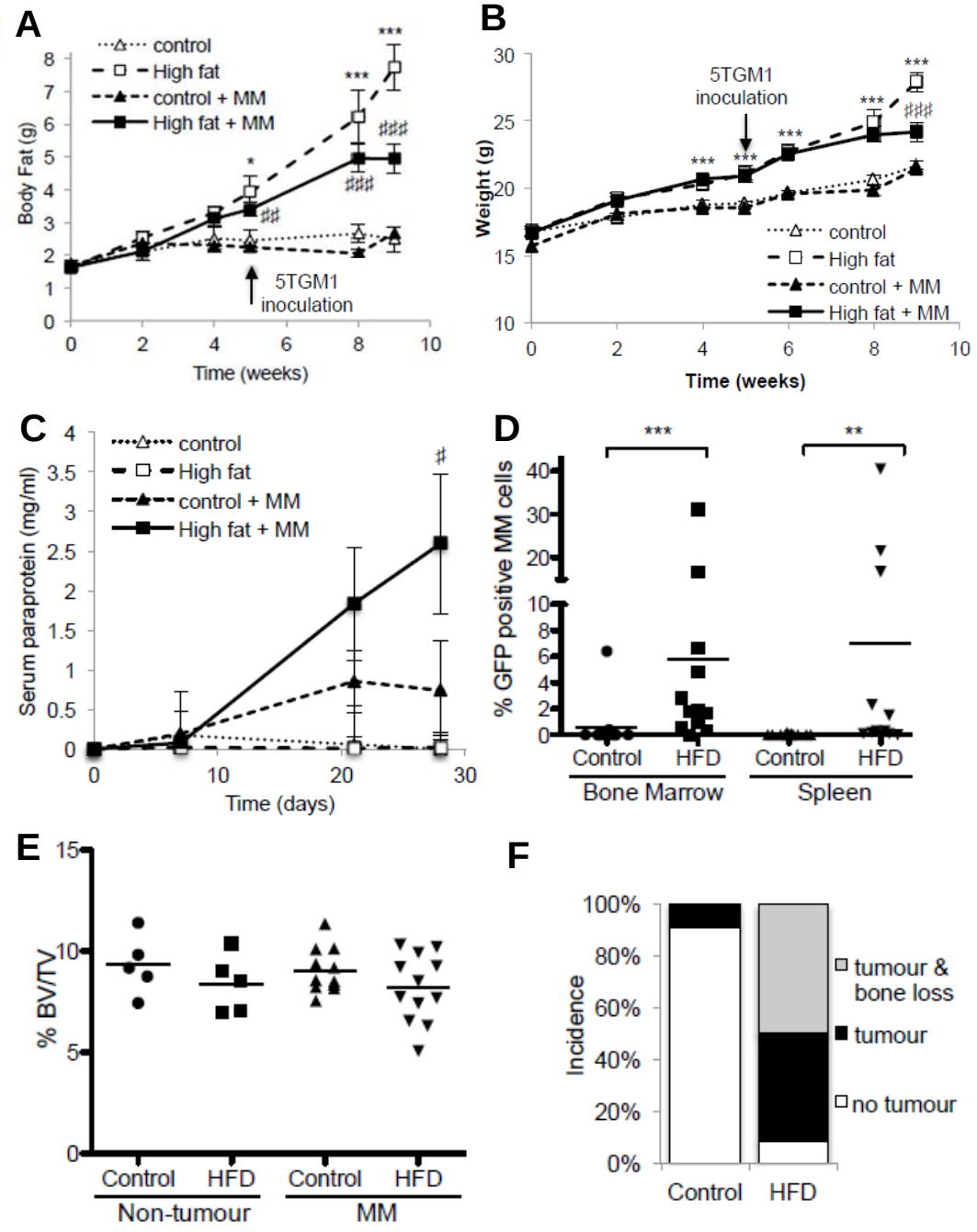

Figure 4.4. A high fat diet increases tumour burden in non-permissive C57Bl6 mice. High fat diet (HFD) significantly increased (A) body fat, measured by body composition analysis (B) body weight, as compared to control diet fed group, following 5 weeks of diet at which point mice were inoculated with either 5TGM1 myeloma cells or vehicle control (PBS) (C) inoculation of myeloma cells into mice on a high fat diet resulted in a significant increase in serum paraprotein (IgG2bk) concentrations and (D) accumulation of myeloma cells within bone marrow and spleen (E) with a trend towards a decrease in trabecular bone volume (F) Tumour incidence with and without bone loss. (control, n=5; high fat n=5; control + MM, n=11; high fat + MM, n=12). **p<0.01, ***p<0.001 as compared to control diet. ♯p<0.05, ♯♯p<0.01, ♯♯♯p<0.001 as compared to control + MM. Data are mean ± SEM.

4.3.3 Removal of high fat diet decreases myeloma tumour burden in C57BL/6 mice

To determine the effect of withdrawal of the high fat diet, in a separate experiment C57BL/6 mice were placed on the high fat diet or control. Two weeks post-tumour inoculation, following detection of an increase in serum paraprotein, mice receiving the high fat diet were either returned to the control diet, or remained on the high fat diet for the duration of the experiment (Figure 4.2). At 5 weeks post-inoculation, all mice were sacrificed and tumour burden was assessed. As before, C57BL/6 mice inoculated with 5TGM1 cells and continuously fed a high fat diet developed features of myeloma, including increased myeloma tumour burden and an increase in the serum concentration of myeloma-specific IgG2bκ, whereas tumour-inoculated mice fed a control diet did not develop significant pathology (Figure 4.5A). Removal of mice from the high fat diet resulted in a reduction in tumour burden, but no change in trabecular bone volume, with the myeloma-induced trabecular bone defect suggestive of a delayed response to tumour regression (Figure 4.5B). Of note, in this experiment, the decrease in % BV/TV in mice on a high fat diet, as compared to control, reached significance.

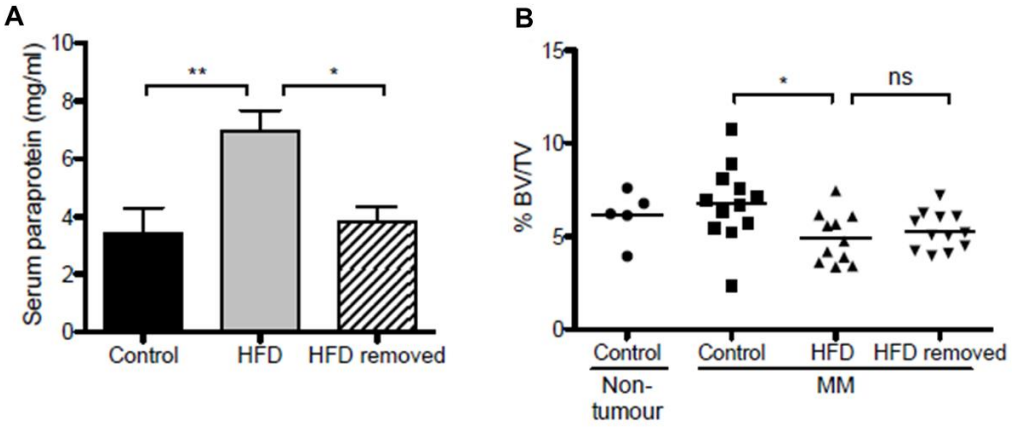

Figure 4.5. Removal of a high fat diet decreases tumour burden in C57Bl6 mice. (A) Removal of the high fat diet two weeks after tumour cell inoculation resulted in a significant reduction in serum paraprotein (B) with no change in trabecular bone loss. *p<0.05, **p<0.01. Data are mean ± SEM.

4.3.4 Effect of high fat diet in myeloma permissive KaLwRij mice

To determine whether diet-induced obesity created a permissive environment for myeloma in non-permissive C57BL/6 mice, or whether the increase in body fat was merely promoting myeloma growth, myeloma-permissive KaLwRij mice were placed on the high fat diet for 5 weeks prior to tumour cell inoculation. 5TGM1 myeloma cell inoculation resulted in tumour growth and osteolytic bone disease, however, despite a significant increase in body fat detected at time of tumour inoculation, no significant difference in serum paraprotein (Figure 4.6A), tumour burden within bone marrow (control; 24.1% ± 2.9%, high fat diet; 26.76 ± 4.1%) or trabecular bone volume (control; 5.9% ± 0.7%, high fat diet; 7.2 ± 1.6%) was detected (Figure 4.6B).

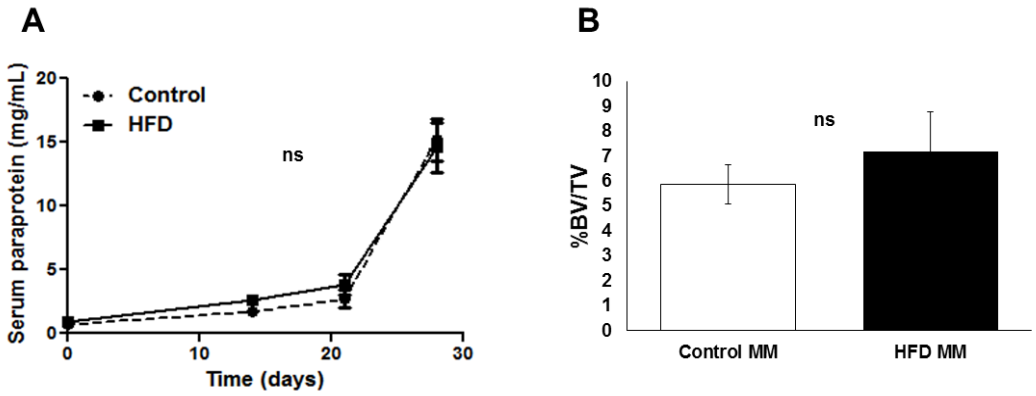

Figure 4.6. A high fat diet in myeloma-permissive KaLwRij mice does not further promote myeloma development. Inoculation of myeloma cells into KaLwRij mice receiving a high fat diet resulted in no change in (A) serum paraprotein (IgG2bκ) concentrations (B) and trabecular bone volume. (Control, n=10; high fat (HFD), n=10). Data are mean ± SEM.

4.3.5 The effect of diet-induced obesity on serum IGF-1, IL-6, DKK1, and adiponectin levels in myeloma development

Our previous studies have identified that a decrease in host-derived adiponectin, or an increase in stromal-derived Dkk1 can create a myeloma-permissive environment (Fowler et al., 2011;Fowler et al., 2012). To further investigate the myeloma-permissive microenvironment created by diet-induced obesity, serum concentrations of Dkk1 and adiponectin were measured, in addition to IL-6 and IGF-1, which are implicated in both obesity and myeloma. Both IL-6 and IGF-1 are major growth factors of myeloma and diet-induced obesity is shown to significantly increase IGF-1 and IL-6 levels (Olivo-Marston et al., 2014;Pini, Rhodes and Fantuzzi, 2011). Diet-induced obesity resulted in a significant increase in IGF-1 detectable prior to tumour inoculation that was maintained during disease development (Figure 4.7A). IL-6 was not significantly altered by diet-induced obesity (Figure 4.7B), but was significantly increased in

myeloma-bearing mice receiving the high fat diet. Diet-induced obesity was found to have no effect on serum DKK1 or total adiponectin (Figure 4.7C and D).

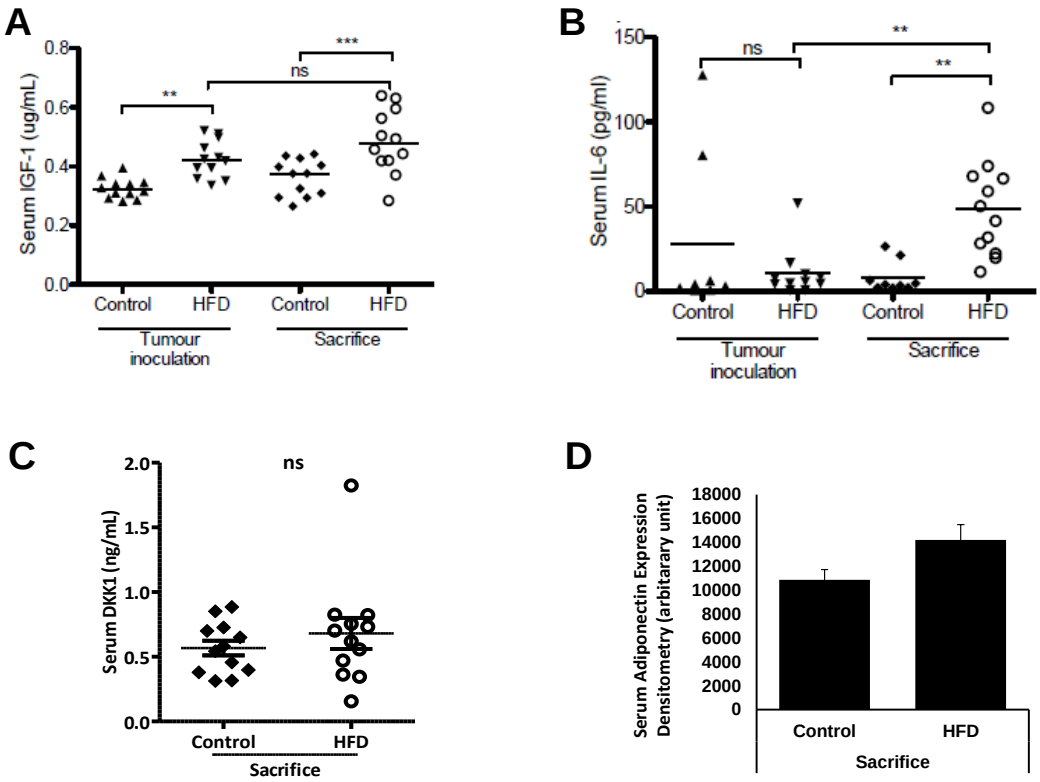

Figure 4.7. Serum concentrations of IGF-1, IL-6, DKK1, and adiponectin in myeloma-inoculated C57Bl6 mice on high fat diet. Serum concentrations of (A) IGF-1 (B) IL-6 (C) DKK1, measured by ELISA, and (D) serum level of adiponectin, measured by western blot analysis, and quantitated by densitometry in C57Bl6 mice with high fat diet. IGF-1and IL-6 were measured at time of tumour inoculation and at sacrifice. DKK1 concentrations and adiponectin level were measured at sacrifice. Data are mean ± SEM. **p<0.01, ***p<0.001.

4.4 Discussion

My data demonstrated that development of myeloma is associated with an increase in overall body weight, fat, and bone marrow adiposity, as myeloma-permissive non-tumour KaLwRij mice possess such characteristics when compared to non-permissive age- and sex-matched C57BL/6 mice. This is supported by clinical evidence demonstrating an association between elevated BMI before diagnosis of myeloma and MGUS, or risk of myeloma (Landgren et al., 2010;Wallin and Larsson, 2011;Murphy et al., 2013). It was notable that despite a significant accumulation of myeloma cells within the bone marrow and spleen in response to diet-induced obesity, the bone marrow was not completely replaced with tumour cells as is observed in 5T myeloma-bearing KaLwRij mice (Radl et al., 1988;Fowler et al., 2011;Fowler et al., 2012). The features are more similar to MGUS, with an increase in tumour-specific immunoglobulins (paraprotein), accumulation of plasma cells within the bone marrow and mild bone loss (Kyle and Rajkumar, 2007;Ng et al., 2011).

Diet-induced obesity has previously been shown to increase mammary tumour growth in ovariectomized mice and a lean body weight phenotype decreased tumour growth both in ovariectomized and non-ovariectomized mice (Núñez et al., 2008). Furthermore, Tuominen et al. studied the effects of regular diet (R), high fat diet (H), regular switched to high fat diet (RH), or high fat diet switched to regular diet (HR) in colon cancer development. All mice on high fat diet had an increase in colon carcinogenesis, with the highest tumour increase being in HR group, suggesting that diet-induced obesity before tumour development was important in promoting colon carcinogenesis (Tuominen et al., 2013). Additionally, various cancer progressions such as liver, prostate, colon, and breast cancer, were shown to be positively associated with diet-

induced or genetically (leptin deficient ob/ob or db/db) obese mice (Koya and Kanasaki, 2011). These studies highlight an important link between a high fat diet and obesity and an increased risk of cancer. Although there is an increasing epidemiological evidence between obesity and MGUS/myeloma, this study is the first to address this *in vivo* and has proven this link.

The present studies have shown that diet-induced obesity can induce a myeloma-permissive microenvironment with associated bone loss in otherwise non-permissive C57BL/6 mice. Withdrawal of a high-fat diet upon detection of a myeloma paraprotein spike can reduce tumour burden as compared to a continuous high fat diet. This implies that a myeloma permissive microenvironment created by diet-induced obesity is altered when the high-fat diet is removed after establishment of myeloma.

In vivo and epidemiological studies have shown an inverse correlation between fat accumulation and bone mass (Cao, 2011). As adipocytes and osteoblasts share common mesenchymal stem cell lineage, increasing fat accumulation may decrease bone formation leading to an overall bone loss. Furthermore, diet-induced obesity was shown to increase bone resorption, with an increase in the bone resorptive marker TRAP, and a decrease in the bone formation marker oseteocalcin in the serum of C57BL/6 mice (Cao, Sun and Gao, 2010). As a result, these mice on high fat diet had a reduction in femoral bone volume, trabecular number with an increase in trabecular separation as compared with mice on the control diet. In the present study, a trend towards a reduction in trabecular bone volume was observed in one experiment and a significant decrease in repeated experiment with mice on high fat diet as compared with mice on control diet. Removal of the high fat diet upon detection of myeloma did not rescue the bone loss, suggesting a delayed response to myeloma regression.

Our group has previously shown that co-inoculation of specific BMSCs with 5TGM1 myeloma cells creates a permissive microenvironment for myeloma development in non-permissive C57BL/6 mice, but with no effect of the BMSCs to enhance myeloma growth in myeloma-permissive KaLwRij mice (Fowler et al., 2012). These studies support the findings from the current study, and highlight the importance of a myeloma-permissive microenvironment. Furthermore, the development of an MGUS-like condition rather than full myeloma, combined with the lack of effect of a high-fat diet in an already permissive KaLwRij environment, supports the notion that while an obese environment prior to disease development significantly promotes the initial stages of myeloma, an obese environment during disease development does not further promote disease progression.

A decrease in host-derived adiponectin, or an increase in stromal-derived DKK1 was associated with creating a myeloma-permissive environment (Fowler et al., 2011;Fowler et al., 2012). In the present study, a high fat diet had no effect on serum DKK1 or total adiponectin, suggesting that these host-derived factors were not responsible for the myeloma-permissive effect created by the high fat diet. IGF-1 is a potent growth factor in myeloma and a regulator of bone growth (Georgii-Hemming et al., 1996;Yakar et al., 2002). Diet-induced obesity increased murine colon cancer progression with a significant increase in IGF-1 level. In the same study, a calorie restricted diet decreased colon carcinogenesis accompanied by a significant decrease in IGF-1 levels (Olivo-Marston et al., 2014). In parallel, my studies have shown that diet-induced obesity significantly increased serum IGF-1, which was detectable prior to tumour inoculation and maintained during disease development. In addition, IL-6 has been shown to be another potent growth factor in patients with myeloma and IL-6 stimulation was shown to induce IGF-1 expression in myeloma cells (Zhang, Klein and

Bataille, 1989;Isaacson et al., 1998). IL-6 was not significantly altered by diet-induced obesity, but was significantly increased in myeloma-bearing mice receiving the high fat diet, most likely reflecting the release of IL-6 from the accumulating myeloma cells. However, these mechanisms need to be further assessed in humans to fully clarify the role of obesity in MGUS and myeloma.

Beason et al. recently demonstrated that patients with multiple myeloma who were overweight or obese at time of diagnosis had a lower mortality than healthy weight patients, suggesting that disease-related weight loss contributes to poor survival (Beason et al., 2013). Disease-related weight loss can also be observed in my study. Moreover, bone marrow adiposity was shown to increase prostate cancer metastasis to bone, through induction of fatty acid binding protein 4 (FABP4) and overexpression of FABP4 was observed in obese mice with prostate skeletal tumours (Herroon et al., 2013). Moreover, an increase in myeloma cell growth was observed when co-cultured with bone marrow adipocytes *in vitro* (Caers et al., 2007). Surprisingly, in the present study, no apparent difference in the number or size of the bone marrow adipocytes was observed. Visceral adiposity was shown to increase the risk of colorectal cancer independent of total adiposity and poor response to chemotherapy with increased complication rates after surgery (Tchernof and Després, 2013). These results suggest the need for more studies dissecting the role of overall adiposity or site-specific adiposity such as bone marrow, visceral, or subcutaneous adiposity, in development.

Additionally, the high fat diet used in my studies is an atherogenic diet and our group has previously shown that an apolipoprotein memetic peptide (L4-F) used in the treatment of atherosclerosis, decreased myeloma tumour burden and increased bone volume in a murine model of myeloma. In parallel, the present study demonstrated that an atherogenic diet created a myeloma permissive environment in an otherwise non-

permissive host environment. These studies strengthen the association between atherosclerosis and myeloma (SPAIN et al., 1956).

In conclusion, my study provides evidence for the significant impact of diet on myeloma pathogenesis, and highlights the potential for dietary intervention strategies. In the current studies, the effect of a high fat diet with 42% fat was explored in myeloma development. Further studies exploring the effect of diet-induced obesity using high or low fat, calories, cholesterol, carbohydrate, or saturated fat diet in myeloma pathogenesis would give a better understanding of the specific dietary effect on disease progression. Combining diets with molecular modification of myeloma cells (eg. knock down of IGF receptor) would be a powerful approach to dissect the mechanisms involved.

Chapter 5 : Pharmacological targeting of adipogenic factor (PPARγ) to alter the myeloma microenvironment

5.1 Introduction

5.1.1 PPARγ, a master regulator of adipogenesis

As obesity and adipogensis appear to be associated with myeloma development as described in section 1.6 and Chapter 4. I have begun to investigate regulators of adipogenesis and adiposity. Peroxisome proliferator-activated receptor γ (PPARγ) belongs to a family of nuclear receptors, expressed mainly by adipose tissue and a transcription factor for adipogenesis (Bishop-Bailey, Hla and Warner, 2001).

The group of PPARγ agonists thiazolodinediones (TZD) have been shown to induce adipogenesis in bone marrow stromal cells (Gimble et al., 1996b). However the increase in TZD-induced adiposity decreases bone formation. The TZD rosiglitazone is a known activator of PPARγ, and can decrease Caco2 colorectal cancer cell and MCF-7 breast cancer cell proliferation by up-regulating the tumour suppressor gene PTEN (Patel et al., 2001). Interestingly, bisphenol A diglycidyl ether (BADGE), a synthetic compound demonstrated by Wright et al. as an inhibitor of adipocyte differentiation in murine 3T3-L1 pre-adipocyte cells *in vitro*, has also been shown to act as a PPARγ agonist in human umbilical vein endothelial cells (ECV304), similar to other known agonists, 15-deoxy-$\Delta^{12,14}$ PGJ2, and ciglitizone. Activation and nuclear translocation of PPARγ, induced cell apoptosis in ECV304 cells (Bishop-Bailey, Hla and Warner,

2001). BADGE also inhibits adipogenesis in the bone marrow of FVB mice *in vivo*, acting as a PPARγ antagonist (Naveiras et al., 2009). Taken together, these studies demonstrate that BADGE could either act as an agonist or antagonist of PPARγ, depending on the cell system or tissue site.

The TZDs troglitazone and rosiglitazone have been used as anti-diabetic drugs to improve insulin sensitivity in genetic models of obesity and diabetes (Wright et al., 2000). Inhibition of PPARγ by BADGE treatment in insulin-deficient diabetic BALB/c mice, decreased bone marrow adiposity with no effect on type 1 diabetes associated bone loss (Botolin and McCabe, 2006). Importantly, activation of PPARγ by the agonist rosiglitazone decreased MCF-7 breast cancer cell proliferation and induced apoptosis *in vitro,* with upregulation of the tumour suppressor gene PTEN and down regulation of survival related Akt phosphorylation (Kim, Kim and Cheon, 2006).

5.1.2 PPARγ ligands

As described in the previous chapter, non-permissive C57BL/6 mice fed a high fat diet develop a permissive environment for the development of myeloma, similar to the human myeloma-like condition. This indicates the importance of the host microenvironment in myeloma development and how changes in diet may alter this. As a result, the role of bone marrow adiposity in myeloma pathogenesis was investigated. Peroxisome proliferator-activated receptors (PPARs) are used as novel targets for anti-diabetic treatment, and exist as α, δ, and γ nuclear isoforms. Their functions include different biological processes such as cellular differentiation, carcinogenesis, and angiogenesis. PPARα is implicated in the regulation of cellular uptake, activation, and β-oxidation of fatty acids. PPARδ is known to be important in myelinogenesis, glial cell maturation, and fertility (Berger and Moller, 2002). The PPARγ agonist rosiglitazone

has been shown to increase insulin sensitivity, promote an anti-inflammatory response and importantly, decrease prostate and breast cancer growth (Patel et al., 2001).

We hypothesized that targeting PPARγ and adiposity within the bone marrow microenvironment using a PPARγ ligand may have an effect on myeloma development. As myeloma pathogenesis is associated with osteolytic bone destruction, the traditional PPARγ agonist such as the TZDs, were avoided due to their known effect to decrease bone volume (Lecka-Czernik, 2010). However, daily intraperitoneal injections of 30mg/kg BADGE increases bone mass in skeletally mature (9 months old) C57BL/6 male mice (Duque et al., 2012). The effect of BADGE on adiposity and bone formation indicates that BADGE represents a reasonable candidate to manipulate the local bone marrow environment in our murine myeloma model to both decrease adiposity and increase bone formation.

In the present study, the effect of BADGE upon myeloma cells was investigated *in vitro* and *in vivo* focusing on AMPK and a down stream target SIRT1.

5.1.3 AMPK signalling

AMP-activated protein kinase (AMPK) plays a crucial role in cell growth, metabolism, autophagy, and cell polarity (Mihaylova and Shaw, 2011). Through these cellular processes, AMPK activation may protect against cancer development by inhibiting tumourigenesis and decreasing cell proliferation (Wang and Guan, 2009). It has been reported that activation of AMPK signalling using AMPK activators, 5-aminoimidazole-4-carboxamide riboside (AICAr) and D942, inhibited cell growth in human myeloma cell lines NCI-H929, U266, RPMI-8226, OPM-2. Interestingly, the same study has shown that one of the activators of PPARγ, troglitazone, decreased

myeloma cell proliferation dose and time dependently by activating AMPK (Baumann et al., 2007).

In addition, regulation of AMPK activation is shown to be important in the treatment of obesity and diabetes (Hardie, 2008). AMPK is a downstream target of adiponectin and our group has previously shown that activation of AMPK, upon treatment with adiponectin, is associated with an increase in myeloma cell apoptosis by increasing the expression of apoptosis markers, cleaved-caspase-3 and cleaved-PARP (Fowler et al., 2011). Medina et al. has reported that the anti-proliferative effect of adiponectin in myeloma cells is mediated through activation of PKA/AMPK signalling and suppression of lipogenesis (Medina et al., 2014;Fowler et al., 2011). SIRT1 is a down stream target of AMPK signalling and importantly, a SIRT1 activator, SRT1720 was shown to induce myeloma cell apoptosis (Chauhan et al., 2011). Moreover, a known activator of SIRT1 resveratrol was shown to inhibit myeloma cell proliferation by suppression of NFκB activity and induce myeloma cell apoptosis through up-regulation of caspase-3, suggesting an potential role for SIRT1 in myeloma (Bhardwaj et al., 2007;Scuto et al., 2013).

5.1.4 Aim

The aim of this study was to investigate the role of bone marrow adiposity in myeloma development by targeting PPARγ using a pharmacological approach. To achieve this, the effects of BADGE were studied *in vivo* using a murine myeloma model and *in vitro* using myeloma, osteoblasts and bone marrow stromal cells.

5.2 Materials and Methods

5.2.1 *In vivo* studies

To determine the effect of the PPARγ ligand BADGE on myeloma (MM) development *in vivo*, KaLwRij mice were treated with a daily intraperitoneal injection of 30mg/kg BADGE for 4 weeks to change the bone marrow microenvironment, prior to intravenous inoculation with $5x10^5$ 5TGM1-GFP murine myeloma cell or vehicle (PBS) (Figure 5.1). Analysis was performed as described in Chapter 2. Non-tumour (NT) vehicle, n=10; NT BADGE, n=10; myeloma-bearing (MM) vehicle, n=7; MM BADGE, n=8.

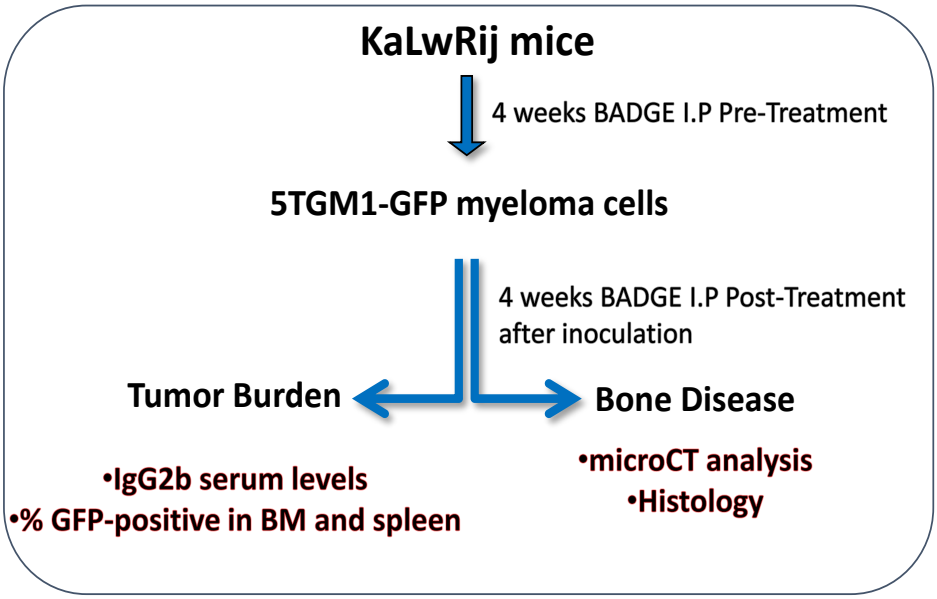

Figure 5.1. Experimental design for *in vivo* studies investigating the role of BADGE in myeloma development.

5.2.2 PPARγ activity assay

PPAR γ activity was measured in bone marrow protein lysates of BADGE and vehicle treated non-tumour (NT) mice according to the manufacturers' instructions using a commercially available PPAR γ activity assay kit (Cayman Chemicals). The assay was based on a 96-well plate ELISA, a non-radioactive, sensitive method for detecting specific transcription factor DNA binding activity in protein extracts. Each well of the 96-well plate was coated with a consensus double stranded DNA sequence containing the peroxisome proliferator response element (PPRE), which specifically binded PPARs contained in the protein sample of interest. Addition of a primary antibody specific against PPARγ detected PPARγ in the sample, followed by the addition of a HRP-conjugated secondary antibody that binded to the primary antibody. Developing solution was added to the wells. The colour developed was proportional to the amount of PPARγ activity in the samples. Colorometric absorbance was read at 450nm using SPECTRA max 384 plus plate reader (Molecular devices), PPARγ activity was then normalized to total protein concentration.

5.2.3 Treatment of myeloma cells *in vitro*

5TGM1-GFP murine myeloma cells were plated at $5x10^5$ cells/mL in 96-well plate and treated with 0-50 μM BADGE (Sigma-Aldrich) for 72h. Adherent cells ST2 BMSCs and 2T3 osteoblasts were plated at $5x10^4$ cells/mL and treated with 0-50 μM BADGE for 72h. 5TGM1-GFP cells were also treated with PPARγ antagonists GW9662 at 500nM, or a more potent antagonist T0070907 at 100nM (Sigma-Aldrich) for 72h, along with BADGE. 5TGM1-GFP cells were also treated with a SIRT1 inhibitor EX527 at 0-5000nM (Sigma-Aldrich) for 24, 48, 72h, or 72h treatment with 50nM, 100nM, or 5μM, along with BADGE. The cells were also pre-treated with 100nM or 1μM EX-527

for 24h, followed by 72h BADGE treatment. A cell viability assay was performed as described in section 2.15 at the end of each time point.

5.2.4 Dual-coloured fluorescence assay with co-culture experiments

HS5-mCherry human BMSCs were plated at $5x10^4$ cells/mL in black 96-well plate. Once HS5 cells adhered after 6 h, $1x10^5$ cells/ml of RPMI 8226-eGFP human myeloma cells were added directly on top of the HS5 cells to set up a direct co-culture *in vitro* system. The cells were then treated with 12.5 μM BADGE for 72h and the number of both RPMI 8226-eGFP human myeloma cells and HS5-mCherry human BMSCs were measured by dual-coloured fluorescence reading using FLUOstar OPTIMA (BMG) (Ramasamy et al., 2012).

5.2.5 Real-time PCR

mRNA expression of PPARγ, adiponectin, CEBPα, XBP1, PTEN, SIRT1, Atg3, VEGF, RUNX2, and OCN were detected using fast SYBR green gene expression assay master mix (Life Technologies). Relative gene expressions were normalized to mouse GAPDH (Life Technologies). All primers were purchased from Eurofins and sequences were described in Appendix I.

5.2.6 Western blotting

Protein expression was measured using polyclonal rabbit anti-cleaved-caspase 3, rabbit anti-cleaved-PARP, rabbit anti-p53, rabbit anti-phosphorylated-AMPK, rabbit anti-AMPK, rabbit anti-SIRT1, rabbit anti-NFκB, or mouse anti-β-actin were investigated using western blot analysis. These antibodies except for β-actin were used at 1:1000 dilution and purchased from Cell Signalling Technologies. Mouse monoclonal anti-β-actin was purchased from Sigma-Aldrich and used at 1:20,000 dilution. Anti-rabbit and

anti-mouse HRP were used at 1:5000 dilution and purchased from Cell signalling Technologies. Western blotting procedure and densitometry were followed as described in section 2.18.

5.3 Results

5.3.1 The PPARγ ligand, BADGE, significantly decreased tumour burden in a murine myeloma model

To assess the role of the PPARγ ligand BADGE in myeloma pathogenesis, KaLwRij mice were given a daily intraperitoneal injection of 30 mg/kg BADGE or control vehicle (200µl of 10% DMSO in PBS) for 4 weeks prior to tumour inoculation in order to change the cellular distribution within the microenvironment (Naveiras et al., 2009). BADGE treatment was continued for 4 weeks after inoculation with GFP-tagged 5TGM1 myeloma cells. Tumour burden was assessed by quantifying the myeloma specific paraprotein IgG2bκ and GFP positive cells in the bone marrow. This revealed a significant decrease in serum IgG2bκ levels in the mice treated with BADGE as compared to vehicle (Figure 5.2A). This finding was supported by a significant decrease in GFP positive myeloma cells in the bone marrow of mice treated with BADGE with no difference in the number of GFP positive myeloma cells noted in the spleen (Figure 5.2B). Since a significant decrease in tumour burden was observed within the bone marrow but importantly not in the spleen, this suggests that BADGE may have an enhanced anti-tumour effect in the local bone marrow microenvironment, compared to extra-osseous sites of different cellular composition.

Since PPARγ ligands have been reported to induce apoptosis in various cancer cells (Elrod and Sun, 2008), myeloma cell apoptosis was measured in the bone marrow by TUNEL staining and quantitated using ImageJ analysis. A significant increase in myeloma cell apoptosis was observed in BADGE treated myeloma-bearing mice as compared to vehicle treated mice (Figure 5.2C).

The effect of BADGE treatment in myeloma bone disease was measured by microCT analysis. There was no difference in trabecular bone volume following BADGE treatment in both non-tumour and myeloma-bearing mice. However, as expected a significant decrease in trabecular bone volume was observed in vehicle treated myeloma-bearing mice as compared with vehicle treated non-tumour mice (Figure 5.2D).

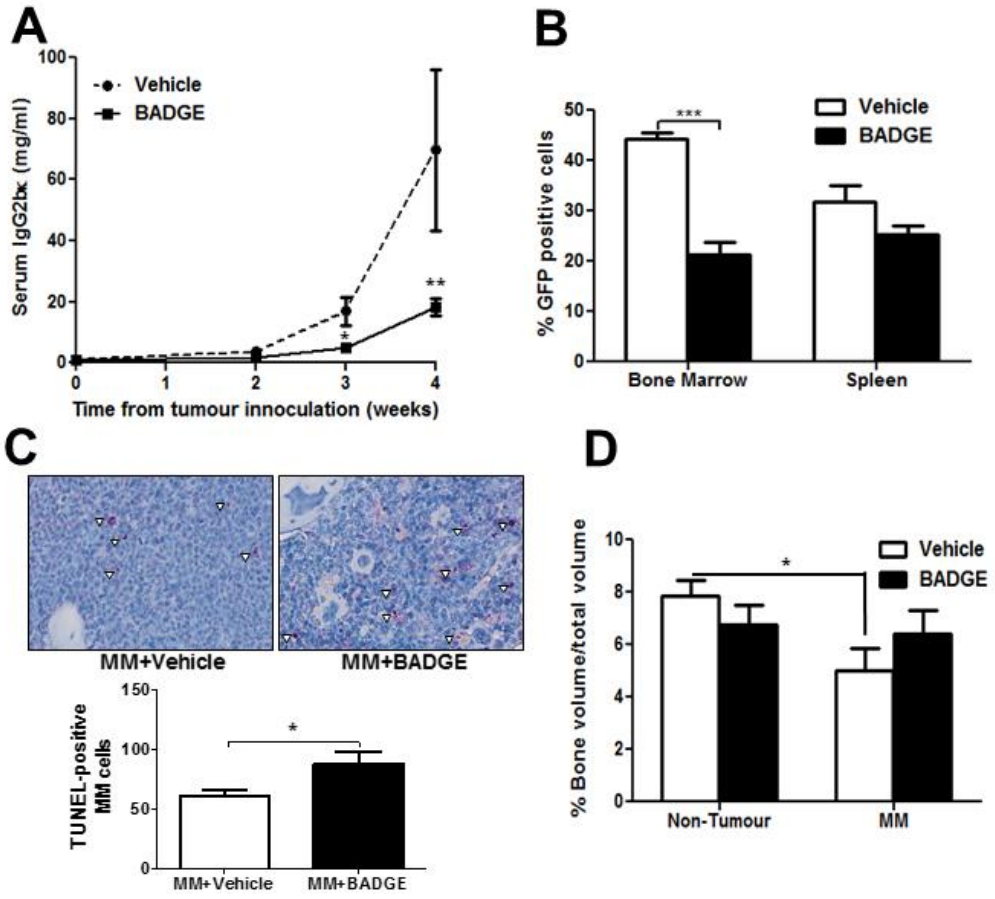

Figure 5.2. PPARγ ligand, BADGE, significantly decreased tumour burden in a murine myeloma model of C57BL/KaLwRij mice inoculated with 5TGM1-GFP myeloma cells. Tumour burden measured by (A) serum IgG2bκ concentrations, (B) FACS analysis of GFP-positive MM cells in the bone marrow and spleen, (C) myeloma cells apoptosis in bone marrow was quantitated by TUNEL staining and ImageJ analysis, (E) trabecular bone volume was measured by microCT analysis, (NT vehicle, n=10; NT BADGE, n=10; MM vehicle, n=7; MM BADGE, n=8). Data are mean ± SEM. *p<0.05, **p<0.01, ***p<0.001 as compared with vehicle treated mice.

5.3.2 BADGE increased bone marrow adipocytes and the mRNA expression of adipocyte markers in myeloma-bearing mice *in vivo*

Since BADGE has been previously reported to decrease adipocytes *in vivo*, I quantitated the number of bone marrow adipocytes in bone marrow sections from BADGE or vehicle treated mice, using ImageJ analysis. Surprisingly, a significant increase in the number of adipocytes in BADGE treated myeloma-bearing mice was found as compared with vehicle treated myeloma bearing mice, with no effect in non-tumour bearing mice (Figure 5.3A).

I also investigated whether BADGE has an effect on overall body fat percentage, by measuring the body composition using a minispec body composition analyser. No difference in overall body fat percentage was observed following BADGE treatment in both non-tumour and myeloma bearing groups (Figure 5.3B).

There was no difference in PPARγ activity in bone marrow protein lysates of BADGE and vehicle treated non-tumour (NT) mice (Figure 5.3C). This was measured by a PPARγ activity assay and normalized to total protein concentration. Due to the limitation of the sample, PPARγ activity was not measured in myeloma-bearing mice with BADGE treatment. To confirm the increase in bone marrow adipocytes seen in myeloma bearing mice following BADGE treatment, and to determine whether the molecular expression of adipocyte markers in the bone marrow is simultaneously altered, the mRNA expressions of PPARγ and downstream targets of PPARγ, (adiponectin and CEBPα) were measured by quantitative RT-PCR in bone marrow cells isolated from either BADGE or vehicle treated myeloma bearing mice. A significant increase in PPARγ, adiponectin, and CEBPα mRNA expression was observed with

BADGE treatment in myeloma mice with no difference in non-tumour mice, as compared to vehicle treated mice (Figure 5.3D).

BADGE has been reported as both a PPARγ antagonist and agonist, with my data suggesting that BADGE might be acting as an agonist in this system. PPARγ agonists have previously been shown to reduce tumour burden in colon, breast and prostate cancers (Patel et al., 2001). However, unlike other agonists, no bone loss was seen in our myeloma model (Figure 5.2D) or overall increase in body fat (Figure 5.3B) with BADGE treatment, suggesting that the PPARγ ligand BADGE may be having differential effects on PPARγ activity depending on the cell types and tissue location.

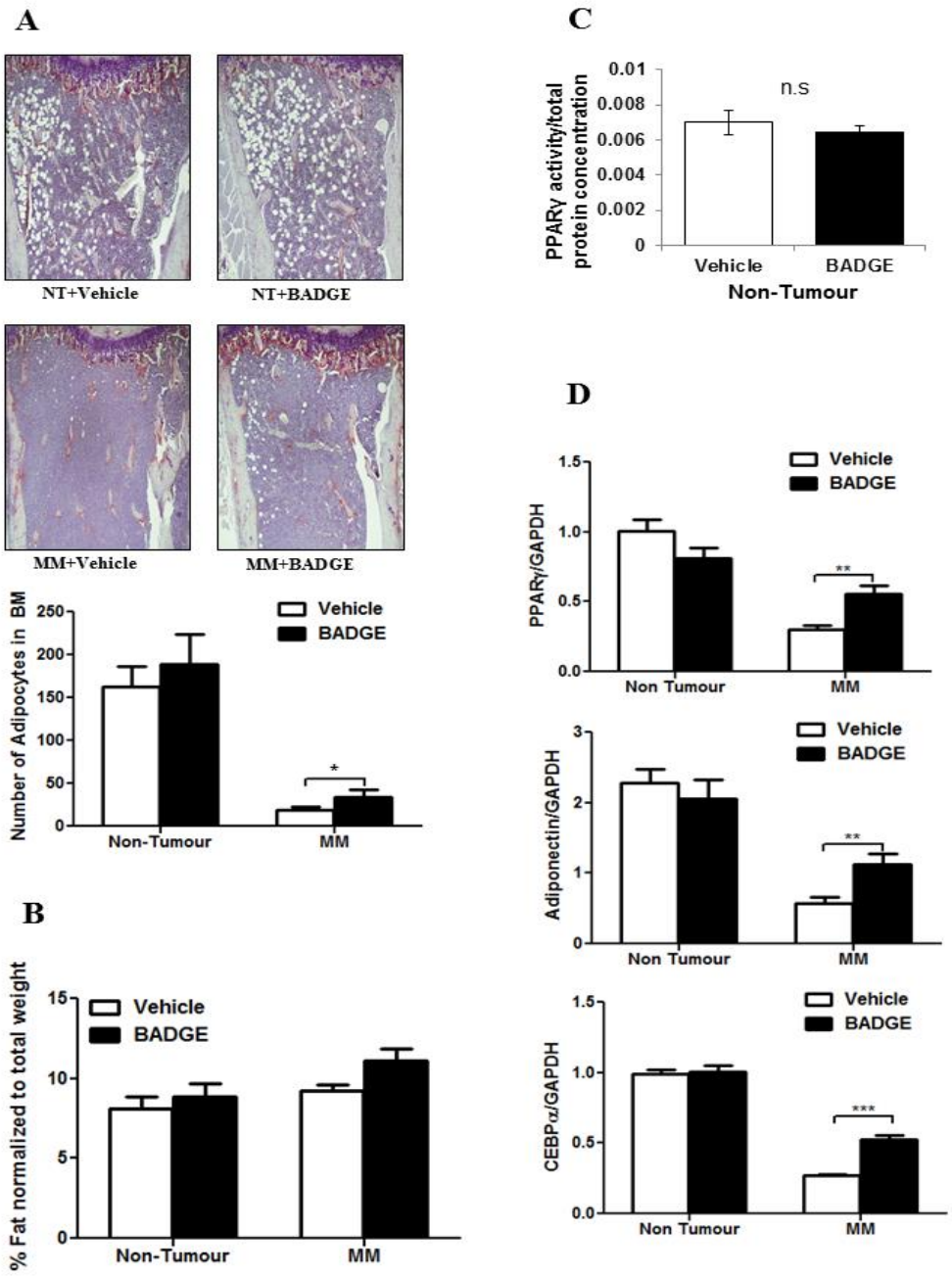

Figure 5.3. Increased number of adipocytes and mRNA expression of adipocyte markers in the bone marrow of myeloma-bearing mice treated with BADGE. (A) The number of adipocytes in the bone marrow quantitated by ImageJ analysis, using TRAP stained sections, (B) fat percentage measured by body composition analysis. (C) PPARγ activity in bone marrow protein lysates of BADGE and vehicle treated non-tumour (NT) mice, measured by PPARγ activity assay and normalized by total protein concentration. (D) *mRNA* expression of adipocyte markers by real-time PCR analysis; Expression of PPARγ, adiponectin, and CEBPα in bone marrow cells isolated from BADGE and vehicle treated non-tumour (NT) and myeloma-bearing (MM) mice. (NT vehicle, n=10; NT BADGE, n=10; MM vehicle, n=7; MM BADGE, n=8). Data are mean ± SEM. *p<0.05, **p<0.01, ***p<0.001.

5.3.3 Direct anti-tumour effects of BADGE on myeloma cells *in vitro*

As BADGE has a significant anti-tumour effect on myeloma development *in vivo*, I looked more closely at the effects of BADGE on myeloma cell growth and survival *in vitro*. Following treatment of 5TGM1 myeloma cells with BADGE at 0-50μM for 72h, BADGE dose dependently decreased 5TGM1 cell viability, whilst demonstrating no effect on the viability of pre-osteoblast 2T3 or bone marrow stromal ST2 cells in the same culture condition (Figure 5.4A). Since BADGE has previously been shown to have PPARγ independent effects. I undertook further studies to determine the mRNA expression of PPARγ, quantitative real-time PCR analysis was conducted in ST2 BMSCs and 5TGM1-GFP myeloma cells used *in vivo* and found that 5TGM1-GFP cells do not express PPARγ (Figure 5.4B).

In addition to murine 5TGM1 myeloma cells, I have looked at the effect of BADGE in human myeloma cells to determine the responses to BADGE. BADGE also decreased human eRPMI 8226 myeloma cell viability, with no effect on the viability of human bone marrow stromal mCherry-HS5 cells in co-culture system. This was using a dual colour fluorescent assay (Figure 5.4C). This confirmed the direct and specific anti-tumour effect of BADGE both in murine and human myeloma cells with no apparent negative effect on bone marrow stromal cells.

To determine whether the direct anti-tumour effect of BADGE in myeloma cells is through the activation of apoptosis, I measured the protein expression of apoptosis markers, cleaved-caspase-3 and cleaved-PARP1, following 0-50μM BADGE treatment for 72h in 5TGM1-GFP myeloma cells *in vitro,* using western blot analysis. No change in the protein expression of cleaved-caspase-3 and cleaved-PARP1 was observed (Figure 5.4D). The protein expression of tumour suppressor p53 was also measured and

an increase in p53 expression was observed with 50μM BADGE treatment (Figure 5.4D).

To begin to determine the mechanism of action of BADGE on myeloma cells, I looked at the mRNA expression of spliced XBP-1 (a regulator of plasma cell differentiation) and the tumour suppressor gene PTEN, following treatment with BADGE (0-50μM for 72h). A significant decrease in spliced XBP-1 and significant up-regulation of PTEN was observed (Figure 5.4E and F).

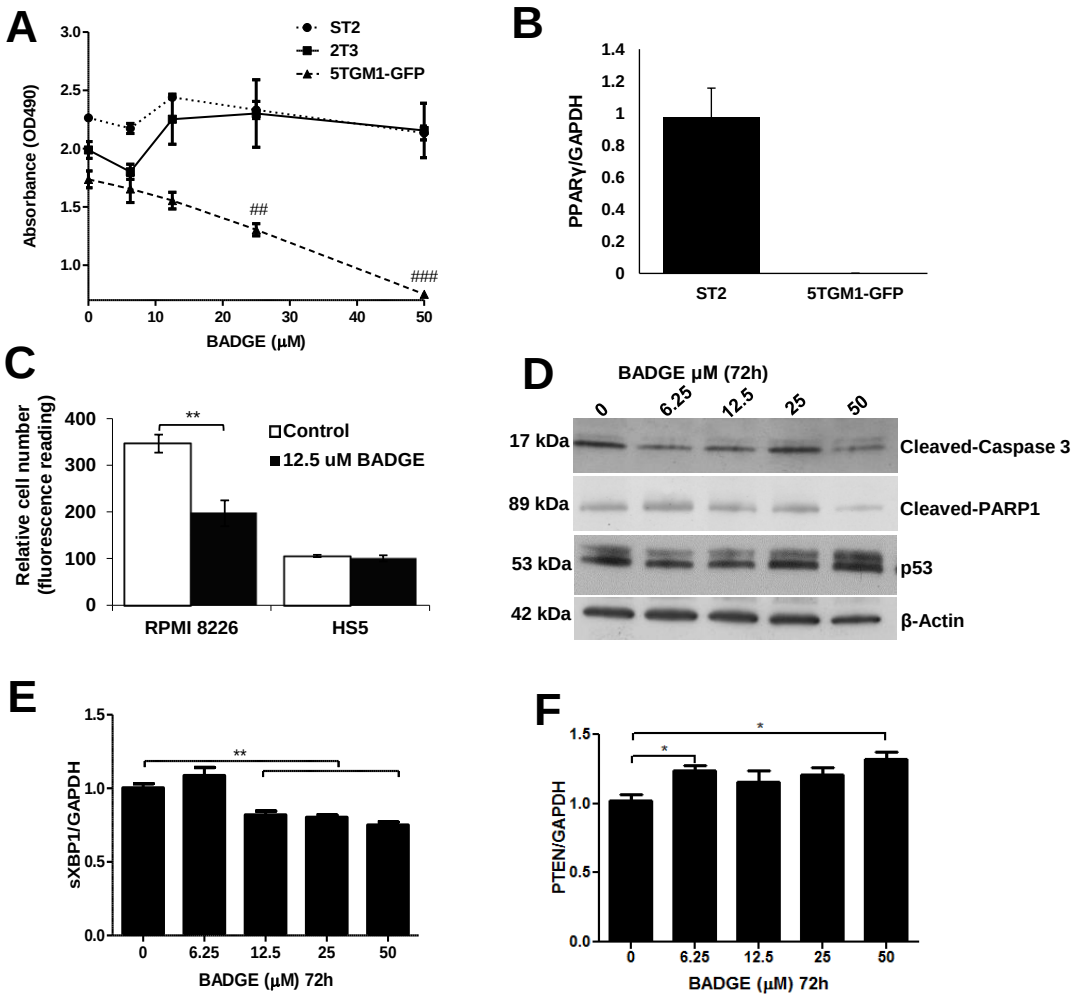

Figure 5.4. Direct anti-tumour effect of BADGE on myeloma cells. Cell viability, as measured by MTS assay, following treatment with 0-50μM BADGE for 72h (A) in 5TGM1-GFP MM cells, 2T3 murine osteoblasts or ST2 murine bone marrow stromal cells, (B) mRNA expression of PPARγ in ST2 BMSCs and 5TGM1-GFP myeloma cells, measured by quantitative real-time PCR analysis (C) cell viability measured by dual colour fluorescence following treatment with 12.5μM BADGE for 72h in human eRPMI8226 myeloma cells and mCherry-HS5 human bone marrow stromal cells, (D) Western blot analysis of apoptosis markers, cleaved-caspase-3, cleaved-PARP1, and tumour suppressor protein p53 expression, following 0-50μM BADGE treatment for 72h in 5TGM1-GFP MM cells *in vitro* (E) mRNA expression of spliced XBP-1 (sXBP1), and (F) PTEN, by quantitative real-time PCR analysis. Data are mean ± SEM. *p<0.05, **p<0.01, ***p<0.001 and ## p<0.01, ### p<0.001 as compared with ST2 and 2T3 cell viability.

5.3.4 Effect of BADGE on the AMPK signalling pathway

As BADGE inhibited the growth of myeloma cells *in vitro*, I looked further into the differential expression of multiple mRNA and protein from different signalling pathways, to investigate the mechanism of action of BADGE in myeloma. Activation of the AMPK signalling pathway has been shown to decrease tumour cell proliferation, suggesting a potential therapeutic approach for cancer therapies (Motoshima et al., 2006). I measured the protein expression of phosphorylated AMPK (p-AMPK) and total AMPK by western blot analysis in 5TGM1-GFP MM cells treated with 0-50μM BADGE for 72h. An increase in p-AMPK protein expression was observed with no difference in total AMPK expression (Figure 5.5A). As BADGE appeared to activate the AMPK signalling pathway, the effect of BADGE on downstream targets of AMPK was investigated.

It has been previously shown that activation of SIRT1 can be mediated by AMPK signalling (Ruderman et al., 2010). Also the SIRT1activator, SRT1720 has been shown to decrease myeloma growth both *in vitro* and *in vivo* (Chauhan et al., 2011). Therefore, I measured SIRT1 protein expression in 5TGM1-GFP myeloma cells treated with 0-50μM BADGE for 72h. A dose dependent increase in SIRT1 protein expression was observed with BADGE treatment, as quantitated by densitometry, using ImageJ analysis (Figure 5.5B).

To determine the effect of BADGE treatment *in vivo*, the mRNA expression of SIRT1 was measured in the bone marrow lysates isolated from vehicle and BADGE treated non-tumour and myeloma bearing mice. A significant increase in SIRT1 mRNA expression was observed in the bone marrow of BADGE treated myeloma bearing mice as compared with the vehicle treated myeloma bearing mice and BADGE treated non-tumour mice. No significant difference in SIRT1 mRNA expression was observed

between vehicle and BADGE treated non-tumour mice (Figure 5.5C). Autophagy is a complex catabolic cellular process that involves cell degradation of unnecessary or dysfunctional cellular components. Autophagy may be influenced by SIRT1, where autophagocytosis associated protein Atg3 is essential for effective autophagy (Salminen et al., 2008). Treatment of 5TGM1-GFP myeloma cells with 50μM BADGE increased Atg3 mRNA expression with no effect on 2T3 osteoblasts (Figure 5.5D).

An increase in angiogenesis has also been shown to promote increased tumour burden in various cancers (Folkman, 1995). VEGF is a well-accepted growth factor and marker of angiogenesis. To determine the effect of BADGE treatment on VEGF *in vitro*, I measured the mRNA expression of VEGFα by quantitative RT-PCR analysis in 5TGM1-GFP myeloma cells treated with 0-50μM BADGE for 72h. A dose dependent decrease in VEGFα mRNA expression was observed in 5TGM1-GFP cells treated with BADGE (Figure 5.5E).

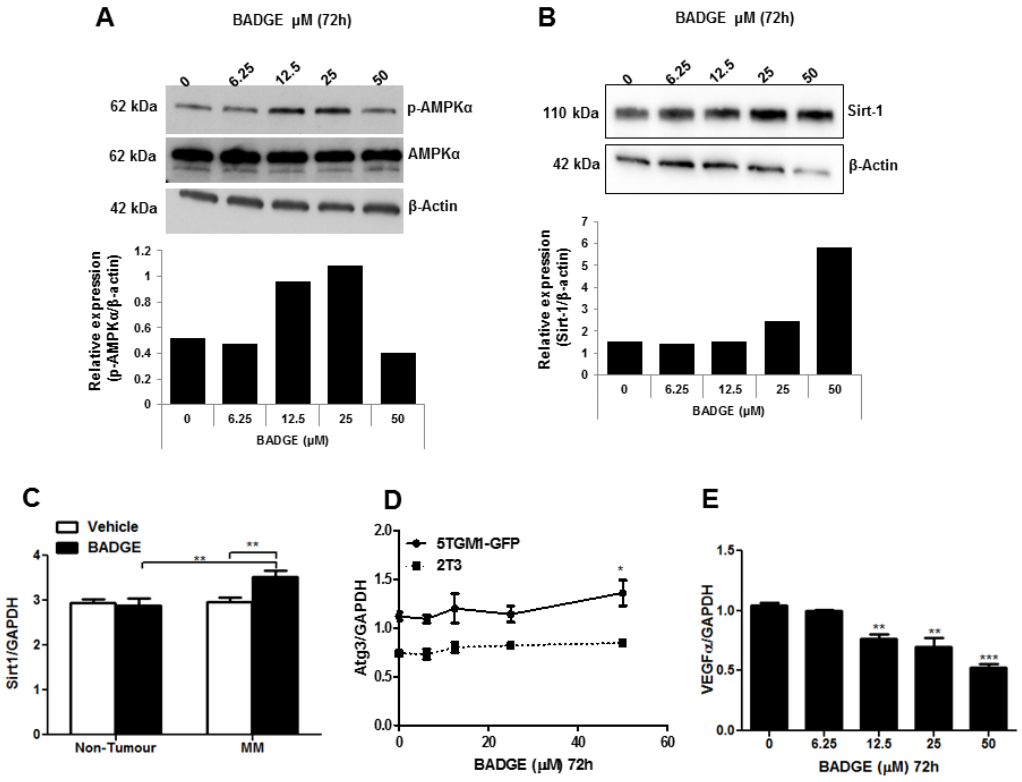

Figure 5.5. BADGE induced activation of AMPK, SIRT1, increased mRNA expression of autophagy marker Atg3 and decreased VEGFα. Western blot and quantitation by ImageJ analysis of (A) AMPK activation and (B) the downstream target, Sirt1, following 0-50μM BADGE treatment for 72h in 5TGM1-GFP MM cells *in vitro* (C) *mRNA* expression of Sirt1 in bone marrow cells isolated from BADGE and vehicle treated non-tumour (NT) and myeloma bearing (MM) mice (NT vehicle, n=10; NT BADGE, n=10; MM vehicle, n=7; MM BADGE, n=8), (D) *mRNA* expression of autophagy marker, Atg3, following 0-50μM BADGE treatment for 72h in 5TGM1-GFP MM cells and 2T3 osteoblast cells *in vitro*, (E) *mRNA* expression of angiogenesis marker, VEGFα, following 0-50μM BADGE treatment for 72h in 5TGM1-GFP MM cells *in vitro*, by quantitative RT-PCR analysis. Data are mean ± SEM. *p<0.05, **p<0.01, ***p<0.001 as compared with control.

5.3.5 The direct anti-tumour effect of BADGE on myeloma cells *in vitro* is independent of SIRT1

As BADGE treatment in myeloma cells increased SIRT1 protein expression dose dependently, I investigated whether the direct anti-tumour effect of BADGE is SIRT1 dependent. 5TGM1 MM cells were treated with a known inhibitor of SIRT1, EX-527 0-5μM for 24, 48, and 72h to determine the effect of SIRT1 inhibition on 5TGM1 myeloma cell viability *in vitro*. Although a significant increase in 5TGM1 cell viability was observed with 100nM and 5000nM (5μM) EX-527 treatment at 24h time point, no clear dose dependent trend was shown. At 72h time point, the effect of EX-527 treatment in increasing 5TGM1 myeloma cell viability was clearer with both high dosages of 1000nM (1μM) and 5000 nM (5μM) (Figure 5.6A). 5TGM1 cells were pre-treated for 24h before treating with BADGE, or treated with 50 nM, 100 nM and 5μM EX-527 for 72h in combination with 0-50μM of BADGE to determine the effect of SIRT1 inhibition in 5TGM1 cell viability *in vitro*. Despite treatment with the SIRT1 inhibitor, BADGE still significantly decreased the viability of 5TGM1 cells, with an enhanced BADGE effect of decreasing myeloma cell viability when pre-treated with 1μM EX-527 (Figure 5.6B and C). This suggests that the direct anti-tumour effect of BADGE may be mediated through a SIRT1-independent mechanism.

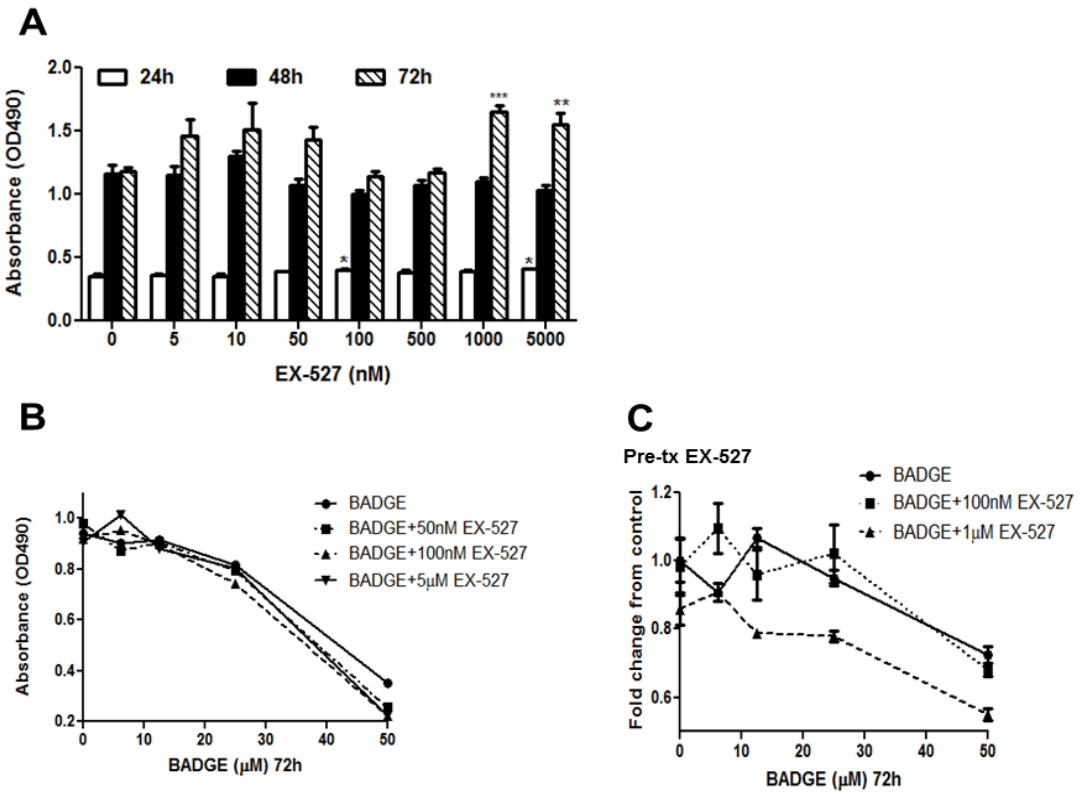

Figure 5.6. Inhibition of SIRT1 activity does not prevent the anti-tumour effect of BADGE. Cell viability of 5TGM1-GFP murine myeloma cells, as measured by MTS assay, (A) following treatment with 0-5000nM EX-527, SIRT1 inhibitor, for 24-72h (B) 0-50μM BADGE treatment combined with EX-527 for 72h (C) 0-50μM BADGE treatment for 72h, following pre-treatment with EX-527 for 24h. Data are mean ± SEM. *p<0.05, **p<0.01, ***p<0.001 as compared with control.

5.3.6 Effect of BADGE on NFκB p65 expression *in vitro*

SIRT1 has been shown to inhibit NFκB (Yeung et al., 2004). Thus the effect of increased SIRT1 protein expression following BADGE treatment was explored on NFκB p65 expression on 5TGM1-GFP cells *in vitro*. Once NFκB is activated, its p65 subunit translocates from the cytoplasm to the nucleus. Therefore, nuclear and cytoplasmic NFκB p65 was measured following 0-50 μM BADGE treatment on

5TGM1-GFP myeloma cells, to determine whether NFκB activation was involved. BADGE treatment had no effect on total, cytoplasmic or nuclear NFκB p65 expression, measured by western blot analysis (Figure 5.7A and B).

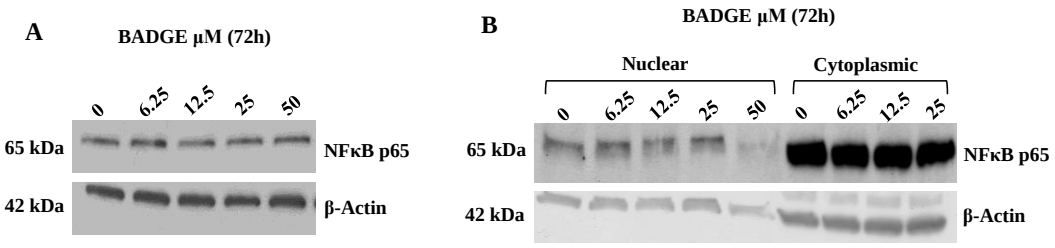

Figure 5.7. BADGE treatment has no effect on NFκB p65 protein expression *in vitro*. Effect of BADGE on 5TGM1-GFP murine myeloma cells in NFκB p65 expression, measured by western blotting analysis, protein expression of (A) total NFκB p65, (B) nuclear and cytoplasmic NFκB p65, following 0-50µM BADGE treatment for 72h *in vitro*.

5.3.7 Effect of BADGE on the expression of osteolineage markers

BADGE treatment has previously been shown to increase bone mass (Duque et al., 2012), although in the current study, no effect of BADGE on bone volume was observed in non-tumour mice. I measured the mRNA expression of RUNX2 and osteocalcin (OCN), by quantitative RT-PCR analysis. The expected bone loss seen in myeloma bearing mice, compared to non-tumour mice, was accompanied by a significant decrease in the RUNX2 and osteocalcin mRNA. In addition, a significant decrease in RUNX2 mRNA expression was observed in non-tumour mice treated with BADGE compared with vehicle treated mice (Figure 5.8A). Interestingly, there was no significant difference in overall trabecular bone volume or in the number of bone marrow adipocytes in BADGE treated non-tumour mice as compared with vehicle treated mice (Figure 5.2D and Figure 5.3A).

To determine the effect of BADGE treatment on the expression of osteogenic markers *in vitro*, the mRNA expression of RUNX2 and osteocalcin was measured by quantitative RT-PCR analysis in 5TGM1-GFP myeloma cells treated with 0-50μM BADGE for 72h. A dose dependent increase of both RUNX2 and osteocalcin mRNA expression was observed in 5TGM1-GFP cells treated with BADGE (Figure 5.8B). The effect of BADGE was also measured on the mRNA expression of RUNX2 and osteocalcin *in vitro* by quantitative RT-PCR analysis in ST2 murine BMSCs and 2T3 pre-osteoblast cells. In contrast to myeloma cell lines, no significant difference was observed in the expression of both RUNX2 and osteocalcin in ST2 and 2T3 cells treated with BADGE (Figure 5.8C and D). This suggests that BADGE selectively increases the mRNA expression of osteolineage markers in myeloma cells with no effect on bone marrow stromal and osteoblast cell lines *in vitro*.

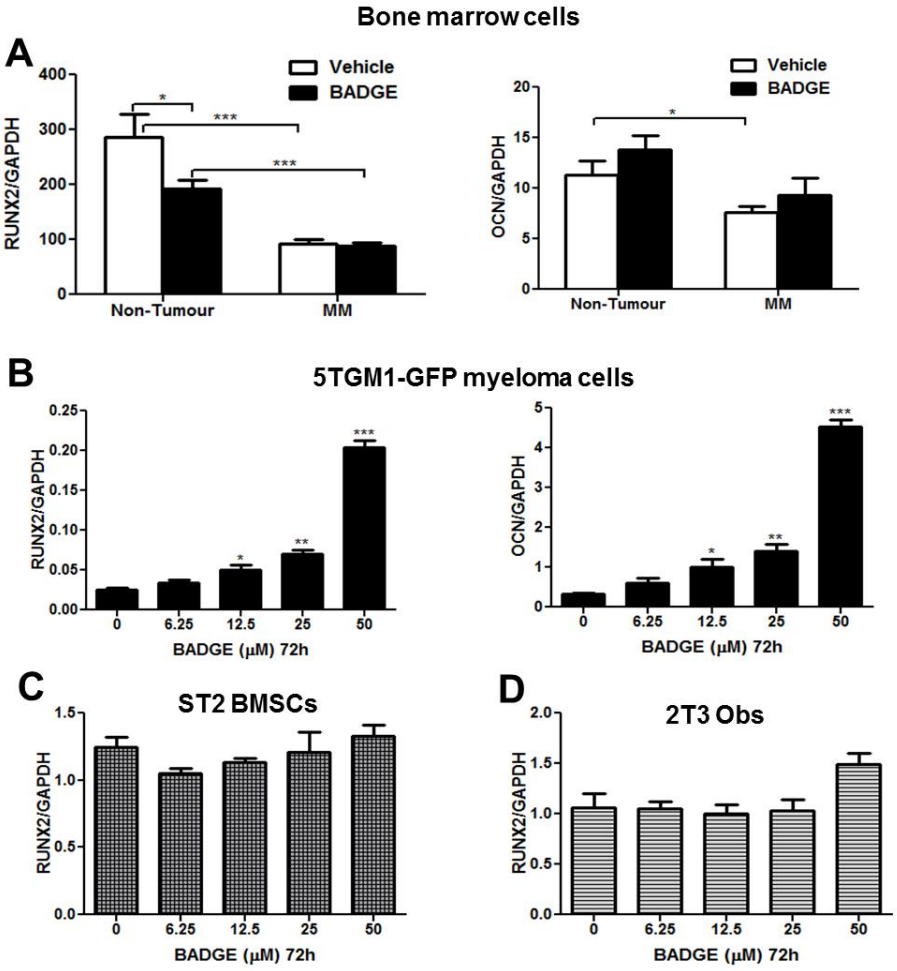

Figure 5.8. BADGE selectively increases *mRNA* expression of osteolineage markers. Measured by quantitative real-time PCR, *mRNA* expression of (A) RUNX2 and OCN in bone marrow cells isolated from BADGE and vehicle treated non-tumour (NT) and myeloma bearing (MM) mice (NT vehicle, n=10; NT BADGE, n=10; MM vehicle, n=7; MM BADGE, n=8), (B) RUNX2 and OCN, in 5TGM1-GFP MM cells (C) RUNX2 in murine ST2 BMSCs, and (D) RUNX2 in murine 2T3 osteoblast cell line, following 0-50μM BADGE treatment for 72h *in vitro*. Data are mean ± SEM. *p<0.05, **p<0.01, ***p<0.001 as compared with control.

5.4 Discussion

Studies in the previous chapter demonstrated that diet-induced obesity created a permissive host microenvironment for the MGUS-like condition in previously non-permissive C57BL/6 mice. Since an increase in bone marrow adiposity was also observed, bone marrow adiposity *in vivo* in a murine model of myeloma was manipulated using a synthetic PPARγ ligand, BADGE. The BADGE treatment regimen has previously been shown to decrease bone marrow adiposity *in vivo* (Naveiras et al., 2009;Bishop-Bailey, Hla and Warner, 2001).

In my studies, although BADGE treatment significantly decreased myeloma tumour burden, surprisingly, a significant increase in bone marrow adipocytes was observed in BADGE treated myeloma-bearing mice with no difference in non-tumour mice. The direct and specific anti-tumour effect of BADGE on myeloma cells *in vitro* suggests that BADGE may have protected the marrow space from becoming taken over by myeloma cells and allowed for other normal cells such as adipocytes to remain in the bone marrow space. As a result, an increase in bone marrow adipocytes was observed in myeloma bearing BADGE treated mice, and an increase in mRNA expression of adipocyte markers in the bone marrow lysates from myeloma bearing BADGE treated mice as compared with vehicle treated mice. This assumption is strengthened by the fact that no significant difference in the number of bone marrow adipocytes or mRNA expression of adipocyte markers in the bone marrow lysates were observed in non-tumour BADGE treated mice as compared with vehicle treated mice. In addition, no difference was observed in overall body fat percentage in both non-tumour and myeloma-bearing mice following BADGE treatment. Taken together, BADGE may be acting purely as an anti-myeloma agent *in vivo* without effecting the bone marrow or

overall adiposity in these mice. Therefore, the direct anti-myeloma effects of BADGE were investigated further.

BADGE has been reported as both an activator and inhibitor of PPARγ (Naveiras et al., 2009;Bishop-Bailey, Hla and Warner, 2001). The activity of PPARγ in the bone marrow lysates of non-tumour mice treated with BADGE did not change as compared to the vehicle treated mice. However, due to the limitation of the sample amount, the PPARγ activity was not measured in the bone marrow protein lysates of the myeloma-bearing mice. From these studies, it is unclear whether BADGE is acting as an agonist or antagonist of PPARγ in this system.

5TGM1-GFP myeloma cells used in the present study do not express PPARγ, suggesting that anti-myeloma effect of BADGE is independent of PPARγ. PPARγ ligands 15-deoxy-$\Delta^{12,14}$-prostaglandin J2 (15d-PGJ2) and ciglitazone have been shown to induce apoptosis in ANBL6 and 8226 human myeloma cell lines through activation of caspase 2 and 3 (Ray, Bernstein and Phipps, 2004). Both ANBL6 and 8226 human myeloma cell lines express PPARγ and addition of the myeloma growth factor IL-6 did not rescue those human myeloma cells from the anti-proliferative effect of PPARγ ligands. In support of this work, Eucker et al. demonstrated that additional PPARγ ligands, pioglitazone and rosiglitazone, also induced apoptosis in LP-1, U-266, RPMI-8226-S, OPM-2 and IM-9 human myeloma cell lines and primary human bone marrow plasma cells (Eucker et al., 2004).

Overexpression of PPARγ in human myeloma cell lines RPMI 8226 and U266 has been shown to decrease myeloma cell proliferation and increase apoptosis in the absence of PPARγ ligand, and the addition of the ligand ciglitazone further enhanced the anti-proliferative and apoptotic effect (Garcia-Bates, Bernstein and Phipps, 2008). The same

study demonstrated that co-culture of myeloma cells with human bone marrow stromal cells HS5, did not protect PPARγ-overexpressed myeloma cells from induction of apoptosis. Overexpression of PPARγ in HS5 bone marrow stromal cells and myeloma cells inhibited the myeloma growth factor IL-6 secretion by bone marrow stromal cells when cultured alone or co-cultured with myeloma cells. These studies suggest that tumour-derived or exogenous PPARγ may have anti-myeloma effect. Further studies investigating the role of host-derived PPARγ effect in myeloma development may give us better insight into its role and activity in myeloma pathogenesis both *in vitro* and *in vivo*.

In vitro studies demonstrated that BADGE specifically decreased the growth of both human RPMI 8226 and 5TGM1-GFP murine myeloma cells, but does not affect human HS5 BMSCs, murine ST2 stromal cells, or 2T3 pre-osteoblasts. Interestingly the anti-tumour effect of BADGE on myeloma cells is independent of the apoptotic markers cleaved-caspase 3 and cleaved-PARP, suggesting that the anti-tumour effect of BADGE in murine myeloma cells is independent of caspase-3 and PARP1 related mechanisms. In contrast, an increase in p53 protein expression was observed in 5TGM1-GFP myeloma cells treated with 50μM of BADGE. Tumour suppressor gene was shown to protect fibroblasts and vascular smooth muscle cells from apoptosis, and p53 was involved in the activation of oxidative stress-induced necrosis or autophagic cell death *in vitro* or *in vivo* (Halasi, Schraufnagel and Gartel, 2009;Mercer et al., 2005;Vaseva et al., 2012). These studies may suggest that p53 is involved in an autophagic or necrotic effect by BADGE in myeloma cells rather than apoptotic effect in the present study. However, more studies will be needed to draw this conclusion.

The anti-proliferative effect of adiponectin in myeloma cells is mediated through the activation of the AMPK pathway (Fowler et al., 2011;Medina et al., 2014). Treatment

with BADGE induced the activation of AMPK in 5TGM1-GFP myeloma cells. SIRT1 is a downstream target of AMPK signalling and an activator of SIRT1, SRT1720 has been shown to increase myeloma cell apoptosis (Chauhan et al., 2011). An increase in SIRT1 protein expression was observed with BADGE treatment in 5TGM1-GFP myeloma cells *in vitro* and a significant increase in SIRT1 mRNA expression in the bone marrow of myeloma-bearing BADGE treated mice as compared to non-tumour mice and myeloma-bearing vehicle treated mice *in vivo.*

Autophagy is a cellular process triggered by activation of SIRT1 (Zeng et al., 2012). A significant increase in mRNA expression of an autophagy marker, Atg3, was observed in 5TGM1-GFP myeloma cells treated with 50μM of BADGE. It has been shown that autophagy protects myeloma cells from apoptosis time dependently upon nutrient depletion, at least in part by an increase in SIRT1 protein expression (Zeng et al., 2012). This suggests that the direct anti-tumour effect of BADGE in my studies *in vitro* might be mediated through increasing autophagy, partly through activation of SIRT1 and/or p53 by protecting against apoptosis in these cells. Finally, the anti-myeloma effect of BADGE *in vitro* appears to be independent of SIRT1, as inhibitors of SIRT1 did not have an effect on the anti-myeloma role of BADGE. Further studies looking into the protein expression of autophagy markers in association with SIRT1 both *in vitro* and *in vivo* will help identify their roles in myeloma.

Furthermore, NFκB was shown to be inhibited by SIRT1 and NFκB activation has been shown to be involved in the progression of myeloma. Inhibitors of NFκB-inducing kinase (NIK) have been recently shown to be cytotoxic to myeloma cells (Demchenko et al., 2014;Yeung et al., 2004). Inactive NFκB remains in the cytosol of the cell and once activated, it translocates to the nucleus. There is no difference in cytoplasmic or nuclear NFκB protein expression in 5TGM1-GFP myeloma cell treated with BADGE,

suggesting that NFκB may not be responsible for the anti-myeloma effect of BADGE *in vitro*.

Taken together, although BADGE did not produce the predicted effects on the host microenvironment, this study is the first to show that BADGE decreases myeloma growth and tumour burden. Although the precise mechanisms are unclear, my studies suggest the response to BADGE is independent of PPARγ and SIRT1. Since the *in vitro* and *in vivo* anti-tumour response is strong and specific to myeloma cells, further study to dissect the key pathways mediating this response is warranted.

Chapter 6 : Conclusion and Significance

My research work has further highlighted the importance of the host microenvironment in the development of myeloma. Firstly, these studies showed the protective role of host-derived MMP7 in myeloma pathogenesis, in contrast to its role to promote disease in prostate and breast cancer (Lynch et al., 2005;Thiolloy et al., 2009). MMPs are involved in different biological processes including tissue remodelling, wound healing and most importantly in the tumour progression of various cancers. Increasing evidence supports a critical role for host-derived MMPs in cancer progression, such as host-derived MMP9 being shown to increase the progression of myeloma, pancreatic cancer, and prostate cancer *in vivo* (Fowler et al., 2009;Bruni-Cardoso et al., 2010;Nakamura et al., 2007).

A significant increase in the negative regulator of MMP7, TIMP1, in serum from myeloma-bearing murine models and patients with myeloma was observed, as compared to controls. No difference in MMP7 expression was found between serum of myeloma patients and controls. These data suggests that the activity, not the expression of MMP7 is important in myeloma pathogenesis. Over-expression of MMP7 in myeloma cells did not have an effect on myeloma tumour burden and bone disease, suggesting that the protective effect of MMP7 is host-derived rather than tumour-derived. However, prolonged culture of MMP7 overexpressed cells due to transduction, prior to inoculation into the mice, could have affected the functionality of these cells. Therefore, a conclusion cannot be drawn definitively from this study.

There is increasing evidence for a protective role of MMPs against cancer. Host-derived MMP13 has been shown to be protective against lung metastasis by generating the anti-angiogenic agent, endostatin (Fukuda et al., 2011). Decock et al. have reported that there is a negative correlation between the plasma level of MMP8 and breast cancer metastasis to lymph nodes, suggesting a potential protective role of MMP8 in breast cancer metastasis. Similarly, MMP8 knockout mice exposed to the carcinogen 4-Nitroquinoline-N-oxide develop increased squamous cell carcinomas (SCC) of the tongue compared to WT mice. In the same report, a positive correlation was noted between an improved patient survival rate and MMP8 expression, determined by IHC staining in tongue SCC tissue sections. These protective and often contrasting roles could explain the failure of broad-spectrum MMP inhibitors to combat cancer growth and metastasis in clinical trials, proving the need for specific inhibitors for individual MMPs and a more robust appreciation of the disease context. Therefore, the roles of individual MMPs in different diseases should be dissected.

Although there are many similarities between the growth or inhibiting factors involved prostate and breast cancer bone metastasis and myeloma, there are also major differences between them. One such example is the differential roles of TGF-β in prostate cancer and myeloma. A negative correlation between the expression of TGF-β receptor type 1 and II (TβR I and II) and prostate cancer progression has been shown previously, where the loss of expression of each receptor was associated with increasing disease progression, measured by immunohistochemical staining of the prostate tissues, and poor prognosis in patients with prostate cancer (Kim et al., 1998). Moreover, increased prostate cancer metastasis was observed in transgenic mice with a dominant negative TβRII expressed in the prostate (Williams et al., 2010). These studies

demonstrated a protective role of TGF-β in prostate cancer in contrast to its promotive effect in myeloma progression.

Similarly, the role of parathyroid hormone (PTH) in breast cancer and myeloma may be different. An association between increased PTH levels and increased risk of breast cancer has been documented (Michels et al., 2004;Nilsson et al., 2007). Additionally, PTH/PTH-related protein (PTHrP) receptor is expressed by human breast cancer cell lines and PTHrP may contribute to the progression of primary tumours and the associated osteolytic bone lesions (Birch et al., 1995;Hiremath and Wysolmerski, 2014). On the other hand, PTH, was shown to reverse bone destruction and restore the trabecular bone structure and strength during postmenopausal osteoporosis (Gallacher and Dixon, 2010). PTH treatment was shown to increase bone formation, decreased osteoclastic markers and reduced myeloma tumour burden *in vivo* (Pennisi et al., 2010). However, PTH effect of stimulating bone formation may increase risk of hypercalcemia, kidney stones, and production of growth factors, which could in turn increase tumour growth in myeloma.

My study demonstrates that the protective role of MMP7 in myeloma development may be mediated through the processing of galectin-3. Furthermore, this study is the first to show that galectin-3 can dose dependently promote myeloma growth. Interestingly, co-localisation of MMP2/MMP9 activity and galectin-3 was found in mouse xenografts and human breast cancer tissue, suggesting a role for cleaved galectin 3 by these MMPs in breast cancer progression. The same study has shown that BT-549 breast cancer cells with non-cleavable galectin-3 expression showed reduced tumour growth and angiogenesis in a mouse xenograft model, as compared with the wild-type BT-549 cells, suggesting that cleaved galectin-3 promotes breast cancer growth *in vivo* (Nangia-Makker et al., 2007). Similarly, increased levels of cleaved galectin-3 is associated

with prostate cancer progression in patient samples, which is contrary to data generated in my study (Wang et al., 2009;Nangia-Makker et al., 2007). These studies support the notion of a contrasting role for MMP7 in tumour progression, promoting prostate and breast cancer induced bone disease, and exerting a protective effect on myeloma pathogenesis as reported in my study (Lynch et al., 2005;Thiolloy et al., 2009). The different roles of galectin-3 in prostate or breast cancer and myeloma (data generated in my current studies) have strengthened the need to identify specific mechanisms for different disease contexts.

Further studies elucidating the effect of different MMP7-cleaved fragments of galectin-3 or other substrates in myeloma pathogenesis will be beneficial. To determine the local effect of cleaved galectin-3, the expression of cleaved galectin-3 could also be explored in the bone marrow sections of patients with myeloma or controls. MMP7 cleavage sites on recombinant murine galectin-3 could also be identified using N-terminal sequencing and investigating the role of mutated individual MMP7 cleavage sites of galectin-3 expressed by ST2 BMSCs or 2T3 osteoblasts in the co-culture system of myeloma cells *in vitro*.

Another aspect of my study highlighting the importance of the host microenvironment, is to investigate the effect of diet-induced obesity in myeloma pathogenesis in previously non-permissive C57Bl/6 mice. My studies showed that changing the host microenvironment using diet-induced obesity resulted in the development of an MGUS-like disorder in non-permissive C57BL/6 mice. Increased IGF-1 serum concentrations were associated with obesity and myeloma. Additionally, a calorie-restricted diet was shown to decrease IGF-1 levels. Therefore, the development of pharmacological mimetics of calorie restriction or inhibition of IGF-1 could be a therapeutic strategy (Hursting et al., 2003). My studies have shown that a high fat diet increased serum IGF-

1 levels prior to inoculation of 5TGM1-GFP myeloma cells, and which might be a factor responsible for creating the permissive environment for the MGUS-like condition in previously non-permissive C57BL/6 mice, by producing a diet-induced obesity. Calorie restriction has been shown to increase bone mass (Tatsumi et al., 2008). As one of the major features of myeloma is an osteolytic bone disease, further studies that involve calorie restriction in myeloma permissive KaLwRij mice may give us a better understanding of the importance of diet in myeloma development and the associated bone disease.

Serum galecin-3 was shown to be elevated in obese or diabetic patients, and treatment with the anti-diabetic drug metformin decreased galectin-3 levels in both patients and primary human adipocytes (Weigert et al., 2010). In contrast, galectin-3 deficient mice have been shown to have accelerated high fat diet induced obesity with increased visceral adiposity and increased phosphorylation of NFκB, suggesting a protective role of galectin-3 in obesity induced inflammation and diabetes (Pejnovic et al., 2013). Further investigation looking into the role of full-length and MMP7-cleaved galectin-3 in diet-induced obesity in murine myeloma model could explain the association between them.

Using the PPARγ ligand, BADGE, as a pharmacological approach resulted in a decrease in myeloma tumour burden *in vivo*. Although BADGE did not show an effect that was expected in the host microenvironment of myeloma, it had a direct-anti-tumour effect in both *in vitro* and *in vivo*. Additionally, this is the first study to show that a PPARγ ligand decreased myeloma growth and tumour burden, through a mechanism which may involve SIRT1. This notion is supported by studies using the SIRT1 activator, SRT1720, which was shown to induce myeloma cell apoptosis (Chauhan et al., 2011). Autophagy is a downstream target of SIRT1, and increased autophagy

protects against myeloma cell apoptosis (Hoang et al., 2009). Treatment of 5TGM1-GFP myeloma cells with BADGE increased the mRNA expression of an autophagy related gene Atg3, *in vitro.* Further studies looking at the protein expression of autophagy markers such as Beclin-1, LC3, and using inhibitors of the different stages of autophagy, in combination with BADGE, would help us dissect the impact of autophagy and BADGE in myeloma pathogenesis. In addition, as the 5TGM1-GFP murine myeloma cells utilized in my studies do not express PPARγ, inoculation of PPARγ-overexpressed 5TGM1-GFP cells in a murine model of myeloma will clarify the role of PPARγ in the development of myeloma.

In conclusion, my studies have demonstrated that the roles of MMP7 and obesity in the host microenvironment are important *in vivo*, with evidence to support the hypothesis that increased obesity and decreased MMP7 activity promoted myeloma growth. A decrease in MMP7 levels in the serum of obese patients was reported previously (Chavey et al., 2003;Ress et al., 2010). Further studies are required to investigate whether this permissive host environment for myeloma development created by diet-induced obesity is mediated through a decrease in MMP7 activity. This connection could be determined by inoculating MMP7-overexpressing 5TGM1-GFP myeloma cells into the non-permissive C57BL/6 mice on a high fat diet, and determine whether tumour derived MMP7 could rescue myeloma development induced by high fat diet in those mice.

In summary, my thesis work has shown that a decrease in MMP7 activity and an increase in adiposity or diet-induced obesity promoted myeloma growth and anti-myeloma effect of BADGE is independent of adiposity. However whether there is a definitive link between MMP7 activity and adiposity in myeloma development remained to be answered (Figure 6.1).

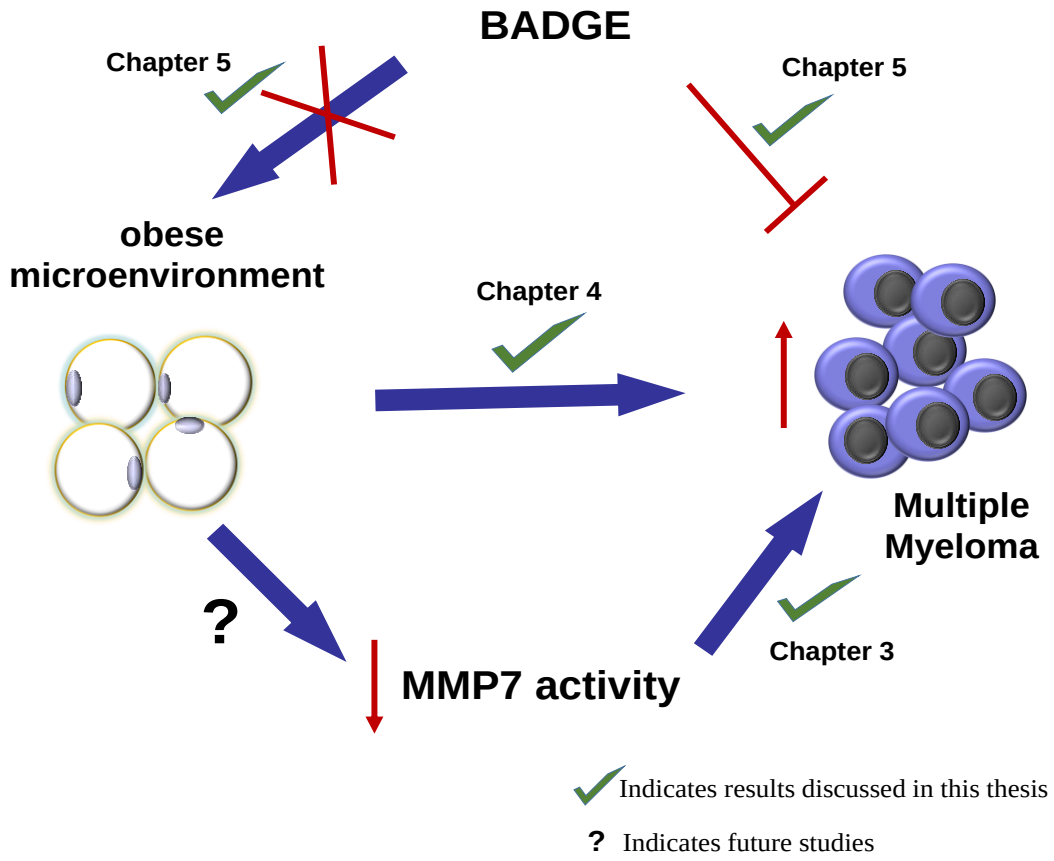

Figure 6.1. Role of MMP7, obese microenvironment, and BADGE in myeloma development.

Appendix I : Primer sequences

Primer sequences for PCR analysis

Name of gene		Sequence 5'-->3'
MMP7	Forward	TGGAGTGCCAGATGTTGCAG
	Reverse	TTTCCATATAGTTTCTGAATGCCT
TIMP1	Forward	TCC CCA GAA ATC AAC GAG AC
	Reverse	TCA CTC TCC AGT TTG CAA GG
GAPDH	Forward	ACC ACA GTC CAT GCC ATC AC
	Reverse	TCC ACC ACC CTG TTG CTG TA

Primer sequences for real-time PCR analysis

Name of gene		Sequence 5'-->3'
MMP7	Forward	CTA GGT CAT GCC TTC GCA CC
MMP7	Reverse	GTT CAC TCC TGC GTC CTC AC
Galectin-3	Forward	CAC TAA TCA GGT GAG CGG CA
	Reverse	GGC ATC GTT AAG CGA AAA GC
PPARγ	Forward	TAT TCT CAG TGG AGA CCG CC
	Reverse	ATC TTC TGG AGC ACC TTG GC
Adiponectin	Forward	GCG GAT CCA TGC TAC TGT TGC AAG CTC TC
	Reverse	GCG AGC TCT CAG TTG GTA TCA TGG TAG AG
CEBPα	Forward	AAT GGC AGT GTG CAC GTC TA
	Reverse	CCC CAG CCG TTA GTG AAG AG
XBP1	Forward	CTG AGT CCG AAT CAG GTG CAG
	Reverse	GTC CAT GGG AAG ATG TTC TGG
PTEN	Forward	AGT GGC GGA ACT TGC AAT CCT CA
	Reverse	ACA TGA ACT TGT CCT CCC GCC G
SIRT1	Forward	CGG CTA CCG AGG TCC ATA TAC
	Reverse	ACA ATC TGC CAC AGC GTC AT
Atg3	Forward	AAG CAA AGC GAG GAC AGC CA
	Reverse	GAG ACC TGA GGT GAG AAG CG
VEGF	Forward	ACT GGA CCC TGG CTT TAC TG
	Reverse	ACT TGA TCA CTT CAT GGG ACT TCT
Runx2	Forward	CCC AGC CAC CTT TAC CTA CA
	Reverse	TAT GGA GTG CTG CTG GTC TG
Osteocalcin	Forward	TGA ACA GAC TCC GGC GCT AC
	Reverse	GAC CAC TCC AGC ACA ACT CC
GAPDH	Forward	TCA ACAGCA ACT CCC ACT CTT CCA
	Reverse	ACC CTG TTG CTG TAG CCG TAT TCA

Appendix II

A-II.1 Publication

- **Lwin, S.T.***, Olechnowicz, S.W.***,** Fowler, J.A., Edwards, C.M. (2014) Diet-induced obesity promotes a myeloma-like condition *in vivo*. *Leukemia,* doi: 10.1038/leu.2014.295. *both authors contributed equally

A-II.2 Manuscript in preparation

- **Lwin, S.T.**, Cheng, T., Fowler, J.A., Drake, M., Edwards, J.R., Lynch, C.C., Edwards, C.M. Host-derived MMP7 inhibits myeloma growth via cleavage of galectin-3. (To be submitted to *Blood*)

A-II.3 Abstract presented

- **Lwin, S.T**., Lynch, C.C., Fowler, J.A., Edwards, J.R., Edwards, C.M. Host-derived MMP-7 decreases myeloma progression in vivo: an unexpected role for MMP-7 and galectin-3 in myeloma pathogenesis. **Oral Presentation** at Nuffield Dept. of Surgical Sciences Away day, Oxford, 2014
- **Lwin, S.T**., Olechnowicz, S.W., Fowler, J.A., Edwards, C.M. Diet-induced obesity promotes an MGUS-like condition, but not multiple myeloma, *in vivo*. **Poster Presentation** at 36th Annual Meeting of the American Society for Bone and Mineral Research, Houston, USA, 2014
- **Lwin, S.T.**, Olechnowicz, S.W., Fowler, J.A., Edwards, C.M. Obesity promotes the development of multiple myeloma and the associated bone disease *in vivo*. **Poster Presentation** at Annual Meeting of Oxford Cancer Research Centre, Oxford, 2014
- **Lwin, S.T**., Fowler, J.A., Olechnowicz, S.W., Edwards, C.M. Obesity promotes the development of multiple myeloma and the associated bone disease *in vivo*. **Oral Presentation** at 4th Joint Meeting of the Bone Research Society and the British Orthopaedic Research Society, 2013
- **Lwin, S.T.**, Edwards, J.R., Edwards, C.M. The PPARγ ligand BADGE reduces tumour burden and increases bone marrow adiposity in multiple myeloma *in vivo*. **Oral Presentation** at 12th International Conference on Cancer-Induced Bone Disease, Lyon, France, 2012

Appendix III : Awards

- Clarendon Scholarship 2011 – 2014
- Endocrine Fellows Foundation Fellowship 2014
  (Eighth Fellows Forum on Metabolic Bone Diseases)
- Travel award, Cancer-induced bone disease conference 2012

References

Abe, M., Hiura, K., Wilde, J., Shioyasono, A., Moriyama, K., Hashimoto, T., Kido, S., Oshima, T., Shibata, H., Ozaki, S., Inoue, D. and Matsumoto, T. (2004) Osteoclasts enhance myeloma cell growth and survival via cell-cell contact: A vicious cycle between bone destruction and myeloma expansion. *Blood,* 104 (8), pp. 2484-2491.

Abramson, S.R., Conner, G.E., Nagase, H., Neuhaus, I. and Woessner Jr., J.F. (1995) Characterization of rat uterine matrilysin and its cDNA: Relationship to human pump-1 and activation of procollagenases. *Journal of Biological Chemistry,* 270 (27), pp. 16016-16022.

Agnihotri, R., Crawford, H.C., Haro, H., Matrisian, L.M., Havrda, M.C. and Liaw, L. (2001) Osteopontin, a Novel Substrate for Matrix Metalloproteinase-3 (Stromelysin-1) and Matrix Metalloproteinase-7 (Matrilysin). *Journal of Biological Chemistry,* 276 (30), pp. 28261-28267.

Alford, A.I. and Hankenson, K.D. (2006) Matricellular proteins: Extracellular modulators of bone development, remodeling, and regeneration. *Bone,* 38 (6), pp. 749-757.

Alsayed, Y., Ngo, H., Runnels, J., Leleu, X., Singha, U.K., Pitsillides, C.M., Spencer, J.A., Kimlinger, T., Ghobrial, J.M., Jia, X., Lu, G., Timm, M., Kumar, A., Côté, D., Veilleux, I., Hedin, K.E., Roodman, G.D., Witzig, T.E., Kung, A.L., Hideshima, T., Anderson, K.C., Lin, C.P. and Ghobrial, I.M. (2007) Mechanisms of regulation of CXCR4/SDF-1 (CXCL12)-dependent migration and homing in multiple myeloma. *Blood,* 109 (7), pp. 2708-2717.

Andersen, N.F., Standal, T., Nielsen, J.L., Heickendorff, L., Borset, M., Sørensen, F.B. and Abildgaard, N. (2005) Syndecan-1 and angiogenic cytokines in multiple myeloma: Correlation with bone marrow angiogenesis and survival. *British Journal of Haematology,* 128 (2), pp. 210-217.

Anderson, D.M., Maraskovsky, E., Billingsley, W.L., Dougall, W.C., Tometsko, M.E., Roux, E.R., Teepe, M.C., DuBose, R.F., Cosman, D. and Galibert, L. (1997) A homologue of the TNF receptor and its ligand enhance T-cell growth and dendritic-cell function. *Nature,* 390 (6656), pp. 175-179.

Anderson, H.C., Sipe, J.B., Hessle, L., Dhamyamraju, R., Atti, E., Camacho, N.P. and Millán, J.L. (2004) Impaired Calcification Around Matrix Vesicles of Growth Plate and Bone in Alkaline Phosphatase-Deficient Mice. *American Journal of Pathology,* 164 (3), pp. 841-847.

Aparicio, A., Gardner, A., Tu, Y., Savage, A., Berenson, J. and Lichtenstein, A. (1998) In vitro cytoreductive effects on multiple myeloma cells induced by bisphosphonates. *Leukemia,* 12 (2), pp. 220-229.

Aref, S., Goda, T. and El-Sherbiny, M. (2003) Syndecan-1 in multiple myeloma: Relationship to conventional prognostic factors. *Hematology,* 8 (4), pp. 221-228.

Ariëns, R.A.S. (2013) Fibrin(ogen) and thrombotic disease. *Journal of Thrombosis and Haemostasis,* 11 (SUPPL.1), pp. 294-305.

Armstrong, A.J., Marengo, M.S., Oltean, S., Kemeny, G., Bitting, R.L., Turnbull, J.D., Herold, C.I., Marcom, P.K., George, D.J. and Garcia-Blanco, M.A. (2011) Circulating tumor cells from patients with advanced prostate and breast cancer display both epithelial and mesenchymal markers. *Molecular Cancer Research,* 9 (8), pp. 997-1007.

Balbín, M., Fueyo, A., Knäuper, V., Pendás, A.M., López, J.M., Jiménez, M.G., Murphy, G. and López-Otín, C. (1998) Collagenase 2 (MMP-8) expression in murine tissue-remodeling processes. Analysis of its potential role in postpartum involution of the uterus. *Journal of Biological Chemistry,* 273 (37), pp. 23959-23968.

Barillé, S., Akhoundi, C., Collette, M., Mellerin, M.-., Rapp, M.-., Harousseau, J.-., Bataille, R. and Amiot, M. (1997) Metalloproteinases in multiple myeloma: Production of matrix metalloproteinase-9 (MMP-9), activation of proMMP-2, and induction of MMP-1 by myeloma cells. *Blood,* 90 (4), pp. 1649-1655.

Barillé, S., Bataille, R., Rapp, M.-., Harousseau, J.-. and Amiot, M. (1999) Production of metalloproteinase-7 (Matrilysin) by human myeloma cells and its potential involvement in metalloproteinase-2 activation. *Journal of Immunology,* 163 (10), pp. 5723-5728.

Baumann, P., Mandl-Weber, S., Emmerich, B., Straka, C. and Schmidmaier, R. (2007) Activation of adenosine monophosphate activated protein kinase inhibits growth of multiple myeloma cells. *Experimental Cell Research,* 313 (16), pp. 3592-3603.

Beason, T.S., Chang, S.-., Sanfilippo, K.M., Luo, S., Colditz, G.A., Vij, R., Tomasson, M.H., Dipersio, J.F., Stockerl-Goldstein, K., Ganti, A., Wildes, T. and Carson, K.R. (2013) Influence of body mass index on survival in veterans with multiple myeloma. *Oncologist,* 18 (10), pp. 1074-1079.

Belaaouaj, A.A., Li, A., Wun, T.-., Welgus, H.G. and Shapiro, S.D. (2000) Matrix metalloproteinases cleave tissue factor pathway inhibitor: Effects on coagulation. *Journal of Biological Chemistry,* 275 (35), pp. 27123-27128.

Belch, A.R., Bergsagel, D.E., Wilson, K., O'Reilly, S., Wilson, J., Sutton, D., Pater, J., Johnston, D. and Zee, B. (1991) Effect of daily etidronate on the osteolysis of multiple myeloma. *Journal of Clinical Oncology,* 9 (8), pp. 1397-1402.

Berenson, J. (2010) Bisphosphonates in the Treatment of Myeloma Bone Disease. In *Myeloma Bone Disease.*, ed. G.D. Roodman, Humana Press, pp. 117-132.

Berenson, J.R., Lichtenstein, A., Porter, L., Dimopoulos, M.A., Bordoni, R., George, S., Lipton, A., Keller, A., Ballester, O., Kovacs, M., Blacklock, H., Bell, R., Simeone, J.F., Reitsma, D.J., Heffernan, M., Seaman, J. and Knight, R.D. (1998) Long-term pamidronate treatment of advanced multiple myeloma patients reduces skeletal events. *Journal of Clinical Oncology,* 16 (2), pp. 593-602.

Berenson, J.R., Lichtenstein, A., Porter, L., Dimopoulos, M.A., Bordoni, R., George, S., Lipton, A., Keller, A., Ballester, O., Kovacs, M.J., Blacklock, H.A., Bell, R., Simeone, J., Reitsma, D.J., Heffernan, M., Seaman, J. and Knight, R.D. (1996) Efficacy of pamidronate in reducing skeletal events in patients with advanced multiple myeloma. *New England Journal of Medicine,* 334 (8), pp. 488-493.

Berenson, J.R., Rosen, L.S., Howell, A., Porter, L., Coleman, R.E., Morley, W., Dreicer, R., Kuross, S.A., Lipton, A. and Seaman, J.J. (2001) Zoledronic acid reduces skeletal-related events in patients with osteolytic metastases. *Cancer,* 91 (7), pp. 1191-1200.

Berger, J. and Moller, D.E. (2002) The mechanism of actions of PPARs. *Annual Review of Medicine,* 53, pp. 409-35.

Bhardwaj, A., Sethi, G., Vadhan-Raj, S., Bueso-Ramos, C., Takada, Y., Gaur, U., Nair, A.S., Shishodia, S. and Aggarwal, B.B. (2007) Resveratrol inhibits proliferation, induces apoptosis, and overcomes chemoresistance through down-regulation of STAT3 and nuclear factor-κB-regulated antiapoptotic and cell survival gene products in human multiple myeloma cells. *Blood,* 109 (6), pp. 2293-2302.

Bianchi, G., Kyle, R.A., Colby, C.L., Larson, D.R., Kumar, S., Katzmann, J.A., Dispenzieri, A., Therneau, T.M., Cerhan, J.R., Melton III, L.J. and Rajkumar, S.V. (2010) Impact of optimal follow-up of monoclonal gammopathy of undetermined significance on early diagnosis and prevention of myeloma-related complications. *Blood,* 116 (12), pp. 2019-2025.

Bini, A., Wu, D., Schnuer, J. and Kudryk, B.J. (1999) Characterization of stromelysin 1 (MMP-3), matrilysin (MMP-7), and membrane type 1 matrix metalloproteinase (MT1-MMP) derived fibrin(ogen) fragments D-dimer and D-like monomer: NH2-terminal sequences of late-stage digest fragments. *Biochemistry,* 38 (42), pp. 13928-13936.

Birch, M.A., Carron, J.A., Scott, M., Fraser, W.D. and Gallagher, J.A. (1995) Parathyroid hormone (PTH)/PTH-related protein (PTHrP) receptor expression and mitogenic responses in human breast cancer cell lines. *British Journal of Cancer,* 72 (1), pp. 90-95.

Bishop-Bailey, D., Hla, T. and Warner, T.D. (2001) Bisphenol A diglycidyl ether (BADGE) is a PPARγ agonist in an ECV304 cell line. *British Journal of Pharmacology,* 131 (4), pp. 651-654.

Body, J.-., Facon, T., Coleman, R.E., Lipton, A., Geurs, F., Fan, M., Holloway, D., Peterson, M.C. and Bekker, P.J. (2006) A study of the biological receptor activator of nuclear factor-κ ligand inhibitor, denosumab, in patients with multiple myeloma or bone metastases from breast cancer. *Clinical Cancer Research,* 12 (4), pp. 1221-1228.

Body, J.-., Greipp, P., Coleman, R.E., Facon, T., Geurs, F., Fermand, J.-., Harousseau, J.-., Lipton, A., Mariette, X., Williams, C.D., Nakanishi, A., Holloway, D., Martin, S.W., Dunstan, C.R. and Bekker, P.J. (2003) A phase I study of AMGN-0007, a recombinant osteoprotegerin construct, in patients with multiple myeloma or breast carcinoma related bone metastases. *Cancer,* 97 (3 SUPPL.), pp. 887-892.

Bonewald, L.F. (2013) Osteocytes. In *Primer on the Metabolic Bone Diseases and Disorders of Mineral Metabolism.* John Wiley & Sons, Inc., pp. 34-41.

Boskey, A.L.and Robey, P.G. (2013) The Composition of Bone. In *Primer on the Metabolic Bone Diseases and Disorders of Mineral Metabolism.* John Wiley & Sons, Inc., pp. 49-58.

Botolin, S. and McCabe, L.R. (2006) Inhibition of PPARγ prevents type I diabetic bone marrow adiposity but not bone loss. *Journal of Cellular Physiology,* 209 (3), pp. 967-976.

Boyden, L.M., Mao, J., Belsky, J., Mitzner, L., Farhi, A., Mitnick, M.A., Wu, D., Insogna, K. and Lifton, R.P. (2002) High bone density due to a mutation in LDL-receptor-related protein 5. *New England Journal of Medicine,* 346 (20), pp. 1513-1521.

Boyle, W.J., Simonet, W.S. and Lacey, D.L. (2003) Osteoclast differentiation and activation. *Nature,* 423 (6937), pp. 337-342.

Bramhall, S.R., Neoptolemos, J.P., Stamp, G.W.H. and Lemoine, N.R. (1997) Imbalance of expression of matrix metalloproteinases (MMPs) and tissue inhibitors of the matrix metalloproteinases (TIMPs) in human pancreatic carcinoma. *Journal of Pathology,* 182 (3), pp. 347-355.

Breitkreutz, I., Raab, M.S., Vallet, S., Hideshima, T., Raje, N., Mitsiades, C., Chauhan, D., Okawa, Y., Munshi, N.C., Richardson, P.G. and Anderson, K.C. (2008) Lenalidomide inhibits osteoclastogenesis, survival factors and bone-remodeling markers in multiple myeloma. *Leukemia,* 22 (10), pp. 1925-1932.

Bruni-Cardoso, A., Johnson, L.C., Vessella, R.L., Peterson, T.E. and Lynch, C.C. (2010) Osteoclast-Derived Matrix Metalloproteinase-9 Directly Affects Angiogenesis in the Prostate Tumor-Bone Microenvironment. *Molecular Cancer Research,* 8 (4), pp. 459-470.

Cackowski, F.C., Anderson, J.L., Patrene, K.D., Choksi, R.J., Shapiro, S.D., Windle, J.J., Blair, H.C. and Roodman, G.D. (2010) Osteoclasts are important for bone angiogenesis. *Blood,* 115 (1), pp. 140-149.

Caers, J., Deleu, S., Belaid, Z., De Raeve, H., Van Valckenborgh, E., De Bruyne, E., DeFresne, M.-., Van Riet, I., Van Camp, B. and Vanderkerken, K. (2007) Neighboring adipocytes participate in the bone marrow microenvironment of multiple myeloma cells [11]. *Leukemia,* 21 (7), pp. 1580-1584.

Caers, J., Günthert, U., De Raeve, H., Valckenborgh, E.V., Menu, E., Riet, I.V., Camp, B.V. and Vanderkerken, K. (2006) The involvement of osteopontin and its receptors in multiple myeloma cell survival, migration and invasion in the murine 5T33MM model. *British Journal of Haematology,* 132 (4), pp. 469-477.

Cancer research UK, U. (2014) *Myeloma incidence statistics.* Available from: <http://www.cancerresearchuk.org/cancer-info/cancerstats/types/myeloma/incidence/uk-multiple-myeloma-incidence-statistics> (Accessed 07/02, 2014).

Cao, J.J. (2011) Effects of obesity on bone metabolism. *Journal of Orthopaedic Surgery and Research,* 6 (1).

Cao, J.J., Sun, L. and Gao, H. (2010) Diet-induced obesity alters bone remodeling leading to decreased femoral trabecular bone mass in mice. *Annals of the New York Academy of Sciences,* 1192, pp. 292-297.

Carrasco, D.R., Sukhdeo, K., Protopopova, M., Sinha, R., Enos, M., Carrasco, D.E., Zheng, M., Mani, M., Henderson, J., Pinkus, G.S., Munshi, N., Horner, J., Ivanova, E.V., Protopopov, A., Anderson, K.C., Tonon, G. and DePinho, R.A. (2007) The differentiation and stress response factor XBP-1 drives multiple myeloma pathogenesis**

**. *Cancer Cell,* 11 (4), pp. 349-360.

Castellano, G., Malaponte, G., Mazzarino, M.C., Figini, M., Marchese, F., Gangemi, P., Travali, S., Stivala, F., Canevari, S. and Libra, M. (2008) Activation of the osteopontin/matrix metalloproteinase-9 pathway correlates with prostate cancer progression. *Clinical Cancer Research,* 14 (22), pp. 7470-7480.

Cawthorn, W., Scheller, E., Learman, B., Parlee, S., Simon, B., Mori, H., Ning, X., Bree, A., Schell, B., Broome, D., Soliman, S., DelProposto, J., Lumeng, C., Mitra, A., Pandit, S., Gallagher, K., Miller, J., Krishnan, V., Hui, S., Bredella, M., Fazeli, P., Klibanski, A., Horowitz, M., Rosen, C. and MacDougald, O. (2014) Bone Marrow Adipose Tissue Is an Endocrine Organ that Contributes to Increased Circulating Adiponectin during Caloric Restriction. *Cell Metabolism,* 20 (2), pp. 368-375.

Chantry, A.D., Heath, D., Mulivor, A.W., Pearsall, S., Baud'Huin, M., Coulton, L., Evans, H., Abdul, N., Werner, E.D., Bouxsein, M.L., Key, M.L., Seehra, J., Arnett, T.R., Vanderkerken, K. and Croucher, P. (2010) Inhibiting activin-A signaling stimulates bone formation and prevents cancer-induced bone destruction in vivo. *Journal of Bone and Mineral Research,* 25 (12), pp. 2357-2370.

Chauhan, D., Bandi, M., Singh, A.V., Ray, A., Raje, N., Richardson, P. and Anderson, K.C. (2011) Preclinical evaluation of a novel SIRT1 modulator SRT1720 in multiple myeloma cells. *British Journal of Haematology,* 155 (5), pp. 588-598.

Chavey, C., Mari, B., Monthouel, M.-., Bonnafous, S., Anglard, P., Van Obberghen, E. and Tartare-Deckert, S. (2003) Matrix metalloproteinases are differentially expressed in adipose tissue during obesity and modulate adipocyte differentiation. *Journal of Biological Chemistry,* 278 (14), pp. 11888-11896.

Chen, P., Abacherli, L.E., Nadler, S.T., Wang, Y., Li, Q. and Parks, W.C. (2009) MMP7 shedding of syndecan-1 facilitates re-epithelialization by affecting a2ß1 integrin activation. *PLoS ONE,* 4 (8), pp. e6565.

Chevallet, M., Luche, S. and Rabilloud, T. (2006) Silver staining of proteins in polyacrylamide gels. *Nature Protocols,* 1 (4), pp. 1852-1858.

Choi, S.J., Cruz, J.C., Craig, F., Chung, H., Devlin, R.D., Roodman, G.D. and Alsina, M. (2000) Macrophage inflammatory protein 1-alpha is a potential osteoclast stimulatory factor in multiple myeloma. *Blood,* 96 (2), pp. 671-675.

Choi, S.J., Oba, Y., Gazitt, Y., Alsina, M., Cruz, J., Anderson, J. and David Roodman, G. (2001) Antisense inhibition of macrophage inflammatory protein 1-a blocks bone destruction in a model of myeloma bone disease. *Journal of Clinical Investigation,* 108 (12), pp. 1833-1841.

Clark, R.A.F., Nielsen, L.D., Howell, S.E. and Folkvord, J.M. (1985) Human keratinocytes that have not terminally differentiated synthesize laminin and fibronectin but deposit only fibronectin in the pericellular matrix. *Journal of Cellular Biochemistry,* 28 (2), pp. 127-141.

Clément-Lacroix, P., Ai, M., Morvan, F., Roman-Roman, S., Vayssière, B., Belleville, C., Estrera, K., Warman, M.L., Baron, R. and Rawadi, G. (2005) Lrp5-independent activation of Wnt signaling by lithium chloride increases bone formation and bone mass in mice. *Proceedings of the National Academy of Sciences of the United States of America,* 102 (48), pp. 17406-17411.

Coleman, R.E., Major, P., Lipton, A., Brown, J.E., Lee, K.-., Smith, M., Saad, F., Zheng, M., Hei, Y.J., Seaman, J. and Cook, R. (2005) Predictive value of bone resorption and formation markers in cancer patients with bone metastases receiving the bisphosphonate zoledronic acid. *Journal of Clinical Oncology,* 23 (22), pp. 4925-4935.

Colla, S., Morandi, F., Lazzaretti, M., Rizzato, R., Lunghi, P., Bonomini, S., Mancini, C., Pedrazzoni, M., Crugnola, M., Rizzoli, V. and Giuliani, N. (2005) Human myeloma cells express the bone regulating gene Runx2/Cbfa1 and produce osteopontin that is involved in angiogenesis in multiple myeloma patients. *Leukemia,* 19 (12), pp. 2166-2176.

Colucci, S., Brunetti, G., Oranger, A., Mori, G., Sardone, F., Specchia, G., Rinaldi, E., Curci, P., Liso, V., Passeri, G., Zallone, A., Rizzi, R. and Grano, M. (2011) Myeloma cells suppress osteoblasts through sclerostin secretion. *Blood Cancer Journal,* 1 (6), pp. e27.

Conway, E.J., Wen, J., Feng, Y., Mo, A., Huang, W.-., Keever-Taylor, C.A., Hari, P., Vesole, D.H. and Chang, C.-. (2009) Phenotyping studies of clonotypic B lymphocytes from patients with multiple myeloma by flow cytometry. *Archives of Pathology and Laboratory Medicine,* 133 (10), pp. 1594-1599.

Corre, J., Mahtouk, K., Attal, M., Gadelorge, M., Huynh, A., Fleury-Cappellesso, S., Danho, C., Laharrague, P., Klein, B., Rème, T. and Bourin, P. (2007) Bone marrow mesenchymal stem cells are abnormal in multiple myeloma. *Leukemia,* 21 (5), pp. 1079-1088.

Crawford, H.C., Scoggins, C.R., Kay Washington, M., Matrisian, L.M. and Leach, S.D. (2002) Matrix metalloproteinase-7 is expressed by pancreatic cancer precursors and regulates acinar-to-ductal metaplasia in exocrine pancreas. *Journal of Clinical Investigation,* 109 (11), pp. 1437-1444.

Crockett, J.C., Rogers, M.J., Coxon, F.P., Hocking, L.J. and Helfrich, M.H. (2011) Bone remodelling at a glance. *Journal of Cell Science,* 124 (7), pp. 991-998.

Croucher, P.I., Shipman, C.M., Lippitt, J., Perry, M., Asosingh, K., Hijzen, A., Brabbs, A.C., Van Beek, E.J.R., Holen, I., Skerry, T.M., Dunstan, C.R., Russell, G.R., Van Camp, B. and Vanderkerken, K. (2001) Osteoprotegerin inhibits the development of osteolytic bone disease in multiple myeloma. *Blood,* 98 (13), pp. 3534-3540.

Dallas, S.L., Garrett, I.R., Oyajobi, B.O., Dallas, M.R., Boyce, B.F., Bauss, F., Radl, J. and Mundy, G.R. (1999) Ibandronate reduces osteolytic lesions but not tumor burden in a murine model of myeloma bone disease. *Blood,* 93 (5), pp. 1697-1706.

De Pergola, G. and Silvestris, F. (2013) Obesity as a major risk factor for cancer. *Journal of Obesity,* 2013, pp. 291546.

Decock, J., Hendrickx, W., Vanleeuw, U., Van Belle, V., Van Huffel, S., Christiaens, M.-., Ye, S. and Paridaens, R. (2008) Plasma MMP1 and MMP8 expression in breast cancer: Protective role of MMP8 against lymph node metastasis. *BMC Cancer,* 8, pp. 77.

Demchenko, Y.N., Brents, L.A., Li, Z., Bergsagel, L.P., McGee, L.R. and Kuehl, M.W. (2014) Novel inhibitors are cytotoxic for myeloma cells with NFkB inducing kinase-dependent activation of NFkB. *Oncotarget,* 5 (12), pp. 4554-4566.

Derycke, L.D.M. and Bracke, M.E. (2004) N-cadherin in the spotlight of cell-cell adhesion, differentiation, invasion and signalling. *International Journal of Developmental Biology,* 48 (5-6), pp. 463-476.

Devlin, M.J., Cloutier, A.M., Thomas, N.A., Panus, D.A., Lotinun, S., Pinz, I., Baron, R., Rosen, C.J. and Bouxsein, M.L. (2010) Caloric restriction leads to high marrow adiposity and low bone mass in growing mice. *Journal of Bone and Mineral Research,* 25 (9), pp. 2078-2088.

DiMascio, L., Voermans, C., Uqoezwa, M., Duncan, A., Lu, D., Wu, J., Sankar, U. and Reya, T. (2007) Identification of adiponectin as a novel hemopoietic stem cell growth factor. *Journal of Immunology,* 178 (6), pp. 3511-3520.

Dimopoulos, M., Spencer, A., Attal, M., Prince, H.M., Harousseau, J.-, Dmoszynska, A., San Miguel, J., Hellmann, A., Facon, T., Foà, R., Corso, A., Masliak, Z., Olesnyckyj, M., Yu, Z., Patin, J., Zeldis, J.B. and Knight, R.D. (2007) Lenalidomide plus dexamethasone for relapsed or refractory multiple myeloma. *New England Journal of Medicine,* 357 (21), pp. 2123-2132.

Dolgin, E. (2011) Stem cells: Transplants on trial. *Nature,* 480 (7377 SUPPL.), pp. S46-S47.

Dowling, J., Yu, Q.-. and Fuchs, E. (1996) ß4 Integrin is required for hemidesmosome formation, cell adhesion and cell survival. *Journal of Cell Biology,* 134 (2), pp. 559-572.

Droin, N., Hendra, J.-., Ducoroy, P. and Solary, E. (2009) Human defensins as cancer biomarkers and antitumour molecules. *Journal of Proteomics,* 72 (6), pp. 918-927.

Ducy, P., Desbois, C., Boyce, B., Pinero, G., Story, B., Dunstan, C., Smith, E., Bonadio, J., Goldstein, S., Gundberg, C., Bradley, A. and Karsenty, G. (1996) Increased bone formation in osteocalcin-deficient mice. *Nature,* 382 (6590), pp. 448-452.

Ducy, P., Schinke, T. and Karsenty, G. (2000) The osteoblast: A sophisticated fibroblast under central surveillance. *Science,* 289 (5484), pp. 1501-1504.

Duque, G., Li, W., Vidal, C., Bermeo, S., Rivas, D. and Henderson, J. (2012) Pharmacological inhibition of PPAR? increases osteoblastogenesis and bone mass in male C57BL/6 mice. *Journal of Bone and Mineral Research,* 28 (2), pp. 639-648.

Durie, B.G.M. (2006) The role of anatomic and functional staging in myeloma: Description of Durie/Salmon plus staging system. *European journal of cancer,* 42 (11), pp. 1539-1543.

Edwards, C.and Mundy, G. (2010) Proteasome Inhibitors and the Wnt Signaling Pathway in Myeloma Bone Disease. In *Myeloma Bone Disease.*, ed. G.D. Roodman, Humana Press, pp. 211-229.

Edwards, C.M., Edwards, J.R., Lwin, S.T., Esparza, J., Oyajobi, B.O., McCluskey, B., Munoz, S., Grubbs, B. and Mundy, G.R. (2008) Increasing wnt signaling in the bone marrow microenvironment inhibits the development of myeloma bone disease and reduces tumor burden in bone in vivo. *Blood,* 111 (5), pp. 2833-2842.

Edwards, C.M., Lwin, S.T., Fowler, J.A., Oyajobi, B.O., Zhuang, J., Bates, A.L. and Mundy, G.R. (2009) Myeloma cells exhibit an increase in proteasome activity and an enhanced

response to proteasome inhibition in the bone marrow microenvironment in vivo. *American Journal of Hematology,* 84 (5), pp. 268-272.

Edwards, C.M., Zhuang, J. and Mundy, G.R. (2008) The pathogenesis of the bone disease of multiple myeloma. *Bone,* 42 (6), pp. 1007-1013.

Edwards, J.R., Nyman, J.S., Lwin, S.T., Moore, M.M., Esparza, J., O'Quinn, E.C., Hart, A.J., Biswas, S., Patil, C.A., Lonning, S., Mahadevan-Jansen, A. and Mundy, G.R. (2010) Inhibition of TGF-ß signaling by 1D11 antibody treatment increases bone mass and quality in vivo. *Journal of Bone and Mineral Research,* 25 (11), pp. 2419-2426.

Ehrlich, L.A., Chung, H.Y., Ghobrial, I., Choi, S.J., Morandi, F., Colla, S., Rizzoli, V., Roodman, G.D. and Giuliani, N. (2005) EL-3 is a potential inhibitor of osteoblast differentiation in multiple myeloma. *Blood,* 106 (4), pp. 1407-1414.

Elomaa, I., Risteli, L., Laakso, M., Lahtinen, R., Virkkunen, P. and Risteli, J. (1996) Monitoring the action of clodronate with type I collagen metabolites in multiple myeloma. *European Journal of Cancer,* 32 (7), pp. 1166-1170.

Elrod, H.A. and Sun, S.-. (2008) PPAR γ and apoptosis in cancer. *PPAR Research,* , pp. e704165.

Engelhardt, M., Terpos, E., Kleber, M., Gay, F., Wäsch, R., Morgan, G., Cavo, M., van de Donk, N., Beilhack, A., Bruno, B., Johnsen, H.E., Hajek, R., Driessen, C., Ludwig, H., Beksac, M., Boccadoro, M., Straka, C., Brighen, S., Gramatzki, M., Larocca, A., Lokhorst, H., Magarotto, V., Morabito, F., Dimopoulos, M.A., Einsele, H., Sonneveld, P. and Palumbo, A. (2014) European myeloma network recommendations on the evaluation and treatment of newly diagnosed patients with multiple myeloma. *Haematologica,* 99 (2), pp. 232-242.

Eucker, J., Bängeroth, K., Zavrski, I., Krebbel, H., Zang, C., Heider, U., Jakob, C., Elstner, E., Possinger, K. and Sezer, O. (2004) Ligands of peroxisome proliferator-activated receptor γ induce apoptosis in multiple myeloma. *Anti-Cancer Drugs,* 15 (10), pp. 955-960.

Faisal Khan, K.M., Laurie, G.W., McCaffrey, T.A. and Falcone, D.J. (2002) Exposure of cryptic domains in the a1-chain of laminin-1 by elastase stimulates macrophages urokinase and matrix metalloproteinase-9 expression. *Journal of Biological Chemistry,* 277 (16), pp. 13778-13786.

Fechtner, K., Hillengass, J., Delorme, S., Heiss, C., Neben, K., Goldschmidt, H., Kauczor, H.-. and Weber, M.-. (2010) Staging monoclonal plasma cell disease: Comparison of the Durie-Salmon and the Durie-Salmon PLUS staging systems. *Radiology,* 257 (1), pp. 195-204.

Feliers, D., Woodruff, K. and Abboud, S. (1999) Potential role of insulin-like growth factor binding protein-4 in the uncoupling of bone turnover in multiple myeloma. *British Journal of Haematology,* 104 (4), pp. 715-722.

Feng, R., Anderson, G., Xiao, G., Elliott, G., Leoni, L., Mapara, M.Y., Roodman, G.D. and Lentzsch, S. (2007) SDX-308, a nonsteroidal anti-inflammatory agent, inhibits NF- κ B activity, resulting in strong inhibition of osteoclast formation/activity and multiple myeloma cell growth. *Blood,* 109 (5), pp. 2130-2138.

Fermand, J.-., Katsahian, S., Divine, M., Leblond, V., Dreyfus, F., Macro, M., Arnulf, B., Royer, B., Mariette, X., Pertuiset, E., Belanger, C., Janvier, M., Chevret, S., Brouet, J.C. and Ravaud, P. (2005) High-dose therapy and autologous blood stem-cell transplantation compared with conventional treatment in myeloma patients aged 55 to 65 years: Long-term results of a randomized control trial from the group myelome-autogreffe. *Journal of Clinical Oncology,* 23 (36), pp. 9227-9233.

Filippov, S., Caras, I., Murray, R., Matrisian, L.M., Chapman Jr., H.A., Shapiro, S. and Weiss, S.J. (2003) Matrilysin-dependent elastolysis by human macrophages. *Journal of Experimental Medicine,* 198 (6), pp. 925-935.

Fingleton, B., Lynch, C.C., Vargo-Gogola, T. and Matrisian, L.M. (2010) Cleavage of E-cadherin by matrix metalloproteinase-7 promotes cellular proliferation in nontransformed cell lines via activation of RhoA. *Journal of Oncology,* 2010, pp. e530745.

Folkman, J. (1995) Angiogenesis in cancer, vascular, rheumatoid and other disease. *Nature Medicine,* 1 (1), pp. 27-31.

Fonseca, H., Moreira-Gonçalves, D., Esteves, J.L.S., Viriato, N., Vaz, M., Mota, M.P. and Duarte, J.A. (2011) Voluntary exercise has long-term in vivo protective effects on osteocyte viability and bone strength following ovariectomy. *Calcified Tissue International,* 88 (6), pp. 443-454.

Fowler, J.A., Lwin, S.T., Drake, M.T., Edwards, J.R., Kyle, R.A., Mundy, G.R. and Edwards, C.M. (2011) Host-derived adiponectin is tumor-suppressive and a novel therapeutic target for multiple myeloma and the associated bone disease. *Blood,* 118 (22), pp. 5872-5882.

Fowler, J.A., Mundy, G.R., Lwin, S.T. and Edwards, C.M. (2012) Bone marrow stromal cells create a permissive microenvironment for myeloma development: A new stromal role for Wnt inhibitor Dkk1. *Cancer Research,* 72 (9), pp. 2183-2189.

Fowler, J.A., Mundy, G.R., Lwin, S.T., Lynch, C.C. and Edwards, C.M. (2009) A murine model of myeloma that allows genetic manipulation of the host microenvironment. *DMM Disease Models and Mechanisms,* 2 (11-12), pp. 604-611.

Fryer, R.A., Graham, T.J., Smith, E.M., Walker-Samuel, S., Morgan, G.J., Robinson, S.P. and Davies, F.E. (2013) Characterization of a Novel Mouse Model of Multiple Myeloma and Its Use in Preclinical Therapeutic Assessment. *PLoS ONE,* 8 (2), pp. e57641.

Fukuda, H., Mochizuki, S., Abe, H., Okano, H.J., Hara-Miyauchi, C., Okano, H., Yamaguchi, N., Nakayama, M., D'Armiento, J. and Okada, Y. (2011) Host-derived MMP-13 exhibits a protective role in lung metastasis of melanoma cells by local endostatin production. *British Journal of Cancer,* 105 (10), pp. 1615-1624.

Galewska, Z., Romanowicz, L., Jaworski, S. and Bańkowski, E. (2010) Matrix metalloproteinases, MMP-7 and MMP-26, in plasma and serum of control and preeclamptic umbilical cord blood. *European Journal of Obstetrics & Gynecology and Reproductive Biology,* 150 (2), pp. 152-156.

Gallacher, S.J. and Dixon, T. (2010) Impact of treatments for postmenopausal osteoporosis (bisphosphonates, parathyroid hormone, strontium ranelate, and denosumab) on bone quality: A systematic review. *Calcified Tissue International,* 87 (6), pp. 469-484.

Galli, L.M., Barnes, T., Cheng, T., Acosta, L., Anglade, A., Willert, K., Nusse, R. and Burrus, L.W. (2006) Differential inhibition of Wnt-3a by Strp-1, Sfrp-2, and Sfrp-3. *Developmental Dynamics,* 235 (3), pp. 681-690.

Galson, D.L.and Roodman, G.D. (2011) 2 - Origins of Osteoclasts. In *Osteoimmunology.*, ed. J.L.C.H. Takayanagi,San Diego: Academic Press, pp. 7-41.

Garcia-Bates, T.M., Bernstein, S.H. and Phipps, R.P. (2008) Peroxisome proliferator-activated receptor γ overexpression suppresses growth and induces apoptosis in human multiple myeloma cells. *Clinical Cancer Research,* 14 (20), pp. 6414-6425.

Garrett, I.R., Dallas, S., Radl, J. and Mundy, G.R. (1997) A murine model of human myeloma bone disease. *Bone,* 20 (6), pp. 515.

Garrett, I.R., Chen, D., Gutierrez, G., Zhao, M., Escobedo, A., Rossini, G., Harris, S.E., Gallwitz, W., Kim, K.B., Hu, S., Crews, C.M. and Mundy, G.R. (2003) Selective inhibitors of the osteoblast proteasome stimulate bone formation in vivo and in vitro. *Journal of Clinical Investigation,* 111 (11), pp. 1771-1782.

Gearing, A.J.H., Beckett, P., Christodoulou, M., Churchill, M., Clements, J., Davidson, A.H., Drummond, A.H., Galloway, W.A., Gilbert, R., Gordon, J.L., Leber, T.M., Mangan, M., Miller, K., Nayee, P., Owen, K., Patel, S., Thomas, W., Wells, G., Wood, L.M. and Wooley, K. (1994) Processing of tumour necrosis factor-α precursor by metalloproteinases. *Nature,* 370 (6490), pp. 555-557.

Georgii-Hemming, P., Jernberg Wiklund, H., Ljunggren, Ö and Nilsson, K. (1996) Insulin-like growth factor I is a growth and survival factor in human multiple myeloma cell lines. *Blood,* 88 (6), pp. 2250-2258.

Gimble, J.M., Robinson, C.E., Wu, X. and Kelly, K.A. (1996a) The function of adipocytes in the bone marrow stroma: An update. *Bone,* 19 (5 SUPPL.), pp. 421-428.

Gimble, J.M., Robinson, C.E., Wu, X., Kelly, K.A., Rodriguez, B.R., Kliewer, S.A., Lehmann, J.M. and Morris, D.C. (1996b) Peroxisome proliferator-activated aeceptor-γ activation by thiazolidinediones induces adipogenesis in bone marrow stromal cells. *Molecular Pharmacology,* 50 (5), pp. 1087-1094.

Giuliani, N., Bataille, R., Mancini, C., Lazzaretti, M. and Barillé, S. (2001) Myeloma cells induce imbalance in the osteoprotegerin/osteoprotegerin ligand system in the human bone marrow environment. *Blood,* 98 (13), pp. 3527-3533.

Giuliani, N., Colla, S., Morandi, F., Lazzaretti, M., Sala, R., Bonomini, S., Grano, M., Colucci, S., Svaldi, M. and Rizzoli, V. (2005) Myeloma cells block RUNX2/CBFA1 activity in human bone marrow osteoblast progenitors and inhibit osteoblast formation and differentiation. *Blood,* 106 (7), pp. 2472-2483.

Glimcher, L.H. and Singh, H. (1999) Transcription Factors in Lymphocyte Development— T and B Cells Get Together. *Cell,* 96 (1), pp. 13-23.

Gong, Y., Slee, R.B., Fukai, N., Rawadi, G., Roman-Roman, S., Reginato, A.M., Wang, H., Cundy, T., Glorieux, F.H., Lev, D., Zacharin, M., Oexle, K., Marcelino, J., Suwairi, W., Heeger, S., Sabatakos, G., Apte, S., Adkins, W.N., Allgrove, J., Arslan-Kirchner, M., Batch, J.A., Beighton, P., Black, G.C.M., Boles, R.G., Boon, L.M., Borrone, C., Brunner,

H.G., Carle, G.F., Dallapiccola, B., De Paepe, A., Floege, B., Halfhide, M.L., Hall, B., Hennekam, R.C., Hirose, T., Jans, A., Jüppner, H., Kim, C.A., Keppler-Noreuil, K., Kohlschuetter, A., LaCombe, D., Lambert, M., Lemyre, E., Letteboer, T., Peltonen, L., Ramesar, R.S., Romanengo, M., Somer, H., Steichen-Gersdorf, E., Steinmann, B., Sullivan, B., Superti-Furga, A., Swoboda, W., Van den Boogaard, M.-., Van Hul, W., Vikkula, M., Votruba, M., Zabel, B., Garcia, T., Baron, R., Olsen, B.R. and Warman, M.L. (2001) LDL receptor-related protein 5 (LRP5) affects bone accrual and eye development. *Cell,* 107 (4), pp. 513-523.

Gonzalo, P., Guadamillas, M.C., Hernández-Riquer, M.V., Pollán, Á, Grande-García, A., Bartolomé, R.A., Vasanji, A., Ambrogio, C., Chiarle, R., Teixidó, J., Risteli, J., Apte, S.S., del Pozo, M.A. and Arroyo, A.G. (2010) MT1-MMP Is Required for Myeloid Cell Fusion via Regulation of Rac1 Signaling. *Developmental Cell,* 18 (1), pp. 77-89.

Goranova-Marinova, V., Goranov, S., Pavlov, P. and Tzvetkova, T. (2007) Serum levels of OPG, RANKL and RANKL/OPG ratios in newly-diagnosed patients with multiple myeloma. Clinical correlations. *Haematologica,* 92 (7), pp. 1000-1001.

Gordon, J.A.R., Tye, C.E., Sampaio, A.V., Underhill, T.M., Hunter, G.K. and Goldberg, H.A. (2007) Bone sialoprotein expression enhances osteoblast differentiation and matrix mineralization in vitro. *Bone,* 41 (3), pp. 462-473.

Govoni, K.E. (2012) Insulin-Like Growth Factor-I Molecular Pathways in Osteoblasts: Potential Targets for Pharmacological Manipulation. *Current Molecular Pharmacology,* 5 (2), pp. 143-152.

Graham-Rowe, D. (2011) Overview: Multiple lines of attack. *Nature,* 480 (7377 SUPPL.), pp. S34-S35.

Groen, R.W.J., de Rooij, M.F.M., Kocemba, K.A., Reijmers, R.M., de Haan-Kramer, A., Overdijk, M.B., Aalders, L., Rozemuller, H., Martens, A.C.M., Bergsagel, P.L., Kersten, M.J., Pals, S.T. and Spaargaren, M. (2011) N-cadherin-mediated interaction with multiple myeloma cells inhibits osteoblast differentiation. *Haematologica,* 96 (11), pp. 1653-1661.

Guedez, L. and Stetler-Stevenson, W.G. (2010) The prognostic value of TIMP-1 in multiple myeloma. *Leukemia Research,* 34 (5), pp. 576-577.

Guo, L.J., Luo, X.H., Xie, H., Zhou, H.D., Yuan, L.Q., Wang, M. and Liao, E.Y. (2006) Tissue inhibitor of matrix metalloproteinase-1 suppresses apoptosis of mouse bone marrow stromal cell line MBA-1. *Calcified Tissue International.,* 78 (5), pp. 285-292.

Habeck, M. (2000) Fibronectin fragment accelerates wound healing in diabetic mice. *Molecular Medicine Today,* 6 (9), pp. 335-336.

Habib, Z.A., Havstad, S.L., Wells, K., Divine, G., Pladevall, M. and Williams, L.K. (2010) Thiazolidinedione use and the longitudinal risk of fractures in patients with type 2 diabetes mellitus. *Journal of Clinical Endocrinology and Metabolism,* 95 (2), pp. 592-600.

Habibi, H., Abroun, S., Hajifathali, A., Soleimani, M., Kavyani, S., Kalantari, N. and Eslahchi, S. (2013) Osteogenic inhibition in multiple myeloma. *Cell Journal,* 15 (3), pp. 266-271.

Halabi, S., Ou, S.-., Vogelzang, N.J. and Small, E.J. (2007) Inverse correlation between body mass index and clinical outcomes in men with advanced castration-recurrent prostate cancer. *Cancer,* 110 (7), pp. 1478-1484.

Halasi, M., Schraufnagel, D.P. and Gartel, A.L. (2009) Wild-type p53 protects normal cells against apoptosis induced by thiostrepton. *Cell Cycle,* 8 (17), pp. 2850-2851.

Halpert, I., Sires, U.I., Roby, J.D., Potter-Perigo, S., Wight, T.N., Shapiro, S.D., Welgus, H.G., Wickline, S.A. and Parks, W.C. (1996) Matrilysin is expressed by lipid-laden macrophages at sites of potential rupture in atherosclerotic lesions and localizes to areas of versican deposition, a proteoglycan substrate for the enzyme. *Proceedings of the National Academy of Sciences of the United States of America,* 93 (18), pp. 9748-9753.

Hardie, D.G. (2008) Role of AMP-activated protein kinase in the metabolic syndrome and in heart disease. *FEBS letters,* 582 (1), pp. 81-89.

Hari, P.N., Zhang, M.-., Roy, V., Pérez, W.S., Bashey, A., To, L.B., Elfenbein, G., Freytes, C.O., Gale, R.P., Gibson, J., Kyle, R.A., Lazarus, H.M., McCarthy, P.L., Milone, G.A., Pavlovsky, S., Reece, D.E., Schiller, G., Vela-Ojeda, J., Weisdorf, D. and Vesole, D. (2009) Is the international staging system superior to the Durie-Salmon staging system? A comparison in multiple myeloma patients undergoing autologous transplant. *Leukemia,* 23 (8), pp. 1528-1534.

Harvey, S.J., Zheng, K., Sado, Y., Naito, I., Ninomiya, Y., Jacobs, R.M., Hudson, B.G. and Thorner, P.S. (1998) Role of distinct type IV collagen networks in glomerular development and function. *Kidney International,* 54 (6), pp. 1857-1866.

Hasegawa, M., Segawa, T., Maeda, M., Yoshida, T. and Sudo, A. (2011) Thrombin-cleaved osteopontin levels in synovial fluid correlate with disease severity of knee osteoarthritis. *Journal of Rheumatology,* 38 (1), pp. 129-134.

Heino, T.J., Hentunen, T.A. and Kalervo Vnnen, H. (2002) Osteocytes inhibit osteoclastic bone resorption through transforming growth factor-ß: Enhancement by estrogen. *Journal of Cellular Biochemistry,* 85 (1), pp. 185-197.

Henry, D.H., Costa, L., Goldwasser, F., Hirsh, V., Hungria, V., Prausova, J., Scagliotti, G.V., Sleeboom, H., Spencer, A., Vadhan-Raj, S., Von Moos, R., Willenbacher, W., Woll, P.J., Wang, J., Jiang, Q., Jun, S., Dansey, R. and Yeh, H. (2011) Randomized, double-blind study of denosumab versus zoledronic acid in the treatment of bone metastases in patients with advanced cancer (excluding breast and prostate cancer) or multiple myeloma. *Journal of Clinical Oncology,* 29 (9), pp. 1125-1132.

Herrmann, J., Turck, C.W., Atchison, R.E., Huflejt, M.E., Poulter, L., Gitt, M.A., Burlingame, A.L., Barondes, S.H. and Leffler, H. (1993) Primary structure of the soluble lactose binding lectin L-29 from rat and dog and interaction of its non-collagenous proline-, glycine-, tyrosine-rich sequence with bacterial and tissue collagenase. *Journal of Biological Chemistry,* 268 (35), pp. 26704-26711.

Herroon, M.K., Rajagurubandara, E., Hardaway, A.L., Powell, K., Turchick, A., Feldmann, D. and Podgorski, I. (2013) Bone marrow adipocytes promote tumor growth in bone via FABP4-dependent mechanisms. *Oncotarget,* 4 (11), pp. 2108-2123.

Hiremath, M. and Wysolmerski, J. (2014) Role of PTHrP in mammary gland development and breast cancer. *Clinical Reviews in Bone and Mineral Metabolism,* 12 (3), pp. 178-189.

Hoang, B., Benavides, A., Shi, Y., Frost, P. and Lichtenstein, A. (2009) Effect of autophagy on multiple myeloma cell viability. *Molecular Cancer Therapeutics,* 8 (7), pp. 1974-1984.

Hofbauer, L.C. and Schoppet, M. (2004) Clinical implications of the osteoprotegerin/RANKL/RANK system for bone and vascular diseases. *Journal of the American Medical Association,* 292 (4), pp. 490-495.

Hofmann, J.N., Liao, L.M., Pollak, M.N., Wang, Y., Pfeiffer, R.M., Baris, D., Andreotti, G., Lan, Q., Landgren, O., Rothman, N. and Purdue, M.P. (2012) A prospective study of circulating adipokine levels and risk of multiple myeloma. *Blood,* 120 (22), pp. 4418-4420.

Houghton, A.M., Hartzell, W.O., Robbins, C.S., Gomis-Rüth, F.X. and Shapiro, S.D. (2009) Macrophage elastase kills bacteria within murine macrophages. *Nature,* 460 (7255), pp. 637-641.

Hughes, V. (2011) Microenvironment: Neighbourhood watch. *Nature,* 480 (7377 SUPPL.), pp. S48-S49.

Hursting, S.D., Lavigne, J.A., Berrigan, D., Perkins, S.N. and Barrett, J.C. (2003) Calorie Restriction, Aging, and Cancer Prevention: Mechanisms of Action and Applicability to Humans. *Annual Review of Medicine,* 54, pp. 131-152.

Imai, K., Hiramatsu, A., Fukushima, D., Pierschbacher, M.D. and Okada, Y. (1997) Degradation of decorin by matrix metalloproteinases: Identification of the cleavage sites, kinetic analyses and transforming growth factor-ß1 release. *Biochemical Journal,* 322 (3), pp. 809-814.

Isaacson, J.A., Arendt, B.K., Tschumper, R.C. and Jelinek, D.F. (1998) IL-6-stimulated myeloma cell proliferation: Evidence for induction of autocrine IGF-I expression. *FASEB Journal,* 12 (5).

Iurisci, I., Tinari, N., Natoli, C., Angelucci, D., Cianchetti, E. and Iacobelli, S. (2000) Concentrations of galectin-3 in the sera of normal controls and cancer patients. *Clinical Cancer Research,* 6 (4), pp. 1389-1393.

Jagannath, S., Barlogie, B., Berenson, J.R., Singhal, S., Alexanian, R., Srkalovic, G., Orlowski, R.Z., Richardson, P.G., Anderson, J., Nix, D., Esseltine, D.L. and Anderson, K.C. (2005) Bortezomib in recurrent and/or refractory multiple myeloma: Initial clinical experience in patients with impaired renal function. *Cancer,* 103 (6), pp. 1195-1200.

Jakob, C., Egerer, K., Liebisch, P., Türkmen, S., Zavrski, I., Kuckelkorn, U., Heider, U., Kaiser, M., Fleissner, C., Sterz, J., Kleeberg, L., Feist, E., Burmester, G.-., Kloetzel, P.-. and Sezer, O. (2007) Circulating proteasome levels are an independent prognostic factor for survival in multiple myeloma. *Blood,* 109 (5), pp. 2100-2105.

Jones, M., Sabatini, P.J.B., Lee, F.S.H., Bendeck, M.P. and Langille, B.L. (2002) N-cadherin upregulation and function in response of smooth muscle cells to arterial injury. *Arteriosclerosis, Thrombosis, and Vascular Biology,* 22 (12), pp. 1972-1977.

Juarez, J. and Bendall, L. (2004) SDF-1 and CXCR4 in normal and malignant hematopoiesis. *Histology and Histopathology,* 19 (1), pp. 299-309.

Juárez-Velázquez, M.R., Salas-Labadía, C., Reyes-León, A., Navarrete-Meneses, M.P., Fuentes-Pananá, E.M. and Pérez-Vera, P. (2013) *Genetic Markers in the Prognosis of Childhood Acute Lymphoblastic Leukemia.* Available from: <http://www.intechopen.com/books/clinical-epidemiology-of-acute-lymphoblastic-leukemia-from-the-molecules-to-the-clinic/genetic-markers-in-the-prognosis-of-childhood-acute-lymphoblastic-leukemia> (Accessed 02/07, 2015).

Karnoub, A.E., Dash, A.B., Vo, A.P., Sullivan, A., Brooks, M.W., Bell, G.W., Richardson, A.L., Polyak, K., Tubo, R. and Weinberg, R.A. (2007) Mesenchymal stem cells within tumour stroma promote breast cancer metastasis. *Nature,* 449 (7162), pp. 557-563.

Karsenty, G. (2001) Minireview: Transcriptional control of osteoblast differentiation. *Endocrinology,* 142 (7), pp. 2731-2733.

Kast, R.E. (2005) Evidence of a mechanism by which etanercept increased TNF-alpha in multiple myeloma: New insights into the biology of TNF-alpha giving new treatment opportunities-the role of bupropion. *Leukemia Research,* 29 (12), pp. 1459-1463.

Kim, H.-., Lee, H.-., Jun, J.-., Oh, Y., Choi, S.-., Kim, H., Chung, C.-., Kim, I.-., Park, I.-., Chae, H.-., Kim, H.-. and Jung, Y.-. (2009) Intracellular cleavage of osteopontin by caspase-8 modulates hypoxia/reoxygenation cell death through p53. *Proceedings of the National Academy of Sciences of the United States of America,* 106 (36), pp. 15326-15331.

Kim, I.Y., Ahn, H.-., Lang, S., Oefelein, M.G., Oyasu, R., Kozlowski, J.M. and Lee, C. (1998) Loss of expression of transforming growth factor-ß receptors is associated with poor prognosis in prostate cancer patients. *Clinical Cancer Research,* 4 (7), pp. 1625-1630.

Kim, K.Y., Kim, S.S. and Cheon, H.G. (2006) Differential anti-proliferative actions of peroxisome proliferator-activated receptor-γ agonists in MCF-7 breast cancer cells. *Biochemical Pharmacology,* 72 (5), pp. 530-540.

Kiviranta, R., Morko, J., Alatalo, S.L., NicAmhlaoibh, R., Risteli, J., Laitala-Leinonen, T. and Vuorio, E. (2005) Impaired bone resorption in cathepsin K-deficient mice is partially compensated for by enhanced osteoclastogenesis and increased expression of other proteases via an increased RANKL/OPG ratio. *Bone,* 36 (1), pp. 159-172.

Korpi, J.T., Kervinen, V., Mäklin, H., Väänänen, A., Lahtinen, M., Läärä, E., Ristimäki, A., Thomas, G., Ylipalosaari, M., Åström, P., Lopez-Otin, C., Sorsa, T., Kantola, S., Pirilä, E. and Salo, T. (2008) Collagenase-2 (matrix metalloproteinase-8) plays a protective role in tongue cancer. *British Journal of Cancer,* 98 (4), pp. 766-775.

Koya, D. and Kanasaki, K. (2011) Biology of obesity: Lessons from animal models of obesity. *Journal of Biomedicine and Biotechnology,* 2011, pp. 197636.

Kraft, P.J., Haynes-Johnson, D.E., Patel, L., Lenhart, J.A., Zivin, R.A. and Palmer, S.S. (2001) Fluorescence polarization assay and SDS-PAGE confirms matrilysin degrades fibronectin and collagen IV whereas gelatinase a degrades collagen IV but not fibronectin. *Connective Tissue Research,* 42 (2), pp. 149-163.

Kralisch, S., Bluher, M., Tonjes, A., Lossner, U., Paschke, R., Stumvoll, M. and Fasshauer, M. (2007) Tissue inhibitor of metalloproteinase-1 predicts adiposity in humans. *European Journal of Endocrinology,* 156 (2), pp. 257-261.

Krause, C., De Gorter, D.J.J., Karperien, M. and ten Dijke, P. (2009) Signal Transduction Cascades Controlling Osteoblast Differentiation. In *Primer on the Metabolic Bone Diseases and Disorders of Mineral Metabolism.*, Seventh ed. John Wiley & Sons, Inc., pp. 10-16.

Kumar, S., Flinn, I., Richardson, P.G., Hari, P., Callander, N., Noga, S.J., Stewart, A.K., Turturro, F., Rifkin, R., Wolf, J., Estevam, J., Mulligan, G., Shi, H., Webb, I.J. and Rajkumar, S.V. (2012) Randomized, multicenter, phase 2 study (EVOLUTION) of combinations of bortezomib, dexamethasone, cyclophosphamide, and lenalidomide in previously untreated multiple myeloma. *Blood,* 119 (19), pp. 4375-4382.

Kyle, R.A. (1978) Monoclonal gammopathy of undetermined significance. Natural history in 241 cases. *American Journal of Medicine,* 64 (5), pp. 814-826.

Kyle, R.A., Finkelstein, S., Elveback, L.R. and Kurland, L.T. (1972) Incidence of monoclonal proteins in a Minnesota community with a cluster of multiple myeloma. *Blood,* 40 (5), pp. 719-724.

Kyle, R.A., Jowsey, J., Kelly, P.J. and Taves, D.R. (1975) Multiple myeloma bone disease. The comparative effect of sodium fluoride and calcium carbonate or placebo. *New England Journal of Medicine,* 293 (26), pp. 1334-1338.

Kyle, R.A. and Rajkumar, S.V. (2007) Monoclonal Gammopathy of Undetermined Significance and Smoldering Multiple Myeloma. *Hematology/oncology clinics of North America,* 21 (6), pp. 1093-1113.

Kyle, R.A., Yee, G.C., Somerfield, M.R., Flynn, P.J., Halabi, S., Jagannath, S., Orlowski, R.Z., Roodman, D.G., Twilde, P. and Anderson, K. (2007) American society of clinical oncology 2007 clinical practice guideline update on the role of bisphosphonates in multiple myeloma. *Journal of Clinical Oncology,* 25 (17), pp. 2464-2472.

Lacey, D.L., Timms, E., Tan, H.-., Kelley, M.J., Dunstan, C.R., Burgess, T., Elliott, R., Colombero, A., Elliott, G., Scully, S., Hsu, H., Sullivan, J., Hawkins, N., Davy, E., Capparelli, C., Eli, A., Qian, Y.-., Kaufman, S., Sarosi, I., Shalhoub, V., Senaldi, G., Guo, J., Delaney, J. and Boyle, W.J. (1998) Osteoprotegerin ligand is a cytokine that regulates osteoclast differentiation and activation. *Cell,* 93 (2), pp. 165-176.

Landgren, O., Rajkumar, S.V., Pfeiffer, R.M., Kyle, R.A., Katzmann, J.A., Dispenzieri, A., Cai, Q., Goldin, L.R., Caporaso, N.E., Fraumeni, J.F., Blot, W.J. and Signorello, L.B. (2010) Obesity is associated with an increased risk of monoclonal gammopathy of undetermined significance among black and white women. *Blood,* 116 (7), pp. 1056-1059.

Lecka-Czernik, B. (2010) Bone loss in diabetes: Use of antidiabetic thiazolidinediones and secondary osteoporosis. *Current Osteoporosis Reports,* 8 (4), pp. 178-184.

Lee, A.-., Iwakoshi, N.N., Anderson, K.C. and Glimcher, L.H. (2003) Proteasome inhibitors disrupt the unfolded protein response in myeloma cells. *Proceedings of the National Academy of Sciences of the United States of America,* 100 (17), pp. 9946-9951.

Lee, J.W., Chung, H.Y., Ehrlich, L.A., Jelinek, D.F., Callander, N.S., Roodman, G.D. and Choi, S.J. (2004) IL-3 expression by myeloma cells increases both osteoclast formation and growth of myeloma cells. *Blood,* 103 (6), pp. 2308-2315.

Lentzsch, S. (2010) Potential Role of IMiDs and Other Agents as Therapy for Myeloma Bone Disease. In *Myeloma Bone Disease.*, ed. G.D. Roodman, Humana Press:, pp. 199-209.

Leung, N., Bridoux, F., Hutchison, C.A., Nasr, S.H., Cockwell, P., Fermand, J.-., Dispenzieri, A., Song, K.W. and Kyle, R.A. (2012) Monoclonal gammopathy of renal significance: When MGUS is no longer undetermined or insignificant. *Blood,* 120 (22), pp. 4292-4295.

Li, J., Sarosi, I., Cattley, R.C., Pretorius, J., Asuncion, F., Grisanti, M., Morony, S., Adamu, S., Geng, Z., Qiu, W., Kostenuik, P., Lacey, D.L., Simonet, W.S., Bolon, B., Qian, X., Shalhoub, V., Ominsky, M.S., Zhu Ke, H., Li, X. and Richards, W.G. (2006) Dkk1-mediated inhibition of Wnt signaling in bone results in osteopenia. *Bone,* 39 (4), pp. 754-766.

Li, J., Sarosi, I., Yan, X.-., Morony, S., Capparelli, C., Tan, H.-., McCabe, S., Elliott, R., Scully, S., Van, G., Kaufman, S., Juan, S.-., Sun, Y., Tarpley, J., Martin, L., Christensen, K., McCabe, J., Kostenuik, P., Hsu, H., Fletcher, F., Dunstan, C.R., Lacey, D.L. and Boyle, W.J. (2000) RANK is the intrinsic hematopoietic cell surface receptor that controls osteoclastogenesis and regulation of bone mass and calcium metabolism. *Proceedings of the National Academy of Sciences of the United States of America,* 97 (4), pp. 1566-1571.

Li, X., Zhang, Y., Kang, H., Liu, W., Liu, P., Zhang, J., Harris, S.E. and Wu, D. (2005) Sclerostin binds to LRP5/6 and antagonizes canonical Wnt signaling. *Journal of Biological Chemistry,* 280 (20), pp. 19883-19887.

Li, Z., Peng, Y. and Li, Z. (2013) GRP78 secreted by tumor cells stimulates differentiation of bone marrow mesenchymal stem cells to cancer-associated fibroblasts. *Biochemical and Biophysical Research Communications,* 440 (4), pp. 558-563.

Lichtman, M.A. (2010) Obesity and the risk for a hematological malignancy: Leukemia, lymphoma, or myeloma. *Oncologist,* 15 (10), pp. 1083-1101.

Lijnen, H.R., Maquoi, E., Hansen, L.B., Van Hoef, B., Frederix, L. and Collen, D. (2002) Matrix metalloproteinase inhibition impairs adipose tissue development in mice. *Arteriosclerosis, Thrombosis, and Vascular Biology,* 22 (3), pp. 374-379.

Lin, H.-., Chang, J.-., Jain, S., Gabison, E.E., Kure, T., Kato, T., Fukai, N. and Azar, D.T. (2001) Matrilysin cleavage of corneal collagen type XVIII NC1 domain and generation of a 28-kDa fragment. *Investigative Ophthalmology and Visual Science,* 42 (11), pp. 2517-2524.

Ling, S.C.W., Lau, E.K.K., Al-Shabeeb, A., Nikolic, A., Catalano, A., Iland, H., Horvath, N., Ho, P.J., Harrison, S., Fleming, S., Joshua, D.E. and Allen, J.D. (2012) Response of myeloma to the proteasome inhibitor bortezomib is correlated with the unfolded protein response regulator XBP-1. *Haematologica,* 97 (1), pp. 64-72.

Lynch, C.C., Hikosaka, A., Acuff, H.B., Martin, M.D., Kawai, N., Singh, R.K., Vargo-Gogola, T.C., Begtrup, J.L., Peterson, T.E., Fingleton, B., Shirai, T., Matrisian, L.M. and Futakuchi, M. (2005) MMP-7 promotes prostate cancer-induced osteolysis via the solubilization of RANKL. *Cancer Cell,* 7 (5), pp. 485-496.

Mahtouk, K., Jourdan, M., De Vos, J., Hertogh, C., Fiol, G., Jourdan, E., Rossi, J.-. and Klein, B. (2004) An inhibitor of the EGF receptor family blocks myeloma cell growth factor activity of HB-EGF and potentiates dexamethasone or anti-IL-6 antibody-induced apoptosis. *Blood,* 103 (5), pp. 1829-1837.

Mancino, A.T., Klimberg, V.S., Yamamoto, M., Manolagas, S.C. and Abe, E. (2001) Breast cancer increases osteoclastogenesis by secreting M-CSF and upregulating RANKL in stromal cells. *Journal of Surgical Research,* 100 (1), pp. 18-24.

Manier, S., Sacco, A., Leleu, X., Ghobrial, I.M. and Roccaro, A.M. (2012) Bone marrow microenvironment in multiple myeloma progression. *Journal of Biomedicine and Biotechnology,* 2012.

Manilay, J.O. and Zouali, M. (2014) Tight relationships between B lymphocytes and the skeletal system. *Trends in Molecular Medicine,* 20 (7), pp. 405-412.

Manning, L.S., Berger, J.D., O'Donoghue, H.L., Sheridan, G.N., Claringbold, P.G. and Harvey Turner, J. (1992) A model of multiple myeloma: Culture of 5T33 murine myeloma cells and evaluation of tumorigenicity in the C57BL/KaLwRij mouse. *British Journal of Cancer,* 66 (6), pp. 1088-1093.

Maquoi, E., Demeulemeester, D., Vörös, G., Collen, D. and Lijnen, H.R. (2003) Enhanced nutritionally induced adipose tissue development in mice with stromelysin-I gene inactivation. *Thrombosis and Haemostasis,* 89 (4), pp. 696-704.

Martin, T.J., Sims, N.A. and Quinn, J.M.W. (2011) 8 - Interactions Among Osteoblasts, Osteoclasts, and Other Cells in Bone. In *Osteoimmunology.*, ed. J.L.C.H. Takayanagi,San Diego: Academic Press, pp. 227-267.

Medina, E.A., Oberheu, K., Polusani, S.R., Ortega, V., Velagaleti, G.V.N. and Oyajobi, B.O. (2014) PKA/AMPK signaling in relation to adiponectin's antiproliferative effect on multiple myeloma cells. *Leukemia,* 28 (10), pp. 2080-2089.

Meissburger, B., Stachorski, L., Röder, E., Rudofsky, G. and Wolfrum, C. (2011) Tissue inhibitor of matrix metalloproteinase 1 (TIMP1) controls adipogenesis in obesity in mice and in humans. *Diabetologia,* 54 (6), pp. 1468-1479.

Mercer, J., Figg, N., Stoneman, V., Braganza, D. and Bennett, M.R. (2005) Endogenous p53 protects vascular smooth muscle cells from apoptosis and reduces atherosclerosis in ApoE knockout mice. *Circulation Research,* 96 (6), pp. 667-674.

Meunier, P., Aaron, J., Edouard, C. and Vignon, G. (1971) Osteoporosis and the replacement of cell populations of the marrow by adipose tissue. A quantitative study of 84 iliac bone biopsies. *Clinical Orthopaedics and Related Research,* 80, pp. 147-154.

Mi, Z., Guo, H., Wai, P.Y., Gao, C., Wei, J. and Kuo, P.C. (2004) Differential osteopontin expression in phenotypically distinct subclones of murine breast cancer cells mediates metastatic behavior. *Journal of Biological Chemistry,* 279 (45), pp. 46659-46667.

Mi, Z., Oliver, T., Guo, H., Gao, C. and Kuo, P.C. (2007) Thrombin-cleaved COOH-terminal osteopontin peptide binds with cyclophilin C to CD147 in murine breast cancer cells. *Cancer Research,* 67 (9), pp. 4088-4097.

Michels, K.B., Xue, F., Brandt, L. and Ekbom, A. (2004) Hyperparathyroidism and subsequent incidence of breast cancer. *International Journal of Cancer,* 110 (3), pp. 449-451.

Michigami, T., Shimizu, N., Williams, P.J., Niewolna, M., Dallas, S.L., Mundy, G.R. and Yoneda, T. (2000) Cell-cell contact between marrow stromal cells and myeloma cells via VCAM-1 and a4ß1-integrin enhances production of osteoclast-stimulating activity. *Blood,* 96 (5), pp. 1953-1960.

Mihaylova, M.M. and Shaw, R.J. (2011) The AMPK signalling pathway coordinates cell growth, autophagy and metabolism. *Nature Cell Biology,* 13 (9), pp. 1016-1023.

Mirandola, L., Yu, Y., Chui, K., Jenkins, M.R., Cobos, E., John, C.M. and Chiriva-Internati, M. (2011) Galectin-3C inhibits tumor growth and increases the anticancer activity of bortezomib in a murine model of human multiple myeloma. *PLoS ONE,* 6 (7), pp. e21811.

Mizuno, A., Amizuka, N., Irie, K., Murakami, A., Fujise, N., Kanno, T., Sato, Y., Nakagawa, N., Yasuda, H., Mochizuki, S.-., Gomibuchi, T., Yano, K., Shima, N., Washida, N., Tsuda, E., Morinaga, T., Higashio, K. and Ozawa, H. (1998) Severe osteoporosis in mice lacking osteoclastogenesis inhibitory factor/osteoprotegerin. *Biochemical and Biophysical Research Communications,* 247 (3), pp. 610-615.

Mochizuki, S., Shimoda, M., Shiomi, T., Fujii, Y. and Okada, Y. (2004) ADAM28 is activated by MMP-7 (matrilysin-1) and cleaves insulin-like growth factor binding protein-3. *Biochemical and Biophysical Research Communications,* 315 (1), pp. 79-84.

Morava, É, Guillard, M., Lefeber, D.J. and Wevers, R.A. (2009) Autosomal recessive cutis laxa syndrome revisited. *European Journal of Human Genetics,* 17 (9), pp. 1099-1110.

Moreau, P. and Minvielle, S. (2013) Multiple myeloma: So much progress, but so many unsolved questions. *Haematologica,* 98 (4), pp. 487-489.

Morgan, G.J., Davies, F.E., Gregory, W.M., Cocks, K., Bell, S.E., Szubert, A.J., Navarro-Coy, N., Drayson, M.T., Owen, R.G., Feyler, S., Ashcroft, A.J., Ross, F., Byrne, J., Roddie, H., Rudin, C., Cook, G., Jackson, G.H. and Child, J.A. (2010) First-line treatment with zoledronic acid as compared with clodronic acid in multiple myeloma (MRC Myeloma IX): A randomised controlled trial. *The Lancet,* 376 (9757), pp. 1989-1999.

Mori, Y., Shimizu, N., Dallas, M., Niewolna, M., Story, B., Williams, P.J., Mundy, G.R. and Yoneda, T. (2004) Anti-a4 integrin antibody suppresses the development of multiple myeloma and associated osteoclastic osteolysis. *Blood,* 104 (7), pp. 2149-2154.

Morvan, F., Boulukos, K., Clément-Lacroix, P., Roman, S.R., Suc-Royer, I., Vayssière, B., Ammann, P., Martin, P., Pinho, S., Pognonec, P., Mollat, P., Niehrs, C., Baron, R. and Rawadi, G. (2006) Deletion of a single allele of the Dkk1 gene leads to an increase in bone formation and bone mass. *Journal of Bone and Mineral Research,* 21 (6), pp. 934-945.

Motoshima, H., Goldstein, B.J., Igata, M. and Araki, E. (2006) AMPK and cell proliferation - AMPK as a therapeutic target for atherosclerosis and cancer. *Journal of Physiology,* 574 (1), pp. 63-71.

Mundy, G.R. (1998) Myeloma bone disease. *European Journal of Cancer,* 34 (2), pp. 246-251.

Mundy, G.R., Raisz, L.G., Cooper, R.A., Schechter, G.P. and Salmon, S.E. (1974) Evidence for the secretion of an osteoclast stimulating factor in myeloma. *New England Journal of Medicine,* 291 (20), pp. 1041-1046.

Murphy, F., Kroll, M.E., Pirie, K., Reeves, G., Green, J. and Beral, V. (2013) Body size in relation to incidence of subtypes of haematological malignancy in the prospective Million Women Study. *British Journal of Cancer,* 108 (11), pp. 2390-2398.

Nagase, H., Visse, R. and Murphy, G. (2006) Structure and function of matrix metalloproteinases and TIMPs. *Cardiovascular Research,* 69, pp. 562-573.

Nakamura, M., Miyamoto, S., Maeda, H., Ishii, G., Hasebe, T., Chiba, T., Asaka, M. and Ochiai, A. (2005) Matrix metalloproteinase-7 degrades all insulin-like growth factor binding proteins and facilitates insulin-like growth factor bioavailability. *Biochemical and Biophysical Research Communications,* 333 (3), pp. 1011-1016.

Nakamura, T., Kuwai, T., Kim, J.-., Fan, D., Kim, S.-. and Fidler, I.J. (2007) Stromal metalloproteinase-9 is essential to angiogenesis and progressive growth of orthotopic human pancreatic cancer in parabiont nude mice. *Neoplasia,* 9 (11), pp. 979-986.

Nangia-Makker, P., Raz, T., Tait, L., Hogan, V., Fridman, R. and Raz, A. (2007) Galectin-3 cleavage: A novel surrogate marker for matrix metalloproteinase activity in growing breast cancers. *Cancer Research,* 67 (24), pp. 11760-11768.

Naveiras, O., Nardi, V., Wenzel, P.L., Hauschka, P.V., Fahey, F. and Daley, G.Q. (2009) Bone-marrow adipocytes as negative regulators of the haematopoietic microenvironment. *Nature,* 460 (7252), pp. 259-263.

Ng, A.C., Khosla, S., Charatcharoenwitthaya, N., Kumar, S.K., Achenbach, S.J., Holets, M.F., McCready, L.K., Melton III, L.J., Kyle, R.A., Rajkumar, S.V. and Drake, M.T. (2011) Bone microstructural changes revealed by high-resolution peripheral quantitative computed tomography imaging and elevated DKK1 and MIP-1 α levels in patients with MGUS. *Blood,* 118 (25), pp. 6529-6534.

NICE (2014) *Bortezomib for induction therapy in multiple myeloma before high-dose chemotherapy and autologous stem cell transplantation.* National Institute for Health and care Excellence (NICE). [Online]. Available from: <https://www.nice.org.uk/guidance/ta311/resources> (Accessed 02/10, 2015).

NICE (2011) *Bortezomib and thalidomide for the first-line treatment of multiple myeloma.* National Institute for Health and care Excellence (NICE). [Online]. Available from: <https://www.nice.org.uk/guidance/TA228> (Accessed 02/10, 2015).

NICE (2009) *Lenalidomide for the treatment of multiple myeloma in people who have received at least one prior therapy.* National Institute for Health and care Excellence (NICE). [Online]. Available from: <https://www.nice.org.uk/guidance/TA171> (Accessed 02/10, 2015).

NICE (2007) *Bortezomib monotherapy for relapsed multiple myeloma.* National Institute for Health and care Excellence (NICE). [Online]. Available from: <https://www.nice.org.uk/guidance/TA129> (Accessed 02/10, 2015).

Niida, A., Hiroko, T., Kasai, M., Furukawa, Y., Nakamura, Y., Suzuki, Y., Sugano, S. and Akiyama, T. (2004) DKK1, a negative regulator of Wnt signaling, is a target of the ß-catenin/TCF pathway. *Oncogene,* 23 (52), pp. 8520-8526.

Niida, S., Kaku, M., Amano, H., Yoshida, H., Kataoka, H., Nishikawa, S., Tanne, K., Maeda, N., Nishikawa, S.-. and Kodama, H. (1999) Vascular endothelial growth factor can substitute for macrophage colony- stimulating factor in the support of osteoclastic bone resorption. *Journal of Experimental Medicine,* 190 (2), pp. 293-298.

Nilsson, I.-., Zedenius, J., Yin, L. and Ekbom, A. (2007) The association between primary hyperparathyroidism and malignancy: Nationwide cohort analysis on cancer incidence after parathyroidectomy. *Endocrine-Related Cancer,* 14 (1), pp. 135-140.

Noll, J.E., Hewett, D.R., Williams, S.A., Vandyke, K., Kok, C., To, L.B. and Zannettino, A.C.W. (2014) SAMSN1 Is a Tumor Suppressor Gene in Multiple Myeloma. *Neoplasia,* 16 (7), pp. 572-585.

Núñez, N.P., Perkins, S.N., Smith, N.C.P., Berrigan, D., Berendes, D.M., Varticovski, L., Barrett, J.C. and Hursting, S.D. (2008) Obesity accelerates mouse mammary tumor growth in the absence of ovarian hormones. *Nutrition and Cancer,* 60 (4), pp. 534-541.

Nuttall, M.E. and Gimble, J.M. (2004) Controlling the balance between osteoblastogenesis and adipogenesis and the consequent therapeutic implications. *Current Opinion in Pharmacology,* 4 (3), pp. 290-294.

Oba, Y., Lee, J.W., Ehrlich, L.A., Chung, H.Y., Jelinek, D.F., Callander, N.S., Horuk, R., Choi, S.J. and Roodman, G.D. (2005) MIP-1α utilizes both CCR1 and CCR5 to induce osteoclast formation and increase adhesion of myeloma cells to marrow stromal cells. *Experimental Hematology,* 33 (3), pp. 272-278.

Ochieng, J., Green, B., Evans, S., James, O. and Warfield, P. (1998) Modulation of the biological functions of galectin-3 by matrix metalloproteinases. *Biochimica et Biophysica Acta (BBA) - General Subjects,* 1379 (1), pp. 97-106.

Ohtsuka, T., Shiomi, T., Shimoda, M., Kodama, T., Amour, A., Murphy, G., Ohuchi, E., Kobayashi, K. and Okada, Y. (2006) ADAM28 is overexpressed in human non-small cell lung carcinomas and correlates with cell proliferation and lymph node metastasis. *International Journal of Cancer,* 118 (2), pp. 263-273.

Olivo-Marston, S.E., Hursting, S.D., Perkins, S.N., Schetter, A., Khan, M., Croce, C., Harris, C.C. and Lavigne, J. (2014) Effects of calorie restriction and diet-induced obesity on murine colon carcinogenesis, growth and inflammatory factors, and MicroRNA expression. *PLoS ONE,* 9 (4), pp. e94765.

Oracki, S.A., Walker, J.A., Hibbs, M.L., Corcoran, L.M. and Tarlinton, D.M. (2010) Plasma cell development and survival. *Immunological Reviews,* 237 (1), pp. 140-159.

Oshima, T., Abe, M., Asano, J., Hara, T., Kitazoe, K., Sekimoto, E., Tanaka, Y., Shibata, H., Hashimoto, T., Ozaki, S., Kido, S., Inoue, D. and Matsumoto, T. (2005) Myeloma cells suppress bone formation by secreting a soluble Wnt inhibitor, sFRP-2. *Blood,* 106 (9), pp. 3160-3165.

Oyajobi, B.O., Franchin, G., Williams, P.J., Pulkrabek, D., Gupta, A., Munoz, S., Grubbs, B., Zhao, M., Chen, D., Sherry, B. and Mundy, G.R. (2003) Dual effects of macrophage inflammatory protein-1 α on osteolysis and tumor burden in the murine 5TGM1 model of myeloma bone disease. *Blood,* 102 (1), pp. 311-319.

Oyajobi, B.O., Garrett, I.R., Gupta, A., Banerjee, M., Esparza, X. and Flores, A. (2004) Role of Dickkopf 1(Dkk) in myeloma bone disease and modulation by the proteasome inhibitor velcade. *Journal of Bone and Mineral Research,* 19 (1).

Oyama, F., Hirohashi, S., Shimosato, Y., Titani, K. and Sekiguchi, K. (1991) Qualitative and quantitative changes of human tenascin expression in transformed lung fibroblast and lung tumor tissues: Comparison with fibronectin. *Cancer Research,* 51 (18), pp. 4876-4881.

Pagani, F., Francucci, C.M. and Moro, L. (2005) Markers of bone turnover: biochemical and clinical perspectives. *Journal of Endocrinological Investigation.,* 28 (10 Suppl), pp. 8-13.

Paizi, M., Manaster, J., Quitt, M. and Spira, G. (1991) High plasma fibronectin levels in multiple myeloma patients: Possible mechanisms and clinical implications. *Scandinavian Journal of Immunology,* 34 (3), pp. 285-289.

Palladino, C., Bruno, B. and Boccadoro, M. (2014) Discovering the Meaning of Monoclonal Gammopathy of Undetermined Significance: Current Knowledge, Future Challenges. *Translational Medicine at UniSa,* 8, pp. 12-18.

Papanicolaou, S.E., Phipps, R.J., Fyhrie, D.P. and Genetos, D.C. (2009) Modulation of sclerostin expression by mechanical loading and bone morphogenetic proteins in osteogenic cells. *Biorheology,* 46 (5), pp. 389-399.

Paszty, C., Turner, C.H. and Robinson, M.K. (2010) Sclerostin: A gem from the genome leads to bone-building antibodies. *Journal of Bone and Mineral Research,* 25 (9), pp. 1897-1904.

Patel, L., Pass, I., Coxon, P., Downes, C.P., Smith, S.A. and Macphee, C.H. (2001) Tumor suppressor and anti-inflammatory actions of PPAR γ agonists are mediated via upregulation of PTEN. *Current Biology,* 11 (10), pp. 764-768.

Patterson, B.C. and Sang, Q.A. (1997) Angiostatin-converting enzyme activities of human matrilysin (MMP-7) and gelatinase B/type IV collagenase (MMP.9). *Journal of Biological Chemistry,* 272 (46), pp. 28823-28825.

Pejnovic, N.N., Pantic, J.M., Jovanovic, I.P., Radosavljevic, G.D., Milovanovic, M.Z., Nikolic, I.G., Zdravkovic, N.S., Djukic, A.L., Arsenijevic, N.N. and Lukic, M.L. (2013) Galectin-3 deficiency accelerates high-fat diet-induced obesity and amplifies inflammation in adipose tissue and pancreatic islets. *Diabetes,* 62 (6), pp. 1932-1944.

Pendás, A.M., Folgueras, A.R., Llano, E., Caterina, J., Frerard, F., Rodríguez, F., Astudillo, A., Noël, A., Birkedal-Hansen, H. and López-Otín, C. (2004) Diet-induced obesity and reduced skin cancer susceptibility in matrix metalloproteinase 19-deficient mice. *Molecular and Cellular Biology,* 24 (12), pp. 5304-5313.

Pendyala, S., Neff, L.M., Suárez-Fariñas, M. and Holt, P.R. (2011) Diet-induced weight loss reduces colorectal inflammation: Implications for colorectal carcinogenesis. *American Journal of Clinical Nutrition,* 93 (2), pp. 234-242.

Pennisi, A., Ling, W., Li, X., Khan, S., Wang, Y., Barlogie, B., Shaughnessy Jr., J.D. and Yaccoby, S. (2010) Consequences of daily administered parathyroid hormone on myeloma growth, bone disease, and molecular profiling of whole myelomatous bone. *PLoS ONE,* 5 (12), pp. e15233.

Pennypacker, B., Shea, M., Liu, Q., Masarachia, P., Saftig, P., Rodan, S., Rodan, G. and Kimmel, D. (2009) Bone density, strength, and formation in adult cathepsin K (-/-) mice. *Bone,* 44 (2), pp. 199-207.

Piazza, F., Manni, S., Tubi, L.Q., Montini, B., Pavan, L., Colpo, A., Gnoato, M., Cabrelle, A., Adami, F., Zambello, R., Trentin, L., Gurrieri, C. and Semenzato, G. (2010) Glycogen Synthase Kinase-3 regulates multiple myeloma cell growth and bortezomib-induced cell death. *BMC Cancer,* 10 (526).

Pini, M., Rhodes, D.H. and Fantuzzi, G. (2011) Hematological and acute-phase responses to diet-induced obesity in IL-6 KO mice. *Cytokine,* 56 (3), pp. 708-716.

Powell, W.C., Fingleton, B., Wilson, C.L., Boothby, M. and Matrisian, L.M. (1999) The metalloproteinase matrilysin proteolytically generates active soluble Fas ligand and potentiates epithelial cell apoptosis. *Current Biology,* 9 (24), pp. 1441-1447.

Prockop, D.J. (1997) Marrow stromal cells as stem cells for nonhematopoietic tissues. *Science,* 276 (5309), pp. 71-74.

Puthenedam, M., Wu, F., Shetye, A., Michaels, A., Rhee, K.-. and Kwon, J.H. (2011) Matrilysin-1 (MMP7) cleaves galectin-3 and inhibits wound healing in intestinal epithelial cells. *Inflammatory Bowel Diseases,* 17 (1), pp. 260-267.

Radl, J., Croese, J.W., Zurcher, C., Van Den Enden-Vieveen, M. and and Margreet de Leeuw, A. (1988) Animal model of human disease; multiple myeloma. *American Journal of Pathology,* 132, pp. 593-597.

Radl, J., De Glopper, E., Schuit, H. and Zurcher, C. (1979) Idiopathic paraproteinemia. II. Transplantation of the paraprotein-producing clone from old to young C57BL/KaLwRij mice. *Journal of Immunology,* 122 (2), pp. 609-613.

Rajkumar, S.V., Leong, T., Roche, P.C., Fonseca, R., Dispenzieri, A., Lacy, M.Q., Lust, J.A., Witzig, T.E., Kyle, R.A., Gertz, M.A. and Greipp, P.R. (2000) Prognostic value of bone marrow angiogenesis in multiple myeloma. *Clinical Cancer Research,* 6 (8), pp. 3111-3116.

Ramasamy, K., Khatun, H., MacPherson, L., Caley, M.P., Sturge, J., Mufti, G.J., Schey, S.A. and Calle, Y. (2012) Fluorescence-based experimental model to evaluate the concomitant effect of drugs on the tumour microenvironment and cancer cells. *British Journal of Haematology,* 157 (5), pp. 564-579.

Ray, D.M., Bernstein, S.H. and Phipps, R.P. (2004) Human multiple myeloma cells express peroxisome proliferator-activated receptor γ and undergo apoptosis upon exposure to PPAR γ ligands. *Clinical Immunology,* 113 (2), pp. 203-213.

Reeves, M.M., Terranova, C.O., Eakin, E.G. and Demark-Wahnefried, W. (2014) Weight loss intervention trials in women with breast cancer: A systematic review. *Obesity Reviews,* 15 (9), pp. 749-768.

Reil, J.-., Gilles, S., Zahler, S., Brandl, A., Drexler, H., Hültner, L., Matrisian, L.M., Welsch, U. and Becker, B.F. (2007) Insights from knock-out models concerning postischemic release of TNF α from isolated mouse hearts. *Journal of Molecular and Cellular Cardiology,* 42 (1), pp. 133-141.

Renehan, A.G., Tyson, M., Egger, M., Heller, R.F. and Zwahlen, M. (2008) Body-mass index and incidence of cancer: a systematic review and meta-analysis of prospective observational studies. *The Lancet,* 371 (9612), pp. 569-578.

Ress, C., Tschoner, A., Ciardi, C., Laimer, M.W., Engl, J.W., Sturm, W., Weiss, H., Tilg, H., Ebenbichler, C.F., Patsch, J.R. and Kaser, S. (2010) Influence of significant weight loss on serum matrix metalloproteinase (MMP)-7 levels. *European Cytokine Network,* 21 (1), pp. 65-70.

Ricciardelli, C., Sakko, A.J., Ween, M.P., Russell, D.L. and Horsfall, D.J. (2009) The biological role and regulation of versican levels in cancer. *Cancer and Metastasis Reviews,* 28 (1-2), pp. 233-245.

Robbiani, D.F., Colon, K., Ely, S., Ely, S., Chesi, M. and Bergsagel, P.L. (2007) Osteopontin dysregulation and lytic bone lesions in multiple myeloma. *Hematological Oncology,* 25 (1), pp. 16-20.

Rosen, L.S., Gordon, D., Kaminski, M., Howell, A., Belch, A., Mackey, J., Apffelstaedt, J., Hussein, M.A., Coleman, R.E., Reitsma, D.J., Chen, B.-. and Seaman, J.J. (2003) Long-term efficacy and safety of zoledronic acid compared with pamidronate disodium in the treatment of skeletal complications in patients with advanced multiple myeloma or breast carcinoma: A randomized, double-blind, multicenter, comparative trial. *Cancer,* 98 (8), pp. 1735-1744.

Rude Voldborg, B., Damstrup, L., Spang-Thomsen, M. and Skovgaard Poulsen, H. (1997) Epidermal growth factor receptor (EGFR) and EGFR mutations, function and possible role in clinical trials. *Annals of Oncology,* 8 (12), pp. 1197-1206.

Ruderman, N.B., Xu, X.J., Nelson, L., Cacicedo, J.M., Saha, A.K., Lan, F. and Ido, Y. (2010) AMPK and SIRT1: A long-standing partnership? *American Journal of Physiology - Endocrinology and Metabolism,* 298 (4), pp. E751-E760.

Saad, S.R., Bendall, L.J., McGowan, E.M., Clarke, C.L., Gottlieb, D.J. and Bradstock, K.F. (2000) Effects of progesterone on the migration of breast cancer cells within bone marrow stroma. *Blood,* 96 (11 PART II).

Saarialho-Kere, U.K., Kerkelä, E., Jeskanen, L., Hasan, T., Pierce, R., Starcher, B., Raudasoja, R., Ranki, A., Oikarinen, A. and Vaalamo, M. (1999) Accumulation of matrilysin (MMP-7) and macrophage metalloelastase (MMP- 12) in actinic damage. *Journal of Investigative Dermatology,* 113 (4), pp. 664-672.

Salminen, A., Kauppinen, A., Suuronen, T. and Kaarniranta, K. (2008) SIRT1 longevity factor suppresses NF- κ B-driven immune responses: Regulation of aging via NF- κ B acetylation? *BioEssays,* 30 (10), pp. 939-942.

Sanchez-Ramos, J., Song, S., Cardozo-Pelaez, F., Hazzi, C., Stedeford, T., Willing, A., Freeman, T.B., Saporta, S., Janssen, W., Patel, N., Cooper, D.R. and Sanberg, P.R. (2000)

Adult bone marrow stromal cells differentiate into neural cells in vitro. *Experimental Neurology,* 164 (2), pp. 247-256.

Scott, L.J., Clarke, N.W., George, N.J.R., Shanks, J.H., Testa, N.G. and Lang, S.H. (2001) Interactions of human prostatic epithelial cells with bone marrow endothelium: Binding and invasion. *British Journal of Cancer,* 84 (10), pp. 1417-1423.

Scuto, A., Kirschbaum, M., Buettner, R., Kujawski, M., Cermak, J.M., Atadja, P. and Jove, R. (2013) SIRT1 activation enhances HDAC inhibition-mediated upregulation of GADD45G by repressing the binding of NF-κB/STAT3 complex to its promoter in malignant lymphoid cells. *Cell Death and Disease,* 4 (5), pp. e635.

Seidel, C., Børset, M., Turesson, I., Abildgaard, N., Sundan, A. and Waage, A. (1998) Elevated serum concentrations of hepatocyte growth factor in patients with multiple myeloma. *Blood,* 91 (3), pp. 806-812.

Sertié, A.L., Sossi, V., Camargo, A.A., Zatz, M., Brahe, C. and Passos-Bueno, M.R. (2000) Collagen XVIII, containing an endogenous inhibitor of angiogenesis and tumor growth, plays a critical role in the maintenance of retinal structure and in neural tube closure (Knobloch syndrome). *Human Molecular Genetics,* 9 (13), pp. 2051-2058.

Sezer, O., Heider, U., Jakob, C., Zavrski, I., Eucker, J., Possinger, K., Sers, C., Krenn, V., Giuilani, N., Bataiile, R., Mancini, C., Lazzaretti, M. and Barlile, S. (2002) Immunocytochemistry reveals RANKL expression of myeloma cells [3] (multiple letters). *Blood,* 99 (12), pp. 4646-4647.

Sezer, O., Heider, U., Zavrski, I., Kühne, C.A. and Hofbauer, L.C. (2003) RANK ligand and osteoprotegerin in myeloma bone disease. *Blood,* 101 (6), pp. 2094-2098.

Shinkai, Y., Rathbun, 0., Lam, K., Oltz, E.M., Stewart, V., Mendelsohn, M., Charron, J., Datta, M., Young, F., Stall, A.M. and Alt, F.W. (1992) RAG-2-deficient mice lack mature lymphocytes owing to inability to initiate V(D)J rearrangement. *Cell,* 68 (5), pp. 855-867.

Shipman, C.M. and Croucher, P.I. (2003) Osteoprotegerin is a soluble decoy receptor for tumor necrosis factor-related apoptosis-inducing ligand/Apo2 ligand and can function as a paracrine survival factor for human myeloma cells. *Cancer Research,* 63 (5), pp. 912-916.

Silbermann, R.and Roodman, G.D. (2013) Hematologic Malignancies and Bone. In *Primer on the Metabolic Bone Diseases and Disorders of Mineral Metabolism.* John Wiley & Sons, Inc., pp. 694-701.

Simone, G., Malara, N., Trunzo, V., Renne, M., Perozziello, G., Di Fabrizio, E. and Manz, A. (2014) Galectin-3 coats the membrane of breast cells and makes a signature of tumours. *Molecular BioSystems,* 10 (2), pp. 258-265.

Smith, M.C.P., Luker, K.E., Garbow, J.R., Prior, J.L., Jackson, E., Piwnica-Worms, D. and Luker, G.D. (2004) CXCR4 regulates growth of both primary and metastatic breast cancer. *Cancer Research,* 64 (23), pp. 8604-8612.

Sobue, T., Hakeda, Y., Kobayashi, Y., Hayakawa, H., Yamashita, K., Aoki, T., Kumegawa, M., Noguchi, T. and Hayakawa, T. (2001) Tissue inhibitor of metalloproteinases 1 and 2 directly stimulate the bone-resorbing activity of isolated mature osteoclasts. *Journal of Bone and Mineral Research,* 16 (12), pp. 2205-2214.

Sonneveld, P., Schmidt-Wolf, I.G.H., Van Der Holt, B., El Jarari, L., Bertsch, U., Salwender, H., Zweegman, S., Vellenga, E., Broyl, A., Blau, I.W., Weisel, K.C., Wittebol, S., Bos, G.M.J., Stevens-Kroef, M., Scheid, C., Pfreundschuh, M., Hose, D., Jauch, A., Van Der Velde, H., Raymakers, R., Schaafsma, M.R., Kersten, M.-., Van Marwijk-Kooy, M., Duehrsen, U., Lindemann, W., Wijermans, P.W., Lokhorst, H.M. and Goldschmidt, H.M. (2012) Bortezomib induction and maintenance treatment in patients with newly diagnosed multiple myeloma: Results of the randomized phase III HOVON-65/ GMMG-HD4 trial. *Journal of Clinical Oncology,* 30 (24), pp. 2946-2955.

SPAIN, D.M., GREENBLATT, I.J., SNAPPER, I. and COHN, T. (1956) The degree of coronary and aortic atherosclerosis in necropsied cases of multiple myeloma. *The American Journal of the Medical Sciences,* 231 (2), pp. 165-167.

Spatz, J.M., Ellman, R., Cloutier, A.M., Louis, L., Van Vliet, M., Suva, L.J., Dwyer, D., Stolina, M., Ke, H.Z. and Bouxsein, M.L. (2013) Sclerostin antibody inhibits skeletal deterioration due to reduced mechanical loading. *Journal of Bone and Mineral Research,* 28 (4), pp. 865-874.

Sprynski, A.C., Hose, D., Caillot, L., Réme, T., Shaughnessy Jr., J.D., Barlogie, B., Seckinger, A., Moreaux, J., Hundemer, M., Jourdan, M., Meißner, T., Jauch, A., Mahtouk, K., Kassambara, A., Bertsch, U., Rossi, J.F., Goldschmidt, H. and Klein, B. (2009) The role of IGF-1 as a major growth factor for myeloma cell lines and the prognostic relevance of the expression of its receptor. *Blood,* 113 (19), pp. 4614-4626.

Standal, T., Abildgaard, N., Fagerli, U.-., Stordal, B., Hjertner, Ø, Borset, M. and Sundan, A. (2007) HGF inhibits BMP-induced osteoblastogenesis: Possible implications for the bone disease of multiple myeloma. *Blood,* 109 (7), pp. 3024-3030.

Streetly, M.J., Maharaj, L., Joel, S., Schey, S.A., Gribben, J.G. and Cotter, F.E. (2010) GCS-100, a novel galectin-3 antagonist, modulates MCL-1, NOXA, and cell cycle to induce myeloma cell death. *Blood,* 115 (19), pp. 3939-3948.

Syrigos, K.N., Harrington, K.J., Karayiannakis, A.J., Baibas, N., Katirtzoglou, N. and Roussou, P. (2004) Circulating soluble E-cadherin levels are of prognostic significance in patients with multiple myeloma. *Anticancer Research,* 24 (3 B), pp. 2027-2031.

Szczepek, A.J., Bergsagel, P.L., Axelsson, L., Brown, C.B., Belch, A.R. and Pilarski, L.M. (1997) CD34+ cells in the blood of patients with multiple myeloma express CD19 and IgH mRNA and have patient-specific IgH VDJ gene rearrangements. *Blood,* 89 (5), pp. 1824-1833.

Takada, I., Mihara, M., Suzawa, M., Ohtake, F., Kobayashi, S., Igarashi, M., Youn, M.-., Takeyama, K.-., Nakamura, T., Mezaki, Y., Takezawa, S., Yogiashi, Y., Kitagawa, H., Yamada, G., Takada, S., Minami, Y., Shibuya, H., Matsumoto, K. and Kato, S. (2007) A histone lysine methyltransferase activated by non-canonical Wnt signalling suppresses PPAR-γ transactivation. *Nature Cell Biology,* 9 (11), pp. 1273-1285.

Takafuji, V., Forgues, M., Unsworth, E., Goldsmith, P. and Wang, X.W. (2007) An osteopontin fragment is essential for tumor cell invasion in hepatocellular carcinoma. *Oncogene,* 26 (44), pp. 6361-6371.

Takeuchi, K., Abe, M., Hiasa, M., Oda, A., Amou, H., Kido, S., Harada, T., Tanaka, O., Miki, H., Nakamura, S., Nakano, A., Kagawa, K., Yata, K., Ozaki, S. and Matsumoto, T. (2010)

TGF-ß inhibition restores terminal osteoblast differentiation to suppress myeloma growth. *PLoS ONE,* 5 (3), pp. e9870.

Tamura, T., Udagawa, N., Takahashi, N., Miyaura, C., Tanaka, S., Yamada, Y., Koishihara, Y., Ohsugi, Y., Kumaki, K., Taga, T., Kishimoto, T. and Suda, T. (1993) Soluble interleukin-6 receptor triggers osteoclast formation by interleukin 6. *Proceedings of the National Academy of Sciences of the United States of America,* 90 (24), pp. 11924-11928.

Tanaka, Y., Abe, M., Hiasa, M., Oda, A., Amou, H., Nakano, A., Takeuchi, K., Kitazoe, K., Kido, S., Inoue, D., Moriyama, K., Hashimoto, T., Ozaki, S. and Matsumoto, T. (2007) Myeloma cell-osteoclast interaction enhances angiogenesis together with bone resorption: A role for vascular endothelial cell growth factor and osteopontin. *Clinical Cancer Research,* 13 (3), pp. 816-823.

Tangye, S.G. (2011) Staying alive: regulation of plasma cell survival. *Trends in Immunology,* 32 (12), pp. 595-602.

Tatsumi, S., Ito, M., Asaba, Y., Tsutsumi, K. and Ikeda, K. (2008) Life-long caloric restriction reveals biphasic and dimorphic effects on bone metabolism in rodents. *Endocrinology,* 149 (2), pp. 634-641.

Tchernof, A. and Després, J.-. (2013) Pathophysiology of human visceral obesity: An update. *Physiological Reviews,* 93 (1), pp. 359-404.

Terpos, E., Dimopoulos, M.A., Shrivastava, V., Leitzel, K., Christoulas, D., Migkou, M., Gavriatopoulou, M., Anargyrou, K., Hamer, P., Kastritis, E., Carney, W. and Lipton, A. (2010) High levels of serum TIMP-1 correlate with advanced disease and predict for poor survival in patients with multiple myeloma treated with novel agents. *Leukemia Research,* 34 (3), pp. 399-402.

Terpos, E., Mihou, D., Szydlo, R., Tsimirika, K., Karkantaris, C., Politou, M., Voskaridou, E., Rahemtulla, A., Dimopoulos, M.A. and Zervas, K. (2005) The combination of intermediate doses of thalidomide with dexamethasone is an effective treatment for patients with refractory/relapsed multiple myeloma and normalizes abnormal bone remodeling, through the reduction of sRANKL/osteoprotegerin ratio. *Leukemia,* 19 (11), pp. 1969-1976.

Terpos, E., Palermos, J., Tsionos, K., Anargyrou, K., Viniou, N., Papassavas, P., Meletis, J.C. and Yataganas, X. (2000) Effect of pamidronate administration on markers of bone turnover and disease activity in multiple myeloma. *European Journal of Haematology,* 65 (5), pp. 331-336.

Terpos, E., Palermos, J., Viniou, N., Vaiopoulos, G., Meletis, J. and Yataganas, X. (2001) Pamidronate increases markers of bone formation in patients with multiple myeloma in plateau phase under interferon-alpha treatment. *Calcified Tissue International,* 68 (5), pp. 285-290.

Terpos, E., Szydlo, R., Apperley, J.F., Hatjiharissi, E., Politou, M., Meletis, J., Viniou, N., Yataganas, X., Goldman, J.M. and Rahemtulla, A. (2003) Soluble receptor activator of nuclear factor κB ligand-osteoprotegerin ratio predicts survival in multiple myeloma: Proposal for a novel prognostic index. *Blood,* 102 (3), pp. 1064-1069.

Thiolloy, S., Edwards, J.R., Fingleton, B., Rifkin, D.B., Matrisian, L.M. and Lynch, C.C. (2012) An osteoblast-derived proteinase controls tumor cell survival via TGF-beta activation in the bone microenvironment. *PLoS ONE,* 7 (1), pp. e29862.

Thiolloy, S., Halpern, J., Holt, G.E., Schwartz, H.S., Mundy, G.R., Matrisian, L.M. and Lynch, C.C. (2009) Osteoclast-derived matrix metalloproteinase-7, but not matrix metalloproteinase-9, contributes to tumor-induced osteolysis. *Cancer Research,* 69 (16), pp. 6747-6755.

Tian, E., Zhan, F., Walker, R., Rasmussen, E., Ma, Y., Barlogie, B. and Shaughnessy Jr., J.D. (2003) The Role of the Wnt-Signaling Antagonist DKK1 in the Development of Osteolytic Lesions in Multiple Myeloma. *New England Journal of Medicine,* 349 (26), pp. 2483-2494.

Tondravi, M.M., McKercher, S.R., Anderson, K., Erdmann, J.M., Quiroz, M., Maki, R. and Teitelbaum, S.L. (1997) Osteopetrosis in mice lacking haematopoietic transcription factor PU.1. *Nature,* 386 (6620), pp. 81-84.

Tuominen, I., Al-Rabadi, L., Stavrakis, D., Karagiannides, I., Pothoulakis, C. and Bugni, J.M. (2013) Diet-Induced Obesity Promotes Colon Tumor Development in Azoxymethane-Treated Mice. *PLoS ONE,* 8 (4), pp. e60939.

Vacca, A., Ribatti, D., Roncali, L., Ranieri, G., Serio, G., Silvestris, F. and Dammacco, F. (1994) Bone marrow angiogenesis and progression in multiple myeloma. *British Journal of Haematology,* 87 (3), pp. 503-508.

Vallet, S., Mukherjee, S., Vaghela, N., Hideshima, T., Fulciniti, M., Pozzi, S., Santo, L., Cirstea, D., Patel, K., Sohani, A.R., Guimaraes, A., Xie, W., Chauhan, D., Schoonmaker, J.A., Attar, E., Churchill, M., Weller, E., Munshi, N., Seehra, J.S., Weissleder, R., Anderson, K.C., Scadden, D.T. and Raje, N. (2010) Activin A promotes multiple myeloma-induced osteolysis and is a promising target for myeloma bone disease. *Proceedings of the National Academy of Sciences of the United States of America,* 107 (11), pp. 5124-5129.

Van Valckenborgh, E., Croucher, P.I., De Raeve, H., Carron, C., De Leenheer, E., Blacher, S., Devy, L., Noël, A., De Bruyne, E., Asosingh, K., Van Riet, I., Van Camp, B. and Vanderkerken, K. (2004) Multifunctional role of matrix metalloproteinases in multiple myeloma: A study in the 5T2MM mouse model. *American Journal of Pathology,* 165 (3), pp. 869-878.

Vande Broek, I., Vanderkerken, K., De Greef, C., Asosingh, K., Straetmans, N., Van Camp, B. and Van Riet, I. (2001) Laminin-1-induced migration of multiple myeloma cells involves the high-affinity 67 kD laminin receptor. *British Journal of Cancer,* 85 (9), pp. 1387-1395.

Vanderkerken, K., De Leenheer, E., Shipman, C., Asosingh, K., Willems, A., Van Camp, B. and Croucher, P. (2003) Recombinant osteoprotegerin decreases tumor burden and increases survival in a murine model of multiple myeloma. *Cancer Research,* 63 (2), pp. 287-289.

Vaseva, A.V., Marchenko, N.D., Ji, K., Tsirka, S.E., Holzmann, S. and Moll, U.M. (2012) P53 opens the mitochondrial permeability transition pore to trigger necrosis. *Cell,* 149 (7), pp. 1536-1548.

Verborgt, O., Tatton, N.A., Majeska, R.J. and Schaffler, M.B. (2002) Spatial distribution of Bax and Bcl-2 in osteocytes after bone fatigue: Complementary roles in bone remodeling regulation? *Journal of Bone and Mineral Research,* 17 (5), pp. 907-914.

Von Bredow, D.C., Cress, A.E., Howard, E.W., Bowden, G.T. and Nagle, R.B. (1998) Activation of gelatinase-tissue-inhibitors-of-metalloproteinase complexes by matrilysin. *Biochemical Journal,* 331 (3), pp. 965-972.

Von Bredow, D.C., Nagle, R.B., Bowden, G.T. and Cress, A.E. (1997) Cleavage of ß4 integrin by matrilysin. *Experimental cell research,* 236 (1), pp. 341-345.

Vu, T.H., Shipley, J.M., Bergers, G., Berger, J.E., Helms, J.A., Hanahan, D., Shapiro, S.D., Senior, R.M. and Werb, Z. (1998) MMP-9/Gelatinase B Is a Key Regulator of Growth Plate Angiogenesis and Apoptosis of Hypertrophic Chondrocytes. *Cell,* 93 (3), pp. 411-422.

Wade-Gueye, N.M., Boudiffa, M., Laroche, N., Vanden-Bossche, A., Fournier, C., Aubin, J.E., Vico, L., Lafage-Proust, M.-. and Malaval, L. (2010) Mice lacking bone sialoprotein (BSP) lose bone after ovariectomy and display skeletal site-specific response to intermittent PTH treatment. *Endocrinology,* 151 (11), pp. 5103-5113.

Wallin, A. and Larsson, S.C. (2011) Body mass index and risk of multiple myeloma: A meta-analysis of prospective studies. *European Journal of Cancer,* 47 (11), pp. 1606-1615.

Wang, W. and Guan, K.-. (2009) AMP-activated protein kinase and cancer. *Acta Physiologica,* 196 (1), pp. 55-63.

Wang, Y., Nangia-Makker, P., Tait, L., Balan, V., Hogan, V., Pienta, K.J. and Raz, A. (2009) Regulation of prostate cancer progression by galectin-3. *American Journal of Pathology,* 174 (4), pp. 1515-1523.

Watelet, J.B., Bachert, C., Claeys, C. and Van Cauwenberge, P. (2004) Matrix metalloproteinases MMP-7, MMP-9 and their tissue inhibitor TIMP-1: Expression in chronic sinusitis vs nasal polyposis. *Allergy: European Journal of Allergy and Clinical Immunology,* 59 (1), pp. 54-60.

Wei, W., Dutchak, P.A., Wang, X., Ding, X., Wang, X., Bookout, A.L., Goetz, R., Mohammadi, M., Gerard, R.D., Dechow, P.C., Mangelsdorf, D.J., Kliewer, S.A. and Wan, Y. (2012) Fibroblast growth factor 21 promotes bone loss by potentiating the effects of peroxisome proliferator-activated receptor γ. *Proceedings of the National Academy of Sciences of the United States of America,* 109 (8), pp. 3143-3148.

Weigert, J., Neumeier, M., Wanninger, J., Bauer, S., Farkas, S., Scherer, M.N., Schnitzbauer, A., Schäffler, A., Aslanidis, C., Schölmerich, J. and Buechler, C. (2010) Serum galectin-3 is elevated in obesity and negatively correlates with glycosylated hemoglobin in type 2 diabetes. *Journal of Clinical Endocrinology and Metabolism,* 95 (3), pp. 1404-1411.

Weinstein, R.S., Nicholas, R.W. and Manolagas, S.C. (2000) Apoptosis of osteocytes in glucocorticoid-induced osteonecrosis of the hip. *Journal of Clinical Endocrinology and Metabolism,* 85 (8), pp. 2907-2912.

Williams, H., Johnson, J.L., Jackson, C.L., White, S.J. and George, S.J. (2010) MMP-7 mediates cleavage of N-cadherin and promotes smooth muscle cell apoptosis. *Cardiovascular Research,* 87 (1), pp. 137-146.

Wilson, C.L., Ouellette, A.J., Satchell, D.P., Ayabe, T., López-Boado, Y.S., Stratman, J.L., Hultgren, S.J., Matrisian, L.M. and Parks, W.C. (1999) Regulation of intestinal a-defensin activation by the metalloproteinase matrilysin in innate host defense. *Science,* 286 (5437), pp. 113-117.

Withold, W., Arning, M., Schwarz, M., Wolf, H.-. and Schneider, W. (1998) Monitoring of multiple myeloma patients by simultaneously measuring marker substances of bone resorption and formation. *Clinica Chimica Acta,* 269 (1), pp. 21-30.

Wolin, K.Y., Carson, K. and Colditz, G.A. (2010) Obesity and cancer. *Oncologist,* 15 (6), pp. 556-565.

Wright, H.M., Clish, C.B., Mikami, T., Hauser, S., Yanagi, K., Hiramatsu, R., Serhan, C.N. and Spiegelman, B.M. (2000) A synthetic antagonist for the peroxisome proliferator-activated receptor γ inhibits adipocyte differentiation. *Journal of Biological Chemistry,* 275 (3), pp. 1873-1877.

Yaccoby, S., Barlogie, B. and Epstein, J. (1998) Primary myeloma cells growing in SCID-hu mice: a model for studying the biology and treatment of myeloma and its manifestations. *Blood,* 92 (8), pp. 2908-2913.

Yakar, S., Rosen, C.J., Beamer, W.G., Ackert-Bicknell, C.L., Wu, Y., Liu, J.-., Ooi, G.T., Setser, J., Frystyk, J., Boisclair, Y.R. and LeRoith, D. (2002) Circulating levels of IGF-1 directly regulate bone growth and density. *Journal of Clinical Investigation,* 110 (6), pp. 771-781.

Yamagata, M. and Kimata, K. (1994) Repression of a malignant cell-substratum adhesion phenotype by inhibiting the production of the anti-adhesive proteoglycan, PG-M/versican. *Journal of Cell Science,* 107 (9), pp. 2581-2590.

Yan, T., Wergedal, J., Zhou, Y., Mohan, S., Baylink, D.J. and Strong, D.D. (2001) Inhibition of human osteoblast marker gene expression by retinoids is mediated in part by insulin-like growth factor binding protein-6. *Growth Hormone and IGF Research,* 11 (6), pp. 368-377.

Yang, H.H., Vescio, R., Schenkein, D. and Berenson, J.R. (2003) A prospective, open-label safety and efficacy study of combination treatment with bortezomib (PS-341, Velcade™) and melphalan in patients with relapsed or refractory multiple myeloma. *Clinical Lymphoma,* 4 (2), pp. 119-122.

Yeung, F., Hoberg, J.E., Ramsey, C.S., Keller, M.D., Jones, D.R., Frye, R.A. and Mayo, M.W. (2004) Modulation of NF-κB-dependent transcription and cell survival by the SIRT1 deacetylase. *EMBO Journal,* 23 (12), pp. 2369-2380.

Yin, J.J., Pollock, C.B. and Kelly, K. (2005) Mechanisms of cancer metastasis to the bone. *Cell Research,* 15 (1), pp. 57-62.

Yoshida, H., Matsui, T., Yamamoto, A., Okada, T. and Mori, K. (2001) XBP1 mRNA is induced by ATF6 and spliced by IRE1 in response to ER stress to produce a highly active transcription factor. *Cell,* 107 (7), pp. 881-891.

Yu, W.-., Huang, P.-., Lou, K.-., Yu, S.-.C. and Lin, C. (2012) A smallest 6 Kda metalloprotease, mini-matrilysin, in living world: A revolutionary conserved zinc-dependent proteolytic domain- helix-Loop-helix catalytic zinc binding domain (ZBD). *Journal of Biomedical Science,* 19 (1).

Yu, W.-., Woessner Jr., F., McNeish, J.D. and Stamenkovic, I. (2002) CD44 anchors the assembly of matrilysin/MMP-7 with heparin-binding epidermal growth factor precursor and ErbB4 and regulates female reproductive organ remodeling. *Genes and Development,* 16 (3), pp. 307-323.

Yu, X., Huang, Y., Collin-Osdoby, P. and Osdoby, P. (2003) Stromal cell-derived factor-1 (SDF-1) recruits osteoclast precursors by inducing chemotaxis, matrix metalloproteinase-9 (MMP-9) activity, and collagen transmigration. *Journal of Bone and Mineral Research,* 18 (8), pp. 1404-1418.

Yue, D.W., De Vos, J., Jourdan, M., Couderc, G., Lu, Z.-., Rossi, J.-. and Klein, B. (2002) Cooperation between heparin-binding EGF-like growth factor and interleukin-6 in promoting the growth of human myeloma cells. *Oncogene,* 21 (16), pp. 2584-2592.

Zangari, M., Esseltine, D., Lee, C.-., Barlogie, B., Elice, F., Burns, M.J., Kang, S.-., Yaccoby, S., Najarian, K., Richardson, P., Sonneveld, P. and Tricot, G. (2005) Response to bortezomib is associated to osteoblastic activation in patients with multiple myeloma. *British Journal of Haematology,* 131 (1), pp. 71-73.

Zannettino, A.C.W., Farrugia, A.N., Kortesidis, A., Manavis, J., To, L.B., Martin, S.K., Diamond, P., Tamamura, H., Lapidot, T., Fujii, N. and Gronthos, S. (2005) Elevated serum levels of stromal-derived factor-1 α are associated with increase osteoclast activity and osteolytic bone disease in multiple myeloma patients. *Cancer Research,* 65 (5), pp. 1700-1709.

Zeng, R., He, J., Peng, J., Chen, Y., Yi, S., Zhao, F. and Cui, G. (2012) The time-dependent autophagy protects against apoptosis with possible involvement of Sirt1 protein in multiple myeloma under nutrient depletion. *Annals of Hematology,* 91 (3), pp. 407-417.

Zhang, X.G., Klein, B. and Bataille, R. (1989) Interleukin-6 is a potent myeloma-cell growth factor in patients with aggressive multiple myeloma. *Blood,* 74 (1), pp. 11-13.

Zou, J., Glinsky, V.V., Landon, L.A., Matthews, L. and Deutscher, S.L. (2005) Peptides specific to the galectin-3 carbohydrate recognition domain inhibit metastasis-associated cancer cell adhesion. *Carcinogenesis,* 26 (2), pp. 309-318.